

THÈSE DE DOCTORAT

PRÉSENTÉE À

Université de Lille

PAR

M. Xinzhe WU

Spécialité de doctorat : Informatique

École doctorale Sciences Pour l'Ingénieur Université Lille Nord-de-France

**Contribution à l'émergence de nouvelles méthodes parallèles
et reparties intelligentes utilisant un paradigme de
programmation multi-niveaux pour le calcul extrême**

Thèse dirigée par SERGE G. PETITON, Université de Lille

MEMBRES DU JURY:

Président	Catherine Lambert	- Directrice de CERFACS
Rapporteurs	Michel Daydé	- Directeur de l'IRT de Toulouse
		- Professeur à l'ENSEEIHT
	<i>Not decided</i>	-
Examinateurs	Yutong Lu	- Directrice de NSCC-Guangzhou
		- Professeur à l'Université de Sun Yat-Sen
	Mitsuhisa Sato	- Directeur adjoint de RIKEN-CCS
		- Professeur à l'Université de Tuskuba
	<i>A German ?</i>	-
Directeur	Serge G. Petiton	- Professeur à l'Université de Lille

Thèse présentée et soutenue à Saclay, le 22 Mars 2019

This thesis is dedicated to my grandmother. Hope you can hear in the heaven.

Acknowledgement

First and foremost I would like to thank my adviser of the dissertation, Serge G. Petiton.

Abstract

The abstract of rapport …

Contents

List of Figures	ix
List of Tables	xii
List of Algorithms	xiv
1 Introduction	1
1.1 Motivations	1
1.2 Objectives and Core Contributions	2
1.3 Outline	4
2 State-of-the-art in High-Performance Computing	7
2.1 Evaluation of HPC	7
2.2 Modern Computing Architectures	9
2.2.1 CPU Architectures and Memory Access	9
2.2.2 Parallel Computer Memory Architectures	11
2.2.3 Nvidia’s GPGPU	13
2.2.4 Intel’s Many Integrated Cores	14
2.2.5 RISC-based (Co)processors	15
2.2.6 FPGA	16
2.3 Parallel Programming Model	17
2.3.1 Shared Memory Level Parallelism	17
2.3.2 Distributed Memory Level Parallelism	19
2.3.3 Partitioned Global Address Space	20
2.3.4 Task/Graph Based Parallel Programming	21
2.4 Exascale Challenges of Supercomputers	22
2.4.1 Increase of Heterogeneity for Supercomputers	23
2.4.2 Potential Architecture of Exascale Supercomputer	24
2.4.3 Parallel Programming Challenges	25
3 Krylov Subspace Methods	27
3.1 Linear Systems and Eigenvalue Problems	27
3.2 Iterative Methods	28

CONTENTS

3.2.1	Stationary and Multigrid Methods	28
3.2.2	Non-stationary Methods	31
3.3	Krylov Subspace methods	31
3.3.1	Krylov Subspaces	32
3.3.2	Basic Arnoldi Reduction	32
3.3.3	Orthogonalization	33
3.3.4	Krylov Subspace Methods	34
3.4	GMRES for Non-Hermitian Linear Systems	35
3.4.1	Basic GMRES Method	35
3.4.2	Variants of GMRES	36
3.5	Arnoldi for Non-Hermitian Eigenvalue Problems	37
3.5.1	Basic Arnoldi Methods	37
3.5.2	Variants of Arnoldi Method	37
3.6	Preconditioners for GMRES	38
3.6.1	Preconditioning by Selected Matrix	39
3.6.2	Preconditioning by Deflation	44
3.6.3	Preconditioning by Polynomials - Introduction in detail on Least Squares Polynomial method	44
3.7	GMRES Convergence Analysis	52
3.7.1	Convergence Analysis by Eigenvalues	53
3.7.2	Convergence Analysis by Pseudo-eigenvalues	53
3.7.3	Convergence Analysis by Polynomial Numerical Hull	53
3.8	Parallel Krylov methods on Large-scale Supercomputers	54
3.8.1	Core Operations in Krylov Methods	54
3.8.2	Existing Softwares	56
3.9	Toward Extreme Computing, Some Correlated Goals	59
4	Sparse Matrix Generator with Given Spectra	67
4.1	Demand of Large Matrices with Given Spectrum	67
4.2	The Existing Collections	69
4.3	Mathematical Framework	69
4.4	Numerical Implementation of SMG2S	70
4.4.1	Matrix Generation Method	71
4.4.2	Numerical Algorithm	73
4.5	Parallel Implementation and Evaluation	74
4.5.1	Basic Implementation on CPUs	74
4.5.2	Implementation on Multi-GPU	75
4.5.3	Communication Optimized Implementation with MPI	75
4.6	Parallel Performance Evaluation	78
4.6.1	Hardware	78
4.6.2	Strong and Weak Scalability Evaluation	78
4.6.3	Speedup Evaluation	81

4.6.4	Performance Analysis	81
4.7	Verification Method	82
4.7.1	Experimental Results	83
4.7.2	Arithmetic Precision Analysis	84
4.8	Package, Interface and Application	86
4.8.1	Package	86
4.8.2	Interface To Scientific Libraries	89
4.8.3	Graphic User Interface for Verification	91
4.8.4	Krylov Solvers Evaluation using SMG2S	91
4.9	Conclusion and Perspectives	94
5	Unite and Conquer GMRES/LS-ERAM Method	95
5.1	Unite and Conquer approach	96
5.2	Asynchronous Unite and Conquer GMRES/LS-ERAM Method	97
5.2.1	Divide of Linear Solvers into Components	97
5.2.2	UCGLE Method	98
5.3	Distributed and Parallel Implementation	99
5.3.1	Component Implementation	100
5.3.2	Parameters Analysis	104
5.3.3	Multi-level Parallelism in UCGLE	106
5.3.4	Distributed and Parallel Manager Engine Implementation	107
5.4	Experiment and Evaluation	110
5.4.1	Hardware Platforms	110
5.4.2	Parameters Evaluation	111
5.4.3	Convergence Evaluation	116
5.4.4	Scalability Evaluation	117
5.4.5	Fault Tolerance Evaluation	121
5.5	Conclusion	122
6	UCGLE for Linear Systems with Sequences of Right-hand-sides	123
6.1	Demand to Solve Linear Systems in Sequence	123
6.2	Existing Methods and Analysis	125
6.2.1	Seeds Method	125
6.2.2	Krylov Subspace Recycling Methods	125
6.2.3	Challenges of Existing Methods	126
6.3	UCGLE method for Linear Systems with Sequent Right-hand-sides	126
6.3.1	Relation between LS Residual and Dominant Eigenvalues	126
6.3.2	Eigenvalues Recycling to Solve Linear Systems in Sequence	128
6.3.3	Experiments of UCGLE for Sequences of Linear Systems	130
6.4	Conclusion	136

7 UCGLE for Linear Systems with Multiple Right-hand-sides	137
7.1 Demand to Solve Linear Systems with Multiple Right-hand-sdes	137
7.2 Existing Methods and Analysis	138
7.2.1 Block Method	138
7.2.2 Cost Comparison	139
7.2.3 Challenges of Existing Methods for Large-scale Platforms	139
7.3 m -UCGLE for Multiple Right-hand-sides	141
7.3.1 Shifted Krylov-Schur Algorithm	141
7.3.2 Least Squares Polynomial for Multiple Right-hand sides	142
7.3.3 Analysis	143
7.3.4 Manager Engine Implementation	146
7.3.5 m -UCGLE Implementation on Multi-GPU	148
7.3.6 Parallel and Numerical Performance Evaluation	148
7.4 Conclusions	156
8 Parameters Autotuning	157
8.1 Autotuning of GMRES/BGMRES Component	158
8.1.1 Krylov Subspace Size	158
8.1.2 LS Applied Times	158
8.1.3 LS Frequence	158
8.1.4 Number of BGMRES Components Allocated	158
8.2 Autotuning of ERAM/ s -KS Component	158
8.2.1 Number of Eigenvalues	158
8.3 Autotuning of LS/BLSP Component	158
8.3.1 LS Plynomial Degree	158
8.4 Adaptive UCGLE/ m -UCGLE	158
8.5 Conclusion	158
9 YML and XMP Multi-level Parallelism Programming Paradigm	159
9.1 YML Framework	159
9.1.1 YML Design	160
9.1.2 Yvette Language	162
9.1.3 YML Example	163
9.1.4 Multi-level Programming Paradigm: YML/XMP	164
9.2 Limitations of YML for UC Approach	166
9.2.1 Workflow of m -UCGLE Analysis	166
9.2.2 Mechanism for Convergence	166
9.2.3 Asynchronous Communications	166
9.3 Proposition of Solution	166
9.3.1 Dynamic Graph Grammar in YML	166
9.3.2 Exiting Parallel Branch	168
9.3.3 Check Pointing	169

9.3.4 Scheduler for YML/MPI	169
9.4 Demand for MPI Correction Mechanism	169
9.5 Conclusion	170
10 Conclusion and Perspectives	171
Scientific Communication	173
Bibliography	175

CONTENTS

List of Figures

2.1	Top 1 Supercomputers' Performance by Year.	8
2.2	Computer architectures.	10
2.3	Memory Hierarchy.	11
2.4	Parallel Computer Memory Architectures.	12
2.5	CPU vs GPU.	14
2.6	The organization of a Knights Landing processor.	15
2.7	The organization of a SW26010 manycores processor.	16
2.8	OpenMP fork-join Model.	18
2.9	Processing flow on CUDA.	19
2.10	MPI send and receive Model.	20
2.11	Number of systems each year boosted by accelerators.	23
2.12	Multiple level parallelism in supercomputers.	24
3.1	Algebraic multigrid hierarchy.	31
3.2	The action of A on V_m gives $V_m H_m$ plus a rank-one matrix.	33
3.3	The polygon of smallest area containing the convex hull of $\lambda(A)$	48
3.4	Communication Scheme of SpMV.	56
3.5	Classic Parallel implementation of Arnoldi reduction.	57
4.1	Nilpotent Matrix. p off-diagonal offset, d number of continuous 1, and n matrix dimension.	72
4.2	Matrix Generation. The left is the initial matrix M_0 with given spectrum on the diagonal, and the h lower diagonals with random values; the right is the generated matrix M_t with nilpotency matrix determined by the parameters d and p	74
4.3	Matrix Generation Pattern Example.	74
4.4	The structure of a CPU-GPU implementation of SpGEMM, where each GPU is attached to a CPU. The GPU is in charge of the computation, while the CPU handles the MPI communication among processes.	76
4.5	(a) AM operation; (b) MA operation.	77
4.6	Strong and weak scaling results of SMG2S on different platforms. A base 2 logarithmic scale is used for X-axis, and a base 10 logarithmic scale for Y-axis.	80

LIST OF FIGURES

4.7	Strong and weak scaling results of SMG2S on different platforms. A base 2 logarithmic scale is used for X-axis, and a base 10 logarithmic scale for Y-axis.	80
4.8	Strong and weak scaling results of SMG2S on different platforms. A base 2 logarithmic scale is used for X-axis, and a base 10 logarithmic scale for Y-axis.	80
4.9	Weak scaling speedup comparison of GPUs on ROMEO.	81
4.10	SMG2S verification workflow.	82
4.11	Spec1: Clustered Eigenvalues I.	84
4.12	Spec1: Clustered Eigenvalues I.	85
4.13	Spec3: Clustered Eigenvalues III.	85
4.14	Spec4: Conjugate and Closest Eigenvalues.	86
4.15	Home Screen Plot Capture	92
4.16	SMG2S Workflow and Interface.	93
5.1	An overview of MERAM (Emad et al. [2005]).	97
5.2	An example of MERAM: MERAM(5,7,10) vs. ERAM(10) with af 23560.mtx matrix. MERAM converges in 74 restarts, ERAM does not converge after 240 restarts (Emad et al. [2005]).	98
5.3	Cyclic Relation of linear solver, eigen-information and preconditioning techniques.	99
5.4	Workflow of UCGLE method's three components	100
5.5	GMRES Component.	101
5.6	ERAM Component.	102
5.7	LS Component.	103
5.8	Convergence comparison of UCGLE method vs classic GMRES.	105
5.9	Communication and different levels parallelism of UCGLE method	106
5.10	Creation of Several Intra-Communicators in MPI.	107
5.11	Data Sending Scheme from one group of process to the other.	108
5.12	Data Receiving Scheme from one group of process to the other.	109
5.13	Evaluation of GMRES subspace size m_g varying from 50 to 180. $l = 10$, $lsa = 10$, $freq = 10$	112
5.14	Convergence comparison of UCGLE method vs classic GMRES.	113
5.15	Evaluation of LS applied times lsa varying from 1 to 25, and $m_g = 100$, $l = 10$, $freq = 1$	114
5.16	Evaluation of LS applied times $freq$	115
5.17	Evaluation of eigenvalue number n_{eigen}	116
5.18	Two strategies of large and sparse matrix generator by a original matrix utm300 of Matrix Market.	116
5.19	<i>MEG1</i> : convergence comparison of UCGLE method vs conventional GMRES . .	117
5.20	<i>MEG2</i> : convergence comparison of UCGLE method vs conventional GMRES . .	118
5.21	<i>MEG3</i> : convergence comparison of UCGLE method vs conventional GMRES . .	118
5.22	<i>MEG4</i> : convergence comparison of UCGLE method vs conventional GMRES . .	119
5.23	Scalability per iteration comparison of UCGLE with GMRES with or without preconditioners on Tianhe-2.	120

5.24 Scalability per iteration comparison of UCGLE with GMRES with or without preconditioners on ROMEO.	121
6.1 GCR-DO workflow.	126
6.2 Convergence comparison of UCGLE method vs classic GMRES.	127
6.3 Workflow of UCGLE to Solve Linear Systems In Sequence.	130
6.4 <i>Mat1</i> : time comparison for solving a sequence of linear systems. (a) shows the solution time for 9 sequent linear systems; (b) shows the cases extracted from (a) after the good selection of parameters in UCGLE.	133
6.5 <i>Mat2</i> : time comparison for solving a sequence of linear systems. (a) shows the solution time for 9 sequent linear systems; (b) shows the cases extracted from (a) after the good selection of parameters in UCGLE.	134
6.6 <i>Mat3</i> : time comparison for solving a sequence of linear systems. (a) shows the solution time for 9 sequent linear systems; (b) shows the cases extracted from (a) after the good selection of parameters in UCGLE.	136
7.1 Manager Engine Implementation for <i>m</i> -UCGLE.	146
7.2 Different strategies to divide the linear systems with 64 RHSs into subsets: (a) divide the 64 RHSs into to 16 different components of <i>m</i> -UCGLE, each holds 4 RHSs; (b) divide the 64 RHSs into to 4 different components of <i>m</i> -UCGLE, each holds 16 RHSs; (c) One classic BGMRES to solve the linear systems with 64 RHSs simultaneously.	149
7.3 Strong scalability test on CPUs of solving time per iteration for <i>m</i> -BGMRES(4) \times 16, <i>m</i> -UCGLE(4) \times 16, <i>m</i> -BGMRES(16) \times 4, <i>m</i> -UCGLE(16) \times 4, BGMRES(64); test matrix size is 1.792×10^6 ; X-axis refers to the total number of CPUs from 224 to 1792; Y-axis refers to the average execution time per iteration. A base 2 logarithmic scale is used for all X-axis, and a base 10 logarithmic scale is used for all Y-axis.	154
9.1 YML Architecture.	162
9.2 Workflow of Sum Application.	163
9.3 Application Execution with YML + OmniRPC-MPI.	165
9.4 <i>m</i> -UCGLE task.	165
9.5 New Scenario with Dynamic Graph.	166
9.6 Exiting Parallel Branch.	169

LIST OF FIGURES

List of Tables

4.1	Details for weak scaling and speedup evaluation.	79
4.2	Accuracy Verification Results.	83
4.3	Krylov Solvers Evaluation by SMG2S with matrix row number = 1.0×10^5 , convergence tolerance = 1×10^{-10} (dnc = do not converge in 8.0×10^4 iterations, the solvers and preconditioners are provided by PETSc.)	93
5.1	Test Matrix from Matrix Market Collection.	111
5.2	Test matrices information	117
5.3	Summary of iteration number for convergence of 4 test matrices using SOR, Jacobi, non preconditioned GMRES,UCGLE_FT(G),UCGLE_FT(G) and UC-GLE: red \times in the table presents this solving procedure cannot converge to accurate solution (here absolute residual tolerance 1×10^{-10} for GMRES convergence test) in acceptable iteration number (20000 here).	119
6.1	<i>Mat1</i> : iterative step comparison for solving a sequence of linear systems.	133
6.2	<i>Mat2</i> : iterative step comparison for solving a sequence of linear systems.	134
6.3	<i>Mat3</i> : iterative step comparison for solving a sequence of linear systems.	135
7.1	Operation Cost.	139
7.2	Storage Requirement.	139
7.3	Extra cost of Block GMRES comparing with s times GMRES.	140
7.4	Extra cost of Block GMRES comparing with s times GMRES.	140
7.5	Memory and Communication Complexity Comparison between m -UCGLE and BGMRES.	147
7.6	Alternative methods for experiments, and the related number of allocated component, Rhs number per component and preconditioners.	151
7.7	Iteration steps of convergence comparison (SMG2S generation suite SMG2S(1, 3, 4, <i>spec</i>), relative tolerance for convergence test = 1.0×10^{-8}), Krylov subspace size $m_g = 40$, $s_{use} = 10$, $d = 15$, $L = 1$, dnc = do not converge in 5000 iteration steps).	152

LIST OF TABLES

7.8 Consumption time (s) comparison on CPUs (SMG2S generation suite SMG2S(1, 3, 4, <i>spec</i>), the size of matrices = 1.792×10^6 , relative tolerance for convergence test = 1.0×10^{-8}), Krylov subspace size $m_g = 40$, $l = 10$, $d = 15$, $L = 1$, <i>dnc</i> = do not converge in 5000 iteration steps).	152
--	-----

List of Algorithms

1	Fine-corse-fine loop of multigrid method	30
2	Arnoldi Reduction	32
3	Arnoldi Reduction with Modified Gram-Schmidt process	34
4	Arnoldi Reduction with Incomplete Orthogonalization process	34
5	Basic GMRES method	35
6	Restarted GMRES method	36
7	Explicitly Restarted Arnoldi Method	38
8	Implicitly Restarted Arnoldi Method	39
9	Krylov-Schur Method	39
10	Left-Preconditioned GMRES	40
11	Right-Preconditioned GMRES	40
12	Incomplete LU Factorization Algorithm	43
13	AMG-Preconditioned GMRES	44
14	GMRES-DR(A, m, k, x_0)	45
15	Polynomial Preconditioned GMRES	48
16	Least Square Polynomial Generation	52
17	Hybrid GMRES Preconditioned by Least Squares Polynomial	52
18	Matrix Generation Method	73
19	Parallel MPI AM Implementation	77
20	Parallel MPI MA Implementation	78
21	Shifted Inverse Power method	82
22	Implementation of Components	102
23	The seed-GMRES algorithm	125
24	UCGLE for sequences of linear systems	131
25	Block Arnoldi Algorithm	138
26	Block GMRES Algorithm	139
27	Shifted Krylov-Schur Method	142
28	Least Square Polynomial Pre-treatment	144
29	Update BGMRES residual by LS Polynomial	144
30	s -KS Component	147
31	B-LSP Component	148

LIST OF ALGORITHMS

32	BGMRES Component	149
33	Manger of m -UCGLE with MPI Spawn	150

CHAPTER 1

Introduction

1.1 Motivations

The exascale era of HPC will come soon, and the first real exascale machine will be available around 2020, in which, the researchers hope to make unprecedented advancements in many fields of sciences and industries. In fact, the most powerful machines now have already over a million cores, and the HPC cluster systems will continue not only to scale up in compute node and Central Processing Unit (CPU) core count, but also the increase of components heterogeneity with the introduction of the Graphics Processing Unit (GPU) and other accelerators. This trend causes the transition to multi- and many cores inside of computing nodes which communicate explicitly through faster interconnection networks. These hierarchical supercomputers can be seen as the combination of distributed and parallel computing. Nevertheless, only a small number of applications may attain sustainable performances due to their lack of good scalability on large clusters.

Many scientific and industrial applications can be formulated as linear systems. A linear system can be described as a operation A , a input x and a output b . The linear solvers which aim to solve these systems, are the kernel of most simulation applications and softwares. When the operation matrix A is sparse, the collection of Krylov subspace methods, such as the Generalized minimal residual method (GMRES), the Conjugate Gradient (CG) and the Biconjugate Gradient Stabilized Method (BiCGSTAB), are well-known tools to solve the linear systems. Krylov subspace methods can approximate the exact solution of linear systems inside the Krylov subspace starting from a given initial guess vector.

Linear systems describe the real applications, such as the fusion operations, the earthquake and weather forecasting, etc., and their dimensions grow quickly (e.g. more than 10 billions unknowns for the earthquake simulation) with the increase of the complexity of applications. Krylov subspace methods should be deployed on the supercomputing platforms to solve such large-scale linear systems. Nowadays, with the increase of computing

unit number and the heterogeneity of supercomputers, the communication of overall reduction and global synchronization of Krylov subspace methods are a bottleneck, which damages heavily their parallel performance. In details, when solving a large-scale problem on parallel architectures by Krylov subspace methods, the cost per iteration of the method becomes the most significant concern, typically because of communication and synchronization overhead. Consequently, large scalar products, overall synchronization, and other operations involving communication among all cores have to be optimized. The numerical applications should be optimized for more local communication and less global communication. To benefit the full computational power of such hierarchical systems, it is central to explore novel parallel methods and models for the solving of linear systems. These methods should not only accelerate the convergence but also have the abilities to adapt to multi-grain, multi-level memory, to improve the fault tolerance, reduce synchronization and promote asynchronous.

1.2 Objectives and Core Contributions

The subject of this dissertation fits within this research context and it concerns on the propose and analyze a distributed and parallel programming paradigm for smart hybrid Krylov methods targetting at the exascale computing. The research relies on the Unite and Conquer approach proposed by Emad ([Emad and Petiton \[2016\]](#)). This approach is a model for the design of numerical methods by combining different computation components together to work for the same objective, with asynchronous communication among them. Unite implies the combination of different calculation components, and conquer represents different components work together to solve one problem. In the unite and conquer methods, different computation parallel components work independently with asynchronous communication. These different components can be deployed on different platforms such as P2P, cloud and the supercomputer systems, or on the same platform with different processors. The idea of unite and conquer approach came from the article of Saad ([Saad \[1984\]](#)) where he suggested using Chebyshev polynomial to accelerate the convergence of Explicitly Restarted Arnoldi Method (ERAM) to solve eigenvalue problems. The ingredients of this thesis to construct a Unite and Conquer linear solver come from the previous research of hybrid methods, e.g. a hybrid Chebyshev Krylov subspace algorithm proposed by Elman ([Elman et al. \[1986\]](#)), a hybrid GMRES algorithm via a Richardson iteration with Leja ordering ([Nachtigal et al. \[1992\]](#)), an approach for solving a system of linear equations which takes a combination of two arbitrary approximate solutions of two methods introduced by Brezinski ([Brezinski and Redivo-Zaglia \[1994\]](#)), and a hybrid gmres/ls-arnoldi method firstly introduced by Essai ([Essai et al. \[1999\]](#)).

Before the investigation on the Krylov subspace methods to solve linear systems, the first contribution of this work is to develop a Scalable Matrix Generator with Given

Spectrum (SMG2S), due to the importance of spectral distribution on the convergence of iterative methods. SMG2S allows generating very large dimension non-Hermitian matrices with user-customized eigenvalues. These matrices are also non-Hermitian and non-trivial, with very high dimension. In fact, recent research related to social networking, big data, machine learning and artificial intelligence has increased the necessity for non-hermitian solvers associated with much larger sparse matrices and graphs. Iterative linear algebra methods are the important parts of the overall computing time of applications in various fields since decades. The analysis of the iterative method behaviors for such problems is complex, and it is necessary to evaluate their convergence to solve extremely large non-Hermitian eigenvalue and linear problems on parallel and/or distributed machines. Since the convergence of iterative methods depends on the properties of spectra, it is necessary to generate large matrices with known spectra to benchmark them. The motivation to propose SMG2S is that it does not exist a collection of test matrices with very large dimension and different kinds of spectral properties to benchmark the linear solvers on supercomputers. SMG2S serves as a very useful tool during my thesis to study the numerical and parallel performance of new designed iterative methods.

After the implementation of SMG2S, the second contribution of my dissertation is to design and implement an asynchronous Unite and Conquer GMRES/LS-ERAM (UCGLE) based on the unite and conquer approach. UCGLE is proposed to solve large-scale linear systems with the reduction of global communications. This method consists of three computation components: ERAM Component, GMRES Component and LS (Least Squares) Component. GMRES Component is used to solve the systems, LS Component and ERAM Component serve as the preconditioning part. The key feature of this hybrid method is the asynchronous communication among these three components, which reduces the number of overall synchronization points and minimizes the global communication. There are three levels of parallelisms in UCGLE method to explore the hierarchical computing architectures. The convergence acceleration of UCGLE method is similar with a deflated preconditioner. The difference between them is that the improvement of the former one is intrinsic to the methods. It means that in the deflated preconditioning methods, for each time of preconditioning, the solving procedure should stop and wait for the temporary preconditioning procedure. Asynchronous communication of the latter can cover the synchronous communication overhead. Obviously, the asynchronous communication among the different computation components improves the fault tolerance and the reusability of this method. The three computation components work independently from each other, when errors occur inside of ERAM Component, GMRES Component or LS Component, UCGLE can continue to work as a normal restarted GMRES method to solve the problems. In fact, the materials for accelerating the convergence are the eigenvalues. With the help of asynchronous communication, we can select to save the computed eigenvalues by ERAM method into a local file and reuse it for the other solving procedures with the

same matrix, which can improve the reusability of linear solvers.

Moreover, both the mathematical model and the implementation of UCGLE are extended to solve a series of linear systems in sequence which share the same operator matrix A but have different Right-hand sides (RHSs) b in sequence. The eigenvalues obtained in solving previous linear systems by UCGLE can be recycled, improved on the fly and applied to construct a new initial guess vector for subsequent linear systems, which can achieve a continuous acceleration to solve linear systems in sequence. Numerical experiments using different test matrices to solve sequences of linear systems on supercomputers indicate a substantial decrease in both computation time and iteration steps when the approximate eigenvalues are recycled to generate the initial guess vectors.

Afterward, since many problems in the field of science and engineering often require to solve simultaneously large-scale non-Hermitian sparse linear systems with multiple RHSs, we develop an extension of UCGLE by combining it with Block GMRES method to solve non-Hermitian linear systems with multiple RHSs. This variant of UCGLE is implemented with novel components and manager engine. This novel engine is capable of allocating multiple Block GMRES at the same time, each Block GMRES solving the linear systems with a subset of RHSs and accelerating the convergence using the eigenvalues approximated by other eigensolvers. Dividing the entire linear system with multiple RHSs into subsets and solving them simultaneously with different allocated linear solvers allow localizing calculations, reducing global communication, and improving parallel performance. Meanwhile, the asynchronous preconditioning using eigenvalues is able to speed up the convergence and improve the fault tolerance and reusability. Numerical experiments using different test matrices on supercomputers indicate that the proposed method achieves a substantial decrease in both computation time and iterative steps with good scaling performance.

Eventually, an adaptive UCGLE is proposed which gives the scheme of auto-tuning the complex parameters inside which have the influence on its numerical and parallel performance. This work was achieved by analyzing the impacts of different parameters on the convergence.

1.3 Outline

The dissertation is organized as follows. In Chapter 2, we will give the state-of-the-art of HPC, including the modern computing architectures for supercomputers (e.g. CPU, Nvidia GPGPU and Intel Many Integrated Cores) and the parallel programming model (including OpenMP, CUDA, MPI, PGAS, the task/graph based programming, etc.). Finally, in this chapter, we will talk about the current challenges of HPC facing the coming of exascale supercomputers.

Chapter 3 covers the existing iterative methods for solving linear systems and eigen-

value problems, especially the Krylov Subspace methods. Firstly, this chapter gives a brief introduction of the stationary and non-stationary iterative methods. Then different Krylov Subspace methods will be presented and compared. Apart from the basic introduction of methods, different preconditioners used to accelerate the convergence will be discussed, especially a Least Squares Polynomial method which is used to construct UCGLE, will be introduced in details. The relation between the convergence of Krylov subspace methods for solving linear systems and the spectral distribution of operator matrix A will also be analyzed in this chapter. Finally, we give a bref introduction of the parallel implementation of the Krylov subspace methods on modern distributed memory systems, then discuss the challenges of iterative methods facing on the coming of exascale platforms, and then summerize the recent efforts to adapt the numerical methods to the much larger clusters/supercomputers.

In Chapter 4, we present the parallel implementation and numerical performance evaluation of SMG2S. SMG2S is able to generate large-scale non-Hermitian test matrices using the user-defined spectrum and ensuring their eigenvalues as the given ones with high accuracy. It is implemented on CPUs and multi-GPU platforms with specific optimized communications. Good strong and weak scaling performance is obtained on several supercomputers. We also propose a method to verify its ability to guarantee the given spectra base on the shift inverse power method. SMG2S is a released open source software which is developed using MPI and C++11. In this chapter, we will analyze the parallel and numerical performance of SMG2S on several supercomputers. Finally, the packaging, the interfaces to other programming laguanges and scientific softwares, and the graphic user interface for verification are introduced in this chapter.

In Chapter 5, the implementation of UCGLE based on the scientific libraries PETSc and SLEPc for both CPUs and GPUs are presented. In this chapter, we describe the implementation of components, the manager engine, and the distributed and parallel asynchronous communications. After the implementation, the selected parameters, the convergence, scalability and fault tolerance are evaluated on several supercomputers.

Chapter 6 presents the extension of UCGLE to solve linear systems in sequence with different RHSs by recycling the eigenvalues. Firstly, we give a survey of existing algorithms, including the seed and deflated methods, and then develop the mathematical model and manager engine of UCGLE to solve linear systems in sequence. The experimental results of the evaluation on different supercomputers are also shown in this chapter.

The variant of UCGLE to solve simultaneously linear systems with multiple RHSs is presented in Chapter 7. Firstly, this chapter introduces the existing block methods to solve linear systems with multiple RHSs, and then analyzes the limitations of block methods on large-scale platforms. Then mathematical extension of Least Squares polynomial for multiple RHSs is given, and then the implementation of the special novel manager engine using MPI Spawn is presented. This engine allows allocating multiple GMRES and ERAM

Components at the same time. This special version of UCGLE is implemented with the block GMRES provided by the Belos package of Trilinos. Finally, we give the experimental results on large-scale machines.

UCGLE is a hybrid method with the combination of three different numerical methods. Thus the autotuning of different parameters is very important. In Chapter 8, we propose the strategy of autotuning for several parameters. (to be developed)

All unite and conquer methods including UCGLE, are able to implement using the workflow/task based environments to manager the fault tolerance, load balance, asynchronous communications of signals, arrays and vectors and the management of different computing units such as GPUs. In Chapter 9, we give a glance at the YML framework, and then analyze the workflow of UCGLE methods and the limitations of YML for UC approach. Then we propose the solutions of Grammar and implementation for YML, including the dynamic graphic grammar, the mechanism of exiting parallel branch, and the check-pointing mechanism to manager the fault tolerance of applications.

In Chapter 10, we summarize the key results obtained in this thesis and present our concluding remarks. Finally, we suggest some possible paths to future research.

CHAPTER 2

State-of-the-art in High-Performance Computing

High-Performance Computing (HPC) most generally refers to the practice of aggregating computing power in a way that delivers much higher performance than one could get out of a typical desktop computer or workstation in order to solve large problems in science, engineering, or business. HPC is one of the most active research areas in Computer Science because it is strategically important to solve the very large challenge problems arising from scientific and industrial applications. The development of HPC relies on the efforts from multi-disciplines, including the computer architecture design, the parallel algorithms, and programming models, etc. This chapter gives the state-of-the-art in HPC: its history of evaluation, modern computing architectures, and parallel programming models. Finally, we discuss the critical challenges to the whole HPC community with the coming of exascale supercomputers in Section 2.4.

2.1 Evaluation of HPC

The terms *high-performance computing* and *supercomputing* are sometimes used interchangeably. HPC technology is implemented in a wide range of computationally intensive applications in multidisciplinary areas including biosciences, geographical data, electronic design, climate research, neuroscience, quantum mechanics, molecular modeling, nuclear fusion, etc. Supercomputers were introduced in the 1960s, and the performance of a supercomputer is measured in floating-point operations per second (FLOPS). Since the first generation of supercomputers, the *megascale* performance was reached in the 1970s, and the *gigascale* performance was passed in less than ten years. Finally, the *terascale* performance was achieved in the 1990s, and then the *petascale* performance was crossed in 2008

with the installation IBM Roadrunner at Los Alamos National Laboratory in the United States. Fig. 2.1 shows the Top 1 supercomputer’s performance by year since 1960s.

Since 1993, the TOP500 project¹ ranks and details the 500 most powerful supercomputing systems in the world and publishes an updated list of the supercomputers twice a year. The project aims to provide a reliable basis for tracking and detecting trends in high-performance computing and bases rankings on HPL, a portable implementation of the high-performance LINPACK benchmark written in Fortran for distributed-memory computers. According to the newest Top500 list of November 2018, the fastest supercomputer is the Summit of the United States, which has a LINPACK benchmark score of 122.3 PFLOPS. The Sunway TaihuLight, Sierra and Tianhe-2A follow closely the Summit, with the performance respectively 93 PFLOPS, 71.6 PFLOPS, and 61.4 PFLOPS.

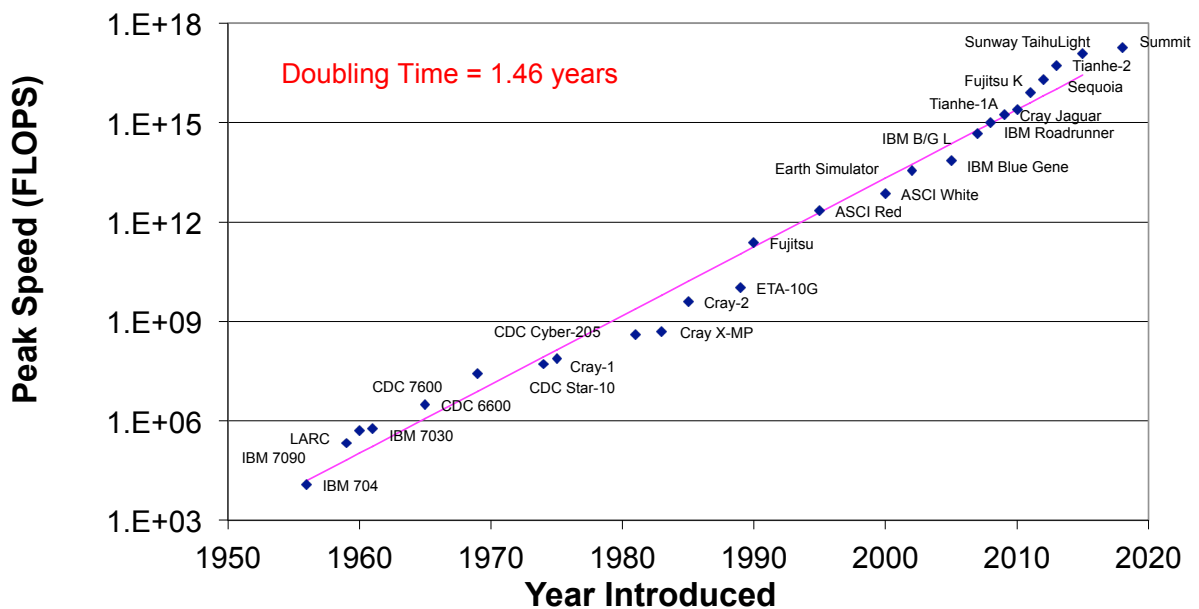


Figure 2.1 – Top 1 Supercomputers’ Performance by Year.

The next barrier for the HPC community to overcome is the *exascale* computing, which refers to the computing systems capable of at least one exaFLOPS (10^{18} floating point operations per second). This capacity represents a thousandfold increase over the first petascale computer which came into operation in 2008. The world first exascale supercomputer will come around 2020. China’s first exascale supercomputer will enter service by 2020 according to the head of the school of computing at the National University of Defense Technology (NUDT). United States’s first exascale computer is planned to be built by 2021 at Argonne National Laboratory. The post-K announced by Japan will start the public service around 2021, and the first exascale supercomputer in Europe will appear around 2022. Exascale computing would be considered as a significant achievement in computer engineering, for it is estimated to be the order of processing power of the human brain at the neural level.

1. <https://www.top500.org>

Considering the evaluation of HPC, there are always two questions proposed to the users who want to develop the applications on supercomputers:

- How to build such powerful supercomputers?
- How to develop the applications to profit efficiently the total computational capacity of supercomputers?

In order to answer these two questions above, firstly, Section 2.2 gives a glance at the modern computing architectures to build the supercomputers. Then different parallel programming models to develop the applications on the supercomputers are given in Section 2.3.

2.2 Modern Computing Architectures

Different architectures of computing units are designed to build the supercomputers. In this section, the state-of-the-art of modern CPUs and accelerators are reviewed.

2.2.1 CPU Architectures and Memory Access

The development of modern CPUs is based on the *Von Neumann architecture*. This proposition of this computer architecture is based on the description by the mathematician and physicist *John von Neumann* and others in the *First Draft of a Report on the EDVAC* ([Von Neumann \[1945\]](#)). All the modern computing units are all evolved from this concept, which consists of five parts:

- A *processing unit* that contains an arithmetic logic unit and processor registers;
- A *control unit* that contains an instruction register and program counter;
- *Memory* that stores data and instructions;
- External mass *storage*;
- *Input/output* mechanisms.

As shown in Fig. 2.2a, the *Von Neumann architecture* uses the shared bus between the program memory and data memory, which leads to its bottleneck. Since the single bus can only access one of the two types of memory at a time, the data transfer rate between the CPU and memory is rather low. With the increase of CPU speed and memory size, the bottleneck has become more of a problem.

The *Harvard architecture* is another computer architecture with physically separate the storage and bus for the instructions and data. As shown in Fig. 2.2b, the limitation of a

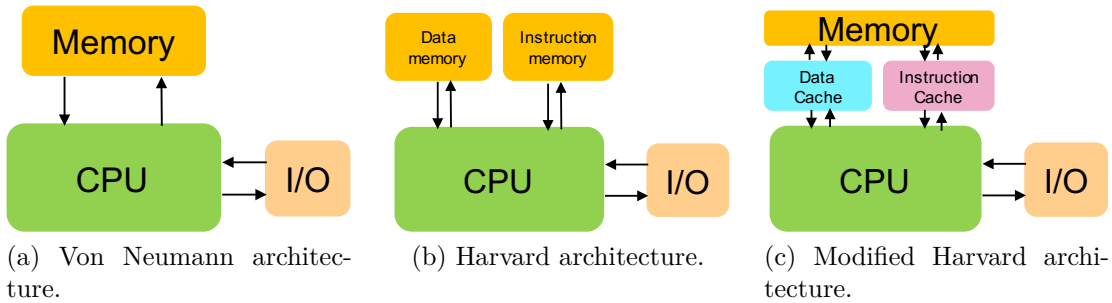


Figure 2.2 – Computer architectures.

pure Harvard architecture is that the mechanisms must be provided to load the program to be executed into instruction memory separately and any data to be operated upon input memory. Additionally, read-only technology for the instruction memory allows the computer to begin execution of a pre-loaded program as soon as power is applied. The data memory will at this time be in an unknown state, so it is not possible to provide any kind of pre-defined data values to the program.

Today, most processors implement the separate pathways as *Harvard architecture* to support the higher performance concurrent data and instruction access, meanwhile loosen the strictly separated storage between code and data. That is named as the *Modified Harvard architecture* (shown as Fig. 2.2c). This model can be seen as the combination of the *Von Neumann architecture* and *Harvard architecture*.

The solution is to provide a hardware pathway and machine language instructions so that the contents of the instruction memory can be read as if they were data. Initial data values can then be copied from the instruction memory into data memory when the program starts. If the data is not to be modified, it can be accessed by the running program directly from instruction memory without taking up space in the data memory.

Nowadays, most CPUs have Von Neumann like unified address space and also separate instruction and data caches as well as memory protection, making them more Harvard-like, and so they could be classified more as *modified Harvard architecture* even using unified address space.

The most common modification on *modified Harvard architecture* for modern CPUs is to build a memory hierarchy with a CPU cache separating instructions and data based on response time. As shown in Fig. 2.3, the top of the memory hierarchy which provides the fastest data transfer rate are the registers. Target data with arithmetic and logic operations will be temporarily held in the register to perform the computations. The number of registers is limited due to the cost. A CPU cache is a hardware cache used by CPU to reduce the average cost (time or energy) to access data from the main memory. A cache is a smaller, faster memory, closer to a processor core, which stores copies of the data from frequently used main memory locations. Most CPUs have different independent

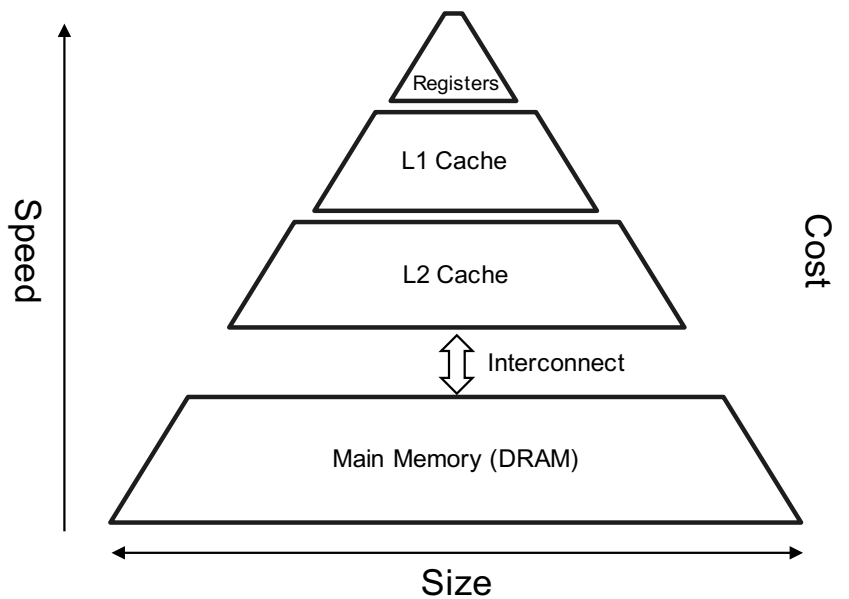


Figure 2.3 – Memory Hierarchy.

caches, including instruction and data caches, where the data cache is usually organized as a hierarchy of more cache levels. The lowest level is the main memory, which is made of Dynamic Random-Access Memory (DRAM) with the lowest bandwidth and the highest latency compared to registers and caches.

2.2.2 Parallel Computer Memory Architectures

The parallel computer memory architectures can be divided into shared and distributed memory types. The shared memory parallel computers vary widely, but generally have in common the ability for all processors to access all memory as global address space. Multiple processors can operate independently but share the same memory resources. Changes in a memory location effected by one processor are visible to all other processors. Historically, shared memory machines have been classified as *Uniform Memory Access (UMA)* (shown as 2.4a) and *Non-Uniform Memory Access (NUMA)* (shown as 2.4b), based upon memory access times. UMA is most commonly represented today by Symmetric Multiprocessor (SMP) machines with Identical processors. These processors require equal access and access times to memory. NUMA is often made by physically linking two or more SMPs, one SMP can directly access memory of another SMP. Not all processors have equal access time to all memories, memory access across link is slower. The advantages of shared memory architectures are: 1) Global address space provides a user-friendly programming perspective to memory; 2) Data sharing between tasks is both fast and uniform due to the proximity of memory to CPUs. The disadvantages are: 1) the lack of scalability between memory and CPUs, in fact, adding more CPUs can geometrically increase traffic on the

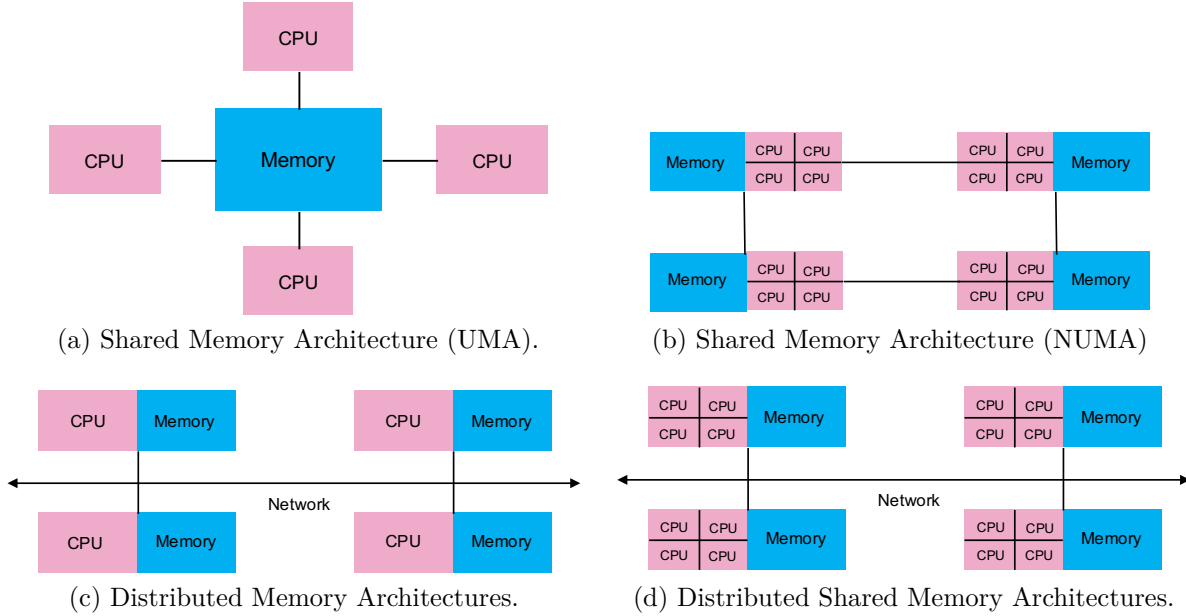


Figure 2.4 – Parallel Computer Memory Architectures.

shared memory-CPU path, and for cache coherent systems, geometrically increase traffic associated with cache/memory management; 2) Programmer responsibility for synchronization constructs that ensure "correct" access of global memory. There is no way we can reach the hundreds of thousands of CPU-cores we need for today's multi-petaflop supercomputers.

Then the distributed-memory architecture is proposed, which takes many multicore computers and connects them together using a network, much like workers in different offices communicating by telephone. With a sufficiently fast network we can in principle extend this approach to millions of CPU-cores and beyond. As shown in Fig. 2.4c, inside distributed memory system, processors have their own local memory. Memory addresses in one processor do not map to another processor, so there is no concept of global address space across all processors. Because each processor has its own local memory, it operates independently. Changes it makes to its local memory have no effect on the memory of other processors. Hence, the concept of cache coherency does not apply. When a processor needs access to data in another processor, it is usually the task of the programmer to explicitly define how and when data is communicated. Synchronization between tasks is likewise the programmer's responsibility. The advantages of distributed memory architecture are: 1) Memory is scalable with the number of processors. Increase the number of processors and the size of memory increases proportionately; 2) Each processor can rapidly access its own memory without interference and without the overhead incurred with trying to maintain global cache coherency; 3) Cost effectiveness. The disadvantages are: 1) the programmer is responsible for many of the details associated with data communication between processors; 2) It may be difficult to map existing data structures, based on global memory, to this memory organization; 3) Non-uniform memory access times - data residing

on a remote node takes longer to access than node local data.

Nowadays, the largest and fastest computers in the world employ both shared and distributed memory architectures (shown as Fig. 2.4d). The shared memory component can be a shared memory machine and/or graphics processing units (GPU). The distributed memory component is the networking of multiple shared memory/GPU machines, which know only about their own memory - not the memory on another machine. Therefore, network communications are required to move data from one machine to another. Current trends seem to indicate that this type of memory architecture will continue to prevail and increase at the high end of computing for the foreseeable future.

In a word, shared-memory systems are difficult to build but easy to use, and are ideal for laptops and desktops. Distributed-shared memory systems are easier to build but harder to use, comprising many shared-memory nodes with their own separate memory. Distributed-shared memory systems introduce much more hierarchical memory and computing with multi-level of parallelism. The important advantage of distributed-shared memory architectures is increasing scalability, and the important disadvantage is increasing the complexity to program.

2.2.3 Nvidia's GPGPU

General-purpose computing on graphics processing units (GPGPU, rarely GPGP) is the use of a graphics processing unit (GPU), which typically handles computation only for computer graphics, to perform computation in applications traditionally handled by the central processing unit (CPU). GPU was first introduced as a specialized electronic circuit designed to rapidly manipulate and alter memory to accelerate the creation of images in a frame buffer intended for output to a display device. Modern GPUs are very efficient at manipulating computer graphics and image processing. Due to its special functionality, GPGPU serves as an accelerator of CPU to improve the overall performance of computers. Nowadays, it is becoming increasingly common to use GPGPU to build the supercomputers. Until now, 5 of top 10 supercomputers in the world use GPGPU.

As shown in Figure 2.5, the architectures of CPU and GPU are different: the CPU has a small number of complex cores and massive caches while the GPU has thousands of simple cores and small caches. The massive Arithmetic Logic Units (ALUs) of GPU are simple, data-parallel, multi-threaded which offer high computing power and large memory bandwidth. In brief, graphics chips are designed for parallel computations with lots of arithmetic operations, and CPUs are for general complex applications. The host character of the CPU requires complicated cores and deep pipelines to deal with all kinds of operations. It usually runs at a higher frequency and supports branch prediction. The GPU only focuses on data-parallel image renderings thus the pipeline is shallow. The same instructions are used on large datasets in parallel with thousands of hardware cores, so



Figure 2.5 – CPU vs GPU.

the branch prediction is not necessary, and memory access latency is hidden by important arithmetic operations instead of caching. GPGPU is also regarded as a powerful backup to overcome the *power wall*.

Introduced in mid-2017, the newest Tesla V100 card can deliver 7.8 TFLOPS in double-precision floating point and 15.7 TFLOPS for single-precision.

2.2.4 Intel's Many Integrated Cores

The performance improvement of processors comes from the increasing number of computing units within the small chip area. Thanks to advanced semiconductor processes, more transistors can be built in one shared-memory system to do multiple things at once: from the view of programmers, this can be realized in two ways: different data or tasks execute in multiple individual computing units (multi-thread) or long uniform instruction decoders (vectorization).

Intel officially first revealed the latest MIC codenamed Knights Landing (KNL) in 2013. Being available as a coprocessor like previous boards, KNL can also serve as a self-boot MIC processor that is binary compatible with standard CPUs and boot standard OS. These second generation chips could be used as a standalone CPU, rather than just as an add-in card. Another key feature is the on-card high-bandwidth memory (HBM) which provides high bandwidth and large capacity to run large HPC workloads. Memory bandwidth is one of the common performance bottlenecks for computational applications due to the memory wall. KNL implements a two-level memory system to address this issue. It shares application areas with GPUs. The main difference between Xeon Phi and a GPGPU like Nvidia Tesla is that Xeon Phi, with an x86-compatible core, can, with less modification, run software that was originally targeted at a standard x86 CPU.

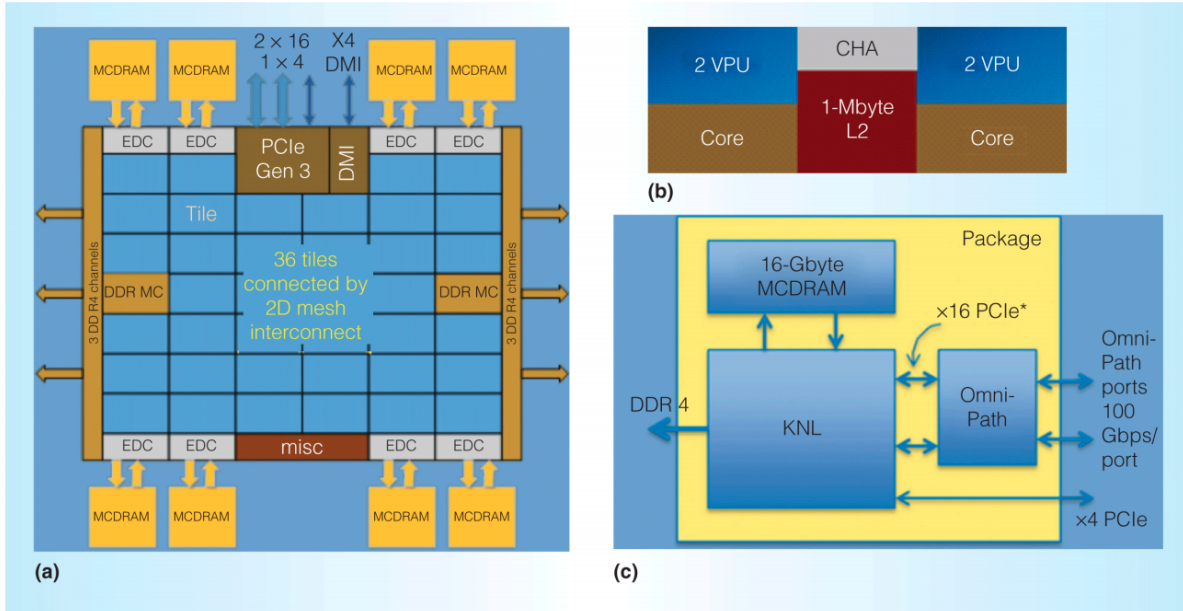


Figure 2.6 – The organization of a Knights Landing processor.

2.2.5 RISC-based (Co)processors

A reduced instruction set computer, or RISC is such a computer has a small set of simple and general instructions, rather than a large set of complex and specialized instructions. A type of well-known RISC-based computing units are the ARM architecture processors. In the 21st century, the use of in smartphones and tablet computers such as the iPad and Android devices provided a wide user base for RISC-based systems. Since the introduction of Sunway TaihuLight², RISC processors are also used in supercomputers. RISC based supercomputers enable low energy consumption per core, less silicon and cheaper chips, since they do not contain complex instruction sets. In this section, we list two types of RISC based processors used on the supercomputers.

The first type of processor is sw26010, which is a 260-core manycore processor ([Fu et al. \[2016\]](#)) designed by the National High-Performance Integrated Circuit Design Center in Shanghai. It implements the Sunway architecture, a 64-bit RISC architecture designed by China. As shown in Fig. 2.7, the sw26010 has four clusters of 64 Compute-Processing Elements (CPEs) which are arranged in an eight-by-eight array. The CPEs support SIMD instructions and are capable of performing eight double-precision floating-point operations per cycle. Each cluster is accompanied by a more conventional general-purpose core called the Management Processing Element (MPE) that provides supervisory functions. Each cluster has its own dedicated DDR3 SDRAM controller and a memory bank with its own address space. The processor runs at a clock speed of 1.45.

Matrix-2000 ([WikiChips \[2017\]](#)) is a 64-bit 128-core many-core processor designed by NUDT and introduced in 2017. This chip was designed exclusively as an accelerator for

2. <http://www.nsccwx.cn/>

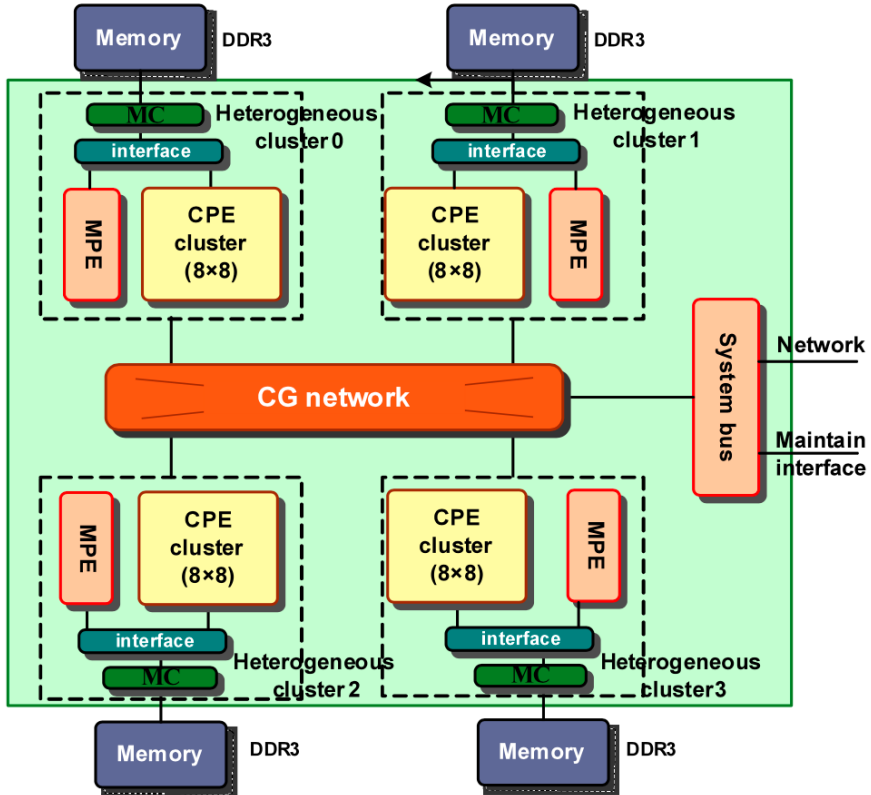


Figure 2.7 – The organization of a SW26010 manycores processor.

China's Tianhe-2A supercomputer installed in the National Supercomputing Center in Guangzhou³ in order to upgrade and replace the aging Intel's Knights Corner accelerators. The Matrix-2000 features 128 RISC cores operating at 1.2 GHz achieving 2.46/4.92 TFLOPS (DP/SP) with a peak power dissipation of 240W. The Matrix-2000 consists of 128 cores, eight DDR4 memory channels, and x16 PCIe lanes. The chip consists of four supernodes (SN) consisting of 32 cores each operating at 1.2 GHz with a peak power dissipation of 240 Watts.

2.2.6 FPGA

Field-programmable gate array (FPGA) is an integrated circuit designed to be configured: an array of programmable logic blocks and reconfigurable interconnects. The FPGA architecture provides the flexibility to create a massive array of application-specified ALUs that enable both instruction and data-level parallelism. FPGA has very high energy efficiency because it requires the low frequency and unused computing blocks do not consume energy. FPGAs can serve as accelerators on the supercomputers, e.g. Paderborn Center for Parallel Computing⁴ installed several prototype hybrid machines by combining FPGAs with intel Xeon CPUs. FPGAs are by no means anything new in the HPC sector –

3. <http://www.nscc-gz.cn>

4. <https://pc2.uni-paderborn.de>

ten years ago they were all the rage but proved very difficult to program, and now they are coming back in vogue as it gets easier to C, C++, and Fortran applications to these devices.

2.3 Parallel Programming Model

After the introduction of hardware architectures, this section presents the different levels of parallel programming models to develop applications on supercomputers. Most of modern supercomputers are of distributed-shared memory architecture, which introduces multi-level parallel programming models, including the shared memory/thread level parallelism models, the distributed memory/process level parallelism models, the Partitioned Global Address Space (PGAS) models and the task/workflow based parallel models.

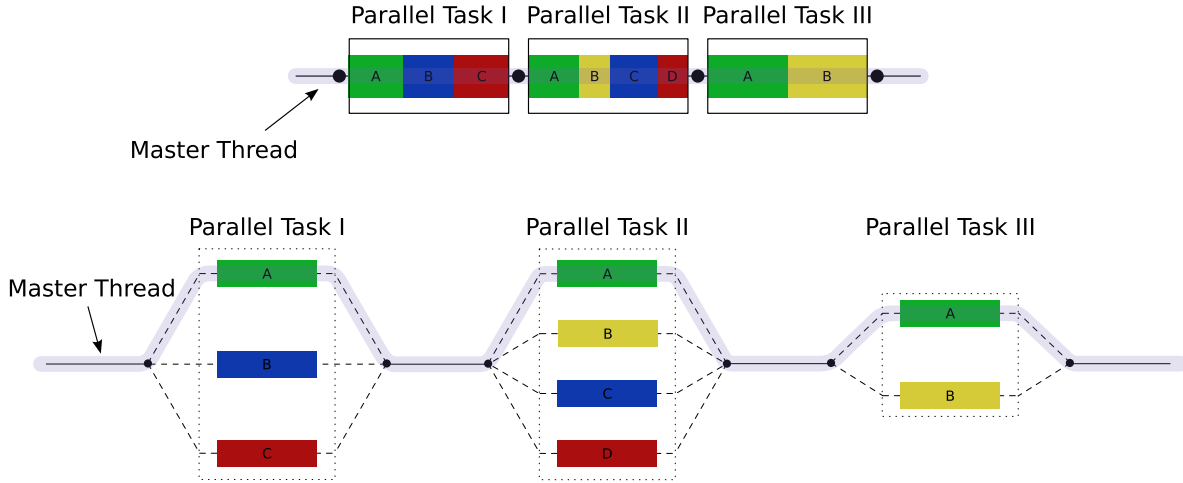
2.3.1 Shared Memory Level Parallelism

In this section, we introduce various runtimes developed to support the shared memory level parallelism of different computing architectures.

2.3.1.1 OpenMP

OpenMP (Open Multi-Processing) ([Dagum and Menon \[1998\]](#)) is an application programming interface (API) that supports multi-platform shared memory parallel programming in C, C++, and Fortran. OpenMP supports most platforms, instruction set architectures, and operating systems. It consists of a set of compiler directives, library routines, and environment variables. OpenMP provides the capability to incrementally parallelize a serial program with by inserting the specific directives. These directives can be ignored by the compiler, and the application can be executed in a sequential way when target machines do not support OpenMP. OpenMP is designed for multi-processor/core, shared memory machines. The underlying architecture can be shared memory UMA or NUMA. OpenMP programs accomplish parallelism exclusively through the use of threads.

As shown in Fig. 2.8, OpenMP uses the **fork-join** model to support parallel execution. All OpenMP programs begin with a single process which executes until the first parallel region construct is encountered. Then this thread creates a team of parallel threads and distributes the workload to them in order to have them work simultaneously. When the team threads complete the statements in the parallel region construct, they synchronize and terminate, leaving only the master thread. The new released OpenMP begins to support task scheduling strategies, the SIMD directives for high-level vectorization and the *offload* directives for heterogeneous systems.


 Figure 2.8 – OpenMP **fork-join** Model.

2.3.1.2 CUDA

CUDA (Compute Unified Device Architecture) ([Nvidia \[2011\]](#)) is a parallel programming platform and application programming interface model created by Nvidia. It allows software developers and software engineers to use a CUDA-enabled GPU for general purpose processing. The CUDA software layer gives direct access to GPU's virtual instruction set de parallel computational elements, for the execution of compute kernels. The CUDA platform is designed to work with programming languages such as C, C++, and Fortran. This accessibility makes it easier for specialists in parallel programming to use GPU resources. Fig. 2.9 gives the four steps processing flow on CUDA:

1. Copy the processing data from main memory to memory for GPU;
2. Load the executable from CPU to GPUs;
3. Execute parallel the operations in each core;
4. Copy back the results from memory for GPU to the main memory.

CUDA supports programming frameworks such as OpenACC ([Wienke et al. \[2012\]](#)) and OpenCL ([Munshi \[2009\]](#)).

2.3.1.3 Others

OpenCL (Open Computing Language) is a framework for writing programs that execute across heterogeneous platforms consisting of CPUs, GPUs, DSPs, FPGAs and other processors or hardware accelerators. OpenCL specifies programming languages (based on C99 and C++11) for programming these devices and application programming interfaces (APIs) to control the platform and execute programs on the compute devices. OpenCL

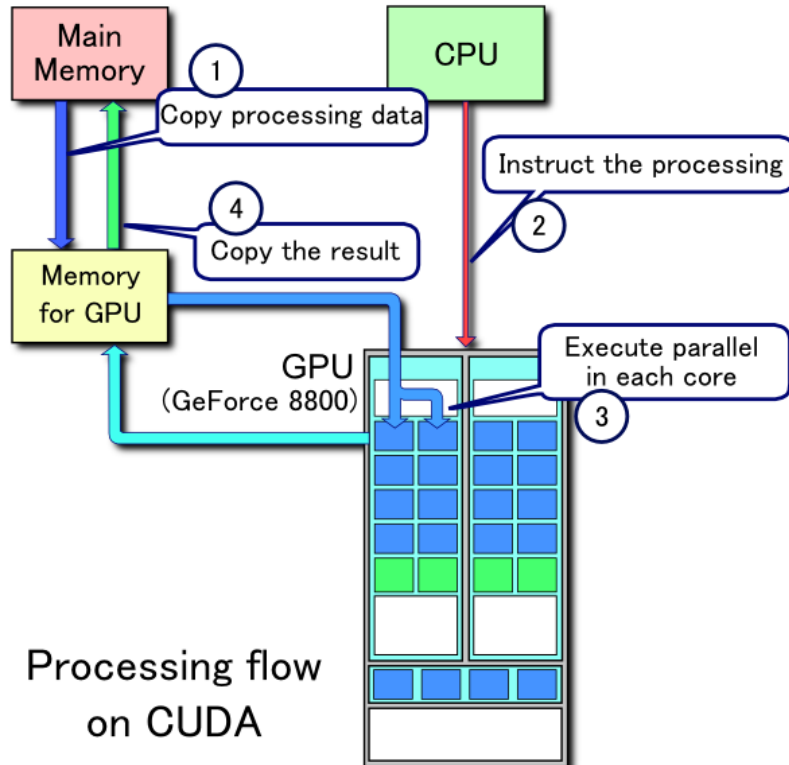


Figure 2.9 – Processing flow on CUDA.

provides a standard interface for parallel computing using task- and data-based parallelism.

OpenACC (for open accelerators) is a programming standard for parallel computing developed by Cray, CAPS, Nvidia and PGI. The standard is designed to simplify parallel programming of heterogeneous CPU/GPU systems. As in OpenMP, the programmer can annotate C, C++ and Fortran source code to identify the areas that should be accelerated using compiler directives and additional functions. Like OpenMP 4.0 and newer, OpenACC can target both the CPU and GPU architectures and launch computational code on them.

Kokkos ([Edwards et al. \[2014\]](#)) core implements a programming model in C++ for writing performance portable applications targeting all major HPC platforms. For that purpose, it provides abstractions for both parallel executions of code and data management. Kokkos is designed to target complex node architectures with N-level memory hierarchies and multiple types of execution resources. It currently can use OpenMP, Pthreads, and CUDA as backend programming models.

2.3.2 Distributed Memory Level Parallelism

In the distributed memory platforms, each processor owns a private memory which is not reachable from other processor. The only way for processors to exchange data is to use explicit communication by sending messages.

2.3.2.1 Message Passing Interface

MPI (Message Passing Interface) ([Gropp et al. \[1999\]](#)) is a standardized and portable message-passing standard designed by a group of researchers from academia and industry to support a wide variety of parallel computing architectures. MPI provides a simple-to-use portable interface for the basic user, yet one powerful enough to allow programmers to use the high-performance message passing operations available on advanced machines. Most MPI implementations consist of a specific set of routines directly callable from C, C++, Fortran and any language able to interface with such libraries. The MPI interface is meant to provide essential virtual topology, synchronization, and communication functionality between a set of processes (that have been mapped to nodes/servers/computer instances) in a language-independent way, with language-specific syntax (bindings), plus a few language-specific features.

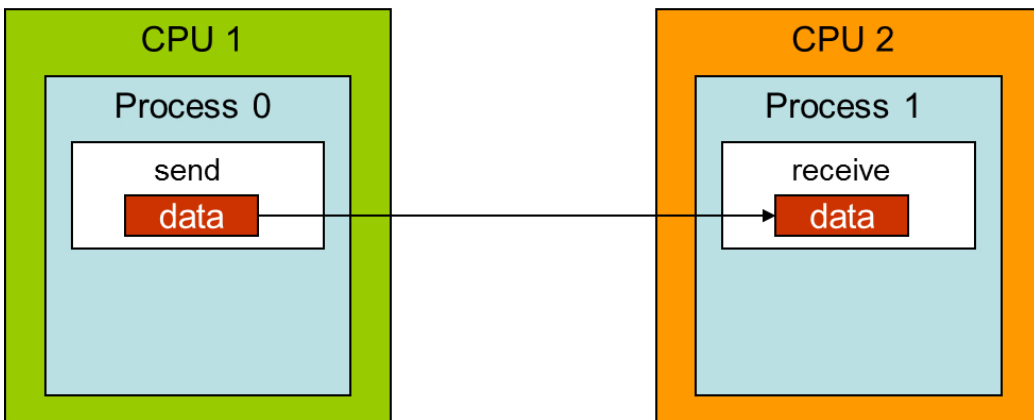


Figure 2.10 – MPI send and receive Model.

MPI library functions include, but are not limited to, basic point-to-point send/receive operations, collective functions involving communication among all processes, synchronizing nodes (barrier operation), the one-sided communication, dynamic process management, I/O and so on. Point-to-point operations support both the communication in both synchronous and asynchronous ways. In modern computing platform with multiple shared-memory nodes, the shared memory programming models such as OpenMP and message passing programming such as MPI can be considered as complementary programming approaches, and can occasionally be used together in a hybrid way.

2.3.3 Partitioned Global Address Space

In computer science, a partitioned global address space (PGAS) is a parallel programming model. It assumes a global memory address space that is logically partitioned and a portion of it is local to each process, thread, or processing element. The novelty of PGAS is that the portions of the shared memory space may have an affinity for a particular process, thereby exploiting locality of reference. There are different implementation based

on PGAS model, such as Unified Parallel C, Coarray Fortran, Split-C, Chapel, X10, UPC++, DASH, XcalableMP, etc. PGAS attempts to combine the advantages of an SPMD programming style for distributed memory systems (as employed by MPI) with the data referencing semantics of shared memory systems. This is more realistic than the traditional shared memory approach of one flat address space because hardware-specific data locality can be modeled in the partitioning of the address space.

2.3.3.1 XcalableMP

XcalableMP ([Lee and Sato \[2010\]](#)) is a language extension of C and Fortran for parallel programming on distributed memory systems that help users to reduce those programming efforts. XcalableMP provides two programming models. The first one is the global view model, which supports typical parallelization based on the data and task parallel paradigm, and enables parallelizing the original sequential code using minimal modification with simple, OpenMP-like directives. The other one is the local view model, which allows using CAF-like expressions to describe inter-node communication. Users can even use MPI and OpenMP explicitly in the XMP language to optimize performance explicitly.

2.3.4 Task/Graph Based Parallel Programming

With the increase of the complexity of applications on the supercomputers, it is more and more difficult for the developers to maintain the parallel codes on the modern computing architectures. The task/graph based parallel programming models are proposed to express the task parallelism and data dependencies of complex codes. In fact, an application can be divided temporally and spatially into inter-dependent tasks of different natures. A good runtime scheduler can manage the complex tasks efficiently across a large number of cores on the supercomputing systems. In this section, we list several well-known task/graph based parallel programming models.

2.3.4.1 YML

YML ([Delannoy \[2008\]](#)) allows you to transparently use one or more grid middleware to run an application. For this, the project is based on a dedicated language named YvetteML. YML can describe a complex parallel application regardless of the execution platform. The YvetteML language is used to express the task graph of the application. The nodes of the graph are the tasks described by components, and the edges correspond to dependencies or communications. The components are written in XML. Each component implementation can contain C++, XMP-C, XMP-FORTRAN or other code. Each component implementation can be expressed with finer grain parallelism. YML will be discussed in details in Chapter [9](#).

2.3.4.2 StarPU

StarPU⁵ ([Augonnet et al. \[2011\]](#)) is a task programming library for hybrid architectures. The application provides algorithms and constraints both the CPU/GPU implementations of tasks and the graphs of tasks, using either the StarPU’s high-level GCC plugin pragmas, StarPU’s rich C/C++ API, or OpenMP pragmas. StarPU handles run-time concerns: the task dependencies, the optimized heterogeneous scheduling, the optimized data transfers/replication between main memory and discrete memories and optimized cluster communications.

2.3.4.3 Swift

Swift⁶ ([Wilde et al. \[2011\]](#)) is a data-flow oriented coarse-grained scripting language that supports dataset typing and mapping, dataset iteration, conditional branching, and procedural composition. Swift programs (or workflows) are written in a language called Swift. Swift scripts are primarily concerned with processing (possibly large) collections of data files, by invoking programs to do that processing. Swift handles execution of such programs on remote sites by choosing sites, handling the staging of input and output files to and from the chosen sites and remote execution of programs.

2.3.4.4 Legion

Legion⁷ ([Grimshaw et al. \[1994\]](#)) is a data-centric parallel programming system for writing portable high performance programs targeted at distributed heterogeneous architectures. Legion presents abstractions which allow programmers to describe properties of program data (e.g., independence, locality). By making the Legion programming system aware of the structure of program data, it can automate many of the tedious tasks programmers currently face, including correctly extracting task- and data-level parallelism and moving data around complex memory hierarchies. A novel mapping interface provides explicit programmer controlled placement of data in the memory hierarchy and assignment of tasks to processors in a way that is orthogonal to correctness, thereby enabling easy porting and tuning of Legion applications to new architectures.

2.4 Exascale Challenges of Supercomputers

The exascale computing era is computing, in this section, we analyze the trends of the increase of heterogeneity for modern supercomputers, and then summarize the challenges of parallel programming for exascale systems.

5. <http://starpu.gforge.inria.fr>

6. <http://swift-lang.org/main/index.php>

7. <http://legion.stanford.edu>

2.4.1 Increase of Heterogeneity for Supercomputers

Hardware architectures have great impacts on the evolution of supercomputers. At the early age, the processor performance improves mainly by increasing the number of transistors per integrated circuit. According to Moore's law, the number of transistors per integrated circuit doubles every 18 months, which means that the size of the transistor is reduced to half, which allows achieving faster clock rate. Moore's law is found to be acceptable until 2002. Since then, the overheating introduced by higher frequency reaches the limit of air cooling. This is the famous *power wall*. Since then, the modern computing architectures with multiple processors on-chip, lower operating frequency and hierarchical architectures come, including the GPGPU, intel MIC, the many-core sw26010, and Matrix-2000 GPDSP. Moreover, Europe (Mont-Blanc (Rajovic et al. [2016]), CEA and Atos (Feldman [2018a])) and Japan (RIKEN and Fujitsu) (Feldman [2018b]) are now pushing the development of ARM supercomputers. Fig. 2.11 shows the trends of supercomputers equipped with accelerators by year. According to the Top 500 list of November 2018, 137 systems out of 500 use accelerator or co-processor technology.

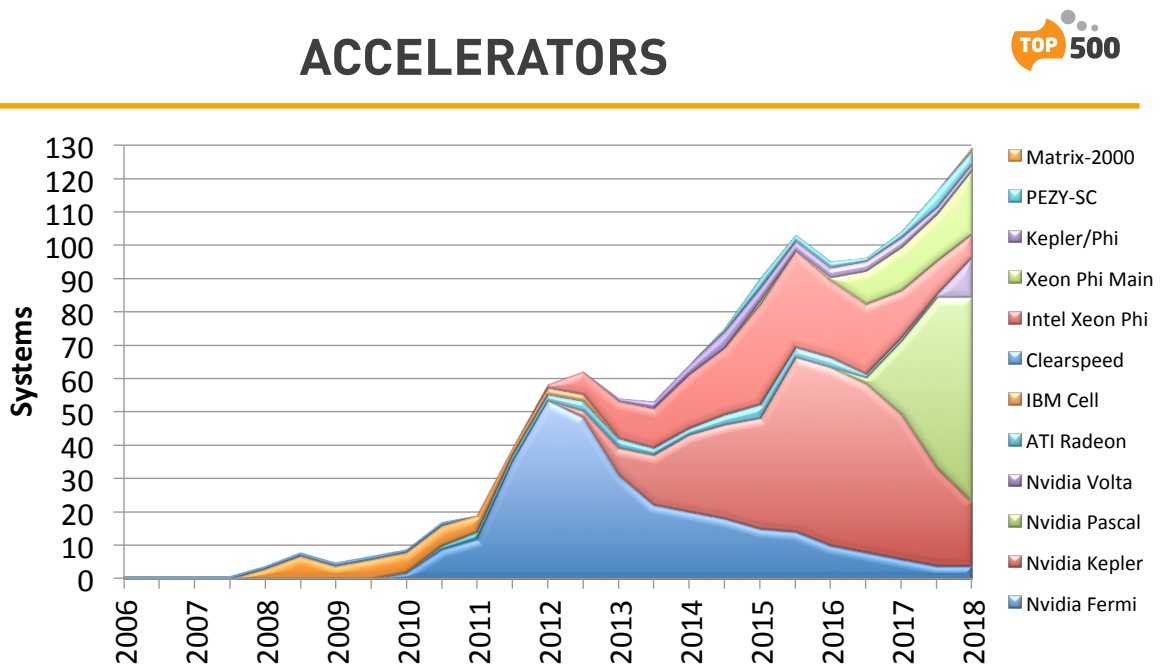


Figure 2.11 – Number of systems each year boosted by accelerators.

Compared with the traditional computing architectures such as Intel, AMD CPUs which dedicate to multiple different purpose that result in bad energy efficiency in HPC, the introduction of low frequency and/or less complex architecture improve the energy efficiency. In the Green500 list⁸ of November 2016, 8 out of 10 the most efficient supercomputers are equipped with the Nvidia GPGPU, and the No.1 machine of Green500 list

8. <https://www.top500.org/green500/>

ZettaScaler-2.2 installed by RIKEN is powered by the intel low frequency processor (*Xeon D-1571 16C 1.3GHz*).

2.4.2 Potential Architecture of Exascale Supercomputer

This section tries to make a blueprint (shown as Fig. 2.12) for the coming exascale supercomputers based on the future architecture of Aurora Exscale system talked in [TheNextPlatform \[2018\]](#).

As shown in Fig. 2.12, the exascale supercomputers will be composed of more than 100,000 interconnected nodes (several millions cores). Each compute node is packed with the thin cores and fat cores. The fat cores refer to the intel, AMD X86 CPUs which dedicate to more complex operations. The thin cores can be the accelerators and co-processors (e.g. GPGPU, Matrix-2000, FPGA, etc.) with low frequency and/or less complex operations. A typical fat-thin mode is the Nvidia *Host* and *device* architecture. The fat cores are connected with RAM which has high capacity and low bandwidth, the thin cores are connected with the memory which has low capacity and high bandwidth.

This fat core-thin core hybrid approach is also used in the sw26010 processor deployed in the Sunway TaihuLight supercomputer. As shown in Fig. 2.7, this processor is designed with one fat core (MPE) which provides supervisory functions and four auxiliary meshes of skinny cores (CPEs) conducted to computing operations, each with 64 cores, for a total of 260 cores.

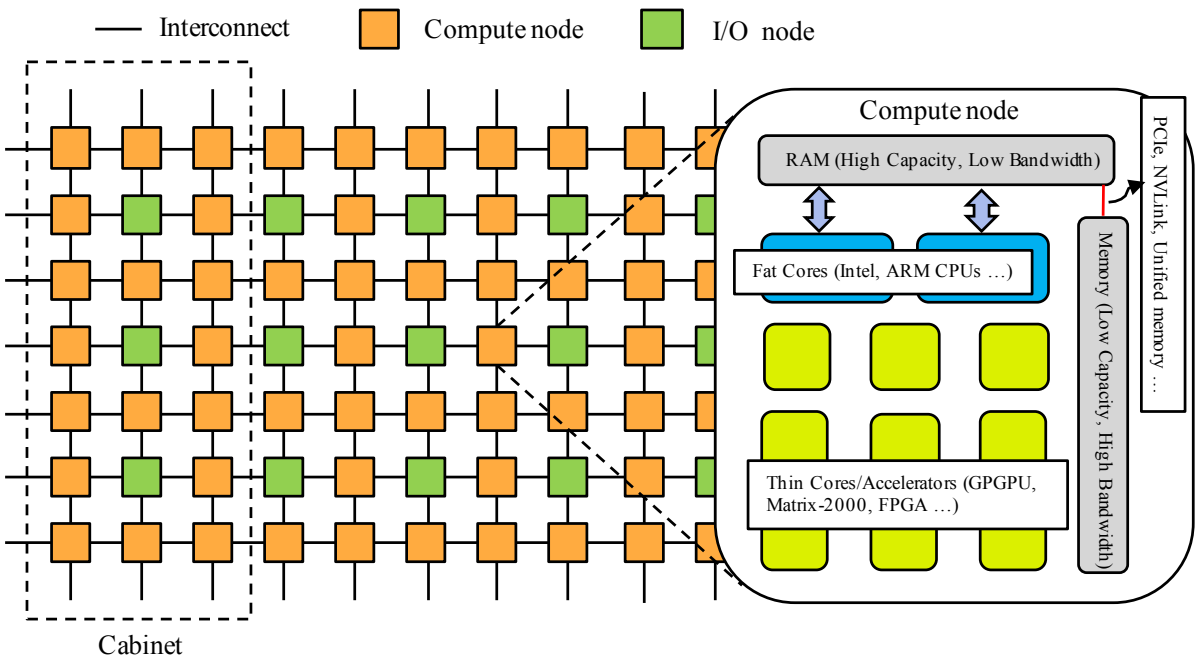


Figure 2.12 – Multiple level parallelism in supercomputers.

This hierarchical computing architectures introduces multiple level parallelism:

1. 1st level is the inter-node parallelism between compute nodes: MPI is the considered model to manage the communication among the compute nodes, manager engine or other complex software stacks are required to handle huge traffic and failure of applications;
2. 2nd level is the intra-node parallelism, including:
 - shared memory parallelism with NUMA among cores and/or sockets in each compute node;
 - heterogeneous computing with different accelerators, memory space and bandwidth;
3. 3rd level are the vectorization techniques, which is able to compute simultaneously a full vector of data with the same set of operations. These techniques include the Single Instruction Multiple Data (SIMD) vectorization on CPUs, and the Single Instruction Multiple Thread (SIMT) vectorization, etc.

2.4.3 Parallel Programming Challenges

With the increase of number of cores and compute nodes in the supercomputers, time spent in communication will overcome the computational time, and it becomes a great bottleneck for the modern applications to take advantages of supercomputers. The parallel programming facing the challenges, which should consider the highly hierarchical architectures of computing and memory, the increasing levels and degrees of parallelism, the heterogeneity of computing, memory, and scalability.

The parallel performance of a common application in HPC is measured by the scalability (also referred to as the scaling efficiency). This measurement indicates how efficient an application is when using increasing numbers of parallel processing elements (CPUs/cores/processes/threads, etc.). There are two basic ways to measure the parallel performance of a given application, depending on whether or not one is cpu-bound or memory-bound. These are referred to as strong and weak scaling, respectively: 1) *strong scaling* which is defined as how the solution time varies with the number of processors for a fixed total problem size; 2) *weak scaling* which is defined as how the solution time varies with the number of processors for a fixed problem size per processor.

In order to improve the parallel performance and get the best scaling efficiency on modern supercomputers, several principles should be considered for the development of applications:

1. Algorithms should have multi-grains of parallelism to fit in the heterogeneity of compute architectures.
2. Applications should be able to adapt to the hierarchical memory on supercomputers.

3. The data movements should be limited, and the number of global communications should be minimized.
4. The parallel programming should reduce synchronizations and promote the asynchronicity;
5. Multi-level scheduling strategies should be proposed, and the manager engine or other complex software stacks should be implemented to handle huge traffic and improve the fault tolerance and resilience.

In following chapters, we focus on the work of design and implementation of novel numerical methods for modern supercomputers based on these principles.

CHAPTER 3

Krylov Subspace Methods

An important application on supercomputers is to solve the linear systems and eigenvalue problems. The chapter gives an overview of the relevant iterative methods to solve large-scale non-Hermitian linear systems and eigenvalue problems. Many applications in science and engineering fields can be formulated as such problems with large dimensions. Large matrices that arise in most applications are almost always sparse. That is, the vast majority of their entries are zero. In numerical linear algebra, these systems are often solved by iterative methods. An iterative method is a mathematical procedure that uses an initial guess to generate a sequence of improving approximate solutions for a class of problems, in which the n -th approximation is derived from the previous ones. Krylov subspace methods are very useful and popular iterative methods to solve large-scale sparse systems since their simplicity and generality. In this chapter, firstly we give a summary on the existing stationery and non-stationary iterative methods, especially the Krylov subspace methods. Then, the mathematical definition of GMRES to solve non-Hermitian linear systems and Arnoldi methods to solve non-Hermitian eigenvalue problems are given in details. For some applications, the convergence of conventional Krylov subspace methods cannot always be guaranteed. Thus various kinds of preconditioners to accelerate the convergence are introduced. In the end, this chapter gives a survey on the parallel implementation on distributed memory platforms, and also the related challenges on the upcoming exascale supercomputers. The material covered in this chapter will be helpful in establishing the mathematical base of this dissertation. Additionally, a large part of consistent efforts in this field are reviewed in this chapter, even some of them have less connection with the motivation of this thesis.

3.1 Linear Systems and Eigenvalue Problems

Given a matrix $A \in \mathbb{C}^{n \times n}$ and a n -vector $b \in \mathbb{C}^n$, the problem considered is: Find $x \in \mathbb{C}^n$ such that:

$$Ax = b. \quad (3.1)$$

This problem is a *linear system*, A is the coefficient matrix, b is the *right hand side (RHS)*, and x is the *vector of unknowns*. In most cases, the linear systems are formulated by solving complex Partial Differential Equations (PDEs) systems. In general, the discretization of these PDEs into a cell-centered Finite Volume scheme in space and an Euler implicit method in time, leads to a nonlinear system which can be solved with a Newton's method. For each Newton step by time, the system is linearized then solved using a linear solver.

Eigenvalue problems occur in many areas of science and engineering, such as structural analysis and electromagnetic applications, and *eigenvalues* are also important in analyzing numerical methods. The standard eigenvalue problem can be defined as: given a matrix $A \in \mathbb{C}^{n \times n}$, find scalar $\lambda \in \mathbb{C}$ and nonzero vector $v \in \mathbb{C}$ such that:

$$Av = \lambda v. \quad (3.2)$$

In this formula, λ is an *eigenvalue* of A , and v is its corresponding *eigenvector*; λ may be complex even if A is real. The *spectrum* of A is the set of all eigenvalues of A , denoted it as $\lambda(A)$, and the *Spectral radius* of A $\rho(A)$ is $\max\{|\lambda| : \lambda \in \lambda(A)\}$.

3.2 Iterative Methods

Iterative methods approach the solution x of Equation (3.1) by a number of steps. Compared with the direct methods such as LU and Gauss Jordan which need an overall computational cost of the order $\frac{2}{3}n^3$, the cost of iterative methods is the order of n^2 operations for each iteration. Iterative methods are especially competitive with direct methods in the case of large sparse matrices, with the potential introduction of the dramatic fill-in by the direct methods. This section gives an overview of both stationary and non-stationary iterative methods.

3.2.1 Stationary and Multigrid Methods

The iterate of stationnary methods to solve Equation (3.1) can be expressed in the simple form

$$x_k = Bx_{k-1} + c \quad (3.3)$$

where neither B nor c depends upon the iteration count k . The four well-known stationary methods are the *Jacobi method* ([Yang and Mittal \[2014\]](#)), *Gauss-Seidel method* ([Yoon and Jameson \[1988\]](#)), *successive overrelaxation method (SOR)* ([Adams and Ortega \[1982\]](#)), and *symmetric successive overrelaxation method (SSOR)* ([Axelsson \[1972\]](#)). Be-

ginning with an initial guess vector, these methods modify one or a few components of the approximation at each iterative step, until the convergence is reached. These medications are called relaxation steps. Theoretically, the stationary methods are applicable for all linear systems, but they are more efficient only for the applications arise from the finite difference discretization of Ellipse Partial Differential Equations. Though the inefficiency of stationary methods for most linear problems, they are often used by combining with the more efficient methods described in later sections of this chapter.

For **Jacobi method**, the Formula (3.3) is extended as:

$$x_k = D^{-1}(L + U)x_{k-1} + D^{-1}b$$

Where the matrices D , $-L$, and $-U$ represent the diagonal, strictly lower triangular, and strictly upper triangular parts of A , respectively. The convergence condition for the Jacobi method is when the spectral radius of the matrix $D^{-1}(L + U)$ is less than 1:

$$\rho(D^{-1}(L + U)) < 1$$

For general cases, the convergence of Jacobi method can be slow. A sufficient (but not necessary) condition for the convergence is that the matrix A is strictly or irreducibly diagonally dominant.

For **Gauss-Seidel method**, the Formula (3.3) is extended as:

$$x_k = (D - L)^{-1}(Ux_{k-1} + b)$$

Where the matrices D , $-L$, and $-U$ represent the diagonal, strictly lower triangular, and strictly upper triangular parts of A , respectively. The Gauss-Seidel method is similar to the Jacobi method except that it uses updated values as soon as they are available. It generally converges faster than the Jacobi method, although still relatively slow. The Gauss-Seidel method can converge if either:

1. The matrix A is strictly or irreducibly diagonally dominant, or
2. A is symmetric positive-definite.

For **SOR method**, the Formula (3.3) is extended as:

$$x_k = (D - \omega L)^{-1}[\omega U + (1 - \omega)D]x_{k-1} + \omega(D - \omega L)^{-1}b$$

Where the matrices D , $-L$, and $-U$ represent the diagonal, strictly lower triangular, and strictly upper triangular parts of A , respectively. The SOR method can be derived from the Gauss-Seidel method by introducing an extrapolation parameter ω . If ω , the SOR method simplifies to the Gauss-Seidel method. A theorem due to Kahan (1958) shows that SOR fails to converge if ω is outside the interval $(0, 2)$. In general, it is not

possible to compute in advance the value of ω that will maximize the rate of convergence of SOR. This method can converge faster than Gauss-Seidel by order of magnitude.

Finally, **SSOR method** is useful as a preconditioner for other methods. However, it has no advantage over the SOR method as a stand-alone iterative method.

In general, many stationary methods have the smoothing property, where oscillatory modes with short wave-length of the errors of linear systems can be eliminated effectively, but the smooth modes with long wave-length are damped very slowly. Thus **multigrid (MG) methods** ([Hutchinson and Raithby \[1986\]](#); [Hiptmair \[1998\]](#); [Bank et al. \[1988\]](#)) are introduced for solving differential equations using a hierarchy of discretizations. The main idea of MG methods is to accelerate the convergence of stationary iterative methods (known as relaxation process) by a global correction on the approximative solution of the fine grid from time to time. This global correction is achieved by solving a coarse problem. The coarse grids can be used to compute an improved initial guess for the fine-grid processes. The reason for the coarse grid are:

1. Relaxation on the coarse-grid is much cheaper;
2. Relaxation on the coarse-grid has a marginally better convergence rate;
3. Smooth error is relatively more oscillatory in the coarse-grid processes, and the relaxation will be more effective

The steps 2 – 4 in Algorithm 1 is the kernel of multigrid method, which gives the restriction-corose solution-interpolation processus. The invovled matrices in this algorithm are:

$$A = A_h = \text{orginal matrix}$$

$$R = R_h^{2h} = \text{restriction matrix}$$

$$I = I_h^{2h} = \text{interpolation matrix}$$

$$A_{2h} = R_h^{2h} A_h I_{2h}^h = RAI = \text{coarse grid matrix}$$

Algorithm 1 Fine-corose-fine loop of multigrid method

- 1: Relaxion **Iterate** on $A_h u = b_h$ by stationary methods to reach u_k .
 - 2: **Restrict** the residual $r_h = b_h - A_h u_h$ to the coarse grid by $r_{2h} = R_h^{2h} r_h$.
 - 3: **Solve** $A_{2h} E_{2h} = r_{2h}$.
 - 4: **Interpolate** E_{2h} as $E_h = I_{2h}^h E_{2h}$. Add E_h to u_h .
 - 5: **Iterative** more times on $A_h u = b_h$ starting from the improved $u_h + E_h$.
-

One extension of multigrid method is the **algebraic multigrid methods (AMG)** ([Ruge and Stüben \[1987\]](#); [Vaněk et al. \[1996\]](#); [Brandt \[1986\]](#); [Brezina et al. \[2001\]](#)). AMG construct their restriction, interpolation, and coarse grid matrices directly from the matrix

of a linear system. AMG is regarded as advantageous when geometric multigrid is too difficult to apply, e.g., unstructured meshes, graph problem, etc. Fig. 3.1 gives an example of hierarchical multi-level AMG.

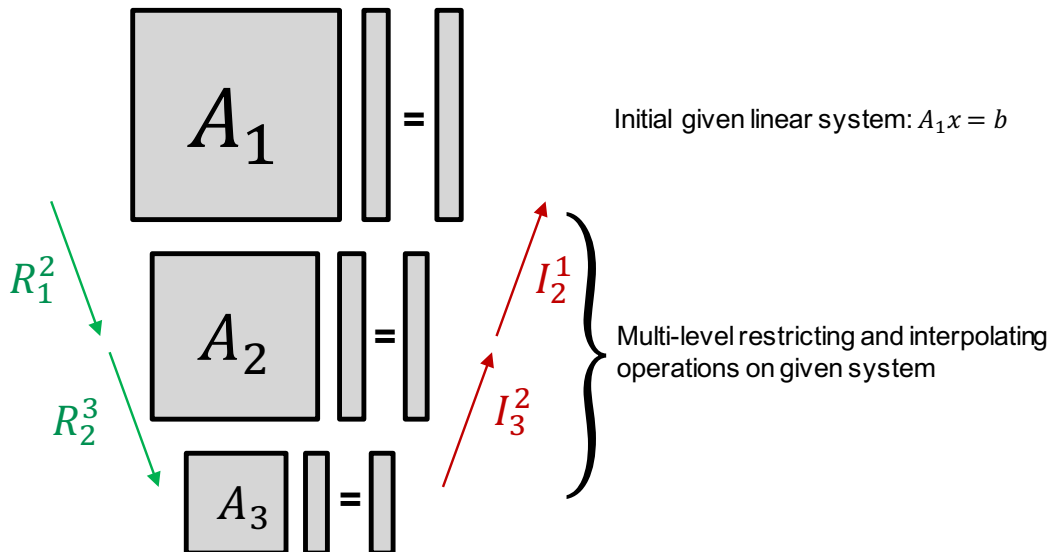


Figure 3.1 – Algebraic multigrid hierarchy.

3.2.2 Non-stationary Methods

In practice, the stationary methods talked in the last section cannot always get the convergence quickly for more general matrices which are not constructed from the Ellipse PDEs. The GMG and AMG which use the relaxation steps of stationary methods' can speed up the convergence for more general matrices, but the construction of restriction, interpolation, and coarse matrices either from geometric PDE problems or the operator matrix A is far more difficult, and these operations matter the convergence. There is no free lunch for AMG which is hard to "control" and get optimal performance. In my dissertation, I will talk more about the **non-stationary methods** which are easy to implement and have better convergence performance than the stationary methods. The difference of non-stationary methods comparing with stationary methods is that the involved computational information changes at each step of the iteration. The most well-known non-stationary methods are the suite of **Krylov subspace methods**.

3.3 Krylov Subspace methods

This section presents the Krylov Subspace projection and the basic Arnoldi reduction in the Krylov subspace.

3.3.1 Krylov Subspaces

In linear algebra, the m -order Krylov subspace (Saad [1981]) generated by a $n \times n$ matrix A and a vector b of dimension n is the linear subspace spanned by the images of b under the first m powers of A , that is

$$K_m(A, b) = \text{span}(b, Ab, A^2b, \dots, A^{m-1}b).$$

The Krylov subspace provides the ability to extract the approximations from an m -dimensional subspace K_m . Since K_m is the subspace of all vectors in \mathbb{R}^n , it can be written as $x = p(A)b$, with p a polynomial of degree not exceeding $m - 1$.

3.3.2 Basic Arnoldi Reduction

Algorithm 2 Arnoldi Reduction

```

1: function AR(input: $A, m, \nu$ , output:  $H_m, \Omega_m$ )
2:    $\omega_1 = \nu / \|\nu\|_2$ 
3:   for  $j = 1, 2, \dots, m$  do
4:     for  $i = 1, 2, \dots, j$  do
5:        $h_{i,j} = (A\omega_j, \omega_i)$ 
6:     end for
7:      $\omega_j = A\omega_j - \sum_{i=1}^j h_{i,j}\omega_i$ 
8:      $h_{j+1,j} = \|\omega_j\|_2$ 
9:     if  $h_{j+1,j} = 0$  then Stop
10:    end if
11:     $\omega_{j+1} = \omega_j / h_{j+1,j}$ 
12:   end for
13: end function

```

Arnoldi procedure is well used to build an orthogonal basis of the Krylov subspace K_m . One variant of basic Arnoldi reduction algorithm is given in Algorithm 2. In this algorithm, at each step of Arnoldi reduction, the algorithm times the previous Arnoldi vector ω_j by matrix A , and get an orthogonal vector ω_j against all previous ω_i by a stand Gram-Schmit procedure. It will stop if the vector computed in line 5 is zero. Then the vectors $\omega_1, \omega_2, \dots, \omega_m$ form an orthonormal basis of the Krylov Subspace.

Denote by V_m , the $n \times m$ matrix with column vectors $\omega_1, \omega_2, \dots, \omega_m$, by \bar{H}_m , the $(m + 1) \times m$ Hessemberg matrix whose nonzero entries $h_{i,j}$ are defined by Algorithm 2, then note H_m as the matrix obtained from \bar{H}_m by deleting its last row (shown as Fig. 3.2). The following relations are given:

$$AV_m = V_m H_m + \omega_m e_m^T = V_{m+1} \bar{H}_m. \quad (3.4)$$

The diagram shows the decomposition of a matrix A into three components. On the left is a large rectangle labeled A . To its right is an equals sign. To the right of the equals sign is another rectangle labeled V_m . To the right of V_m is a plus sign. To the right of the plus sign is a rectangle labeled H_m , which has a diagonal line from top-left to bottom-right. To the right of H_m is a plus sign. To the right of the plus sign is the expression $\omega_m e_m^T$.

Figure 3.2 – The action of A on V_m gives $V_m H_m$ plus a rank-one matrix.

$$V_m^T A V_m = H_m. \quad (3.5)$$

In case that the norm of ω_j in line 5 of Algorithm 2 vanishes at a certain step j , the next vector ω_{j+1} cannot be computed and the algorithm steps, H_m turns to be H_j with dimension $j \times j$.

3.3.3 Orthogonalization

There are different orthogonalization schemes to construct the orthogonal basis of Krylov subspace, in this section, we list four variants.

1. **Classic Gram-Schmit Orthogonalization (CGS):** Algorithm 2 gives an example of Arnoldi reduction using the CGS to create a basis vector by vector. The benefit of CGS is the parallelism in computing $h_{i,j}$ and ω_j in step 5 and 7.
2. **Modified Gram-Schmit Orthogonalization (MGS):** An alternative (See Algorithm 3), in which the number of subtractions is reduced, resulting in a less chance of cancellations. Though MGS is more stable than CGS, it is less parallel than CGS. In CGS, the orthogonalization process from line 5 to line 7 can be overlapped, while the same process of MGS has a data dependency. Thus the parallel implementation of Arnoldi reduction still prefers CGS, and a preconditioner or a reorthogonalization process can compensate its deficiency of numerical stability.
3. **Householder Orthogonalization:** the Arnoldi reduction can also be operated by the householder orthogonalization, which is more numerically robust than the Gram-Schmit orthogonalization.
4. **Incomplete Orthogonalization:** This orthogonalization process in Arnoldi is expensive because each vector accumulated in the basis is orthogonalized against all previous ones. Thereby, the orthogonalization process number of iterations k is bounded to the Krylov subspace size, thus higher values of m will imply More

Algorithm 3 Arnoldi Reduction with Modified Gram-Schmidt process

```
1: function AR-MGS(input: $A, m, \nu$ , output:  $H_m, \Omega_m$ )
2:    $\omega_1 = \nu / \|\nu\|_2$ 
3:   for  $j = 1, 2, \dots, m$  do
4:     for  $i = j, 2, \dots, j$  do
5:        $h_{i,j} = (A\omega_j, \omega_i)$ 
6:        $\omega_j = \omega_j - h_{i,j}v_i$ 
7:     end for
8:      $h_{j+1,j} = \|\omega_j\|_2$ 
9:     if  $h_{j+1,j} = 0$  then Stop
10:    end if
11:     $\omega_{j+1} = \omega_j / h_{j+1,j}$ 
12:   end for
13: end function
```

Algorithm 4 Arnoldi Reduction with Incomplete Orthogonalization process

```
1: function AR-INCOMPLETE(input: $A, m, \nu$ , output:  $H_m, \Omega_m$ )
2:    $\omega_1 = \nu / \|\nu\|_2$ 
3:   for  $j = 1, 2, \dots, m$  do
4:     for  $i = \max\{1, j - q + 1\}, \dots, j$  do
5:        $h_{i,j} = (A\omega_j, \omega_i)$ 
6:        $\omega_j = \omega_j - h_{i,j}v_i$ 
7:     end for
8:      $h_{j+1,j} = \|\omega_j\|_2$ 
9:     if  $h_{j+1,j} = 0$  then Stop
10:    end if
11:     $\omega_{j+1} = \omega_j / h_{j+1,j}$ 
12:   end for
13: end function
```

computations and memory space in order to create the Krylov orthonormalized vector basis. With the aim to reduce the cost induced by the Arnoldi orthogonalization process, it is possible to truncate it by orthogonalizing each vector against a subset of the basis vectors, i.e. the q precedent basis vectors (Algorithm 4). In this case, the resulting upper Hessenberg matrix H_m is not fully orthogonalized and has the propriety to be banded of bandwidth q . Incomplete orthogonalization can speed up the construction of Krylov subspace basis, with the loose of numerical accuracy.

3.3.4 Krylov Subspace Methods

The best known Krylov subspace methods are the Arnoldi ([Voß \[2004\]](#)), Lanczos ([Widlund \[1978\]](#)), Conjugate gradient ([Lasdon et al. \[1967\]](#)), IDR(s) (Induced dimension reduction) ([van Venetië and Westerdiep \[2015\]](#)), GMRES (generalized minimum residual), BiCGSTAB (biconjugate gradient stabilized) ([Sleijpen and Fokkema \[1993\]](#)), QMR (quasi

minimal residual) ([Freund and Nachtigal \[1991\]](#)), TFQMR (transpose-free QMR) ([Basermann \[1996\]](#)), and MINRES (minimal residual) ([Paige and Saunders \[1975\]](#)) methods. This dissertation concentrates on GMRES which is used to solve non-Hermitian linear systems.

3.4 GMRES for Non-Hermitian Linear Systems

GMRES is a well-known Krylov iterative method to solve non-Hermitian linear systems $Ax = b$. This section gives an introduction in-depth about the fundamentals of GMRES.

3.4.1 Basic GMRES Method

GMRES (Algorithm 5) is a kind of projection method which extracts an approximated solution x_m of given problem in a well-selected m -dimensional Krylov subspace $K_m(A, v)$ from a given initial guess vector x_0 . GMRES method was introduced by Youssef Saad and Martin H. Schultz in 1986 ([Saad and Schultz \[1986\]](#)).

Algorithm 5 Basic GMRES method

```

1: function BASICGMRES(input:  $A, m, x_0, b$ , output:  $x_m$ )
2:    $r_0 = b - Ax_0$ ,  $\beta = \|r_0\|_2$ , and  $\nu_1 = r_0/\beta$ 
3:   Compute an AR(input: $A, m, \nu_1$ , output:  $H_m, \Omega_m$ )
4:   Compute  $y_m$  which minimizes  $\|\beta e_1 - H_m y\|_2$ 
5:    $x_m = x_0 + \Omega_m y_m$ 
6: end function
```

In fact, any vector x in subspace $x_0 + K_m$ can be written as

$$x = x_0 + V_m y. \quad (3.6)$$

with y an m -vector, V_m an orthonormal basis of the Krylov Subspace K_m . The norm of residual $R(y)$ of $Ax = b$ is given as:

$$\begin{aligned} R(y) &= \|b - Ax\|_2 = \|b - A(x_0 + V_m y)\|_2 \\ &= \|V_{M+1}(\beta e_i - \bar{H}_m y)\|_2 = \|\beta e_i - \bar{H}_m y\|_2. \end{aligned} \quad (3.7)$$

The GMRES approximation x_m can be obtained as $x_m = x_0 + V_m y_m$ where $y_m = \text{argmin}_y \|\beta e_i - \bar{H}_m y\|_2$. The minimizer y_m is inexpensive to compute since it requires the solution of an $(m + 1) \times m$ least-squares problem if m is typically small. This gives the basic GMRES method as Algorithm 5.

If m is very large, GMRES can be restarted after a number of iterations, to avoid enormous memory and computational requirements with the increase of Krylov subspace projection number. It is called the restarted GMRES. The restarted GMRES won't stop

until the condition $\|b - Ax_m\| < \epsilon_g$ is satisfied. See Algorithm 6 for restarted GMRES algorithm in detail. A well-known difficulty with the restarted GMRES algorithm is that it can stagnate when the matrix is not positive definite. A typical method is to use preconditioning techniques whose goal is to reduce the number of steps required to converge.

Algorithm 6 Restarted GMRES method

```
1: function RESTARTEDGMRES(input:  $A, m, x_0, b, \epsilon_g$ , output:  $x_m$ )
2:   BASICGMRES(input:  $A, m, x_0, b$ , output:  $x_m$ )
3:   if ( $\|b - Ax_m\| < \epsilon_g$ ) then
4:     Stop
5:   else
6:     set  $x_0 = x_m$  and GOTO 2
7:   end if
8: end function
```

3.4.2 Variants of GMRES

Several variants of GMRES are proposed, such as:

1. **Restarted GMRES (Morgan [1995])**: the cost of the iterations grow as $\mathcal{O}(n^2)$, where n is the iteration number. Therefore, the method is sometimes restarted after a number, say k , of iterations, with x_k as an initial guess. The resulting method is called Restarted GMRES. This method suffers from stagnation in convergence as the restarted subspace is often close to the earlier subspace.
2. **Truncated GMRES (De Sturler [1999])**: a version of GMRES with incomplete orthogonalization, which reduces the computing and memory requirement of the Arnoldi process in GMRES with the cost of the accuracy of orthogonalization.
3. **GMRES-DR (Erhel et al. [1996])**: Restarted GMRES with deflation. As we have just seen, restarting results in a loss of useful information, thus a slowing of convergence after a restart. To overcome this problem, GMRES with deflated restarting (GMRES-DR) was introduced. The deflation in GMRES-DR makes restarted GMRES more robust and makes it converge much faster for tough problems with small eigenvalues.
4. **Pipelined GMRES (Ghysels and Vanroose [2014])**: A particular variant of GMRES which hides the global communication latency for parallel implementation.
5. **FGMRES (Frayssé et al. [2008])**: Flexible GMRES presented by Saad is a variant of GMRES with the advantage of being able to switch preconditioners on the fly according to specific heuristics in the GMRES process without any additional computation. This method is interesting because it allows developing robust and easily

parallelizable methods. FGMRES is developed based on the right-preconditioner which will be presented later in Section 3.6.1.1.

3.5 Arnoldi for Non-Hermitian Eigenvalue Problems

The dominant eigenvalues of a non-Hermitian eigenvalue problem can be approximated by the Arnoldi method. In the section, we present the basic algorithm of the Arnoldi method and its variants.

3.5.1 Basic Arnoldi Methods

Arnoldi algorithm ([Arnoldi \[1951\]](#)) is widely used to approximate the eigenvalues of large sparse matrices. The kernel of Arnoldi algorithm is the Arnoldi reduction, which gives an orthonormal basis $\Omega_m = (\omega_1, \omega_2, \dots, \omega_m)$ of Krylov subspace $K_m(A, v)$, by the Gram-Schmidt orthogonalization, where A is $n \times n$ matrix, and v is a n -dimensional vector. As shown Arnoldi reduction can transfer a matrix A to be an upper Hessenberg matrix H_m with relation $V_m^T A V_m = H_m$, the eigenvalues of H_m are the approximated ones of A , which are called the Ritz values of A . With the Arnoldi reduction, the r desired Ritz values $\Lambda_r = (\lambda_1, \lambda_2, \dots, \lambda_r)$, and the corresponding Ritz vectors $U_r = (u_1, u_2, \dots, u_r)$ can be calculated by Basic Arnoldi method.

The numerical accuracy of the computed eigenpairs of basic Arnoldi method depends highly on the size of the Krylov subspace and the orthogonality of Ω_m . Generally, the larger the subspace is, the better the eigenpairs approximation is. The problem is that firstly the orthogonality of the computed Ω_m tends to degrade with each basis extension. Also, the larger the subspace size is, the larger the Ω_m matrix gets. Hence available memory may also limit the subspace size, and so the achievable accuracy of the Arnoldi process. To overcome this, Saad ([Saad \[2011\]](#)) proposed to restart the Arnoldi process, which is the ERAM. Inside ERAM, the subspace size is fixed as m , and only the starting vector will vary. After one restart of the Arnoldi process, the starting vector will be initialized by using information from the computed Ritz vectors. In this way, the vector will be forced to be in the desired invariant subspace. The Arnoldi process and this iterative scheme will be executed until a satisfactory solution is computed. The Algorithm of ERAM is given by Algorithm 7, where ϵ_a is a tolerance value, r is desired eigenvalues number and the function g defines the stopping criterion of iterations.

3.5.2 Variants of Arnoldi Method

There are various strategies to restart the basic Arnoldi method and to accelerate the convergence by the deflation of unwanted eigenvalues. This section lists three variants:

Algorithm 7 Explicitly Restarted Arnoldi Method

```
1: function ERAM(input:  $A, r, m, \nu, \epsilon_a$ , output:  $\Lambda_r$ )
2:   Compute an AR(input:  $A, m, v$ , output:  $H_m, \Omega_m$ )
3:   Compute  $r$  desired eigenvalues  $\lambda_i$  ( $i \in [1, r]$ ) of  $H_m$ 
4:   Set  $u_i = \Omega_m y_i$ , for  $i = 1, 2, \dots, r$ , the Ritz vectors
5:   Compute  $R_r = (\rho_1, \dots, \rho_r)$  with  $\rho_i = \|\lambda_i u_i - Au_i\|_2$ 
6:   if  $g(\rho_i) < \epsilon_a$  ( $i \in [1, r]$ ) then
7:     stop
8:   else
9:     set  $v = \sum_{i=1}^d \text{Re}(\nu_i)$ , and GOTO 2
10:  end if
11: end function
```

1. **Explicitly Restarted Arnoldi Method (ERAM)** ([Morgan \[1996\]](#)): Arnoldi algorithm restarted explicitly by the combination of Ritz values and vectors.
2. **Implicitly Restarted Arnoldi Method (IRAM)** ([Sorensen \[1997\]](#)): IRAM is a variant of Arnoldi algorithm with deflation of unwanted eigenvalues. It can shift the unwanted eigenvalues of matrix implicitly without the explicit construction of filter polynomial during the process of Arnoldi reduction. The Algorithm 8 illustrates this method. The shift of unwanted values of matrix A can be transferred to be a shifted QR factorization of Hessemberg matrix H_m . IRAM can operate in parallel to solve the large problem without extra memory space.
3. **Krylov-Schur Method** ([Stewart \[2002\]](#)): It is another implementation of Arnoldi algorithm with deflation of unwanted eigenvalues. Krylov-Schur method is mathematically equal to IRAM. Its two advantages over IRAM: 1) it is easier to deflate converged Ritz vectors; 2) it avoids the potential forward instability of the QR algorithm. The Algorithm 9 gives this method. During the Arnoldi reduction procedure, the Hessemberg matrix H_m is decomposed by the Schur deposition as $H_m = S_m * T_m S_m$ with unitary matrix S_m and upper triangular matrix T_m . The upper triangular form of T_m eases the analysis of Ritz pairs. The wanted and unwanted Ritz values in T_m can be reordered into two separate parts as T_{m-k} and T_k . T_{m-k} can be extended to m -dimension without unwanted values through further k steps of Krylov subspace projection.

3.6 Preconditioners for GMRES

In practice, one weakness of GMRES discussed in the previous section is the lack of robustness, it is likely to suffer from slow convergence for some problems. Preconditioning is a kind of techniques to accelerate the convergence of Krylov subspace methods by

Algorithm 8 Implicitly Restarted Arnoldi Method

```

1: function IRAM(input:  $A, r, m, \nu, \epsilon_a$ , output:  $\Lambda_r$ )
2:   Compute an AR(input:  $A, m, v$ , output:  $H_m, \Omega_m$ )
3:   Compute the spectrum of  $H_m$ :  $\Lambda(H_m)$ . If converge, stop. Otherwise, select set of
    $p$  shifts  $\mu_1, \mu_2, \dots, \mu_p$ 
4:    $q^T = e_m^T$ 
5:   for  $j = 1, 2, 3, \dots, p$  do
6:     Factor  $[Q_j, R_j] = QR(H_m - \mu_j I)$ 
7:      $H_m = q_j^T H_m Q_j, V_m = V_m Q_j, q^T = q^T Q_j$ 
8:   end for
9:    $f_k = v_{k+1} H_{m(k+1,k)} + f_m q^T(k), V_k = V_{m(1:n,1:k)}, H_k = H_{m(1:k,1:k)}$ 
10:  Begining with the  $k$ -step Arnoldi factorization,  $AV_k = V_k H_k + f_k e_k^T$ , apply  $p$  ad-
    ditional steps of the Arnoldi process to obtain a new  $m$ -step Arnoldi factorization as
     $AV_m = V_m H_m + f_m e_m^T$ 
11: end function

```

Algorithm 9 Krylov-Schur Method

```

1: function KRYLOV-SCHUR(input:  $A, x_1, m$ , output:  $\Lambda_k$  with  $k \leq p$ )
2:   Build an initial Krylov decompostion of order  $m$ 
3:   Apply orthogonal transformations to get a Krylov-Schur decompostion
4:   Reorder the diagonal blocks of the Krylov-Schur decompostion
5:   Truncate to a Krylov-Schur decompostion of order  $p$ 
6:   Extend to a Krylov decomposition of order  $m$ 
7:   If not satisfied, go to step 3
8: end function

```

transforming the original linear systems from one to another. In this section, we summarize different kinds of existing preconditioners, including the preconditioning by a selected matrix, by the deflation, and by a selected polynomial.

3.6.1 Preconditioning by Selected Matrix

The first alternative is to use the preconditioning matrix M . This M can be defined in many different ways, and it makes it is much easier to solve linear systems $Mx = b$ compared with the original linear systems $Ax = b$. After the selection of M , there are two ways to apply this preconditioning matrix M to the original systems: the left, right and split preconditioning.

3.6.1.1 Left, Right and Split Preconditioning

The **left preconditioning** of matrix on the original linear can be defined as:

$$M^{-1}Ax = M^{-1}. \quad (3.8)$$

The GMRES is applied to solve the Equation (3.8) instead of the original matrix. The

left preconditioned version GMRES is given as Algorithm 10.

Algorithm 10 Left-Preconditioned GMRES

```

1:  $r_0 = M^{-1}(b - Ax_0)$ ,  $\beta = \|r_0\|_2$ , and  $\nu_1 = r_0/\beta$ 
2: for  $i = 0, \dots, m-1$  do
3:    $z \leftarrow M^{-1}A\nu_i$ 
4:    $h_{j,i} \leftarrow \langle z, \nu_j \rangle$ ,  $z = z - h_{j,i}\nu_j$   $j = 1, \dots, i$ 
5:   if  $h_{j+1,j} == 0$  then
6:     stop
7:   else
8:      $\nu_{i+1} = z/h_{i+1,i}$ , and  $h_{i+1,i} = \|z\|_2$ 
9:   end if
10: end for
11: Compute  $y_m$  which minimizes  $\|\beta e_1 - H_m y\|_2$ 
12:  $x_m = x_0 + V_m y_m$ 

```

As shown in Algorithm 10, M is applied to each step of GMRES iteration, and the Krylov subspace constructed by the Arnoldi process tends to be:

$$\text{span}\{r_0, M^{-1}Ar_0, \dots, (M^{-1}A)^{m-1}r_0\}. \quad (3.9)$$

The residual vectors in this algorithm can be defined as $r_m = M^{-1}(b - Ax_m)$, instead of the unpreconditioned one $b - Ax_m$.

The **right preconditioning** of M makes GMRES solve linear systems as follows instead of the original systems:

$$AM^{-1}u = b, \quad u = Mx. \quad (3.10)$$

The right-preconditioned GMRES is given as Algorithm 11.

Algorithm 11 Right-Preconditioned GMRES

```

1:  $r_0 = b - Ax_0$ ,  $\beta = \|r_0\|_2$ , and  $\nu_1 = r_0/\beta$ 
2: for  $i = 0, \dots, m-1$  do
3:    $z \leftarrow AM^{-1}\nu_i$ 
4:    $h_{j,i} \leftarrow \langle z, \nu_j \rangle$ ,  $z = z - h_{j,i}\nu_j$   $j = 1, \dots, i$ 
5:   if  $h_{j+1,j} == 0$  then
6:     stop
7:   else
8:      $\nu_{i+1} = z/h_{i+1,i}$ , and  $h_{i+1,i} = \|z\|_2$ 
9:   end if
10: end for
11: Compute  $y_m$  which minimizes  $\|\beta e_1 - H_m y\|_2$ 
12:  $x_m = x_0 + M^{-1}V_m y_m$ 

```

As shown in this algorithm, the Krylov subspace spanned by the right preconditioning can be defined as:

$$Span\{r_0, AM^{-1}r_0, \dots, (AM^{-1})^{m-1}r_0\}. \quad (3.11)$$

The essential difference of right preconditioning comparing with left preconditioning is that the residual vectors in the algorithm can be obtained as $b - Ax_m = b - AM^{-1}u_m$, which is equal the ones of unpreconditioned systems, and independent from the selection of M . Thus this preconditioning matrix can vary with different selections for each iteration of GMRES, that is the flexible GMRES, which can be useful for several linear systems.

Another alternative is to use the split preconditioning, which can be seen as a combination of left and right preconditioning. Suppose that a preconditioning matrix M can be factorized as the form:

$$M = LU. \quad (3.12)$$

Then, the split preconditioned linear systems to be solved by GMRES can be defined as:

$$L^{-1}AU^{-1}u = L^{-1}b, \quad x = U^{-1}u. \quad (3.13)$$

The residual vectors of this type of GMRES is that form $L^{-1}(b - Ax_m)$. In fact, a split preconditioner may be much better if A is nearly symmetric.

3.6.1.2 Jacobi, SOR, and SSOR Preconditioners

The preconditioners based on stationary methods, such as Jacobi, SOR and SSOR methods is a special collection of left-preconditioners.

The general form for the preconditioning can be given as:

$$x_{k+1} = M^{-1}Nx_k + M^{-1}b, \quad (3.14)$$

where M and N are created by the splitting of A as:

$$A = M - N. \quad (3.15)$$

The above formula can be rewritten as:

$$x_{k+1} = Gx_k + f \quad (3.16)$$

with $f = M^{-1}b$ and $G = M^{-1}N = I - M^{-1}A$.

The Expression (3.16) is attempting to solve:

$$(I - G)X = f. \quad (3.17)$$

which can be rewritten as:

$$M^{-1}Ax = M^{-1}b. \quad (3.18)$$

For Jacobi Preconditioner, the preconditioning matrix M can be defined as:

$$M_{Jacobi} = D^{-1}. \quad (3.19)$$

For Gauss-Seidel Preconditioner, the preconditioning matrix M can be defined as:

$$M_{Gauss} = (D - E)D^{-1}(D - F). \quad (3.20)$$

For SSOR Preconditioner, the preconditioning matrix M can be defined as:

$$M_{SSOR} = (D - \omega E)D^{-1}(D - \omega F). \quad (3.21)$$

3.6.1.3 Incomplete LU Preconditioners

In numerical linear algebra, an incomplete LU factorization (abbreviated as ILU) of a matrix is a sparse approximation of the LU factorization often used as a preconditioner.

For a linear system $Ax = b$, it is often solved by computing the factorization $A = LU$, with L a lower triangular and U upper triangular. One then solves efficiently $Ly = b$ and $Ux = y$ in sequence since U , and L are all triangular. It is well known that usually in the factorization procedure, the matrices L and U have more non zero entries than A . These extra entries are called fill-in entries.

An incomplete factorization ([Saad \[1994b\]](#); [Sertel and Volakis \[2000\]](#); [Lee et al. \[2003\]](#); [Malas and Gürel \[2007\]](#)) instead seeks triangular matrices L and U such that

$$A \approx LU.$$

For a typical sparse matrix, the LU factors can be much less sparse than the original matrix - a phenomenon called fill-in. The memory requirements for using a direct solver can then become a bottleneck in solving linear systems. One can combat this problem by using fill-reducing reorderings of the matrix's unknowns, such as the Cuthill-McKee ordering.

Let S be a subset of all positions of the original matrix generally including the main diagonal, and $\forall(i, j)$ such as $a_{i,j} \neq 0$. An incomplete LU factorization of A only allows fill-in positions which are in S , which is designated by the elements to drop at each step. S has to be specified in advance in a static way by defining a zero pattern which must exclude the main diagonal. Therefore, for any zero pattern P , such that

$$P \subset \{(i, j) | i \neq j; 1 \leq i, j \leq n\} \quad (3.22)$$

Algorithm 12 Incomplete LU Factorization Algorithm

```

1: for  $i = 2, \dots, n$  do
2:   for  $k = 1, \dots, i - 1$  do
3:     if  $(i, k) \notin P$  then
4:        $a_{i,k} = a_{i,k}/a_{k,k}$ 
5:       for  $j = k + 1, \dots, n$  do
6:         if  $(i, j) \notin P$  then
7:            $a_{i,j} = a_{i,j} - a_{i,k}a_{k,j}$ 
8:         end if
9:       end for
10:      end if
11:    end for
12:  end for

```

Solving for $LUX = b$ can be done quickly but does not hold the exact solution to the given problem. So a matrix is

$$M_{LU} = LU$$

often used as a preconditioner for another iterative method such as GMRES. For an incomplete factorization with no-fill, named ILU(0), we define the pattern P as the zero pattern of A . However, more accurate factorization can be obtained by allowing some fill-in, denoted by ILU(p) where p stands for the desired level of fill. This class of preconditioner has some difficulties to converge in a reasonable number of iterations on ill-conditioned systems.

3.6.1.4 Preconditioning by Multigrid solvers

Multigrid methods, including GMG and AMG, are the most complex preconditioners. The MG methods speed up the convergence of stationary iterative methods by smoothing the low-frequency modes of the errors of linear systems with the construction of a series of coarse representations. The main difference between the GMG and AMG is the strategy to construct the restriction, and coarsening matrices. AMG preconditioners need an amount of time for the pre-processing, but they can accelerate convergence much more significantly.

When AMG is applied as a preconditioner (e.g. [Plank et al. \[2007\]](#); [Leem et al. \[2004\]](#); [Yang et al. \[2002\]](#); [Mifune et al. \[2003\]](#)), the setup phase of restriction matrix R_h^{2h} and the interpolation matrix I_h^{2h} need to be complex as the standalone AMG solvers. The creation of a given number of sub-domains, and each domain representing by only one value at the coarse level is enough. After dividing the nodes of mesh into groups, the projection matrix can be defined as W . W is used to build the coarse-system matrix A_{2h} of an original matrix A :

$$A_{2h} = W^T A W. \quad (3.23)$$

Thus, W is the restriction operation R_h^{2h} , and W^T is the interpolation matrix I_h^{2h} . After the creation of transfer operation W , it can be applied into the Fine-Coarse-Fine loop of MG method to generate an approximate solution of original linear systems. Algorithm 13 gives an example of AMG preconditioned GMRES.

Algorithm 13 AMG-Preconditioned GMRES

```

1:  $r_0 = b - Ax_0$ ,  $\beta = \|r_0\|_2$ , and  $\nu_1 = r_0/\beta$ 
2: for  $i = 0, \dots, m-1$  do
3:   Get  $u_p$  by  $p$  relaxions on  $Au = \nu_i$  starting from  $u_0$  using stationary methods.
4:   Find the residual:  $r_p = \nu_i - Au_p$ .
5:   Project  $r_p$  one the coarse level:  $r_{pc} = W^T r_p$ .
6:   Solve the coarse-level residual system:  $A_{2h} E_{pc} = r_{pc}$ .
7:   Project back  $E_{pc}$  the fine level:  $E_p = We_{pc}$ .
8:   Correct the fine-level approximation:  $u_p = u_p + E_p$ .
9:   Iterate  $p$  times on  $Au = \nu_i$  starting from  $u_p$ , get the final approximation  $\hat{u}$ .
10:  set  $\nu_i = \hat{u}$ .
11:   $z \leftarrow A\nu_i$ 
12:   $h_{j,i} \leftarrow \langle z, \nu_j \rangle$ ,  $z = z - h_{j,i}\nu_j$   $j = 1, \dots, i$ 
13:  if  $h_{j+1,j} == 0$  then
14:    stop
15:  else
16:     $\nu_{i+1} = z/h_{i+1,i}$ , and  $h_{i+1,i} = \|z\|_2$ 
17:  end if
18: end for
19: Compute  $y_m$  which minimizes  $\|\beta e_1 - H_m y\|_2$ 
20:  $x_m = x_0 + M^{-1}V_m y_m$ 

```

3.6.2 Preconditioning by Deflation

TO DO

3.6.3 Preconditioning by Polynomials - Introduction in detail on Least Squares Polynomial method

In the context of iterative methods for solving linear systems, polynomial preconditioners have been studied extensively. In this section, we recall some of the results regarding common polynomial preconditioners, and then give an introduction about the Least Squares Polynomial preconditioner.

3.6.3.1 Polynomial Preconditioners for Linear Solvers

In order to an approximate solution of linear system

$$Ax = b,$$

Algorithm 14 GMRES-DR(A, m, k, x_0)

```

1:  $r_0 = b - Ax_0$ ,  $\beta = \|r_0\|_2$ , and  $\nu_1 = r_0/\beta$ 
2: for  $i = 0, \dots, m-1$  do
3:    $z \leftarrow M^{-1}A\nu_i$ 
4:    $h_{j,i} \leftarrow \langle z, \nu_j \rangle$ ,  $z = z - h_{j,i}\nu_j$   $j = 1, \dots, i$ 
5:   if  $h_{j+1,j} == 0$  then
6:     stop
7:   else
8:      $\nu_{i+1} = z/h_{i+1,i}$ , and  $h_{i+1,i} = \|z\|_2$ 
9:   end if
10: end for
11: Compute  $y_m$  which minimizes  $\|\beta e_1 - H_m y\|_2$ 
12:  $x_m = x_0 + V_m y_m$ 
13: Compute the  $k$  smallest eigenpairs  $(\lambda_k, g_K)$  of  $Hm + \beta H_m^{-T}e_m e_m^T$ 
14: Set  $Q_{k+1}$  from  $G_k = [g_1, g_2, \dots, g_k]$ 
15: Set  $V_{k+1}^{new} = V_{k+1} Q_{k+1}$  and  $\bar{H}_k^{new} = Q_{k+1}^H \bar{H}_m$  with Arnoldi reduction
16: if  $\|r_m\| < tol$  then
17:   Stop
18: end if
19: set  $x_0 = x_m$  and Go to Step 1

```

one approach is to get the inverse of A , denote it as A^{-1} , and then the solution gets to be easily obtained as

$$x = A^{-1}b$$

Suppose that the characteristic polynomial for A :

$$q(A) = \gamma_n A^n + \gamma_{n-1} A^{n-1} + \dots + \gamma_1 A + \gamma_0 I = 0. \quad (3.24)$$

The polynomial representation of A^{-1} with $\gamma_0 \neq 0$ can be given as:

$$A^{-1} = \frac{1}{\gamma_0}(-\gamma_n A^{n-1} - \gamma_{n-1} A^{n-2} - \dots - \gamma_1 I) = p(A). \quad (3.25)$$

Therefore, it makes sense to approximate A^{-1} by a polynomial in A . Better selection of this kind of polynomial can approximate more quickly the solution of linear systems.

3.6.3.2 Neumann series polynomials

The simplest p is the polynomial with the Neumann series expansion:

$$I + N^1 + N^2 + \dots \quad (3.26)$$

with:

$$N = I - \omega A. \quad (3.27)$$

and ω is a scaling parameter. The above series can be obtained by the expansion of the inverse of ωA :

$$\begin{aligned} (\omega A)^{-1} &= [D - (D - \omega D^{-1} A)]^{-1} \\ &= [I - (I - \omega D^{-1} A)]^{-1} D^{-1}. \end{aligned} \quad (3.28)$$

where D can be the Identity matrix I , the diagonal of A , or even a block diagonal of A .

Setting:

$$N = I - \omega D^{-1} A, \quad (3.29)$$

and truncating this series, we define a polynomial preconditioner of degree k as:

$$p_k(A) = [I + N^1 + N^2 + \cdots + N^k] D^{-1}. \quad (3.30)$$

Denote the exact solution of $Ax = b$ as $x = A^{-1}b$ and the approximate solution by $p_k(A)$ as $x' = p_k(A)b$. The error of between x' and x is bounded as:

$$\begin{aligned} \|x - x'\| &= \|A^{-1}b - p_k(A)b\| \\ &= \|(I - p_k(A)A)A^{-1}b\| \\ &= \|N^{k+1}A^{-1}b\| \leq \|N\|^{k+1}\|A^{-1}b\|. \end{aligned} \quad (3.31)$$

The performance of precondition by Neumann can be improved with the enlargement of polynomial degree of p_k , but matrix operation can be difficult numerically for large k .

3.6.3.3 Minimum-maximum Polynomials

In order to accelerate the convergence with the degree k as small as possible, a kind of minimum-maximum polynomials are proposed. Let us define a polynomial preconditioner more abstractly as any polynomial $P_d(A)$ of degree d .

The iterates of this polynomial to approximate the solution can be written as

$$x_d = x_0 + P_d(A)r_0. \quad (3.32)$$

Where x_0 is a selected initial approximation to the solution, r_0 the corresponding residual norm, and P_d a polynomial of degree $d - 1$. We set a polynomial of d degree R_d such that

$$R_d(\lambda) = 1 - \lambda P_d(\lambda). \quad (3.33)$$

The residual of d^{th} steps iteration r_d can be expressed as equation

$$r_d = R_d(A)r_0. \quad (3.34)$$

with the constraint $R_d(0) = 1$. We want to find a kind of polynomial which can minimize $\|R_d(A)r_0\|_2$, with $\|\cdot\|_2$ the Euclidean norm.

If A is a $n \times n$ diagonalizable matrix with its spectrum denoted as $\sigma(A) = \lambda_1, \dots, \lambda_n$, and the associated eigenvectors u_1, \dots, u_n . Expanding the initial residual vector r_0 in the basis of these eigenvectors as

$$r_0 = \sum_{i=1}^n \rho_i u_i \quad (3.35)$$

moreover, then the residual vector r_d can be expanded in this basis of these eigenvectors as

$$r_d = \sum_{i=1}^n R_d(\lambda_i) \rho_i u_i \quad (3.36)$$

which allows to get the upper limit of $\|r_d\|$ as

$$\|r_d\|_2 \leq \|r_0\|_2 \max_{\lambda \in \sigma(A)} |R_d(\lambda)| \quad (3.37)$$

In order to minimize the norm of r_d , it is possible to find a polynomial P_d which can minimize the Equation (7.2). And it tends to be a minimum-maximum problem with the constraint $R_d(0) = 1$ and $\lambda \in \sigma(A)$

$$\min \max_{\lambda \in \sigma(A)} |R_d(\lambda)| \quad (3.38)$$

In order to resolve the last problem, a well known method is the Chebyshev iterative method, where H is taken to be an ellipse with center c and focal distance d , which contains the convex hull of $\lambda(A)$. If the origin is outside of this ellipse, the minimal polynomial can be reduced to a scaled and shifted Chebyshev polynomial:

$$R_n(\lambda) = \frac{T_n(\frac{c-\lambda}{d})}{T_n(\frac{c}{d})} \quad (3.39)$$

The three terms recurrence of Chebyshev polynomial induces an elegant algorithm (shown as Algorithm 15) for generating the approximation x_n that uses only three vectors of storage. But there are several constraints with this method, the most important is that the optimal ellipse which encloses the spectrum, often does not accurately represent the spectrum, which may result in slow convergence.

Algorithm 15 Polynomial Preconditioned GMRES

- 1: Start or Restart:
 - 2: Compute current residual vector $r = b - Ax$
 - 3: Adaptive GMRES step:
 - 4: Run m_1 steps of GMRES for solving $Ad = r$.
 - 5: Update x by $x = x + d$.
 - 6: Get eigenvalue estimates from the eigenvalues of the Hessenberg matrix.
 - 7: Compute new polynomial:
 - 8: Refine H from previous hull H and new eigenvalue estimates.
 - 9: Get new best polynomial p_k .
 - 10: Polynomial Iteration:
 - 11: Compute the current residual vector $r = b - Ax$.
 - 12: Run m_2 steps of GMRES applied to $p_k(A)Ad = p_kAr$.
 - 13: Update x by $x = x + d$.
 - 14: Test for convergence.
 - 15: If solution converged then Step, else GoTo 1.
-

3.6.3.4 Least Squares Polynomial Method

Based on the normalized Chebyshev polynomial, the Least Squares polynomials methods are introduced. In fact, the spectrum of A is discrete, it is possible to introduce one or more polygonal regions without the origin, which has a relatively small number of edges instead of ellipses ([Smolarski \[1982\]](#)). The problem tends to find a polynomial P_n on the boundary of H which we note as ∂H , that maximizes the modulus of $|1 - \lambda P_n(\lambda)|$. And then we get the least square problem with respect to some weight $w(\lambda)$ on the boundary of H and the constraint $R_n(0) = 1$.

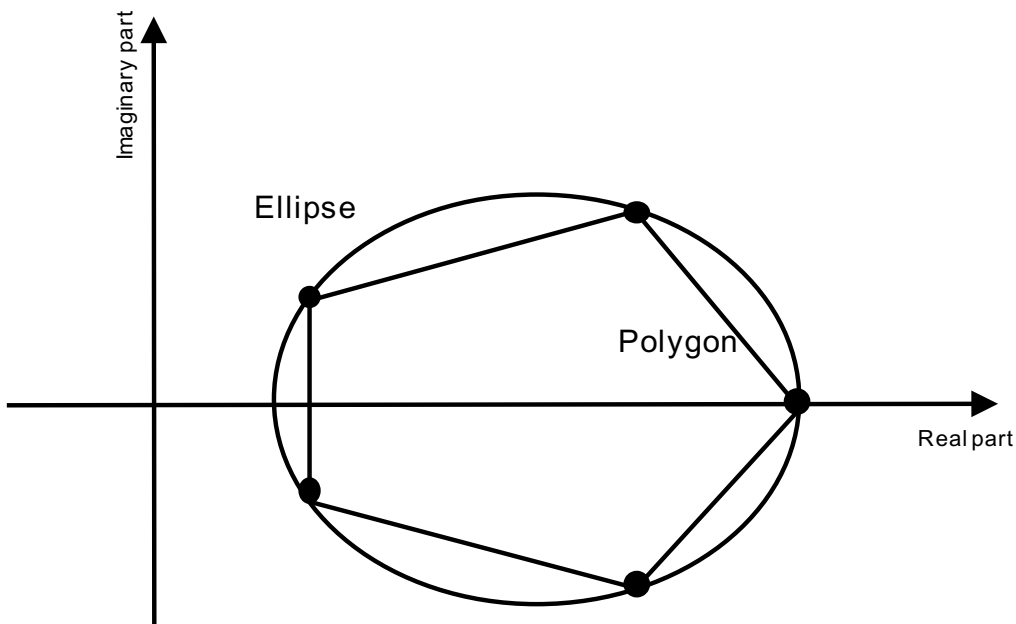


Figure 3.3 – The polygon of samllest area containing the convex hull of $\lambda(A)$.

Weight Function and Gram Matrix

Suppose that matrix A is real, we know that its spectrum is symmetric with the real axis, which means we will only need the upper half part H^+ of the convex hull H .

Suppose that ∂H^+ the upper part of boundary H and $v = 1, \dots, \mu$ that $\partial H^+ = \cup_{v=1}^{\mu} E_v$. And then, suppose c_v and d_v , the center and focal distance of edge E_v . The inner product of two complex polynomials associated with the weight function ω_v on the edge E_v can be expressed as the expression (11).

$$(p, q)_w = 2\Re(\sum_{v=1}^{\mu} \int_{E_v} p(\lambda) \overline{q(\lambda)} w_v(\lambda) d\lambda) \quad (3.40)$$

$$w_v(\lambda) = \frac{2}{\pi} |d_v^2 - (\lambda - c_v)^2|^{-\frac{1}{2}} \quad (3.41)$$

The function (12) is the weight function sur one edge E_v generated by the basis of Chebyshev polynomials (expression 13), which facilite to calculate the inner product.

$$T_i\left(\frac{\lambda - c_v}{d_v}\right) \quad (3.42)$$

When we project p and q into this basis on the edge E_v , we could get the equations (14) and (15), then the inner product will result into equation (16).

$$p(\lambda) = \sum_{i=0}^n \xi^v T_i\left(\frac{\lambda - c_v}{d_v}\right) \quad (3.43)$$

$$q(\lambda) = \sum_{i=0}^n \zeta^v T_i\left(\frac{\lambda - c_v}{d_v}\right) \quad (3.44)$$

$$(p, q)_w = 2\Re\left[\sum_{v=1}^{\mu} 2\xi_0^v \bar{\zeta}_0^v + \sum_{i=1}^{\mu} 2\xi_1^v \bar{\zeta}_1^v\right] \quad (3.45)$$

And then, suppose that t_j the Chebyshev basis on the ellipse $\xi(c, d, a)$ with $j \geq 0$, and we can obtain the three terms recurrence with $i \geq 0$ such as equation (18).

$$t_j(\lambda) = \frac{T_j \frac{\lambda - c}{d}}{T_j \frac{a}{d}} \quad (3.46)$$

$$\beta_{i+1} t_{i+1}(z) = (z - a) t_i(z) - \delta_i t_{i-1}(z) \quad (3.47)$$

With this polynomial basis, we can obtain a so-called modified Gram matrix $M_n = m_{i,j}$, which is well-conditioned. The entries of M_n defined by the relation (19) where $i, j \in 1, \dots, n+1$, and we can express the inner production formula (16) into the equation (20) with $\eta = (\eta_1, \dots, \eta_n)$ and $\theta = (\theta_1, \dots, \theta_n)$, which are the coordinates of polynomials p and q in basis t_i .

$$m_{i,j} = (t_{i-1}, t_{j-1})_{\omega} \quad (3.48)$$

$$(p, q)_\omega = (M_n \eta, \theta) \quad (3.49)$$

Expanding the polynomial P_n into the Chebyshev basis, and then we can get R_n as equation (22), and in the end we obtain the equation (23) with the three terms recurrence (18).

$$P_n = \sum_{i=0}^{n-1} \eta_i t_i \quad (3.50)$$

$$\begin{aligned} R_n(\lambda) &= 1 - \lambda P_n(\lambda) \\ &= 1 - \sum_{i=0}^{n-1} \eta_i \lambda t_i(\lambda) \end{aligned} \quad (3.51)$$

$$R_d(\lambda) = t_0 - \sum_{i=0}^{n-1} \eta_i (\beta_{i+1} t_{i+1} + \alpha_i \eta_i + \delta_i \eta_{i+1}) t_i. \quad (3.52)$$

Then we can express R_n into $e_1 - T_n \eta$ with its coordinates in the polynomial t_i , where T_n is a $(n+1) \times n$ matrix as (24).

$$T_n = \begin{bmatrix} \alpha_0 & \delta_1 & & & & \\ \beta_1 & \alpha_1 & \delta_2 & & & \\ & \beta_2 & \alpha_2 & \delta_3 & & \\ & & & & \ddots & \\ & & & & & \delta_{n-1} \\ & & & & \beta_{n-1} & \alpha_{n-1} \\ & & & & & \beta_n \end{bmatrix} \quad (3.53)$$

With the definition of inner product in the polynomial basis, the function which needs to be minimized can be expressed under the form of equation (25). As M_n is symmetric, we can get the factorization of M_n under the form $M_n = L_n L_n^T$, and in the end we obtain the equation (26) with $F_n = L_n^T T_k$ a $(n+1) \times n$ upper Hessenberg matrix.

$$\begin{aligned} \|R_n\| &= (R_n, R_n)_\omega \\ &= (M_n(e_1 - T_n \eta), e - T_n \eta). \end{aligned} \quad (3.54)$$

$$\begin{aligned} \|R_n\| &= (R_n, R_n)_\omega \\ &= (L_n^T(e_1 - T_n \eta), L_n^T(e_1 - T_n \eta)) \\ &= \|L_n^T(e_1 - T_n \eta)\|_2 \\ &= \|l_{1,1} - F_n \eta\| \end{aligned} \quad (3.55)$$

The coefficients η_i are the solution of problem $\min \|l_{1,1}e_1 - F_n \eta\|_2$ with $\eta \in IR^n$. This problem can maybe resolved easily by Givens rotations and QR fatorization. The process

to generate the least polynomials by the eigenvalues are given in Algorithm 16.

Non-Hermitian Linear Systems

TO DO

Calcul the Iteration Form

In order to resolve the minimum-maximum problem, a well known method is to use the Chebyshev polynomial, where H_k is taken to be an ellipse with center c and focal distance d . This ellipse contains the convex hull of $\sigma_k(A)$. If the origin is outside of this ellipse, the minimal polynomial can be reduced to a scaled and shifed Chebyshev polynomial:

$$R_d(\lambda) = \frac{T_d\left(\frac{c-\lambda}{d}\right)}{T_d\left(\frac{c}{d}\right)} \quad (3.56)$$

The three terms recurrence of Chebyshev polynomial introduces an elegant algorithm for generating the approximation x_d that uses only three vectors of storage. The choice of ellipses as enclosing regions in Chebyshev acceleration maybe overly restrictive and ineffective if the shape of the convex hull of the unwanted eigenvalues bears little resemblance to an ellipse. There are several research to find the acceleration polynomial to minimize its L_2 -norm on the boundary of the convex hull of the unwanted eigenvalues with respect to some suitable weight function ω . An algorithm based on the modified moments for computing the least square polynomial was proposed by Youcef Saad ([Saad \[1987b\]](#)). The problem tends to find a polynomial P_d on the boundary of H_k which we note as ∂H_k , that maximizes the modulus of $|1 - \lambda P_d(\lambda)|$. And then we get the least square problem with respect to some weight $w(\lambda)$ on the boundary of H_k and the constraint $R_d(0) = 1$.

The iteration form of Least Square is $x_d = x_0 + P_d(A)r_0$ with P_d the least square polynomial of degree $d - 1$ under the Formula (3.57). The polynomial basis t_i meet the three terms recurrence relation (3.58).

$$P_d = \sum_{i=0}^{d-1} \eta_i t_i. \quad (3.57)$$

$$t_{i+1}(\lambda) = \frac{1}{\beta i + 1} [\lambda t_i(\lambda) - \alpha_i t_i(\lambda) - \delta_i t_{i-1}] \quad (3.58)$$

For the computation of parameters $H = (\eta_0, \eta_1, \dots, \eta_{d-1})$, we construct a modified gram matrix M_d with dimension $d \times d$, and matrix T_d with dimension $(d + 1) \times d$ by the three terms recurrence of the basis t_i . M_d can be factorized to be $M_d = LL^T$ by the Cholesky factorization. The parameters H can be computed by a least squares problem of the formula

$$\min \|l_{11}e_1 - F_d H\| \quad (3.59)$$

We therefore need to compute the vectors $\omega_i = t_i(A)r_0$, and get the linear combination

of formula (3.57). The recurrence expression of ω_i is given as (3.60) and the final solution value as (3.61). The hybrid GMRES preconditioned by least squares polynomial methods is given as Algorithm 17.

$$\omega_{i+1} = \frac{1}{\beta_{i+1}}(A\omega_i - \alpha_i\omega_i - \delta_i\omega_{i-1}) \quad (3.60)$$

$$\begin{aligned} x_d &= x_0 + P_d(A)r_0 \\ &= x_0 + \sum_{i=1}^{d-1} \eta_i \omega_i. \end{aligned} \quad (3.61)$$

Algorithm 16 Least Square Polynomial Generation

```

1: function LSP(input:  $A, b, d, \Lambda_r$ , output:  $A_d, B_d, \Delta_d, H$ )
2:   construct the convex hull  $C$  by  $\Lambda_r$ 
3:   construct ellispe( $a, c, d$ ) by the convex hull  $C$ 
4:   compute parameters  $A_d, B_d, \Delta_d$  by ellispe( $a, c, d$ )
5:   construct matrix  $T$   $(d+1) \times d$  matrix by  $A_d, B_d, \Delta_d$ 
6:   construct Gram matrix  $M_d$  by Chebyshev polynomials basis
7:   Cholesky factorization  $M_d = LL^T$ 
8:    $F_d = L^T T$ 
9:    $H_d$  satisfies  $\min \|l_{11}e_1 - F_d H\|$ 
10: end function

```

Algorithm 17 Hybrid GMRES Preconditioned by Least Squares Polynomial

```

1: Compute current residual vector  $r = b - Ax$ 
2: Run  $m_1$  steps of GMRES for solving  $Ad = r$ .
3: Update  $x$  by  $x = x + d$ .
4: Get eigenvalue estimates from the eigenvalues  $\Lambda_r$  of the Hessenberg matrix.
5: LSP(input:  $A, b, d, \Lambda_r$ , output:  $A_d, B_d, \Delta_d, H$ )
6:  $r_0 = f - Ax_0$ ,  $\omega_1 = r_0$  and  $x_0 = 0$ 
7: for  $k = 1, 2, \dots, s_{use}$  do
8:   for  $i = 1, 2, \dots, d-1$  do
9:      $\omega_{i+1} = \frac{1}{\beta_{i+1}}[A\omega_i - \alpha_i\omega_i - \delta_i\omega_{i-1}]$ 
10:     $x_{i+1} = x_i + \eta_{i+1}\omega_{i+1}$ 
11:   end for
12: end for
13: set  $x_0 = x_d$ 
14: Test for convergence.
15: If solution converged then Step, else GoTo 1.

```

3.7 GMRES Convergence Analysis

Many things have been proposed over the years to explain GMRES convergence:

- Eigenvalues of A ;
- Pseudo-eigenvalues;
- Polynomial numerical hull.

This section summarize these discussions.

3.7.1 Convergence Analysis by Eigenvalues

TO DO

Gérard MEURANT completely describes GMRES convergence for normal matrices. Convergence depends on the eigenvalues of A and on its eigenvectors and b through the weights.

When A is normal, GMRES convergence depends on the eigenvalues and eigenvectors of A .

TO DO

GMRES convergence is governed by the distribution of the eigenvalues of $V^T W$ on the unit circle (and also the weights ω_i). When A is non-normal, GMRES convergence depends on the eigenvalues and eigenvectors of $Q = V^T W$.

Theorem 3.7.1. Denote x_m be the approximate solution obtained from the m -th step of GMRES, and the related residual is $r_m = b - Ax_m$. Then, x_m is of the form:

$$x_m = x_0 + q_m(A)r_0 \quad (3.62)$$

and

$$\|r_m\|_2 = \|(I - Aq_m(A))r_0\|_2 = \min_{q \in \mathbb{P}_{m-1}} \|(I - Aq(A))r_0\|_2 \quad (3.63)$$

Theorem 3.7.2. If A is a $n \times n$ diagonalizable matrix and let $A = P\Lambda P^{-1}$ with $\Lambda = \text{diag}(\lambda_1, \lambda_2, \dots, \lambda_n)$ is the diagonal matrix of eigenvalues. Then the residual norm achieved by the m -th step of GMRES satisfies the inequality

$$\|r_m\|_2 \leq c_2(P)\epsilon^{(m)}\|r_0\|_2. \quad (3.64)$$

where $\epsilon^{(m)} = \min_{p \in \mathbb{P}_m, p(0)=1} \max_{\lambda \in \sigma(A), i=1, \dots, n} |p(\lambda_i)|$, and $c_2(P) = \|P\|_2\|P^{-1}\|_2$.

The exact proof can be found in ([Saad \[2003\]](#)).

3.7.2 Convergence Analysis by Pseudo-eigenvalues

3.7.3 Convergence Analysis by Polynomial Numerical Hull

Corollary 3.7.2.1. If A is a $n \times n$ diagonalizable matrix and let $A = P\Lambda P^{-1}$ with $\Lambda = \text{diag}(\lambda_1, \lambda_2, \dots, \lambda_n)$ is the diagonal matrix of eigenvalues. Assume that all the eigenvalues

of A are located in the ellipse $E(c, d, a)$ which excludes the origin. The residual norm achieved at the m -th step of GMRES satisfies the inequality.

$$\|r_m\|_2 \leq c_2(P) \frac{C_m(\frac{a}{d})}{|C_m \frac{c}{d}|} \|r_0\|_2. \quad (3.65)$$

3.8 Parallel Krylov methods on Large-scale Supercomputers

Krylov subspace methods are generally implemented in parallel on the supercomputers to solve very large linear systems and eigenvalue problems. This section discusses the scheme to implement Krylov methods in parallel.

3.8.1 Core Operations in Krylov Methods

It is necessary to identify the main operations in Krylov methods before the parallel implementation. Consider Algorithm 2, 5 and 7. We distinguish four types of operations, which are:

- Matrix-vector products in step 5 of Algorithm 2;
- AXPY operation in step 7 of Algorithm 2;
- Dot products in step 8 of Algorithm 2;
- Orthogonalization of vector for the loop from step 4 to 6 in of Algorithm 2.

This section gives the parallel implementation of these four operations in details.

3.8.1.1 AXPY Operation

AXPY is in the form:

$$y = \alpha x + y. \quad (3.66)$$

With x and y two vectors, and α is a scalar. This operation is used to *update vectors* inside Krylov subspace methods. On distributed memory platforms, it is necessary to assume that the vectors x and y should be distributed in the same manner across all the processor. The distributed AXPY is simple without requiring communication. It can be regarded as several AXPY of local vectors in serial on each processor.

3.8.1.2 Dot product and Global Reduction Operation

The dot product is the operation that use all the components of given vectors to compute a single floating-point scalar. In the Arnoldi reduction process, this scalar is always needed by all processors. Equation (3.67) gives the formula of dot product operation.

$$v \cdot w = \langle v_1, v_2, \dots, v_n \rangle \cdot \langle w_1, w_2, \dots, w_n \rangle = v_1w_1 + v_2w_2 + \dots + v_nw_n. \quad (3.67)$$

The distributed version of the dot-product is needed to compute the inner product of two vectors v and w and then distribute the result across all the processors. This types of operations are termed the *All Reduction Operations*, which can be seen as the combination *Reduction Operations* and *Broadcast Operations*. In Krylov subspace methods, the dot-product operation is typically needed to perform the vector update on each processor. If the number of processors is large, this kind of operations can introduce enormous communication costs. The computation of the Euclidean norm of distributed vectors is also a global reduction operation which is similar to the dot-product.

3.8.1.3 Orthogonalization of Vector

In the Arnoldi reduction (as shown by Algorithm 2) for non-Hermitian matrices, the vector Av_i should be orthogonalized against all the previous vectors. In practice, the classic Gram-Schmidt process is preferred than the Modified Gram-Schmidt, even the presence of round-offs and cancellations within CGS diminish its numerical stability. In CGS, the orthogonalization process is overlapped, while the same process of MGS has a data dependency, which is not possible to get good parallel performance. A preconditioner or a reorthogonalization process can compensate the deficiency of numerical stability.

3.8.1.4 Matrix-vector products

In practice, the parallel version of Arnoldi orthogonalization is memory/communication bounded. The most critical operation with the high communication intensity is the substantial number of matrix-vector multiplications Av_i . Krylov subspaces are often used to solve linear systems and eigenvalue problems associated with the sparse matrix. Its parallel implementation depends heavily on the data structure to store the matrix. Different distributed sparse matrix format introduces different matrix-vector implementation scheme and finally results in the different parallel performances.

The standard used sparse matrix storage format includes: COO (Coordinate lists) which stores respectively the row index, column index and values into three arrays; CSR (Compressed Sparse Row) which stores respectively the row offset, the column index and data values into three arrays; ELLPACK which stores the column index and values into

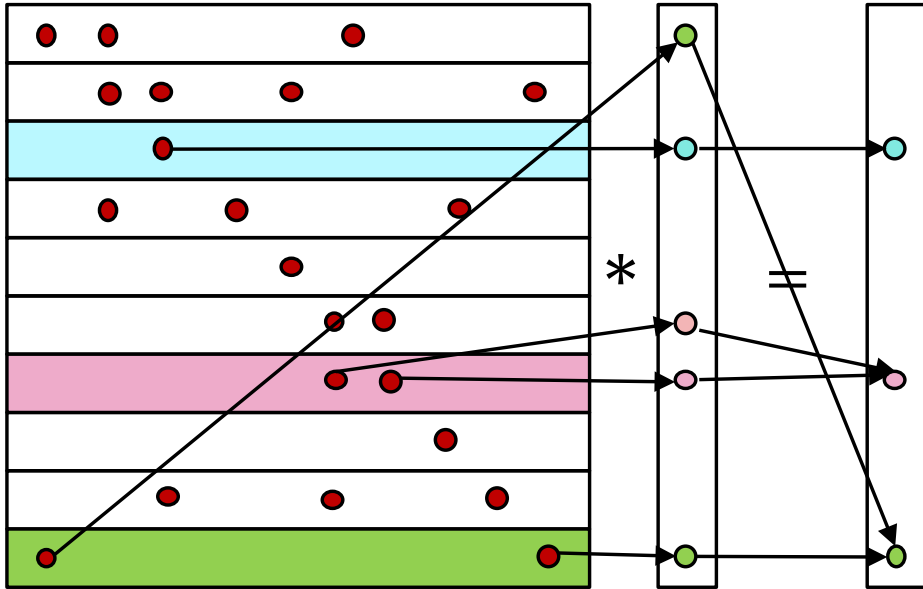


Figure 3.4 – Communication Scheme of SpMV.

two two-dimensional arrays according their row index; and DIA (Diagonal format) which store the diagonal offsets into one-dimensional array, and the values sorted by diagonal into a two-dimensional array.

For the parallel implementation of SpMV on modern parallel systems, the matrix with selected storage format should be distributed across different processors with considering the load balance and reduction of communications. Fig. 3.4 gives the communication scheme of SpMV on distributed memory memory systems.

3.8.1.5 Parallel GMRES on Distributed Memory Systems

Fig. 3.5 describes the parallel implementation of the Arnoldi reduction process inside GMRES. For each loop inside, it can be divided into two parts: the Gram-Schmidt and the normalization processes. The SpMV in Gram-Schmidt process is implemented in parallel with the communication among the processors, and the distributed version of dot-product operation is the combination of *Reduction* and *Broadcast* Operations, which introduce a synchronization point, and the AXPY is implemented in parallel without communications. In the normalization process, the computation of the norm of the distributed vectors also introduce the synchronization points. In the Arnoldi reduction, this loop is executed in sequence for m times to generate an orthonormal basis in the m -dimensional Krylov subspace.

3.8.2 Existing Softwares

Recent years, there are several efforts to provide the parallel Krylov methods on different computing architectures. This section gives a glance at two famous ones of them.

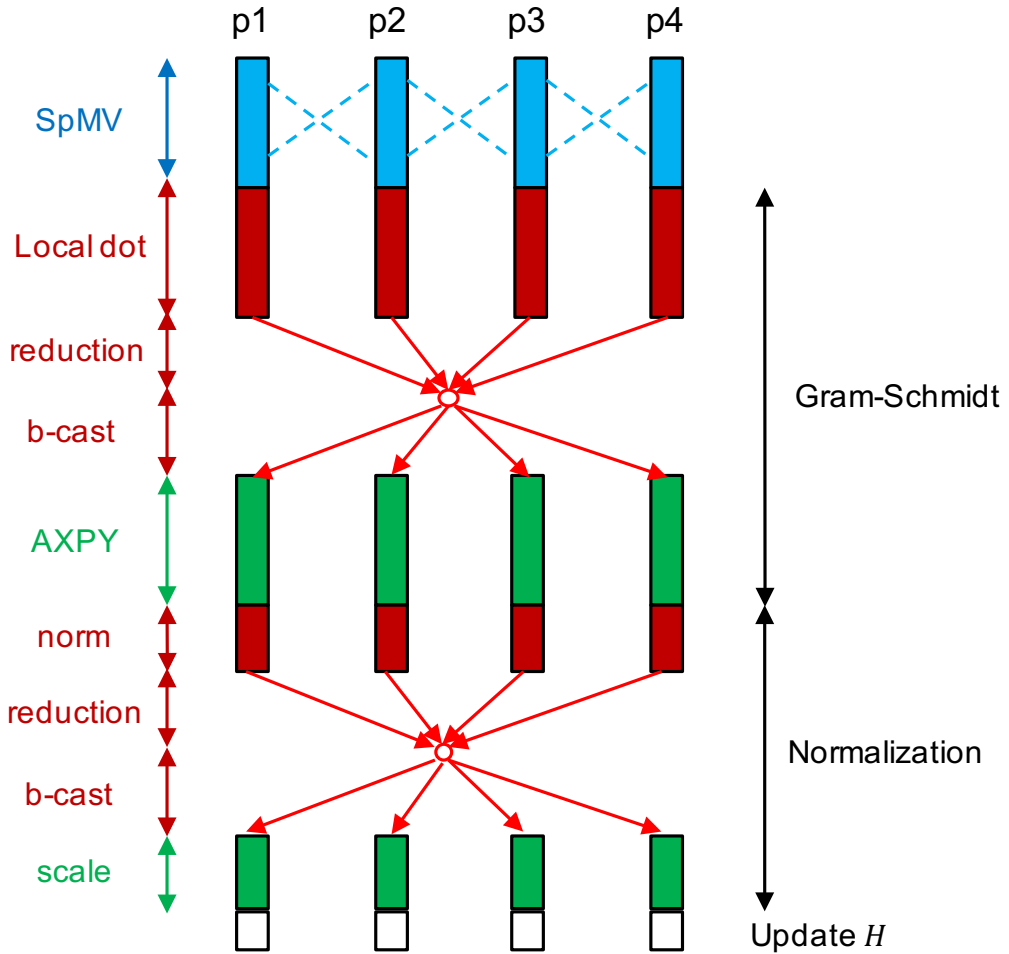


Figure 3.5 – Classic Parallel implementation of Arnoldi reduction.

3.8.2.1 PETSc/SLEPc

The Portable, Extensible Toolkit for Scientific Computation (**PETSc**) ([Balay et al. \[2001\]](#)), is a suite of data structures and routines developed by Argonne National Laboratory for the scalable (parallel) solution of scientific applications modeled by partial differential equations. It employs the Message Passing Interface (MPI) standard for all message-passing communication. PETSc provides many of the mechanisms needed within parallel application code, such as simple parallel matrix and vector assembly routines that allow the overlap of communication and computation. PETSc provides the parallel implementation of Krylov methods and several preconditioners.

The Scalable Library for Eigenvalue Problem Computations (**SLEPc**) ([Hernandez et al. \[2005b\]](#)) is a software library for the parallel computation of eigenvalues and eigenvectors of large, sparse matrices. It can be seen as a module of PETSc that provides solvers for different types of eigenproblems, including linear (standard and generalized) and nonlinear (quadratic, polynomial and general), as well as the SVD. Recent versions also include support for matrix functions. It uses also the MPI standard for paralleliza-

tion. Both real and complex arithmetic are supported, with single, double and quadruple precision. When using SLEPc, the application programmer can use any of the PETSc's data structures and solvers. Other PETSc features are incorporated into SLEPc as well. The module *EPS* in SLEPc provides Krylov subspace methods such as Krylov-Schur, Arnoldi and Lanczos to solve sparse eigenvalue problems.

3.8.2.2 Trilinos

Trilinos ([Heroux et al. \[2005\]](#)) is a collection of open-source software libraries, intended to be used as building blocks for the development of scientific applications. The word "Trilinos" is Greek and conveys the idea of "a string of pearls," suggesting a number of software packages linked together by a common infrastructure. Trilinos was developed at Sandia National Laboratories from a core group of existing algorithms and utilizes the functionality of software interfaces such as the BLAS, LAPACK, and MPI (the message-passing interface for distributed-memory parallel programming). Fortunately, Trilinos supports many different packages which are defined to implement the iterative linear and eigen-solvers methods. There are some packages which are widely used as follows:

- **Kokkos** ([Edwards et al. \[2014\]](#)): Kokkos Core implements a programming model in C++ for writing performance portable applications targeting all major HPC platforms. For that purpose, it provides abstractions for both parallel executions of code and data management. Kokkos is designed to target complex node architectures with N-level memory hierarchies and multiple types of execution resources. It currently can use OpenMP, Pthreads, and CUDA as backend programming models.
- **Epetra** ([Heroux \[2005\]](#)): Epetra provides the fundamental construction routines and services function that are required for serial and parallel linear algebra libraries. Epetra provides the underlying foundation for all Trilinos solvers.
- **Tpetra** ([Baker and Heroux \[2012\]](#)): Tpetra is the next version of Epetra with better support for shared-memory parallelism. It implements linear algebra objects including sparse graphs, sparse matrices, and dense vectors. Many Trilinos packages and applications produce, modify, or consume Tpetra's linear algebra objects, or depend on Tpetra's parallel data redistribution facilities. Tpetra is “hybrid parallel,” meaning that it uses at least two levels of parallelism: MPI for distributed-memory parallelism and Any of various shared-memory parallel programming models within an MPI process, Tpetra uses the Kokkos package's shared-memory parallel programming model for data structures and computational kernels. Kokkos makes it easy to port Tpetra to new computer architectures and to extend its use of parallel computational kernels and thread-scalable data structures. Kokkos supports several different parallel programming models, including OpenMP, POSIX Threads and

Nvidia’s CUDA programming model for graphics processing units (GPUs). Tpetra has the following unique features:

- Native support for representing and solving very large graphs, matrices, and vectors. “Very large” means over two billion unknowns or other entities;
 - Matrices and vectors may contain many different kinds of data, such as floating-point types of different precision and complex-valued types;
 - Support for many different shared-memory parallel programming models based on Kokkos.
- **AztecOO** ([Heroux \[2004\]](#)): Preconditioners and Krylov subspace methods (conjugate gradient, GMRES, etc.), compatible with Epetra only.
 - **Belos** ([Bavier et al. \[2012\]](#)): Classical and block Krylov subspace methods (implementations of iterated classical Gram-Schmidt (ICGS), classical Gram-Schmidt with a DGKS correction step, implementations of conjugate gradient (CG), block CG, block GMRES, pseudo-block GMRES, block flexible GMRES, and GCRO-DR iterations). Belos is compatible with Epetra and Tpetra.
 - **Anasazi** ([Baker et al. \[2009\]](#)): Parallel eigensolvers, Anasazi is compatible with Epetra and Tpetra. It is a package within the Trilinos Project that uses ANSI C++ and modern software paradigms to implement algorithms for the numerical solution of large-scale eigenvalue problems.
 - **Komplex** ([Day and Heroux \[2001\]](#)): Complex-valued system solver, KOMPLEX is an add-on module to AztecOO that allows users to solve complex-valued linear systems. KOMPLEX solves a complex-valued linear system $Ax=b$ by solving an equivalent real-valued system of twice the dimension.

3.9 Toward Extreme Computing, Some Correlated Goals

This section gives the challenges of numerical methods facing the development of HPC platforms. In Section 2.4, we discussed the tendance of future exascale supercomputing architectures and the related challenges of parallel programming to develop the applications to profit efficiently from these supercomputers. The main objective for the parallel implementation of numerical methods is to minimize the global computing time. The global computing time of an algorithm can be reduced by either accelerating the convergence or improve its parallel scaling performance using much more computing units. In section,

we list in details the correlated goals of iterative methods toward the extreme computing below:

1. **Accelerate the convergence:** When solving linear systems by Krylov subspace, the convergence cannot be guaranteed for the ill-conditioned matrix or the restart strategy all used. Thus, one important issue for the iterative methods is to propose different kinds of preconditioners which have better speedup on the convergence, and also enough numerical stability. Moreover, facing the coming exascale computing, the proposed preconditioners should either with better parallel performance across large number of cores, or be able to promote the asynchronicity, and benefit from the more complex architectures of modern supercomputers.
2. **Minimize the number of communications:** When solving very large problems on parallel architectures, the most significant concern becomes the cost per iteration of the method – typically because of communication and synchronization overheads. In general, the complexity of algorithms (number of operations performed) is used to express their performance rather than the quantity of data movement and communications. In fact, on the exascale computers, the global communications across millions of cores are very expensive and the computing operations inside each core will be nearly free. To address the critical issue of communication costs, researchers need to investigate algorithms that minimize communication. Considering inside the Krylov iterative methods such as such as GMRES, CG, and Lanczos, the operations of loop inside Arnoldi reduction much more global communications.

When matrix A in Krylov subspace methods is very sparse, the sparse matrix-vector multiplication (SpMV) invokes even more communications. Hence, strategies for reducing communication overheads in Arnoldi orthogonalization have been proposed to address this bottleneck. In order to reduce the global communication of SpMV for sparse matrices, the first approach is to select the best sparse matrix storage format, which can produce less communications (e.g. [Montagne and Ekambaram \[2004\]](#); [Liu and Vinter \[2015\]](#); [Stathis et al. \[2003\]](#); [Merrill and Garland \[2016\]](#); [Bell and Garland \[2008, 2009\]](#); [Kreutzer et al. \[2014\]](#); [Ashari et al. \[2014\]](#)). Another approach is to use the Hypergraph Partitioning Models to optimize the SpMV scheme on parallel computers, e.g. in 1999, Catalyurek et al. proposed two computational hypergraph models which avoid this crucial deficiency of the graph model for SpMV ([Catalyurek and Aykanat \[1999\]](#)); Vastenhouw et al. tried to reduce the communication volume of SpMV through a recursive bipartitioning of the sparse matrix ([Vastenhouw and Bisseling \[2005\]](#)); Chen et al. proposed a communication optimization scheme based on the hypergraph for basis computation of krylov subspace methods on multi-GPUs ([Chen et al. \[2014\]](#)); a Locality-aware parallel sparse matrix-vector and matrix-transpose-vector multiplication on many-core processors is introduced

by Karsavuran et al. ([Karsavuran et al. \[2016\]](#)); and spatiotemporal graph and hypergraph partitioning models for SpMV on manycore architectures is presented by Abubaker et al. with better scaling performance through enhancing data locality in the operations [Abubaker et al. \[2018\]](#), etc.

3. **Promote the asynchronicity and reduce the synchronization:** One algorithm often must do the synchronize operations during the computation. The global data synchronization across amount of cores in the distributed memory systems is expensive especially for a hybrid platform with accelerators. Inside Krylov subspace methods, dot product is a good example which needs the global synchronization after its *global reduction*. For the extreme-scale platforms, synchronizations become bottlenecks. Hence, the algorithm should be designed with as few synchronization points as possible.

Attempts have been made to restructure existing algorithms for the exascale computing so that the number of synchronizations is reduced. Communication-avoiding and pipelined variants of Krylov solvers are critical for the scalability of linear system solvers on future exascale architectures. Firstly, the impact of global communication latency at extreme scales on Krylov methods are analyzed by Ashby et al. ([Ashby et al. \[2012\]](#)). The strategy of hiding global synchronization latency in GMRES and the preconditioned CG was presented by Ghysels ([Ghysels et al. \[2013\]](#); [Ghysels and Vanroose \[2014\]](#)); Fujino et al. evaluated performance of parallel computing of revised BiCGSafe and BiCGStar-plus method, and made clear that the revised single synchronized BiCGSafe method outperforms other methods from the view points of elapsed time and speedup on parallel computer with distributed memory ([Fujino and Iwasato \[2015\]](#)); Rupp et al. implemented pipelined iterative solvers with kernel fusion for GPUs [Rupp et al. \[2016\]](#); Sanan et al. presented variants of CG, CR, GMRES which both piplined and flexible ([Sanan et al. \[2016\]](#)); Yamazaki et al. proposed to improving the performance of GMRES by reducing communication and pipelining global collectives ([Yamazaki et al. \[2017\]](#)); Swirydowicz et al. presented low synchronization variants of iterated classical (CGS) and modified Gram-Schmidt (MGS) algorithms that require one and two global reduction communication steps; the reduction operations are overlapped with computations and pipelined to optimize performance ([Swirydowicz et al. \[2018\]](#)), etc. Moreover, on important considerationin for the restructuring an algorithm to reduce synchronization and communication is their numerical stability.

4. **Memory and cache optimization for the heterogeneity and scale:** Extracting the desired performance from environments that offer massive parallelism, especially where additional constraints (e.g., limits on memory bandwidth and energy) are in play, requires more sophisticated scheduling and memory management tech-

niques than have heretofore been applied to linear algebra libraries. Confronting the limits of domain-decomposition in the face of massive, explicit parallelism introduces another form of heterogeneity. Feed-forward pipeline parallelism can be used to extract additional parallelism without forcing additional domain-decomposition, but it exposes the user to dataflow hazards. Ideas relating to a data-flow-like model, where parallelism is expressed explicitly in DAGs, allows for dynamic scheduling of tasks, support of massive parallelism, and application of common optimization techniques to increase throughput. Approaches for isolating side-effects include explicit approaches that annotate the input arguments to explicitly identify their scope of reference and implicit methods, such as using language semantics or strongly typed elements to render code easier to analyze for side-effects by compiler technology. New primitives for memory management techniques are needed that enable diverse memory management systems to be managed efficiently and in coordination with the execution schedule.

5. **Mixed arithmetic:** One important for the development of numerical methods for the exascale computing is to recognize and exploit the presence of mixed-precision mathematics. Low-precision floating-point arithmetic is a powerful tool for accelerating scientific computing applications, especially those in artificial intelligence. In fact, on the modern computing architectures, the 32-bits operation can achieve at least two times speedup over the performance of 64-bits operations. Additionally, through the combination of 32-bits and 64-bits floating-point arithmetic, where the performance of many linear algebra algorithms can be significantly enhanced by the 32-bits precision operations while maintaining the 64-bit accuracy of the resulting solution. The mixed archmetic can be applied to the different computing architectures including the conventional CPUs and the accelerators such as GPUs. The creation of mixed-precision algorithms allows more effectively utilizing of the heterogeneous hardwares. Little modification of exsiting codes can provide significant speedup by taking into account existing hardware properties.

In 2014, Kouya et al. ([Kouya \[2014\]](#)), evaluate the performance of Krylov subspace methods by using highly efficient multiple precision SpMV. They show that SpMV implemented in these functions can be more efficient. ([Yamazaki et al. \[2015\]](#)), Yamazaki present a mixed-precision Cholesky factorization, which has $1.4\times$ speedup over the standard approach on GPU. Additionally, their studies of using the mixed-precision Cholesky factorization within communication-avoiding variants of Krylov subspace projectionmethods demonstrate that by using the higher precision for this small but critical segment of the Krylov methods, we can improve not only the overall numerical stability of the solvers but also, in some cases, their performance. In 2018, Haidar et al. ([Haidar et al. \[2018\]](#)) investigate how HPC applications can

be accelerated by the mixed arithmetic technique. In details, they developed the architecture-specific algorithms and highly tuned implementations of a solver based on mixed-precision (FP16-FP64) iterative refinement for the general linear system, $Ax = b$, where A is a large dense matrix, and a double precision (FP64) solution is needed for accuracy. Their paper show how using half-precision Tensor Cores (FP16-TC) for the arithmetic can provide up to $4\times$ speedup. Maynard et al. ([Maynard and Walters \[2018\]](#)) present a mixed-precision implementation of Krylov solver for the numerical weather prediction and climate modelling, the beneficial effect on run-time and the impact on solver convergence. The complex interplay of errors arising from accumulated round-off in floating-point arithmetic and other numerical effects is discussed. They employ now the mixed-precision solver in the operational forecast to satisfy run-time constraints without compromising the accuracy of the solution.

6. **Minimize energy consumption:** The generated heat also affects the performance of clusters such as the arising failure rate of hardware, and the energy consumption also becomes a tremendous financial burden for supercomputer centers, because it takes up a large portion in the total cost of ownership (TCO), that is the *Power wall*, another roadrock to approach the exascale computing. The HPC community starts to address this problem in recent years, and it is necessary to build power and energy awareness, control, and efficiency of numerical methods and libraries.

In 2013, an analysis of energy-optimized lattice-Boltzmann CFD simulations from the chip to the highly parallel level is introduced by Wittmann et al. ([Wittmann et al. \[2013\]](#)). Padoin et al. ([Padoin et al. \[2013\]](#)) evaluated the application performance and energy consumption on hybrid CPU+ GPU architecture. In 2015, Anzt et al. ([Anzt et al. \[2015\]](#)) unveil some energy efficiency and performance frontiers for sparse computations on GPU-based supercomputers. Aliaga et al. ([Aliaga et al. \[2015\]](#)) unveil the performance-energy trade-off in iterative linear system solvers for multithreaded processors. In order to gain insights about the benefits of hands-on optimizations, they analyze the runtime and energy efficiency results for both out-of-the-box usage relying exclusively on compiler optimizations, and implementations manually optimized for target architectures, that range from CPUs and DSPs to manycore GPUs.

7. **Multi-level Parallelism:**
8. **Adaptive response to load imbalance:** For the exascale computing with millions of cores and accelerators, even naturally load-balanced algorithms on homogeneous hardware will present many of the same load-balancing problems. Dynamic scheduling based on directed acyclic graphs (DAGs) has been identified as a path

forward, but this approach will require new approaches to optimize for resource utilization without compromising spatial locality. The current implementation DAGs based runtime including StarPU ([Augonnet et al. \[2011\]](#)), OmpSs ([Duran et al. \[2011\]](#)), etc.

9. **Autotuning:** Numerical algorithms and libraries need the ability to adapt to the possibly heterogeneous environment in which they operate. Such adaptation must deal with the complexity of discovering and applying the best algorithm for diverse and rapidly evolving architectures. An automated process would be best, both for productivity and for correctness, where productivity refers both to the development time of the implementation and to the user’s time to solution. The objective is to provide a consistent library interface that, independent of scale and processor heterogeneity, can achieve good performance and efficiency by binding to different underlying code, depending on the configuration. The diversity and rapid evolution of today’s platforms mean that autotuning of libraries such as the BLAS will be indispensable to achieving good performance, energy efficiency, and load balancing across the range of systems. In addition, autotuning has to be extended to frameworks that go beyond libraries, such as optimizing data layout (e.g., blocking strategies for sparse matrix/SpMV kernels), stencil autotuners (since stencils kernels are diverse and not amenable to library calls), and even tuning of the optimization strategy for multigrid solvers (optimizing the transition between the multigrid coarsening cycle and bottom-solver to minimize runtime). Adding heuristic search techniques and combining these with traditional compiler techniques will enhance the ability to address generic problems extending beyond linear algebra.

Aquilanti et al. ([Aquilanti et al. \[2011\]](#)) present a general parallel auto-tuned linear solver approach based on the tuning of the Arnoldi incomplete orthogonalization process within GMRES by monitoring the convergence in order to reduce the time of computation needed for a solver to attain solution. Katagiri et al. ([Katagiri et al. \[2012\]](#)) presented a smart tuning strategy for restart frequency of GMRES with hierarchical cache sizes.

10. **Fault tolerance, resilience:** Computing an incorrect answer quickly is of no use to a scientist. Yet computing with exascale hardware poses several challenges in assessing and assuring the correctness of numerical simulation results. Resilience to faults has been identified as a critical need for future HPC systems [57]; the thousandfold increase in computational capabilities expected over the next decade, along with incorporation of techniques for reducing energy consumption, is predicted to increase the error rate of the largest systems. DOE has several critical mission deliverables, including annual stockpile certification and safety assurance for the NNSA and future energy generation technologies for the Office of Science. Computer simulations

are key to meeting these deliverables and must be resilient enough to complete in time and correctly, in order to meet the respective critical mission need. In many cases, these simulations can take days, weeks, or even months to complete, which increases the computation's exposure to faults. Both hard and soft faults are expected to occur with much greater frequency than on previous hardware. Uncorrected soft faults have the potential to corrupt computed solutions. Hard faults will need to be handled on the fly; halting and restarting an entire application because of the loss of a node, for instance, will be prohibitively expensive at the exascale. Dynamically recovering from either type of fault will introduce nondeterministic variability in resource usage, as will dynamic scheduling of tasks. Because of the nonassociativity of floating-point arithmetic, such nondeterminism will make bitwise reproducibility difficult at best and will complicate code correctness testing procedures, including code verification, where reproducible execution behavior is assumed. Preventing all faults during exascale simulation will be impossible, and nondeterministic execution is likewise unavoidable without potentially severe performance penalties. Fault management will require developments in hardware, programming environments, runtime systems, and programming models; but mathematics will play an important role as well. The issue of correctness is ultimately a mathematical one and will require mathematics-informed solutions. Research will be required in order to devise efficient application-level fault-tolerance mechanisms and new procedures to verify code correctness at scale.

The work of this dissertation try to propose a potential smart multi-level parallel programming with auto-tuning scheme for solving linear systems which address on the goals of acceleration of convergence, minimizing the number of communications, promoting the asynchronicity, reducing the synchronize points and fault tolerance.

CHAPTER 4

Sparse Matrix Generator with Given Spectra

In Chapter 3, we have discussed the convergence of iterative methods and its relation with spectral distribution of linear systems. Indeed, algorithms and applications from diverse fields can be formulated as an eigenvalue problem. The eigenvalues are also extremely important for the preconditioners of solving linear systems. In machine learning and pattern recognition, it is often demanded to solve the eigenvalue problems for both supervised and unsupervised learning algorithms, such as principal component analysis (PCA) ([Croux and Haesbroeck \[2000\]](#)), Fisher discriminant analysis (FDA) ([Berkes \[2005\]](#)), and clustering ([Fender et al. \[2017\]](#)), etc. An insufficient accuracy and a failure of eigenvalue solvers and linear solvers usually result in, respectively, a poor approximation to original discrete problems and a failure of entire algorithms. A good selection of solvers becomes especially essential. Thus it is crucial to have the test matrices to benchmark the numerical performance and parallel efficiency of different methods. In this section, we present the Scalable Matrix Generator with Given Spectra (SMG2S), including its parallel implementation and optimization of both CPU and GPU clusters, the verification mechanism, and the release of open source package.

4.1 Demand of Large Matrices with Given Spectrum

As presented in Chapter 3, nowadays, the size of eigenvalue problems and the supercomputer systems continue to scale up. The whole ecosystem of High-Performance Computing (HPC), especially the linear system applications, should be adjusted to this kind of large clusters. Under this background, there are four special requirements on the test matrices for the evaluation of numerical algorithms on extreme-scale platforms:

1. their spectra must be known and can be customized;

2. they should be both sparse, non-Hermitian and non-trivial;
3. they could have a very high dimension, including the non-zero element numbers and/or the matrix dimension, to evaluate the numerical algorithms on large-scale systems, which means that the proposed matrix generator should be able to be parallelized to profit from the large distributed memory clusters.
4. their sparsity patterns should be controllable.

In order to provide numerically robust solvers of eigenvalue or linear system problems, the researchers need the matrices whose spectra are known, which help to analyze the numerical accuracy. Some scientific communities may be interested in matrices with clustered, conjugated eigenvalues, the closest eigenvalues in random distribution or contained in a specified interval. It is significant to develop a suite of very large Non-Hermitian test matrices whose eigenvalues can be given.

The properties of being sparse, non-Hermitian and non-trivial together can add many mathematical features to simulate the matrices in reality. Besides, the test matrices should have very high dimensions for the experiments on large-scale platforms. This means that the proposed generation method should be easily parallelized to exploit the modern cluster platforms. Furthermore, since the enormous matrix is generated in a parallel way, its different slices are already distributed on separate computing units, which can be directly used to evaluate the required linear and eigenvalue solvers, without concerning loading the large matrix file from the filesystems. It can save time and improve the efficiency for the applications.

In this chapter, we present a Scalable Matrix Generator from Given Spectra (SMG2S) for testing the linear and eigenvalue solvers on large-scale platforms. In Section 4.2, we introduce the related work to propose test matrix collections. In Section 4.3, we give the proof of mathematical framework of SMG2S to generate matrices with given spectra. In Section 4.4, the numerical algorithm and practical implementation of SMG2S are presented. In section 4.5, firstly, we give a naive implementation of SMG2S based on PETSc¹ for homogenous platforms and PETSc+CUDA² for heterogeneous machines with multi-GPU. Then an open source package³ with specific communication optimization based on MPI⁴ and C++ is available. In Section 4.6, the evaluations of its scalability and the accuracy to keep the given spectra are presented on different supercomputing platforms. A mechanism to verify the capacity of the generated matrix to keep the given spectra has been proposed based on the Shifted Inverse Power Method in Section 4.7, and the accuracy verification for various spectral distribution is also presented in this section.

1. Portable, Extensible Toolkit for Scientific Computation.
2. Compute Unified Device Architecture
3. <https://github.com/smg2s/SMG2S>
4. Message Passing Interface.

In Section 4.8, we introduce the SMG2S package as a released software, including the interfaces to different programming languages and scientific computational libraries, the Graphic User Interface (GUI) for verification, and also an example to evaluate the Krylov solvers.

4.2 The Existing Collections

It's rare but there are already several efforts to supply test matrix collections for linear problems. SPARSEKIT ([Saad \[1994a\]](#)) implemented by Y. Saad contains various simple matrix generation subroutines. Z. Bai et al. ([Bai et al. \[1996\]](#)) presented a collection of test matrices for the development of numerical algorithms for solving nonsymmetric eigenvalue problems. There are also two widely spread matrix providers, the Tim Davis collection ([Davis and Hu \[2011\]](#)) and Matrix Market ([Boisvert et al. \[1997\]](#)). They all contain many matrices with various mathematical properties coming from different scientific fields. However, the spectra of matrices in these collections are fixed, and that cannot be whatever we want. A test matrix generation suite with given spectra was already introduced by J. Demmel et al. ([Demmel and McKenney \[1989\]](#)) in 1989 for the benchmark of LAPACK⁵. They proposed the method to transfer the diagonal matrix with given spectra into a dense matrix with same spectra using the orthogonal matrices, and then reduce them to unsymmetric band ones by the Householder transformation. This method requires $\mathcal{O}(n^3)$ time and $\mathcal{O}(n^2)$ storage even for generating a small bandwidth matrix. Moreover, this method was implemented for the shared memory systems, not for larger distributed memory systems, thus it is difficult to generate large-scale test matrices customized for the tests on extreme scale clusters. That is the motivation for us to propose SMG2S which can generate large-scale non-Hermitian matrices with given spectra on modern parallel platforms with much less time and storage, and easily be implemented in distributed memory systems.

4.3 Mathematical Framework

In this Section, we give a summary of the theorem and related proof based on the preliminary theoretical research of H. Gachlier et al. ([Galicher et al.](#)).

Theorem 4.3.1. *Let's consider the matrices $A \in \mathbb{C}^{n \times n}$, $M_0 \in \mathbb{C}^{n \times n}$, $n \in \mathbb{N}^*$. If M verifies:*

$$\begin{cases} \frac{dM(t)}{dt} = AM(t) - M(t)A, \\ M(t = 0) = M_0. \end{cases}$$

5. Linear Algebra PACKage

Then the matrices $M(t)$ and M_0 are similar, $\forall A \in \mathbb{C}^{n \times n}$.

Proof. Denote respectively $\sigma(M_0)$ and $\sigma(M_t)$ the spectra of M_0 and M_t . If M_0 is a diagonalisable matrix, $\forall \lambda \in \sigma(M_0)$, it exists an eigenvector $v \neq 0$ satisfies the relation:

$$M_0 v = \lambda v. \quad (4.1)$$

Denote $v(t)$ by the matrix $B \in I_n$:

$$v(t) = B_t v = e^{tA} B v. \quad (4.2)$$

We can get:

$$\begin{aligned} \frac{d(M_t v(t) - \lambda v(t))}{dt} &= \frac{dM_t}{dt} v(t) + M_t \frac{dv(t)}{dt} - \lambda \frac{dv(t)}{dt} \\ &= A(M_t v(t) - \lambda v(t)) + \lambda A v(t) \\ &\quad - M_t A v(t) + M_t \frac{dB_t}{dt} v - \lambda \frac{dB_t}{dt} v. \end{aligned} \quad (4.3)$$

With the definition of B_t in Equation (4.2), we have:

$$\frac{dB_t}{dt} = AB_t. \quad (4.4)$$

Thus the Equation (4.3) can be simplified as

$$\frac{d(M_t v(t) - \lambda v(t))}{dt} = A(M_t v(t) - \lambda v(t)). \quad (4.5)$$

The initial condition for the Equation (4.5) is:

$$\begin{aligned} M_t v(t) - \lambda v(t)|_{t=0} &= M_0 B v - \lambda B v \\ &= M_0 v - \lambda v \\ &= 0. \end{aligned} \quad (4.6)$$

Hence the solution of the differential Equation (4.5) is 0 and $\forall \lambda \in \sigma(M_0)$, we have $\lambda \in \sigma(M_t)$. Since $\dim(M_0) = \dim(M_t)$, we have $\sigma(M_0) = \sigma(M_t)$. Thus, M_0 and M_t are similiar with same eigenvalues, but different eigenvectors.

□

4.4 Numerical Implementation of SMG2S

Base on the previous mathematical work by H. Gachlier, a matrix M_0 with given spectra can be transferred to another one $M(t)$ that verifies *Theorem 4.3.1* and keeps the spectra

of M_0 . We propose a matrix generation method by selecting many parameters including the matrices A and M_0 .

4.4.1 Matrix Generation Method

The idea is to impose the desired spectra to M_0 and obtain a M_t matrix that verifies the Theorem 1 and our hypothesis. The M_t spectra is the same as M_0 however we recall that the M_t eigenvectors are not the same as M_0 . The idea may seem very simple but many parameters need to be fixed to achieve our objective.

Firstly, we define the linear operator \bar{A} such that:

$$\begin{cases} A_A : M_{n \times n} \rightarrow M_{n \times n}, \\ M \rightarrow AM - MA. \end{cases} \quad (4.7)$$

At the present time, we did not imposed any conditions on the matrix A . The \bar{A}_A operator verifues that:

$$\bar{A}_A(I_d) = 0, \forall A \in M_{n \times n}. \quad (4.8)$$

Based on the Theorem 1 and the linear operator \bar{A}_A definition, we can rewritte the ordinary differential equation such that:

$$\begin{cases} \frac{dM(t)}{dt} = \bar{A}_A(M(t)), \\ M(t=0) = M_0. \end{cases} \quad (4.9)$$

Starting out the Equation (4.9), we apply the exponential operator (which is possible as \bar{A}_A has no time dependency). This leads to the fact that the solution of Equation (4.9), can be expressed as follows:

$$\begin{cases} M_t = e^{(\bar{A}_A t)} M_0, \\ M_t = \sum_{k=0}^{\infty} \frac{t^k}{k!} (\bar{A}_A)^k M_0. \end{cases} \quad (4.10)$$

The k -times power operation of $\widetilde{A}_A(M_0)$ can be given as

$$(\widetilde{A}_A)^k(M_0) = \sum_{m=0}^k (-1)^m C_k^m A^{k-m} M_0 A^m. \quad (4.11)$$

With the loop

$$M_{i+1} = M_i + \frac{1}{i!} (\widetilde{A}_A)^i(M_0), i \in (0, +\infty), \quad (4.12)$$

a very simple initial matrix $M_0 \in \mathbb{C}^{n \times n}$ can be transferred into a new sparse, non-trivial and non-Hermitian matrix $M_{+\infty} \in \mathbb{C}^{n \times n}$, which has the same spectra but different

eigenvectors with M_0 .

However, it is not reasonable to generate a matrix by infinity times of iterations. Thus a good selection of matrix A which can make $\widetilde{(A_A)}^i$ tends to $\mathbf{0}$ in limited steps is very necessary. We define the matrix A as the formula $A = Q^{-1}PQ$ with $Q \in \mathbb{R}^{n \times n}$ and $P \in \mathbb{N}^{n \times n}$. In addition, the matrix P is set to be a nilpotent matrix, which means that there exists an integer k such that: $P^i = 0$ for all $i \geq k$. Such k is called the nilpotency of P . In this paper, we set the matrix Q to be the identity matrix $I \in \mathbb{N}^{n \times n}$ for simplification. Thus A is also a nilpotent matrix. The selection of a nilpotent matrix will influence the sparsity pattern of the upper band of the generated matrix.

The exact shape of A is given in Fig. 4.1. Inside an $n \times n$ matrix A , its entries are default 0, except in the upper diagonal with the distance p to the diagonal. In this diagonal, its entries start with d continuous 1 and a 0, this term repeats until the end. Matrix A should be nilpotent with good choices of the parameters of p , d and n . The determination of this series of matrices to be nilpotent or not might be difficult, but the cases that $p = 1$ or $p = 2$ are straightforward, which can completely fulfill our demands.

If $p = 1$, with $d \in \mathbb{N}^*$, or $p = 2$ with $d \in \mathbb{N}^*$ to be even, the nilpotency of A and the upper band's bandwidth of generated matrix are respectively $d + 1$ and $2pd$. Obviously, there is another constraint that the matrix size n should be greater or equal to the upper band's width $2pd$. For $p = 2$, if d is odd, the matrix A will not be nilpotent, thus we do not take it into account.

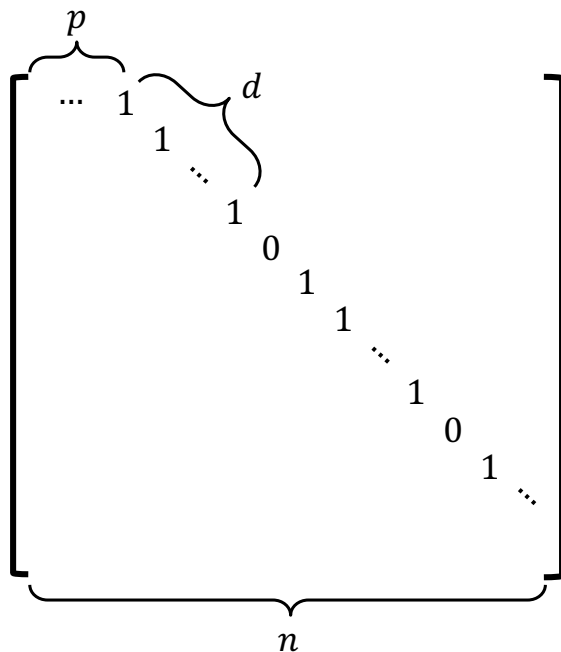


Figure 4.1 – Nilpotent Matrix. p off-diagonal offset, d number of continuous 1, and n matrix dimension.

4.4.2 Numerical Algorithm

As shown in Algorithm 18, the procedure of SMG2S is simple. Firstly, it reads an array $Spec_{in} \in \mathbb{C}^n$, as the given eigenvalues. Then it inserts random elements in h lower diagonals of the initial matrix M_0 , and sets its diagonal to be $Spec_{in}$, and scale it with $(2d)!$. Meanwhile, it generates a nilpotent matrix A with the parameters d and p . The final matrix M_t can be generated as $M_t = \frac{1}{(2d)!} M_{2d}$, where M_{2d} is the result after $2d$ times of loop $M_{i+1} = M_i + (\prod_{k=i+1}^{2d} k)(\widetilde{A}_A)^i(M_0)$. The slight modification of the loop formula is to reduce the potential rounding errors coming from numerous division operations on modern computer systems.

Algorithm 18 Matrix Generation Method

```

1: function MATGEN(input: $Spec_{in} \in \mathbb{C}^n$ ,  $h$ ,  $d$ , output:  $M_t \in \mathbb{C}^{n \times n}$ )
2:   Insert the entries in  $h$  lower diagonals of  $M_o \in \mathbb{N}^{n \times n}$ 
3:   Insert  $Spec_{in}$  on the diagonal of  $M_0$ 
4:    $M_0 = (2d)!M_0$ 
5:   Generate nilpotent matrix  $A \in \mathbb{C}^{n \times n}$  with selected parameters  $d$  and  $p$ 
6:   for  $i = 0, \dots, 2d - 1$  do
7:      $M_{i+1} = M_i + (\prod_{k=i+1}^{2d} k)(\widetilde{A}_A)^i(M_0)$ 
8:   end for
9:    $M_t = \frac{1}{(2d)!} M_{2d}$ 
10: end function
```

For M_t , if M_0 is a lower triangular matrix having h non zero diagonals, it will be a band diagonal matrix, whose number of new diagonals in the upper triangular zone will be at most $2pd - 1$. Thus the maximal number of the bandwidth of matrix M_t is: $width = h + 2pd - 1$, as in Fig. 4.2. In general, researchers use these matrices to test the iterative methods of sparse linear systems. Thus after the generation of band matrix, it can be transferred to be sparse with the help of permutation matrices. Fig. 4.3 gives an example showing the pattern of the generated matrix by SMG2S. In general, researchers use these matrices to test the iterative methods for sparse linear systems. The h lower diagonals of the initial matrix can set to be sparse, which ensures the sparsity of the final generated matrix, as shown in Fig. 4.3. Moreover, the permutation matrix can also be applied to change the sparsity of the generated matrix further.

The operations complexity C of Algorithm 18 is given as:

$$C \approx 2(2d^2 + (4h - 2)d - (h + 5))n - h(h + 1)(h + 4d - 4). \quad (4.13)$$

In Equation (4.13), the complexity of SMG2S is $\max(\mathcal{O}(hdn), \mathcal{O}(d^2n))$. The worst case would be an $\mathcal{O}(n^3)$ problem for operations with large d and h , and it would require $\mathcal{O}(n^2)$ memory storage. But if we want to generate a band matrix with small bandwidth which means $d \ll n$ and $h \ll n$, it turns to be a $\mathcal{O}(n)$ problem with good potential scalability and to consume $\mathcal{O}(n)$ memory storage.

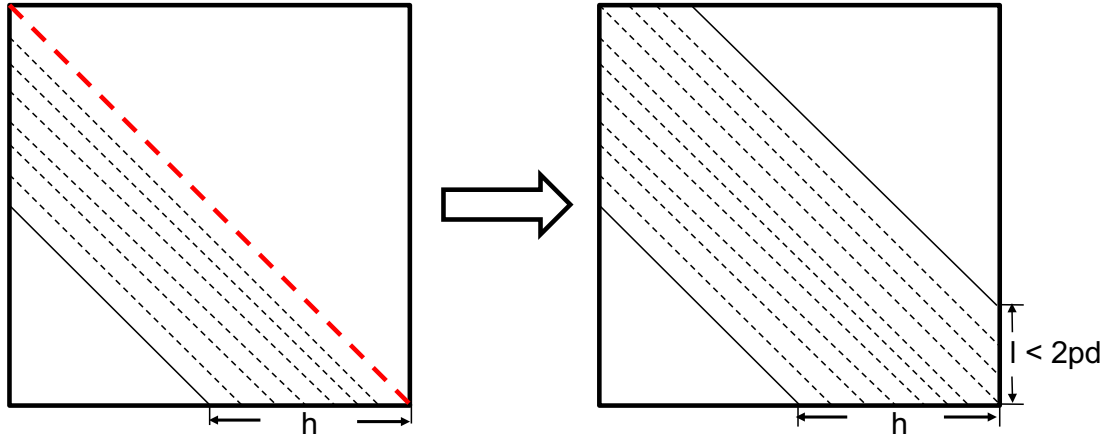


Figure 4.2 – Matrix Generation. The left is the initial matrix M_0 with given spectrum on the diagonal, and the h lower diagonals with random values; the right is the generated matrix M_t with nilpotency matrix determined by the parameters d and p .

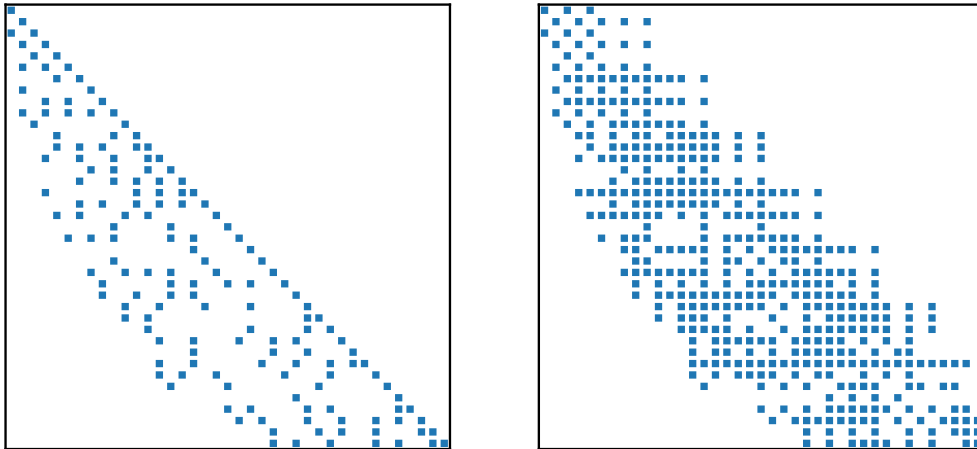


Figure 4.3 – Matrix Generation Pattern Example.

4.5 Parallel Implementation and Evaluation

In this section, we present the parallel implementation of SMG2S for homogeneous and heterogeneous clusters. The former is initially implemented based on MPI and PETSc, and the latter is based on MPI, CUDA, and PETSc. We select the mature library PETSc firstly since it provides several methods to verify the generated matrices, and also the basic operations inside are optimized for different computer architectures. After the validation of matrix generation based on PETSc, an open source parallel software with specific optimized communication is also implemented based on MPI and C++.

4.5.1 Basic Implementation on CPUs

For the initial CPU implementation, we chose PETSc instead of ScaLAPACK because we would like to evaluate the solvers for sparse linear systems. As shown in Algorithm

[18](#), the kernel of generation is the sparse matrix-matrix multiplication (SpGEMM) of AM and MA , and the matrix-matrix addition (AYPX operation) as $AM - MA$. All the sparse matrices during the generation procedure are stored by the block diagonal Compressed Sparse Row (CSR) format which is provided in default by PETSc. We use the matrix operations supported by PETSc to facilitate the implementation. The block diagonal parallel matrix based on MPI are partitioned and stored into several submatrices. For example, if there are three MPI process: $proc1$, $proc2$ and $proc3$, the matrix can be divided into blocks as the Formula (4.14). The submatrix A , B and C is stored in $proc1$, D , E and F in $proc2$, and G , H and I is stored in $proc3$. On each process, the diagonal part and the off-diagonal are separately stored into two sequence block matrices. The parallel SpGEMM and AXPY operations for CPUs are already supported by PETSc ([Balay et al. \[2016a\]](#)). We use these functions directly to facilitate the implementation.

$$\left[\begin{array}{c|c|c} A & B & C \\ \hline D & E & F \\ \hline G & H & I \end{array} \right] \quad (4.14)$$

4.5.2 Implementation on Multi-GPU

PETSc does not supply the SpGEMM and AXPY operations for GPU clusters. Thus we implemented them using MPI, CUDA and cuSPARSE library based on the PETSc data structure definitions. The structure of implementation is given in Fig. 4.4 which uses sparse matrix A and B multiplication as an example. Firstly, the same as in PETSc, A and B are divided into slices, and each slice is saved in a process. In each process of number i , the local matrices are all saved as two separate sequence matrix, noted as A_{dia}^i and A_{off}^i for matrix A^i , B_{dia}^i and B_{off}^i for matrix B^i . Then B_{dia}^i and B_{off}^i are combined together as a novel sequence matrix noted as B_{loc}^i in each process i . With MPI functionalities, each CPU gather all the remote data of matrix B from the other processes, and construct them to a new sequence matrix B_{oth}^i . These matrices from each process are copied to one attached GPU, and calculate $C^i = A_{dia}^i B_{loc}^i + A_{off}^i B_{oth}^i$. The matrix operations on each GPU device is supported by the cuSPARSE. The final result C can be obtained by gathering all slices C_i from all the devices.

4.5.3 Communication Optimized Implementation with MPI

The implementation of SMG2S, especially the parallel SpGEMM kernel's communication can be specifically optimized based on the particular property of nilpotent matrix A . In fact, A can be determined by three parameters p , d and n that we have mentioned in Section 4.4, thus it is not necessary to explicitly implement this parallel matrix. We note this nilpotent matrix as $A(p, d, n)$. Denote that for any matrix J , $J(i, j)$ represents the entry in row i and column j ; $J(i, :)$ represents all the entries of row i ; and $J(:, j)$ represents

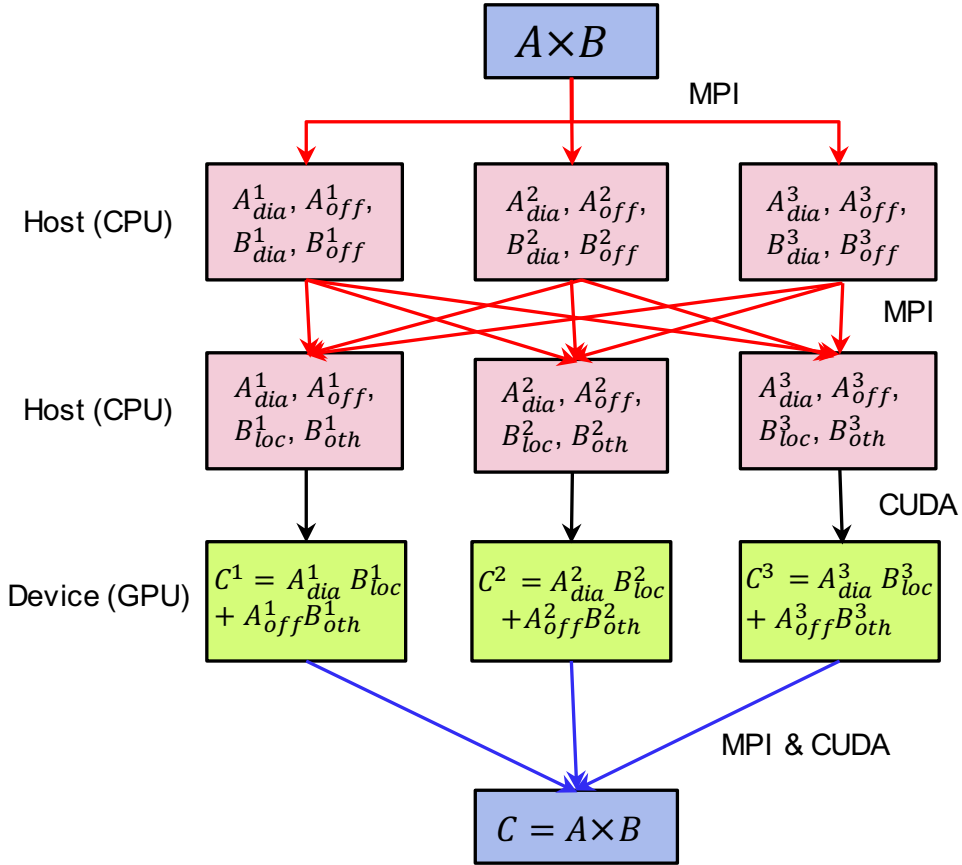


Figure 4.4 – The structure of a CPU-GPU implementation of SpGEMM, where each GPU is attached to a CPU. The GPU is in charge of the computation, while the CPU handles the MPI communication among processes.

all the entries of column j . Then, we observe the effects of right and left-multiplying this nilpotent matrix $A(p, d, n)$ on a general matrix M by basic mathematical matrix operations. As shown in Fig. 4.5, the right-multiplication operation of $A(p, d, n)$ will shift all the entries of first $n - p$ columns to right side with an offset p . Denote MA the result matrix gotten by the right-multiplying A on M (the result of MA operation). We have $MA(:, j) = M(:, j - p), \forall j \in p, \dots, n - 1$, and $MA(:, j) = 0, \forall j \in 0, \dots, p - 1$. Similarly, the left-multiplying $A(p, d, n)$ on M will shift the whole entries of last $n - p$ rows to up side with an offset p . Denote AM the matrix gotten by the left-multiplying A on M (the result of AM operation). We have $AM(i, :) = M(i + p, :), \forall i \in 0, \dots, n - p - 1$, and $AM(i, :) = 0, \forall i \in p, \dots, n - 1$. Moreover, the parameter d decides that $MA(:, r(d + 1)) = 0$ and $AM(r(d + 1), :) = 0$ with $r \in 1, \dots, \lfloor \frac{n}{d+1} \rfloor$.

When thinking about the implementation in parallel on distributed memory systems, the three integer parameters p , d and n can be shared by all MPI processes, and the parallel operations AM and MA are different from the general parallel SpGEMM, which is communication bounded. We analyze these two operations in Fig. 4.5. Firstly, the general matrix M is one-dimensional distributed by row across m MPI process. As shown

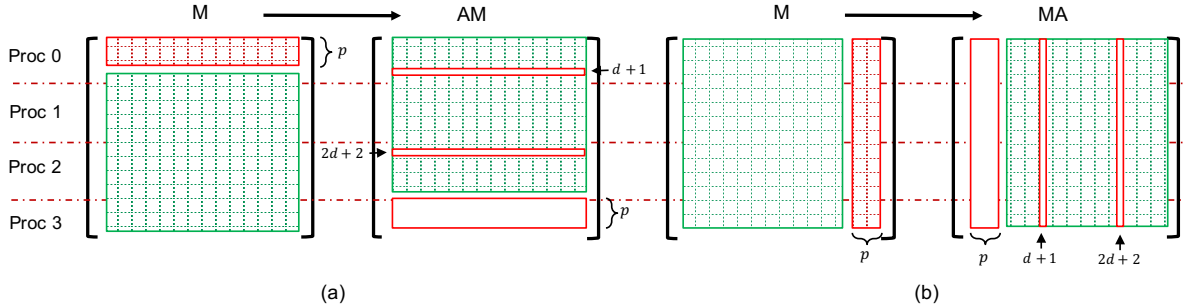


Figure 4.5 – (a) AM operation; (b) MA operation.

in Fig. 4.5 (b), for MA , there is no communication inter different MPI processes since the data are moved inside each row. Assume that $\lfloor \frac{n}{m} \rfloor \geq p$, for AM , the inter communication of MPI takes place when the MPI process k ($k \in 1, \dots, m - 1$) should send the first p rows of their sub-matrix to the closest previous MPI process numbering $k - 1$. The communication complexity for each process is $\mathcal{O}(np)$. When generating the band matrix with low bandwidth b , it tends to be a $\mathcal{O}(bp)$ with $p = 1$ or 2 . The MPI-based optimization implementations of AM and MA are respectively given by Algorithm 19 and 20. The communication inter MPI process is assumed by the asynchronous sending and receiving functions. In this algorithm, M_k , MA_k and AM_k imply the sub-matrices on process k with t rows. The rows and columns of these sub-matrices in Algorithm 19 and 20 are all indexed by the local indices.

Algorithm 19 Parallel MPI AM Implementation

```

1: function AM(input: matrix  $M$ , matrix row number  $n$ ,  $p$ ,  $d$ , proc number  $m$ ; output: matrix  $AM$ )
2:   Distribute  $t$  row blocks  $M_k$  of  $M$  to MPI process  $k$ 
3:   for  $p + 1 \leq i < t$  do
4:     for  $0 \leq j < n$  do
5:       if  $M(i, j) \neq 0$  then
6:          $AM_k(i - p, j) = M_k(i, j)$ 
7:       end if
8:     end for
9:   end for
10:  for  $0 \leq i < p$  do
11:    if  $k \neq 0$  then
12:      isend  $i$ th row  $M_k(i)$  to  $k - 1$ 
13:    end if
14:    if  $k \neq m - 1$  then
15:      irecv  $i$ th row  $M_k(i)$  from  $k + 1$ 
16:       $AM_k(t - p + i) = M_k(i)$ 
17:    end if
18:  end for
19: end function

```

The communication-optimized SMG2S is implemented based on MPI and C++. The submatrix on each process is stored in ELLPACK format, using the key-value map containers provided by C++. The key-value map implementation facilitates the indexing and moving of the rows and columns. We did not implement a GPU version of SMG2S with this kind of communication since its core is the data movement among different computing units, which is not well suitable for multi-GPU architecture.

Algorithm 20 Parallel MPI MA Implementation

```
1: function MA(input: matrix  $M$ , matrix row number  $n, p, d$ , proc number  $m$ ; output:  
    matrix  $MA$ )  
2:   Distribute  $t$  row blocks  $M_k$  of  $M$  to process  $k$   
3:   for  $0 \leq i < t$  do  
4:     for  $p + 1 \leq j < n$  do  
5:       if  $M_k(i, j) \neq 0$  then  
6:          $MA_k(i, j + p) = M_k(i, j)$   
7:       end if  
8:     end for  
9:   end for  
10: end function
```

4.6 Parallel Performance Evaluation

4.6.1 Hardware

In experiments, we implement SMG2S on the supercomputers *Tianhe-2* and *Romeo*. *Tianhe-2* system has been 6 times No.1 and is No.2 in the Top500 list, which is installed at the National Super Computer Center in Guangzhou of China. It is a heterogeneous system made of Intel Xeon CPUs and Intel Knights Corner (KNC), with 16000 compute nodes in total. Each node composes 2 Intel Ivy Bridge 12 cores @ 2.2 GHz. *Romeo* is located at University of Reims Champagne-Ardenne, France. It is also a heterogeneous system made of Xeon CPUs and Nvidia GPUs, with 130 BullX R421 nodes. Each node composes 2 Intel Ivy Bridge 8 cores @ 2.6 GHz and 2 NVIDIA Tesla K20x GPUs. In this article, we do not test SMG2S using the KNC on *Tianhe-2* since our parallel implementation does not support it with good performance.

4.6.2 Strong and Weak Scalability Evaluation

In this section, we will use double-precision real and complex values to evaluate the strong and weak scalability of SMG2S’s different implementations on CPU and multiple GPUs. All the test matrices in this paper are generated with the h set to be 10 and d to be 7. The details of the weak scaling experiments are given in Table 4.1. The matrix size

Table 4.1 – Details for weak scaling and speedup evaluation.

(a) Matrix size for the CPU weak scaling tests on *Tianhe-2*.

CPU number	48	96	192	384	768	1536
matrix size	1×10^6	2×10^6	4×10^6	8×10^6	1.6×10^7	3.2×10^7

(b) Matrix size for the CPU weak scaling on *ROMEO*.

CPU number	16	32	64	128	256
matrix size	4×10^5	8×10^5	1.6×10^6	3.2×10^6	6.4×10^6

(c) Matrix size for the GPU weak scaling and speedup evaluation on *ROMEO*.

CPU or GPU number	16	32	64	128	256
matrix size	2×10^5	4×10^5	8×10^5	1.6×10^6	3.2×10^6

of the strong scaling experiments on *Tianhe-2* with CPUs, *ROMEO* with CPUs and *ROMEO* with GPUs are respectively 1.6×10^7 , 3.2×10^6 and 8.0×10^5 . The results are given in Fig. 4.6, Fig. 4.7 and Fig. 4.8. The weak scaling for the PETSc implementation of SMG2S on *Tianhe-2* trends to be bad when MPI processes number is larger than 768, where the communication overhead becomes dominant for computation. But for the communication optimized SMG2S, both the strong and weak scaling perform well when the MPI process number is larger than 768. The experiments show that SMG2S implemented with GPUs can still have good strong and weak scalability. In conclusion, SMG2S has always good strong scaling performance when d and h are much smaller than the dimension of the matrix n , because it turns to be a $\mathcal{O}(n)$ problem. The weak scalability is good enough for most cases. The reason is that the nilpotent matrix A in SpGEMM is simple with not many non-zero elements, therefore there is not enormous communication among different computing units. The weak scalability has its drawback in case that the computing unit number come to be huge for the SMG2S implementation based on PETSc, where the communication overhead become dominant. The special implementation of communication-optimized SMG2S makes his strong and weak scalability better. It is also shown that the double precision complex type matrix generation takes almost two times time over the double precision real type for the basic SMG2S implementation, but the time consumption of complex and real type matrix generation of optimized SMG2S seems similar. The reason is that there is no numerical values multiplication anymore in the optimized implementation of SMG2S.

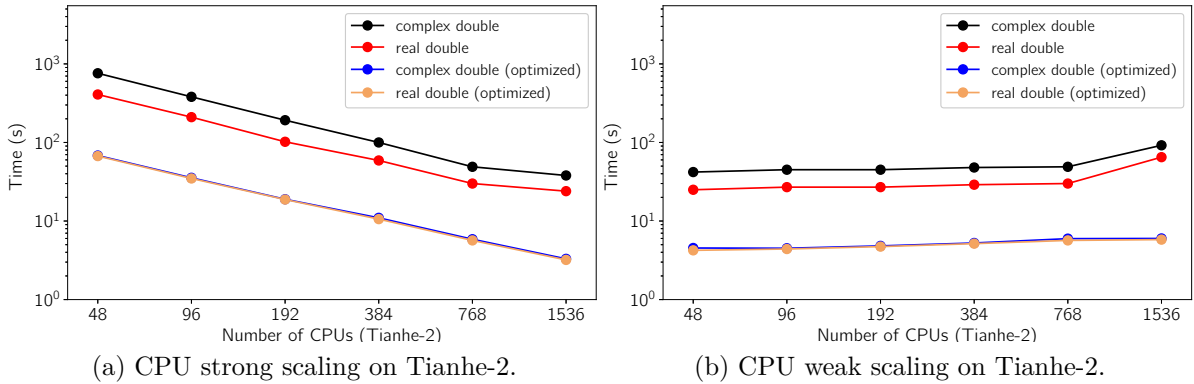


Figure 4.6 – Strong and weak scaling results of SMG2S on different platforms. A base 2 logarithmic scale is used for X-axis, and a base 10 logarithmic scale for Y-axis.

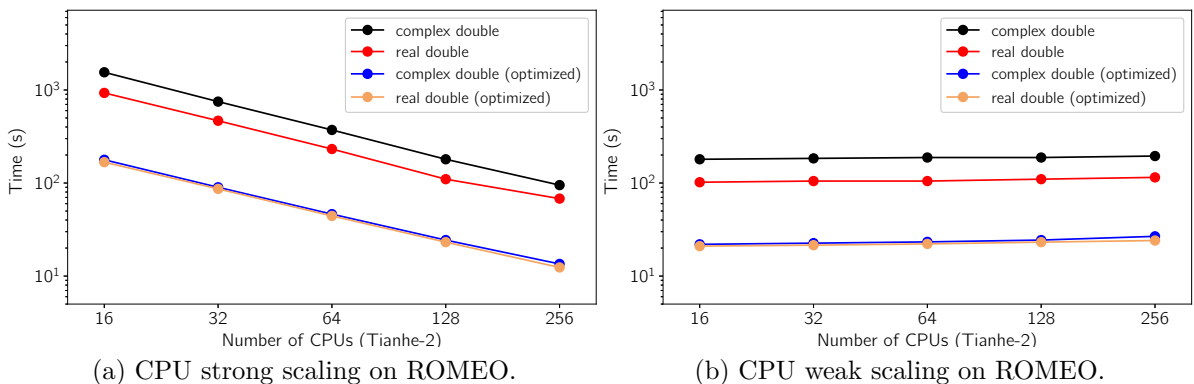


Figure 4.7 – Strong and weak scaling results of SMG2S on different platforms. A base 2 logarithmic scale is used for X-axis, and a base 10 logarithmic scale for Y-axis.

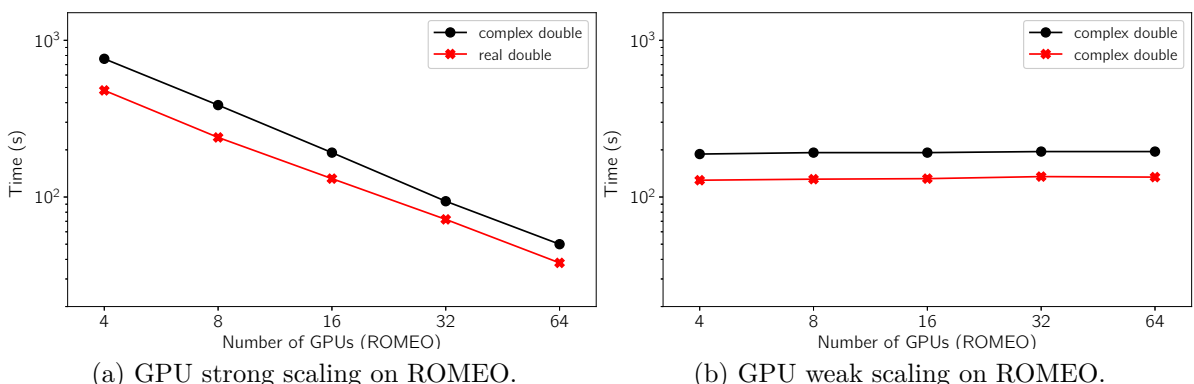


Figure 4.8 – Strong and weak scaling results of SMG2S on different platforms. A base 2 logarithmic scale is used for X-axis, and a base 10 logarithmic scale for Y-axis.

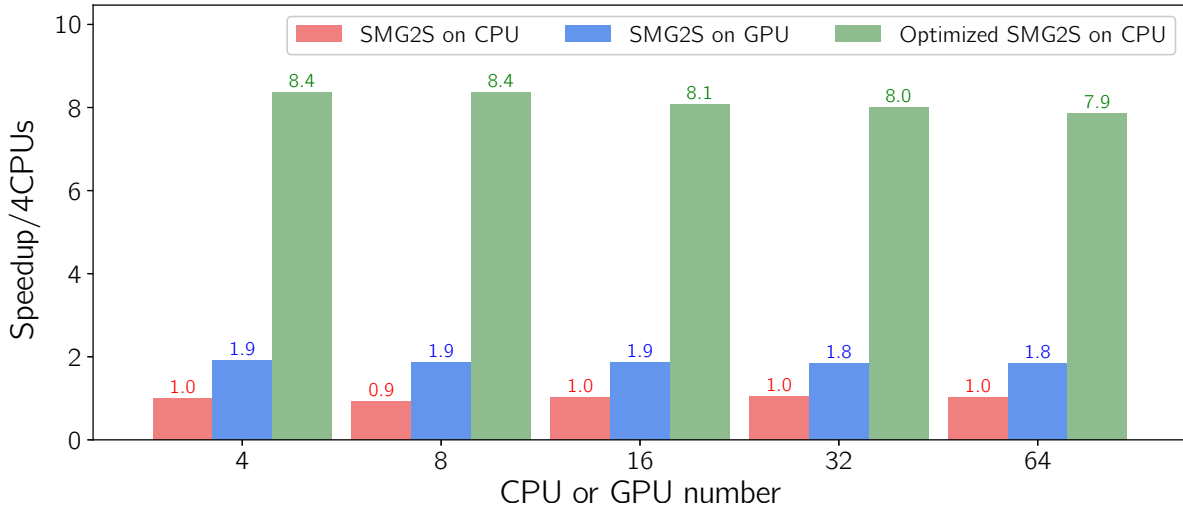


Figure 4.9 – Weak scaling speedup comparison of GPUs on ROMEO.

4.6.3 Speedup Evaluation

The speedup of both SMG2S on multi-GPU and communication-optimized SMG2S on the CPUs compared with the PETSc-based implementation on CPU are also tested on *Romeo*. According to the previous evaluation that complex and real value types always have good scalability, we select the double precision complex values for the speedup evaluation. The details of experiments are also given in Table 4.1c. The results are shown in Fig. 4.9. We can find that the GPU version of SMG2S has almost $1.9\times$ speedup over the PETSc CPU version. The communication-optimized SMG2S on CPUs has about $8\times$ speedup over the basic PETSc CPU version.

4.6.4 Performance Analysis

In conclusion, SMG2S always has good strong scalability when d and h are much smaller than the dimension of the matrix to be generated n , because It turns to be a $\mathcal{O}(n)$ problem. The weak scalability is good enough for most cases. The reason is that the matrices dealt with in SpGEMM are simple with not many non-zero elements. Therefore there are not enormous communication among different computing units. The weak scalability has its drawback in case that the computing unit number come to be huge for the SMG2S implementation based on PETSc, where the communication overhead become dominant. The strong and weak scaling for communication optimized SMG2S is good with its special implementation. It is also shown that the double-complex type matrix generation takes almost two times time over the double-real type for the basic SMG2S implementation. The time consumption of complex and real type matrix generation of optimized SMG2S seems similar. The reason is that in the optimized implementation of SMG2S, there are not numerical values multiplication anymore. It also has the capacity to take advantage of GPUs to accelerate the computation with about 1.9x speedup than CPUs.

The communication optimized version has 8x speedup over the basic implementation.

4.7 Verification Method

In the last section, we show the good parallel performance of SMG2S, and then it is necessary to verify if the generated matrices are able to keep the given spectra with enough accuracy. Generally, the iterative eigenvalue solvers such as the Arnoldi or other Krylov methods ([Petiton \[1992\]](#)) are applied to approximate the dominant eigenvalues. However, the accuracy verification is an opposite case. Now there exists a value, and we want to check if it is an eigenvalue of a given matrix. These iterative methods cannot directly and efficiently deal with this kind of verification. In this section, we present a method for accuracy verification using the Shifted Inverse Power method, which was easily implemented in parallel.

The Power method is an algorithm to approximate the greatest eigenvalue. Meanwhile, the Inverse Power method is a similar iterative algorithm to find the smallest eigenvalue. The middle eigenvalues can be obtained by the Shifted Inverse Power method ([Hernandez et al. \[2005a\]](#)). This method is given in Algorithm 21. Its operation complexity is $\mathcal{O}(n^3)$. The Shifted Inverse Power method is used to compute the eigenvalue which is the nearest one to a given value in a few steps of iterations. The related eigenvector can be easily calculated by its definition and used to check if this given value is an eigenvalue of the matrix.

Algorithm 21 Shifted Inverse Power method

```

1: function SIPM(input: Matrix  $A$ , initial guess for desired eigenvalue  $\sigma$ , initial vector
    $v_0$ , output: Approximate eigenpair  $(\theta, v)$ )
2:    $y = v_0$ 
3:   for  $i = 1, 2, 3 \dots$  do
4:      $\theta = \|y\|_\infty$ 
5:      $v = y/\theta$ 
6:     Solve  $(A - \sigma I)y = v$ 
7:   end for
8: end function

```

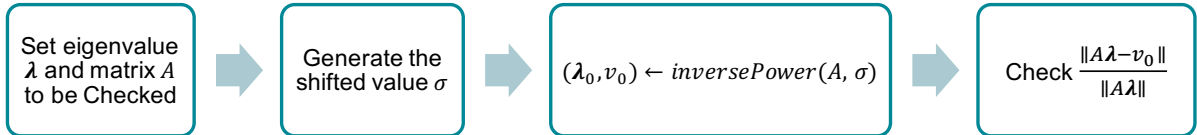


Figure 4.10 – SMG2S verification workflow.

In details, for checking if the given value λ is the eigenvalue of a matrix, we select a shifted value σ which is close enough to λ . An eigenpair (λ', v') with the relation $Av' = \lambda'v'$

can be approximated in very few steps by Shifted Inverse Power method, with λ' is the closest eigenvalue to σ . Since σ is very close to λ , it should be that λ and λ' are the same eigenvalue of a system, and v' should be the eigenvector related to λ . In reality, even if the computed eigenvalue is very close to the true one, the related eigenvector may be quite inaccurate. For the right eigenpairs, the formula $Av' \approx \lambda v'$ should be satisfied. Based on this relation, we define the relative error as Formula (4.15) to quantify the accuracy.

$$\text{error} = \frac{\|Av' - \lambda v'\|}{\|Av'\|} \quad (4.15)$$

If $\lambda' = \lambda$, this *error* should be 0, if not, this generated matrix do not have an exact eigenvalue as λ . In real experiments, the exact solution cannot always be guaranteed with the arithmetic rounding errors of floating operations during the generation. A threshold could be set for accepting it or not.

Table 4.2 – Accuracy Verification Results.

Matrix N^o	Size	Spectra	Acceptance (%)	max <i>error</i>
1	100	<i>Spec1</i>	93	2×10^{-2}
2	100	<i>Spec2</i>	94	3×10^{-2}
3	100	<i>Spec3</i>	100	7×10^{-5}
4	100	<i>Spec4</i>	100	3×10^{-7}

4.7.1 Experimental Results

In the experiments, we test the accuracy of SMG2S with four selected cases among the various tests of different spectral distributions. Fig. 7.3 and Fig. ?? are cases of clustered eigenvalues with different scales. Fig. 4.12 is a special case with the dominant part of eigenvalues clustered in a small region. Fig. 4.14 is a case that composes the conjugate and closest pair eigenvalues. These figures compare the difference between the given spectra (noted as initial eigenvalues in the figures) and the approximated ones (noted as computed eigenvalues) by the Shifted Inverse Power Method. Clearly, the matrices generated by SMG2S can keep almost all the given eigenvalues in the four cases even they are very clustered and close. The acceptance threshold is set to be 1.0×10^{-3} .

This acceptance for cases of Fig. 7.3, Fig. ??, Fig. 4.12 and Fig. 4.14 are respectively 93%, 100%, 94% and 100%. The maximum *error* for them are respectively 3×10^{-2} , 7×10^{-5} , 3×10^{-2} and 3×10^{-7} . After the tests, we conclude that SMG2S is able to keep accurately the given spectra even for the very clustered and closest eigenvalues. In some cases, a very little number of too clustered eigenvalues may result in the inaccuracy of given ones, but in general, the generated matrix can fulfil the need to evaluate the linear

system and eigenvalue solvers.

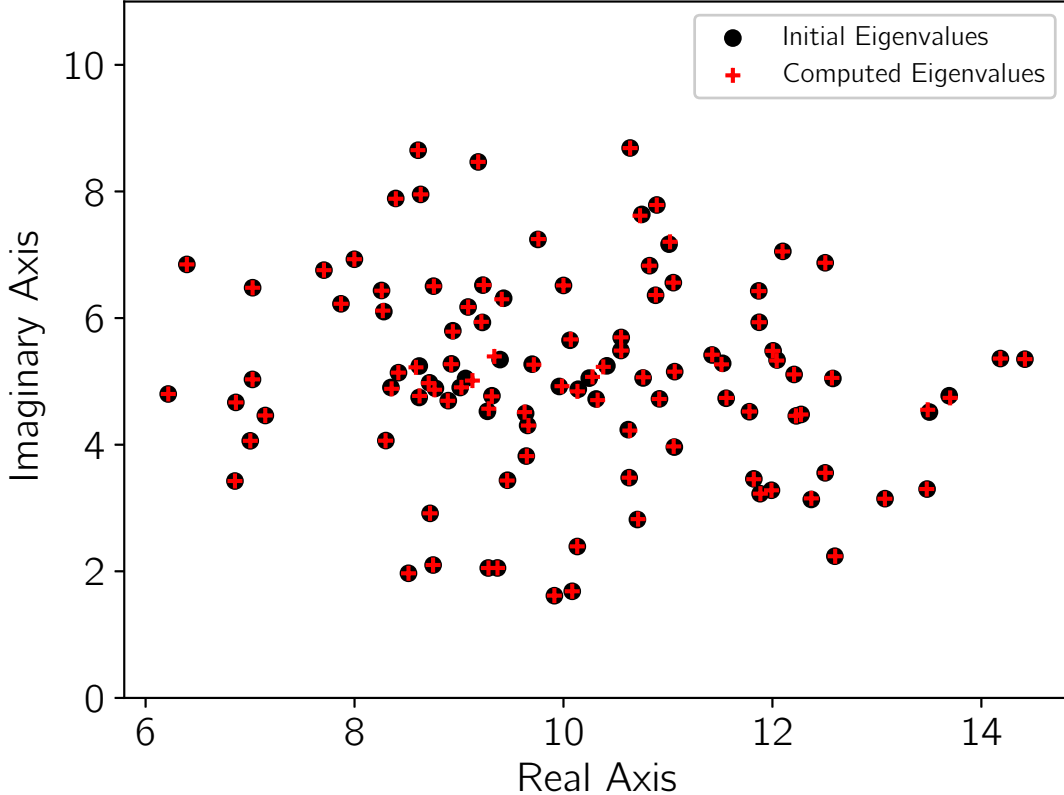


Figure 4.11 – Spec1: Clustered Eigenvalues I.

4.7.2 Arithmetic Precision Analysis

Any floating operations will introduce rounding errors, which cannot be ignored for the generation of large matrices. Regarding the non-Hermitian matrix, its eigenvalues may be extremely sensitive to perturbation. This sensibility is bounded by $\text{bound}(\lambda) \leq \|E\|_2 \text{Cond}(\lambda)$, with $\text{Cond}(\lambda)$ the condition number of related eigenvalue λ and $\|E\|_2$ the Euclidean norm of errors (Saad [2011]). $\text{Cond}(\lambda) = 1$ for the Hermitian matrices, but for the non-Hermitian ones, it can be excessively high. There are two solutions facing this problem. The first one is to ensure the eigenvalue to be well-conditioned. The second is to use the integer value for the matrix generation, since only integers and the operations $+$, $-$, and \times on the microprocessor can make absolutely exact computations. As shown in Algorithm 18, most of the operations in SMG2S are $+$, $-$ and \times , except the step 8 with a division operation. Without step 8, we could introduce a special SMG2S fully using integers to avoid the risks of rounding errors. The spectra of the generated matrix will be $(2d)!$ times of the given one. Moreover, the upper band's width of generated depends on the parameter d . The factorial of $2d$ can easily reach the limit of integer, even with unsigned long long type. Thus a special factorial function using multiple integers should be implemented in order to enlarge the upper band's width.

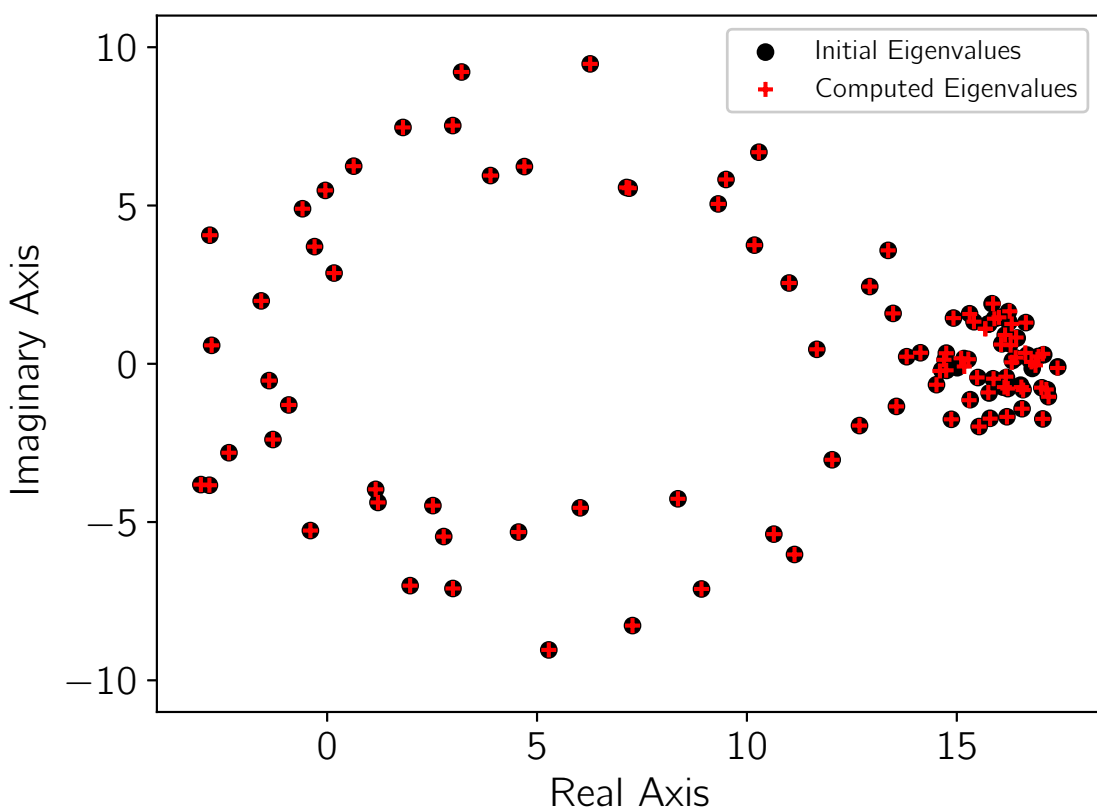


Figure 4.12 – Spec1: Clustered Eigenvalues I.

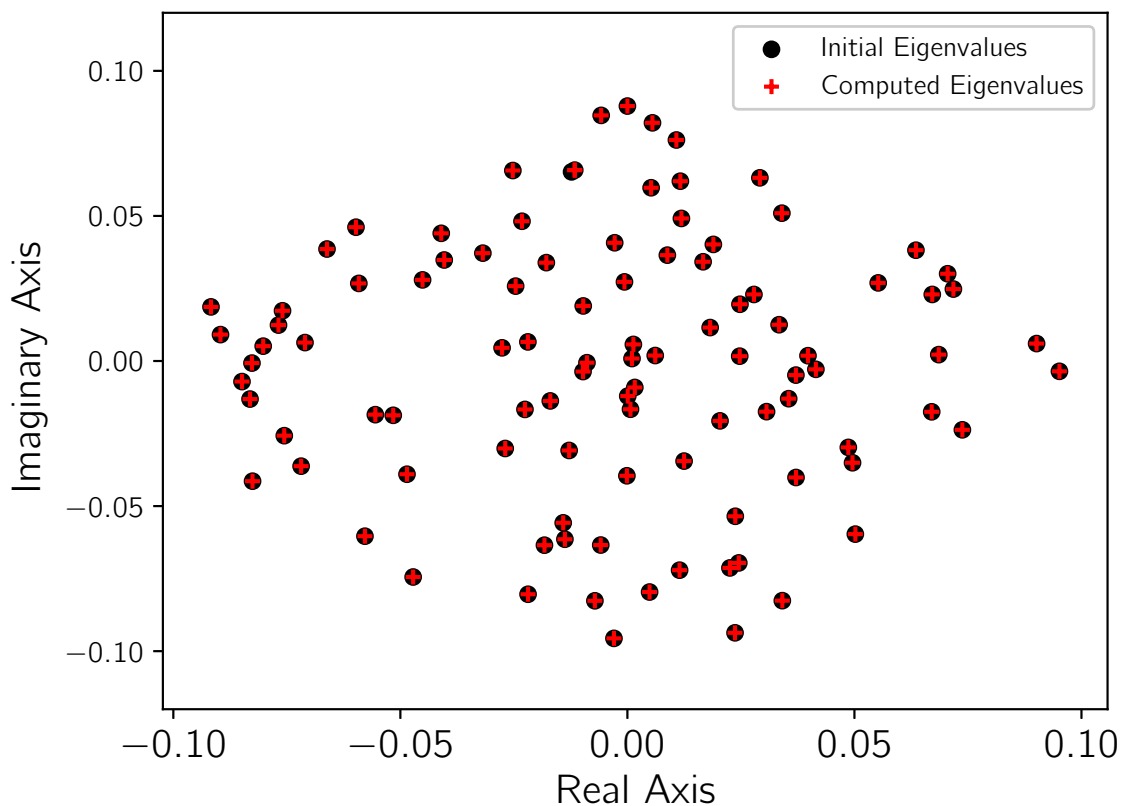


Figure 4.13 – Spec3: Clustered Eigenvalues III.

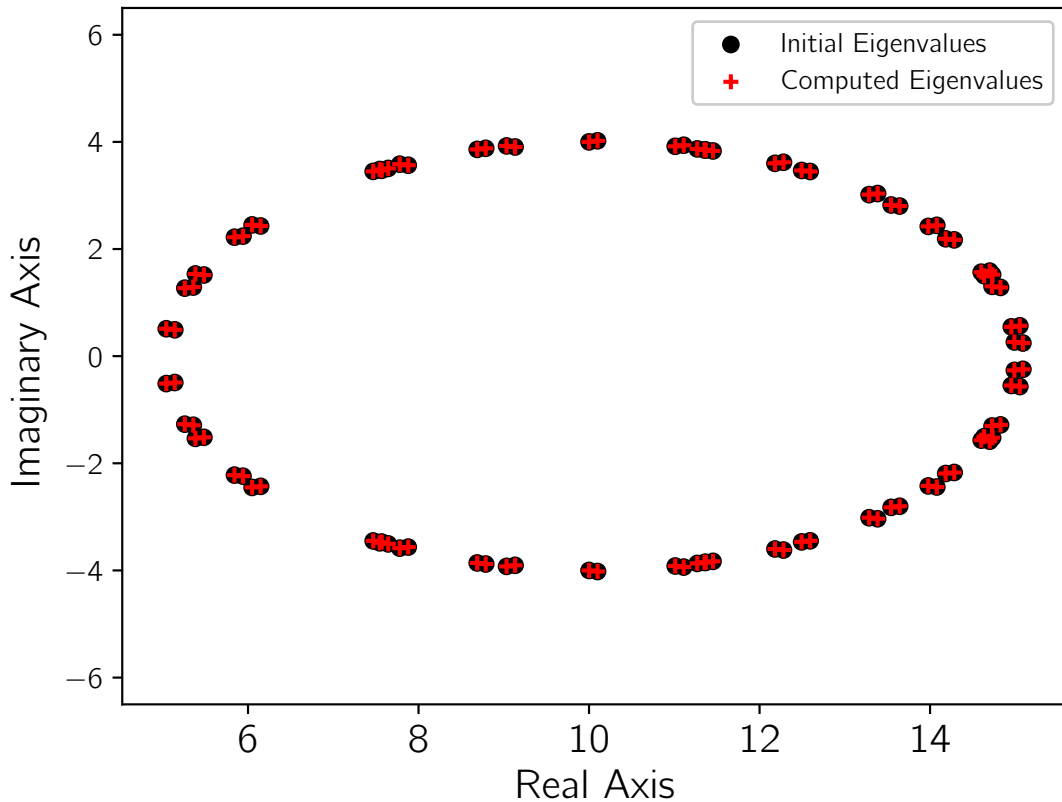


Figure 4.14 – Spec4: Conjugate and Closest Eigenvalues.

4.8 Package, Interface and Application

SMG2S is packaged and released as an open source software based on MPI and C++. In this section, we present firstly the package information of SMG2S and its interface to various programming languages and scientific computational libraries. More details of package can be found in the related manual ([Wu \[2018\]](#)). Then, we give an example which uses SMG2S to evaluate different Krylov solvers.

4.8.1 Package

4.8.1.1 Installation Prerequisites

Before the use of SMG2S, the below packages and libraries should be available on the computer platforms:

1. C++ Comiler with c++11 support;
2. MPI;
3. CMake (version minimum 3.6)
4. (Optional) PETSc and SLEPc are necessary for the verification of accuracy of generated matrices to keep the given spectra.

4.8.1.2 Functions and Directory Structure

SMG2S provides the following subsets of function, including the setup of parallel matrix and vector, the construction of special nilpotent matrix, the matrix generation function, the interfaces to other languages/libraries and the verification mechanism.

- **Parallel Vector and Matrix:** this part presents the functions implemented in SMG2S to establish parallel vector and matrix over distributed memory platforms.
- **Nilpotent Matrix Object:** this part presents a special nilpotent matrix object for the matrix generation procedure in SMG2S.
- **Generating Matrix with prescribed eigenvalues:** this part gives the way to use SMG2S to generate required test matrices.
- **Interface to Other Languages/Libraries:** this part introduces the interface of SMG2S to other languages and existing scientific computational libraries such as PETSc and Trilinos.
- **Verification of Eigenvalues of Generated Matrix:** this part gives the way to verify the accuracy of eigenvalues of generated matrices comparing with given spectrum. A graphic user interface is also provided to facilitate the comparison.

4.8.1.3 Generation Workflow

SMG2S is a collection of C++ include headers, this section gives the workflow to generate test matrices by SMG2S. The C++ template support of SMG2S allows generating matrices of different sizes, scalar types, and precisions.

1. Include the head file

```
#include <smg2s/sm2s.h>
```

2. Generate the Nilpotent Matrix Object:

```
Nilpotency<int> nilp;
nilp.NilpType1(length, probSize);
```

3. Create the parallel Sparse Matrix Object Mt:

```
parMatrixSparse<std::complex<double>, int> *Mt;
```

4. Generate a new matrix by SMG2S:

```
MPI_Comm comm; //working MPI Communicator
Mt = smg2s<std::complex<double>, int>(probSize, nilp,
lbandwidth, spectrum, comm);
```

Here, in step 4, the **probsize** parameter represent the matrix size, **nilp** is the nilpotency matrix object that we have declared previously in step 2, **lbandwidth** is the bandwidth of lower-diagonal band. **spectrum** is the file path of spectra file, if **spectrum** is set as " ", SMG2S will use the function provided inside to generate the spectral distribution. **comm** is the basic object used by MPI to determine which processes are involved in a communication.

The given spectra file is in **pseudo-Matrix Market Vector format**. For the complex eigenvalues, the given spectrum is stored in three columns as below, the first column is the coordinates, the second column is the real part of complex values, and the third column is the imaginary part of complex values.

```
%%MatrixMarket matrix coordinate complex general
3 3 3
1 10 6.5154
2 10.6288 3.4790
3 10.7621 5.0540
```

For the eigenvalues values, the given spectrum is stored in two columns as below, the first column is the coordinates, the second column is related values.

```
%%MatrixMarket matrix coordinate real general
3 3
1 10
2 10.6288
3 10.7621
```

If the users want to generate the eigenvalues in time without loading from local file, they can customize their eigenvalues generation by the function **specGen** in the file [./verification/tests/specGen.h](#), and set the parameter **spectrum** of **smg2s** to be " ".

```
template<typename T, typename S>
void parVector<T,S>::specGen( std :: string spectrum )
```

In this function, the eigenvalues are stored by the distributed vector **textcolor{blue}{parVector}**. And the filling of values on this **parVector** can be done by the method **SetValueGlobal** implemented in **parVector**, which takes the global indices to set values.

We know that the low band bandwidth of initial matrix can be set by the parameter **lbandwidth** of **smg2s**. Additionaly, the distribution of entries of initial matrix can also be customized by the function **matInit** provided by the file [./verification/tests/specGen.h](#). En default, these entries are filled in random. The different mechanism to fill them will influence the sparsity of final generated sparse matrix.

```
template<typename T, typename S>
```

```
void matInit(
    parMatrixSparse<T, S> *Am,
    parMatrixSparse<T, S> *matAop,
    S probSize,
    S lbandwidth
)
```

In this function, distributed matrix *Am* and *matAop* should be filled with the same way. And these entries of matrix can be filled by the method [Loc_SetValue](#) implemented in [parMatrixSparse](#). [Loc_SetValue](#) uses the [global indices](#) of matrix to set values.

4.8.2 Interface To Scientific Libraries

Until now, SMG2S provides interfaces to C, Python, PETSc and Trilinos.

4.8.2.1 Interface to C

SMG2S install command will generate a shared library [libsmg2s.so](#) ([libsmg2s2c.dylib](#) on OS X platform) into `${INSTALL_DIRECTORY}/lib`. It can be used to profit the C wrapper of SMG2S.

A minimum example to use the interface of SMG2S to C:

```
#include <interface/C/c_wrapper.h>

/*create Nilpotency object*/
struct NilpotencyInt *n;
n = newNilpotencyInt();
NilpType1(n, 2, 10);
/*create the parallel Sparse Matrix Object*/
struct parMatrixSparseRealDoubleInt *m;
m = newParMatrixSparseRealDoubleInt();
/*Generation by SMG2S*/
smg2sRealDoubleInt(m, 10, n, 3, "□", MPI_COMM_WORLD);
/*Release Nilpotency Object and parMatrixSparse Object*/
ReleaseNilpotencyInt(&n);
ReleaseParMatrixSparseRealDoubleInt(&m);
```

SMG2S provides the C interface to different data types. For the data type of matrix size, it can be either *int* or *longint*; for the data type of matrix entries, it can be either *complex* or *real* with *single* or *double* precision.

C interface implements the Nilpotent Matrix object for both *int* and *long int* as below:

```
struct NilpotencyInt;
struct NilpotencyLongInt;
```

For all the public functions in parMatrixSparse Object and smg2s function, **SUFFIX** below can be added them to provides the implementations for different data types:

- *ComplexDoubleLongInt*;
- *RealDoubleLongInt*;
- *ComplexDoubleInt*;
- *RealDoubleInt*;
- *ComplexSingleLongInt*;
- *RealSingleLongInt*;
- *ComplexSingleInt*;
- *RealSingleInt*.

4.8.2.2 Interface to Python

SMG2S uses SWIG to generate the wrapper of SMG2S to Python. This interface is available through the Python pacjage management system *pip*

```
#install online from pypi
CC=mpicxx pip install smg2s
#run
mpirun -np 2 python generate.py
```

Before the utilization, make sure that **mpi4py** is installed.

4.8.2.3 Interface to PETSc

SMG2S provides the interface to scientific computational softwares PETSc/SLEPc.

The way of Usage:

1. Include the header file:

```
#include <interface/PETSc/petsc_interface.h>
```

2. Create parMatrixSparse type matrix :

```
parMatrixSparse<std :: complex<double>,int> *Mt;
```

3. Restore this matrix into CSR format :

```
Mt->Loc_ConvertToCSR();
```

4. Create PETSc MAT type :

```
MatCreate(PETSC_COMM_WORLD,&A);
```

5. Convert to PETSc MAT format :

```
A = ConvertToPETSCMat(Mt);
```

Here are the example of [Arnoldi](#), [GMRES](#), and another [Krylov](#) method.

4.8.2.4 Interface to Trilinos/Teptra

SMG2S is able to convert its distributed to the CSR one-dimensional distributed matrix defined by Teptra in Trilinos.

The way of usage:

1. Include header file

```
#include <interface/Trilinos/trilinos_interface.hpp>
```

2. Create parMatrixSparse type matrix :

```
parMatrixSparse<std :: complex<double>,int> *Mt;
```

3. Create Trilinos/Teptra MAT type :

```
parMatrixSparse<std :: complex<double>,int> *Mt;
```

4. Convert to Trilinos MAT format :

```
K = ConvertToTrilinosMat(Mt);
```

[Here is a full example of Trilinos.](#)

4.8.3 Graphic User Interface for Verification

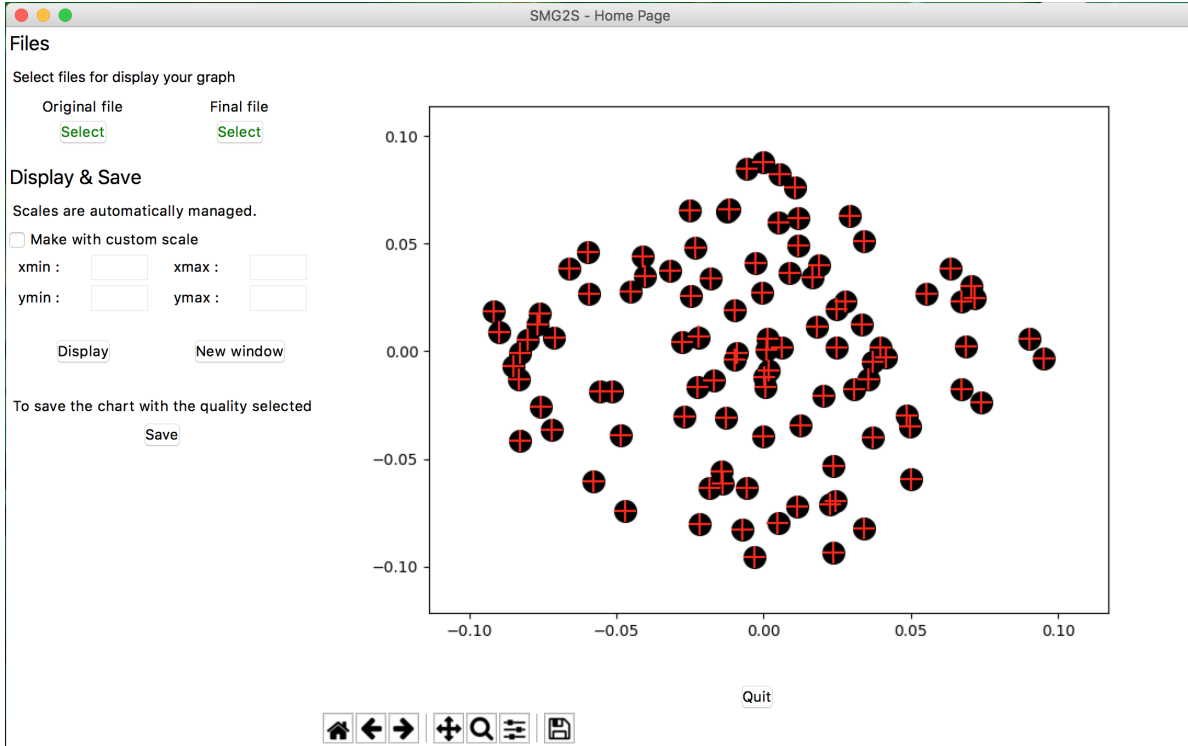
When you launch the program, a new windows opens like Fig. ?? :

After that, you can click on "Display" to build and open the graphic on the right side of the window. Click on "New window" to open your graphic on a new window. It's possible to open as many windows as you want like Fig. ??:

4.8.4 Krylov Solvers Evaluation using SMG2S

SMG2S is suitable to evaluate different kinds of linear system and eigenvalue solvers. We give an example to demonstrate its workflow by evaluating the Krylov solvers. In this section, we do not mean to propose novel points on the Krylov methods, but to show the benefits of SMG2S. A class of Krylov subspace iterative methods is one of the most powerful tools to solve large and sparse linear systems. Their significant advantages such as low memory requirements and a good approximation of solution make them widely be used in applications throughout science and engineering. Convergence analysis of these methods is not only of a great theoretical importance but it can also help to answer practically relevant questions about improving their performance using the preconditioners.

Figure 4.15 – Home Screen Plot Capture



As we introduced in Section ??, the convergence of Krylov solvers depends on the spectral distribution of matrices. And most preconditioners are applied to change the spectral distribution in order to accelerate the convergence. Anyway, the spectrum has a great impact on the convergence of Krylov methods. We can use SMG2S to generate the test matrices with different spectral distributions and to study their influence on the convergence.

4.8.4.1 SMG2S workflow to evaluate Krylov Solvers

SMG2S workflow for evaluating the solvers is shown in Fig. 4.16. It generates the matrix in parallel, which means that the different parts of the matrix are already distributed into the computing units of the platform. An interface can be provided to PETSc, Trilinos, and any public or personal parallel solvers. This interface can restore the distributed data into the necessary data structures of different libraries. This feature can significantly reduce the I/O of applications and improve their efficiency to evaluate the numerical methods.

4.8.4.2 Experiments

We evaluate three different restarted Krylov linear system solvers by SMG2S. The test methods include GMRES, BiCGStab (BiConjugate Gradient Stabilized method), and TFOMR (Transpose Free Quasi-Minimal Residual), with/without the basic parallel preconditioners SOR or Jacobi. In the experiments, matrices with different spectral distributions are generated by SMG2S, including the clustered, closest, conjugate eigenvalues,

Table 4.3 – Krylov Solvers Evaluation by SMG2S with matrix row number = 1.0×10^5 , convergence tolerance = 1×10^{-10} (dnc = do not converge in 8.0×10^4 iterations, the solvers and preconditioners are provided by PETSc.)

Krylov Methods	Preconditioner	Case 1	Case 2	Case 3	Case 4	Case 5	Case 6
GMRES	None	2160	dnc	dnc	dnc	50773	dnc
	Jacobi	17	dnc	129	dnc	12056	dnc
	SOR	3	dnc	4	dnc	dnc	dnc
BiCGStab	None	220	6859	dnc	771	53	dnc
	Jacobi	9	1097	66	214	56	dnc
	SOR	2	168	3	12	8	dnc
TFQMR	None	510	dnc	dnc	dnc	dnc	dnc
	Jacobi	18	dnc	128	dnc	dnc	dnc
	SOR	3	dnc	5	22	dnc	dnc

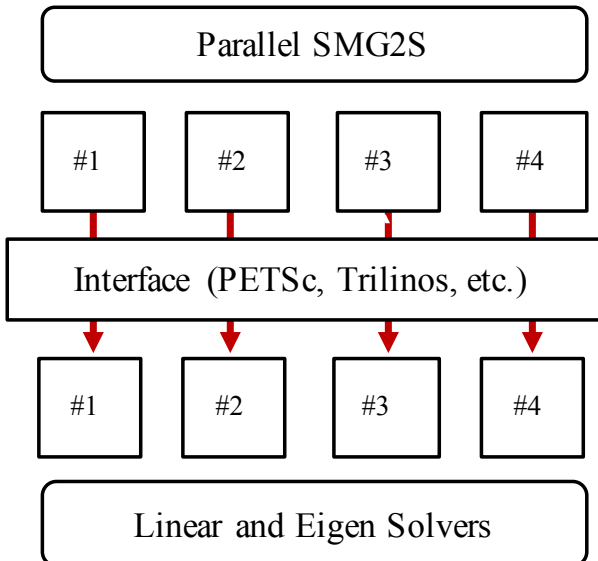


Figure 4.16 – SMG2S Workflow and Interface.

eigenvalues with dominant values, etc. With the interface implemented between SMG2S and PETSc, we use the parallel Krylov solvers and preconditioners provided by PETSc to do the evaluations.

Table 4.3 shows iterative steps for convergence of different solvers. We can conclude that different matrices generated by SMG2S with different spectral distributions have divers convergence performance with different solvers and preconditioners. The 6 cases listed in Table 4.3 are not cover much more different types of spectral distributions, and the tested preconditioners are relatively simple because it is not the main purpose of this paper. But we can say that SMG2S is a reliable tool which can be used to evaluate the different numerical methods, and in the future, we will make use of it to do more tests with different solvers and novel preconditioners and to analyze their performance with

different spectral distributions.

4.9 Conclusion and Perspectives

In this chapter, we have presented a scalable matrix generator with the given spectra and its parallel implementation on homogenous and heterogenous clusters. This method allows generating large-scale test matrices with customized eigenvalues to evaluate the influence of spectra on the linear and eigenvalue solvers targeting the large-scale platform. We have evaluated the parallel scalability and the accuracy to keep the spectra of matrices generated by this matrix generator. The experiments proved that this method has good scalability and acceptable accuracy to keep the given spectra. One more important benefit of SMG2S is that the matrices are generated in parallel, thus the data are already allocated on different processes. These distributed data can be used directly for the users to efficiently evaluate the numerical linear methods of the scientific libraries or their personal implementation without concerning the I/O operation, whose time consumption is enormous if the matrix size is large. In future, in order to augment the bandwidth of generated matrix, a special data structure and function for the very large factorial operation should be implemented. And the interface to more scientific linear and eigenvalue solver libraries should be provided.

CHAPTER 5

Unite and Conquer GMRES/LS-ERAM Method

Facing the challenges of numerical linear algebra methods on a large-scale machine discussed in Section 3, the new programming model should be proposed with well-suited characteristics on modern architectures. These features include optimized communications, asynchronicity, diversity of natural parallelism and fault tolerance. In such numerical methods, the avoidance of operations involving synchronous communications is most important. Indeed, with a very large number of cores, the overall reductions or global synchronization are a bottleneck. Consequently, large scalar products and overall synchronization, and other operations involving communications between all cores have to be avoided. On the other hand, everywhere that is possible, asynchronicity of communications has to be promoted. Indeed, this kind of communications could allow their overlapping with computation operations inside a task and between the tasks constituting these methods. The communication avoiding techniques could also be integrated allowing a general reduction of communications in the algorithm. The diversity of natural parallelism existing in such methods can be exploited by taking advantage of heterogeneity of targeted architectures. Fault tolerance and the ability to load balancing should be integral parts of these methods. These characteristics allow the improvement of the performance of applications built on the basis of these methods. Moreover, based on these properties, auto/smart-tuned versions of algorithms can be proposed. In this chapter, we present an asynchronous distributed and parallel Unite and Conquer GMRES/LS-ERAM (UCGLE) method to solve sparse non-Hermitian systems on large platforms. The key feature of UCGLE comparing with the classical hybrid methods using LS polynomial preconditioner ([Essai et al. \[1999\]](#); [He et al. \[2006\]](#)) is its distributed and parallel asynchronous communication and the manager engine implementation among three components, which are specified for the extreme-scale supercomputing platforms. We summarize the UC approach in Section 5.1. The theoretical parts of UCGLE are given in Section 5.2. In Section 5.3, we present the distributed and parallel implementation of UCGLE, including the computing components, the manager engine, and the distributed and parallel asynchronous communications. The experimental results on different supercomputers which evaluate the convergence, the parameters, the scalability, and the

fault tolerance are shown in Section 5.5.

5.1 Unite and Conquer approach

In general, Unite and Conquer approach is to make collaborate several iterative methods in order to accelerate the convergence of one of them. It is important to recall that the hybrid methods defined according to this approach are particularly interesting when underlying computing platforms are constituted by parallel and/or distributed heterogeneous components. This approach is a model for the design of numerical methods by combining different computation components together to work for the same objective, with asynchronous communication among them. Unite implies the combination of different calculation components, and conquer represents different components work together to solve one problem. Different independent components with asynchronous communication can be deployed on various platforms such as P2P, cloud and the supercomputer systems. The idea of unite and conquer approach came from the article of Saad ([Saad \[1984\]](#)) in 1984, where he suggested using Chebyshev polynomial to accelerate the convergence of Explicitly Restarted Arnoldi Method (ERAM) to solve eigenvalue problems. Brezinski ([Brezinski and Redivo-Zaglia \[1994\]](#)) proposed in 1994 an approach for solving a system of linear equations which takes a combination of two arbitrary approximate solutions of two methods. In 2005, Emad ([Emad et al. \[2005\]](#)) proposed a hybrid approach based on a combination of multiple ERAMs, which showed significant improvement in solving different eigenvalue problems. In 2016, Fender ([Fender et al. \[2016\]](#)) studied a variant of multiple IRAMs and generated multiple subspaces in a nested fashion in order to dynamically pick the best one inside each restart cycle.

The multiple explicitly restarted Arnoldi method (MERAM) is a technique based upon an ERAM with multiple projections. This method projects an eigenproblem on a set of subspaces and thus creates a whole range of differently parameterized ERAM processes which cooperate to compute a solution of this problem efficiently. As shown in Fig. 5.1, in MERAM the restarting vector of an ERAM is updated by taking into account the interesting eigeninformation obtained by the other ones. In other words, the ERAM processes of a MERAM begin with several subspaces spanned by a set of initial vectors and a set of subspace sizes. If the convergence does not occur for any of them, then the new subspaces will be defined with initial vectors updated by taking into account the intermediary solutions computed by all the ERAM processes. Each of these differently sized subspaces is defined with a new initial vector v . To overcome the storage dependent shortcoming of ERAM, a constraint on the subspace size of each ERAM is imposed. As

shown in Fig. 5.2, which is an experimental results extracted from ([Emad et al. \[2005\]](#)), MERAM is able to accelerates the convergence of ERAM. The numerical experiments have demonstrated that this variant of MERAM is often much more efficient than ERAM.

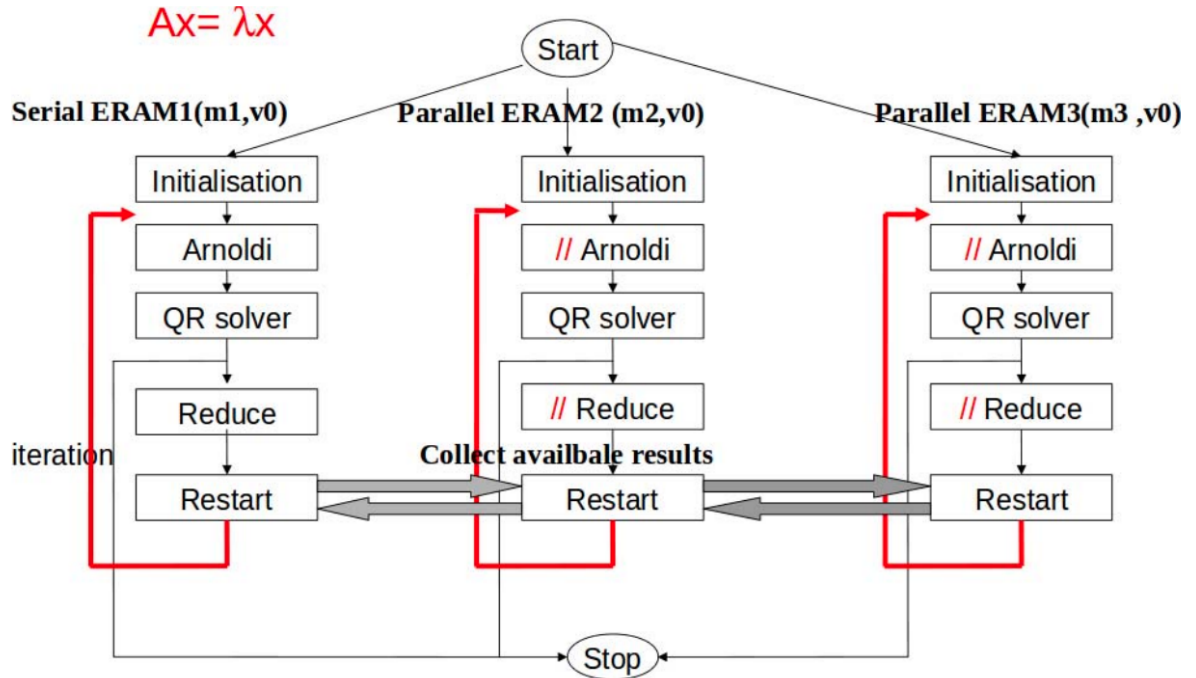


Figure 5.1 – An overview of MERAM ([Emad et al. \[2005\]](#)).

5.2 Asynchronous Unite and Conquer GMRES/LS-ERAM Method

In this section, we try to propose a new multi-level parallelism programming paradigm to solve linear systems based on the unite and conquer approach. Thus, firstly Section 5.2.1 divide the preconditioned linear solvers into three components, and then discuss in details the proposed paradigm. In Section 5.2.2, we give an implementation using this programming model by combining the restarted GMRES with the Least Squares polynomial preconditioner.

5.2.1 Divide of Linear Solvers into Components

As shown in Chapter 3, the convergence of linear solvers can be accelerated:

1. by preconditioning matrix;
2. by the deflation of eigenvalues/eigenvectors;
3. by the selected polynomials.

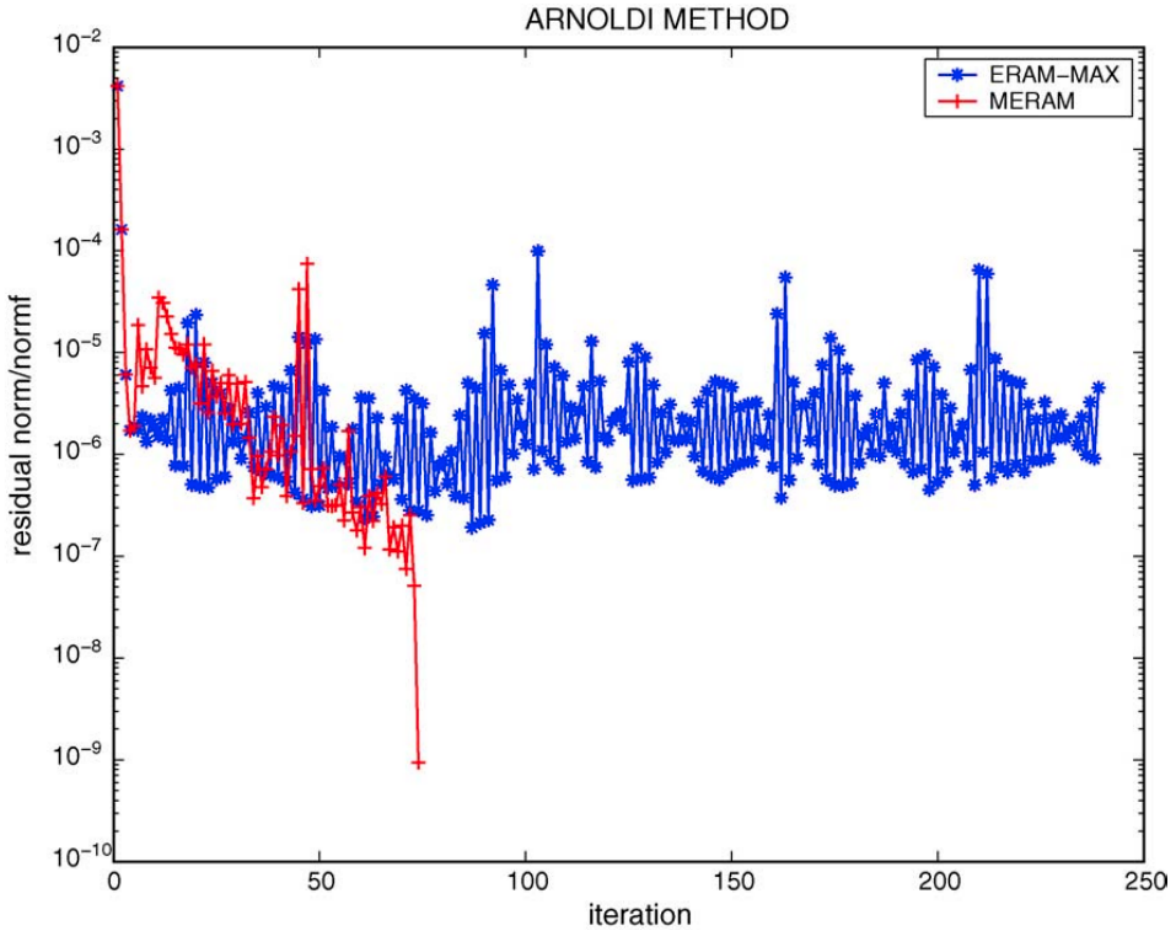


Figure 5.2 – An example of MERAM: MERAM(5,7,10) vs. ERAM(10) with af 23560.mtx matrix. MERAM converges in 74 restarts, ERAM does not converge after 240 restarts ([Emad et al. \[2005\]](#)).

For the first type solver, which is preconditioned by selected matrix, It is difficult to separate the linear solver and preconditioning matrix into two independant computing components with asynchronous communications. When thinking about to construct a linear solver based on the *Unite and Conquer approach* by combining several methods with asynchronous communications, the deflation and the polynomial preconditioning are the good candidates.

- Linear solver;
- Eigen-Information;
- Preconditioning.

5.2.2 UCGLE Method

It is difficult to separate the linear solver and preconditioning matrix with asynchronous communications. Thus, we select the hybrid method which is preconditioned by the least

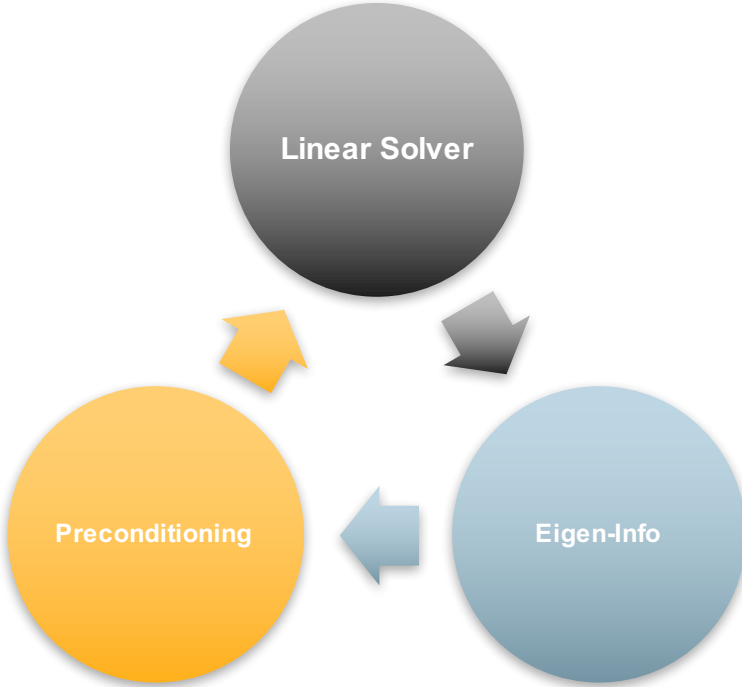


Figure 5.3 – Cyclic Relation of linear solver, eigen-information and preconditioning techniques.

squares polynomial to construct our new model. In the conventional implementation of this method, the eigenvalues used to construct the least squares polynomials are computed by the Hessemberg matrix H_m after each time restart of GMRES. In UCGLE, the linear solver, the approximation of eigenvalues and the construction of least squares polynomials are separated into three different parts. These three computing components work independently with each other and they share the necessary information by the asynchronous communications.

UCGLE method comprises mainly two parts: the first part uses the restarted GMRES method to solve the linear systems; in the second part, it computes a specific number of approximated eigenvalues, and then applies them to the Least Squares method and gets a new preconditioned residual, as a new initial vector for restarted GMRES.

Figure 5.4 gives the workflow of UCGLE method with three computation components. ERAM Component and GMRES Component are implemented in parallel, and the communication among them is asynchronous. ERAM Component computes a desired number of eigenvalues, and then sends them to LS Component; LS Component uses these received eigenvalues to output a new residual vector, and sends it to GMRES Component; GMRES Component uses this residual as a new restarted initial vector for solving non-Hermitian linear systems.

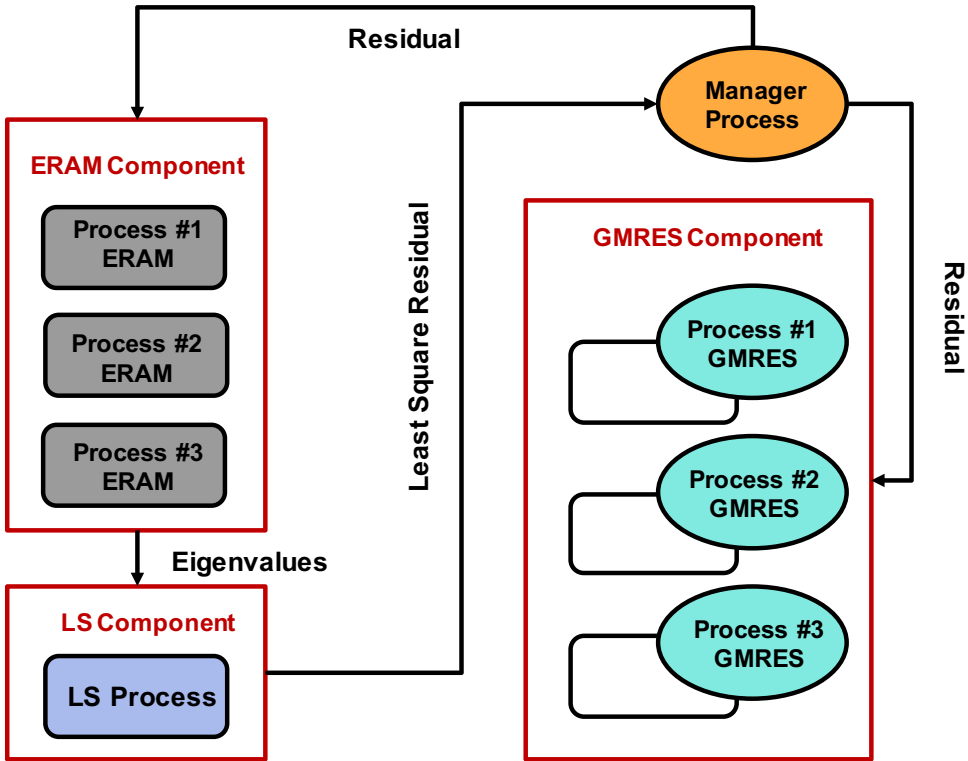


Figure 5.4 – Workflow of UCGLE method’s three components

5.3 Distributed and Parallel Implementation

This section gives the distributed and parallel implementation, including the components, the multi-level parallelism, the manager engine, and the asynchronous communications.

5.3.1 Component Implementation

This section gives the basic implementation and workflow for each component in UCGLE, and Algorithm 22 gives the implementation of UCGLE in details.

5.3.1.1 GMRES Component

GMRES Component aims to complete the solving a linear system $Ax = b$. It takes as input an operator matrix A and two vectors, x the initial guess vector and b the related RHS. GMRES approximates the solution starting from this initial guess vector until the exact solution is found or if a stopping criterion is met, for example, that the residual norm is below a given threshold (e.g., $\|r\|_2 \leq 10e^{-8}$). In practice, GMRES are restarted after m steps of iterations in order to reduce the memory requirement. Before each time of restart, GMRES Component check if it receives asynchronously the LS parameters from LS Component. If received, it will provide these parameters to generate a new residual vector and use it as the restart vector, if not, GMRES will be normally restarted. Fig. 5.5

gives the workflow of GMRES Component.

GMRES Component loads the parameters $A, m_g, x_0, b, \epsilon_g, L, s_{use}$ to solve the linear systems. At the beginning of the execution, it behaves like the basic GMRES method. When it finishes the m^{th} iteration, it will check if the condition $\|b - Ax_m\| < \epsilon_g$ is satisfied, if yes, x_m is the solution of linear system $Ax = b$, or GMRES Component will be restarted using x_m as a new initial vector. A parameter $count$ is used to count the times of restart. All these processes are similar to a Restarted GMRES. However, when $count$ is an integer multiple of L (number of GMRES restarts between two times preconditioning of LS), it will check if it has received the parameters A_d, B_d, Δ_d, H_d from LS Component. If yes, these parameters will be used to construct a preconditioning polynomial P_d , which can be used to generate a preconditioned residual x_d , then set the initial vector x_0 as x_d , and restart the basic GMRES, until the exit condition is satisfied.

The GMRES component has the role of solving the linear system. We reused PETSc's GMRES resolution method and modified it to include sending and receiving data and calculating the new residual. After going through a configuration phase of the numerical method, relating to parameters as important as the size of subspace to be used, as well as the residual standard to be achieved.

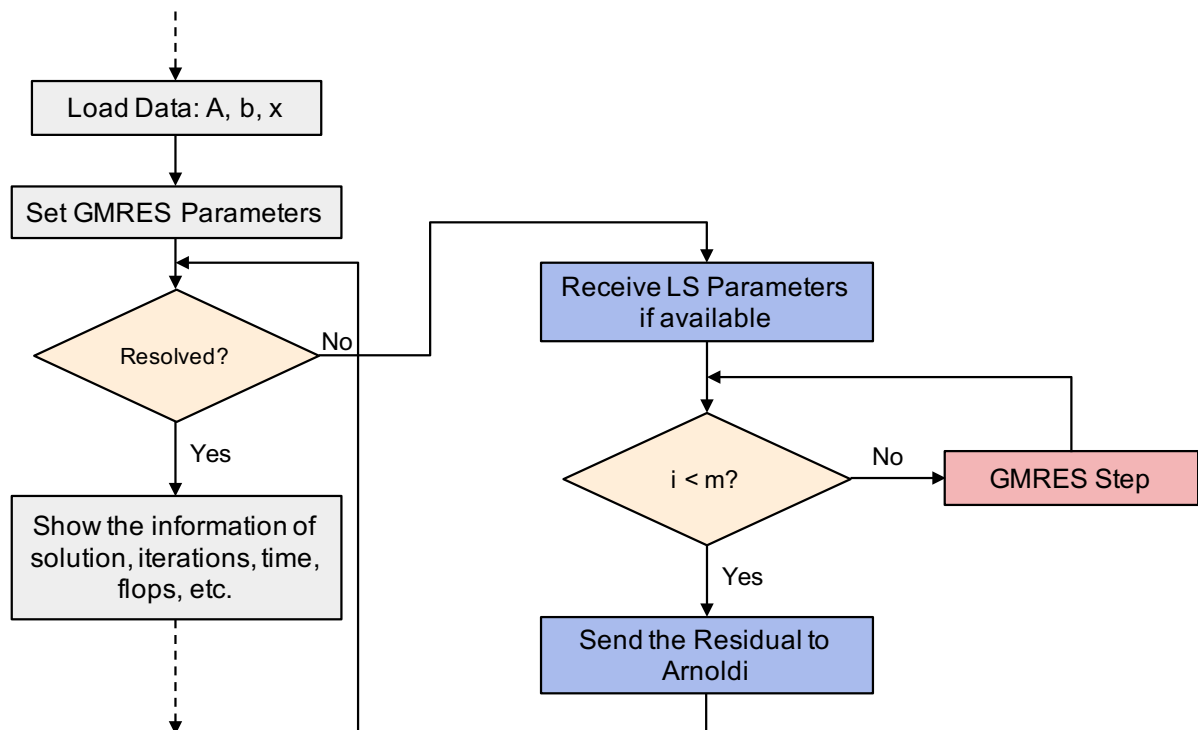


Figure 5.5 – GMRES Component.

5.3.1.2 ERAM Component

Fig. 5.6 gives the workflow of ERAM Component. ERAM Component loads the parameters m_a, v, r, ϵ_a and the operator matrix A , then launches ERAM function. When it

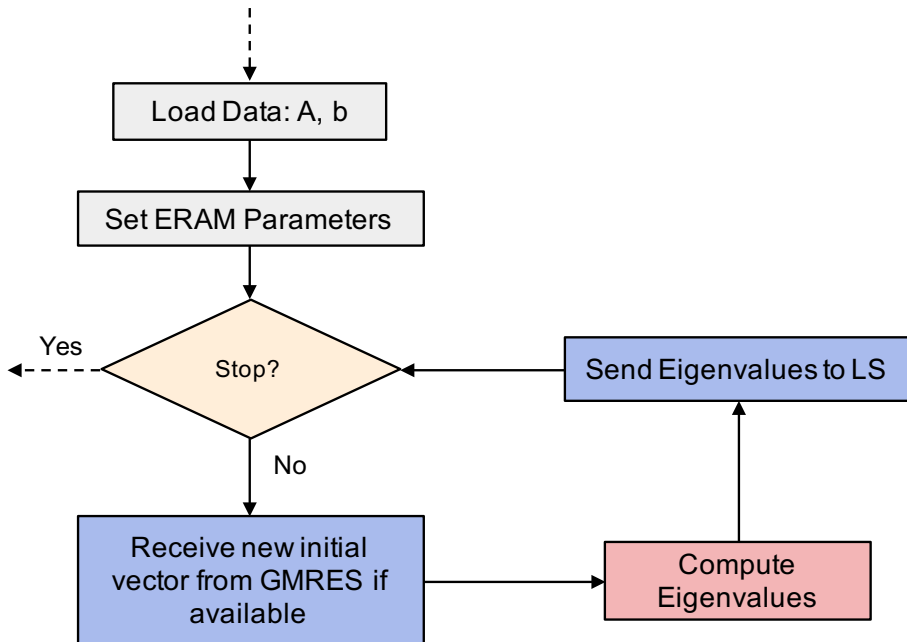


Figure 5.6 – ERAM Component.

receives a new vector X_TMP from GMRES Component, this vector will be stored in ERAM Component. This vector is updated with the continuous receiving of a new one from GMRES Component. If the r eigenvalues Λ_r are approximated by ERAM Component, it will send them to LS Component, at the same time, it is able to save the eigenvalues into the local file.

5.3.1.3 LS Component

Fig. 5.7 gives the workflow of ERAM Component. LS Component won't start work until it receives the eigenvalues Λ_r sent from ERAM Component. Then it will use them to compute the parameters A_d, B_d, Δ_d, H_d , whose dimensions are related to LS parameter d , the Least Squares polynomial degree, and send these parameters to GMRES Component.

Algorithm 22 Implementation of Components

```

1: function LOADERAM(input:  $A, m_a, \nu, r, \epsilon_a$ )
2:   while exit==False do
3:     ERAM( $A, r, m_a, \nu, \epsilon_a$ , output:  $\Lambda_r$ )
4:     Send ( $\Lambda_r$ ) to LS
5:     if saveflg == TRUE then
6:       write ( $\Lambda_r$ ) to file eigenvalues.bin
7:     end if
8:     if Recv ( $X\_TMP$ ) then
9:       update  $X\_TMP$ 
10:    end if
11:    if Recv (exit == TRUE) then

```

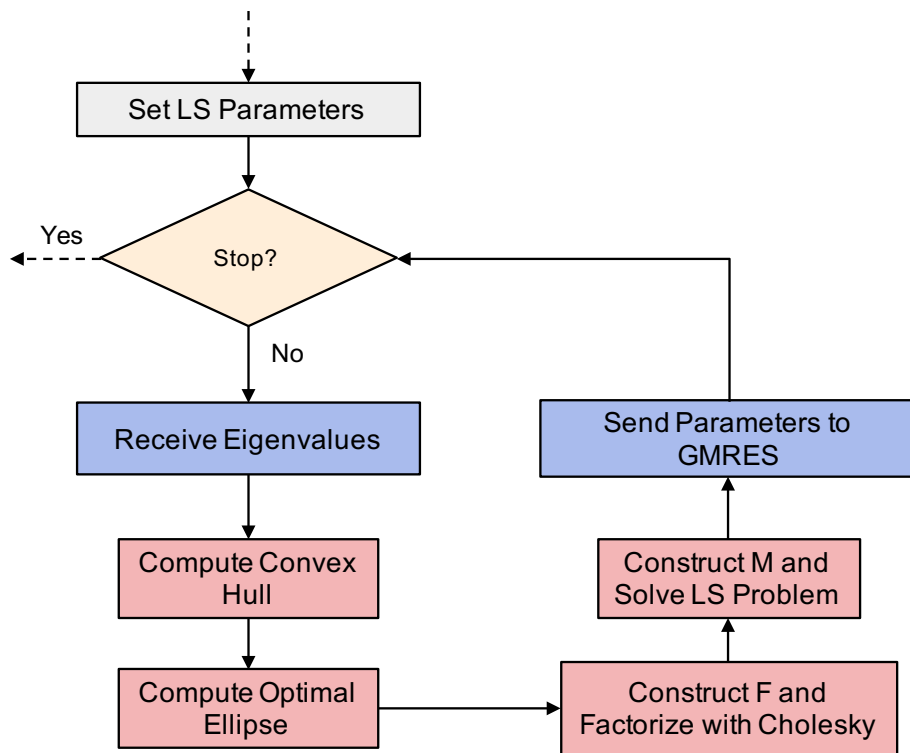


Figure 5.7 – LS Component.

```

12:      Send (exit) to LS Component
13:      stop
14:  end if
15: end while
16: end function
17: function LOADLS(input:  $A, b, d$ )
18:  if Recv( $\Lambda_r$ ) then
19:    LS(input:  $A, b, d, \Lambda_r$ , output:  $A_d, B_d, \Delta_d, H_d$ )
20:    Send ( $A_d, B_d, \Delta_d, H_d$ ) to GMRES Component
21:  end if
22:  if Recv (exit == TRUE) then
23:    stop
24:  end if
25: end function
26: function LOADGMRES(input:  $A, m_g, x_0, b, \epsilon_g, L, s_{use}$ , output:  $x_m$ )
27:  count = 0
28:  BASICGMRES(input:  $A, m, x_0, b$ , output:  $x_m$ )
29:   $X\_TMP = x_m$ 
30:  Send ( $X\_TMP$ ) to ERAM Component
31:  if  $\|b - Ax_m\| < \epsilon_g$  then
32:    return  $x_m$ 

```

```

33:      Send (exit == TRUE) to ERAM Component
34:      Stop
35:      else
36:          if count | L then
37:              if recv (Ad, Bd,  $\Delta_d$ , Hd) then
38:                   $r_0 = f - Ax_0$ ,  $\omega_1 = r_0$  and  $x_0 = 0$ 
39:                  for k = 1, 2, ..., suse do
40:                      for i = 1, 2, ..., d - 1 do
41:                           $\omega_{i+1} = \frac{1}{\beta_{i+1}}[A\omega_i - \alpha_i\omega_i - \delta_i\omega_{i-1}]$ 
42:                           $x_{i+1} = x_i + \eta_{i+1}\omega_{i+1}$ 
43:                      end for
44:                  end for
45:                  set  $x_0 = x_d$ , and GOTO 1
46:                  count ++
47:              end if
48:          else
49:              set  $x_0 = x_m$ , and GOTO 1
50:              count ++
51:          end if
52:      end if
53:      if Recv (exit == TRUE) then
54:          stop
55:      end if
56:  end function

```

5.3.2 Parameters Analysis

UCGLE method is a combination of three different methods, there are a number of parameters, which have impacts on its convergence rate. We summarize these different related ones, and classify them according to their relations with different components.

1. GMRES Component
 - (a) m_g : GMRES Krylov Subspace size
 - (b) ϵ_g : absolute tolerance for the GMRES convergence test
 - (c) P_g : GMRES core number
 - (d) s_{use} : number of times that polynomial applied on the residual before taking account into the new eigenvalues
 - (e) L : number of GMRES restarts between two times of LS preconditioning

2. ERAM Component

- (a) m_a : ERAM Krylov subspace size
- (b) r : number of eigenvalues required
- (c) ϵ_a : tolerance for the ERAM convergence test
- (d) P_a : ERAM core number

3. LS Component

- (a) d : Least Squares polynomial degree

Suppose that the computed convex hull by Least Squares contains eigenvalues $\lambda_1, \dots, \lambda_m$, the residual given by Least Square polynomial of degree $d - 1$ is

$$r = \sum_{i=1}^k \rho_i R_d(\lambda_i) u_i + \sum_{i=m+1}^n \rho_i R_d(\lambda_i) u_i$$

The first part of this residual is minimized by the Least Square polynomial method using the eigenvalues inside convex hull H_k , and the second part is large since the related eigenvectors associated with the eigenvalues outside H_k . With the number of approximated eigenvalues d increasing, the first part will be much closer to zero and the second part keeps enormous. The next restart process of GMRES can be still accelerated since it restarts with the combination of eigenvectors. The more eigenvalues are known, the more significant acceleration will be. The convergence comparison of UCGLE and classic GMRES is given in Fig. 5.8. The large peaks appear in the UCGLE curve for each time restart. It means that the residual turns to be large, and then will drop down very quickly with the acceleration of LS polynomial method.

The Algorithm 22 shows the implementation of UCGLE's three components and their asynchronous communication in detail.

5.3.3 Multi-level Parallelism in UCGLE

UCGLE method is a distributed parallel method which can profit both shared memory and distributed memory of computational architectures. As shown in Figure 5.9, it has two levels of parallelism for distributed memory: 1) Coarse Grain/Component level: UCGLE allows the distribution of different numerical components, including the preconditioning part (LS and ERAM) and the solving part (GMRES) on different platforms or processors; 2) Medium Grain/Intra-component level, GMRES and ERAM components are both deployed in parallel; the third level for shared memory is the Fine Grain/Thread parallelism: the OpenMP thread level parallelism in CPU, or the accelerator level parallelism if GPUs or other accelerators are available.

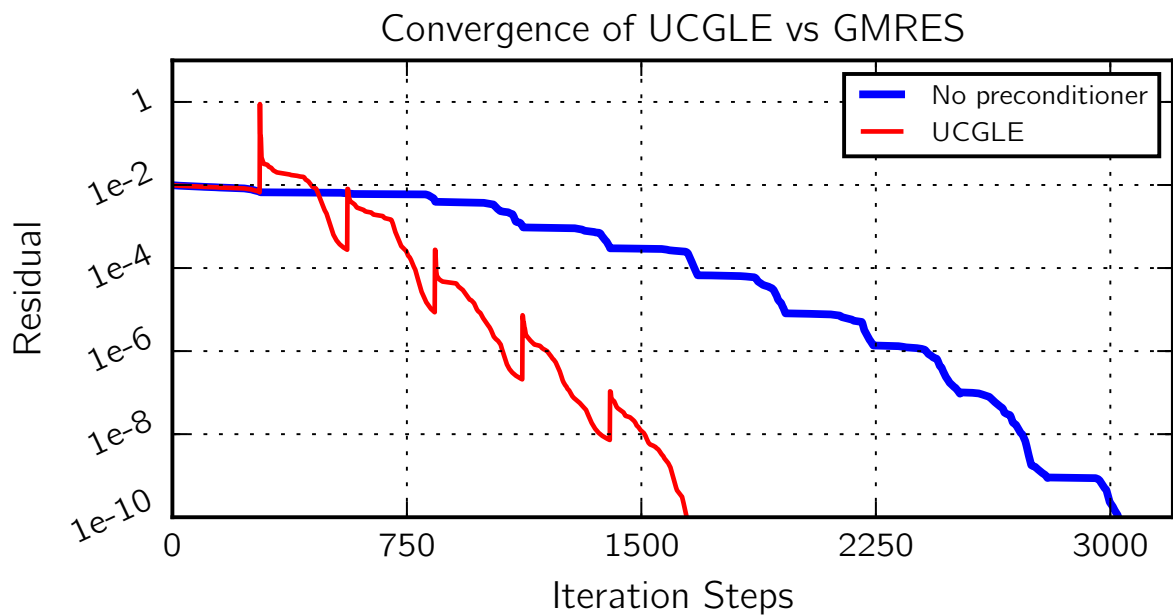
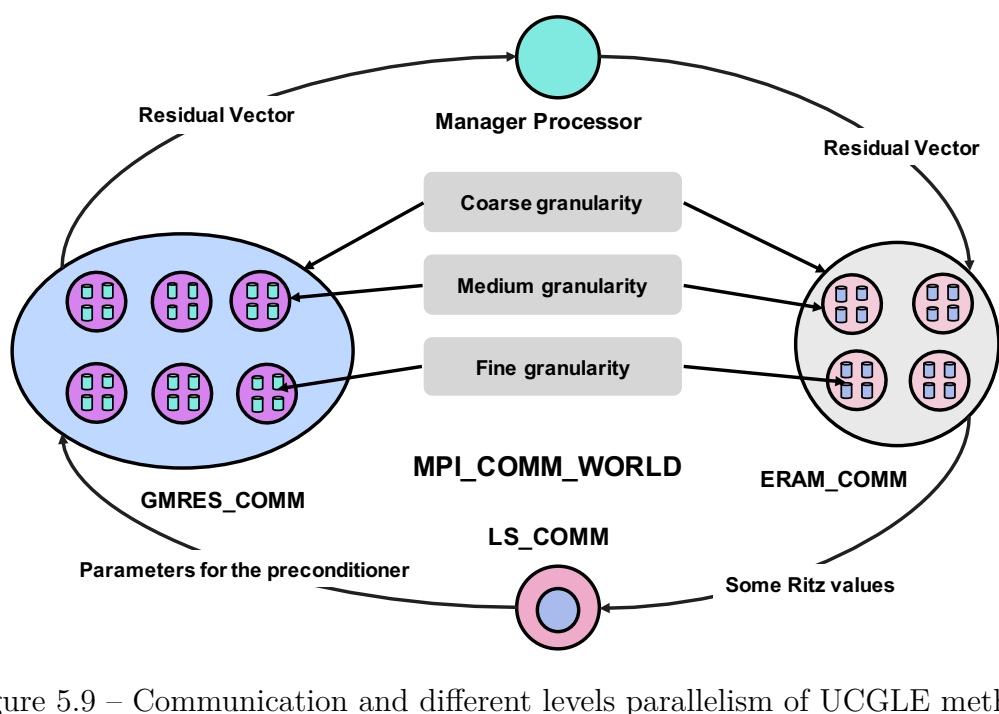


Figure 5.8 – Convergence comparison of UCGLE method vs classic GMRES.



The GMRES method has been implemented by PETSc, and the ERAM method is provided by SLEPc. Additional functions have been added to the GMRES and ERAM provided by PETSc and SLEPc in order to include the sending and receiving functions of different types of data. For the implementation of LS Component, it computes the convex hull and the ellipse encircling the Ritz values of matrix A , which allows generating a novel Gram matrix M of selected Chebyshev polynomial basis. This matrix should be factorized into LL^T by the Cholesky algorithm. The Cholesky method is ensured by PETSc as a preconditioner but can be used as a factorization method. The implementation based on these libraries allows the recompilation of the UCGLE codes to adapt to both CPU and GPU architectures. The experimentation of this paper does not consider the OpenMP thread level of parallelism since the implementation of PETSc and SLEPc is not thread-safe due to their complicated data structures. The data structures of PETSc and SLEPc makes it more difficult to partition the data among the threads to prevent conflict and to achieve good performance ([Balay et al. \[2016b\]](#)).

5.3.4 Distributed and Parallel Manager Engine Implementation

5.3.4.1 Implementation of the Inter-component Communication Network

From a view of asynchronous communication, the implementation of UCGLE is to establish several communicators inside of *MPI_COMM_WORLD* and their inter-communication. The topology of communication among these groups is a circle shown in Figure [5.9](#). The total number of computing units supplied by the user is thus divided into four groups according to the following distribution: P_t is the total number of processes, then $P_t = P_g + P_a + P_l + P_m$, where P_g is the number of processes assigned to GMRES Component, P_a the number of processes to ERAM component, P_l the number of processes allocated to LS Component and P_f the number of processes allocated to *ManagerProcess* proxy. P_g and P_a are greater than or equal to 1, P_l and P_m are both exactly equal to 1. LS Component is a serial component because the Least Squares polynomial method cannot be parallelized.

P_t is thus divided into several MPI groups according to a color code. The minimum number of processes that our program requires is 4. We utilize the mechanism of MPI standard to support the communication of our application fully. The communication layer that does not depend on the application, this allows the replacement and scalability of various components provided.

5.3.4.2 Asynchronous Communication Mechanism

The main characteristic of UCGLE method is its asynchronous communication. But the synchronous communication takes place inside of GMRES and ERAM components. Distributed and parallel communication involves different types of exchange data, such as

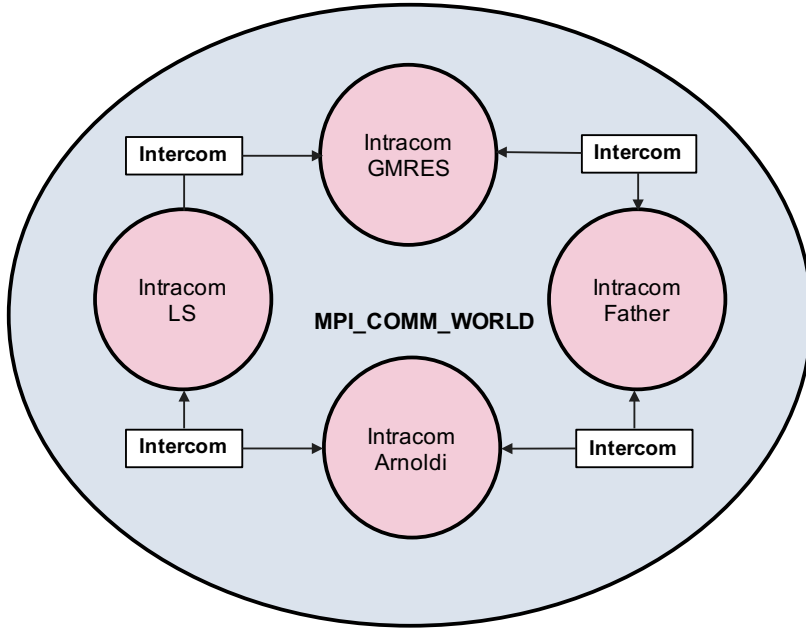


Figure 5.10 – Creation of Several Intra-Communicators in MPI.

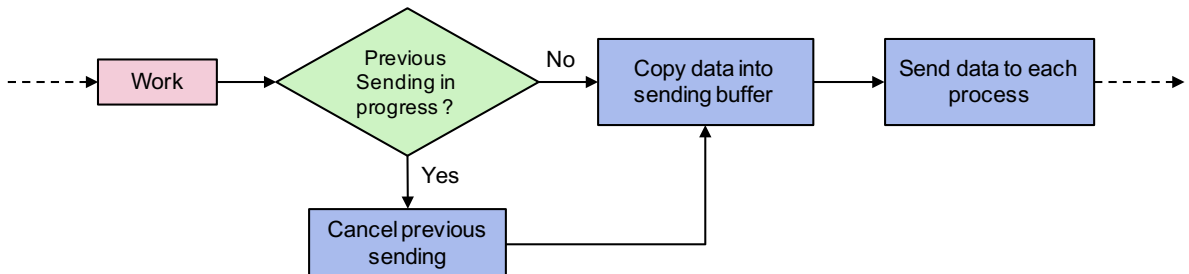


Figure 5.11 – Data Sending Scheme from one group of process to the other.

vectors, scalar tables, and signals among different components. When the data are sent and received in a distributed way, it is essential to ensure the consistency of data. In our case, we choose to introduce an intermediate node as a proxy to carry out only several types of exchanges and thus facilitate the implementation of asynchronous communication. This proxy is called *Manager Process* as in Figure 5.9. One process can fulfill all the data exchanges.

Asynchronous communication allows each computation component to conduct independently the work assigned to it without waiting for the input data. The asynchronous data sending and receiving operations are implemented by the non-blocking communication of Message Passing Interface (MPI). Sending takes place after the sender has completed the task assigned to it. Before any prior shipment, the component checks whether several transactions are now on the way. If yes, this task will be canceled to avoid the competition of different types of sending tasks. Sent data are copied into a buffer to prevent them from being modified while sending. For the asynchronous data receiving, before starting this task, the component will check if data is expected to be received. Once the receiving buffer is allocated, the component performs the receiving of data while respect-

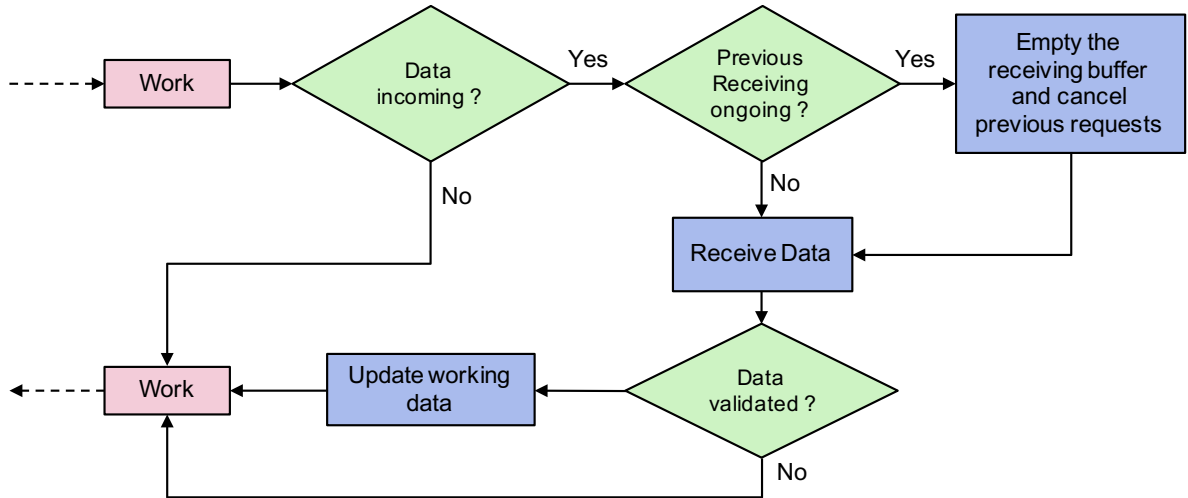


Figure 5.12 – Data Receiving Scheme from one group of process to the other.

ing the distribution of data globally according to the rank of sending processes. It is also essential to validate the consistency of receiving data before any use of them by the tasks assigned to the components.

Asynchronous Sending: The sending operation, as we described, will start by verifying if the previous sending operations are pending or not. If some operations are not finished, they are canceled so as not to be in a state where several shipments with different data are in competition. In the practical implementation, we use the MPI_Request to track the state of an asynchronous request. Once the verification is validated, then the data to be sent will be copied to a buffer to prevent them overwritten by other work operations. Then, this data is sent to the different nodes of the other components, respecting the distribution negotiated during the initialization of the communications via the standard asynchronous sending function MPI_Isend.

This last function is asynchronous in the sense that the data sent with this function will only be effective when the recipient (s) decide to receive them. In practice, it may be interesting to know that this is not entirely true. Indeed, the actual sending of data only occurs when the receiver or receivers are available, but also during a subsequent call to the MPI library whatever it is. Thus it may be that the sending cannot be done because the communicating nodes do not find the time to communicate.

Asynchronous Receiving: In the context of send-and-receive communication mechanisms, the sending operation is often the most difficult to implement because it requires a synchronization point. As far as we are concerned, we have hidden this synchronization point thanks to an input verification step. Indeed, we have chosen to implement a test function before proceeding with asynchronous reception instead of going through a purely asynchronous reception function. The data input test is done via the MPI_Iprobe function and the MPI_Recv reception. The latter is blocking or synchronous, that is, once called the computation node will wait for data to be received before returning to the

calling function.

At first glance, it would seem wiser to go through the non-blocking reception function MPI_Irecv, but in practice, this function requires to know in advance the size of the data that will be received, which is not the case in the case where our components exchange tables of scalars. Indeed, the component Arnoldi goes throughout its task, calculate more and more eigenvalues, more and more precise. In advance, it is not possible to know the number of eigenvalues that will be obtained, in fact, impossible to predict the size of the input buffer. Also, we made a choice to work with a dynamic reception buffer. In our implementation, this one is allocated thanks to the information provided by the operation MPI_Get_count using structure MPI_Status filled in by the function MPI_Iprobe.

Also, apart from this difference, our reception mechanism is fundamentally similar to the MPI_Irecv function in that it only receives data if it is available. In our case we also do not receive data if they are not available, the component to continue its task in case they were not.

In addition to having reimplemented MPI's asynchronous receive mechanism, we integrated a mechanism for checking the consistency of the received data. In order to allow different independent groups of compute nodes (our components), we have used the tools that are the intracomunicators and inter-communicators MPI (see explanations in 5.2.3.1). The problem of this type of implementation (at the same time there is no other possible, at least without falling into the experimental unstable) is that it does not allow collective communications between the different nodes of two communicating groups. In fact, the communications between groups of nodes (or components) pass through the intercommunication that only allow collective communications between those between the master of a group and the set of nodes of the other. This is therefore quite limiting when the goal (ours) is to carry out entirely collective communications, that is to say to allow all the nodes of a group to communicate with all the nodes of another group. This is what we have completed through our implementation of the sending and receiving mechanisms. The real problem is as to the coherence of the received data.

Indeed, even if we go through the proxy to facilitate communication control, data consistency must be checked before any prior use. For example, take the case of a vector. If a vector is partially received, it can not be used, and if it was the case, we could witness a disaster from a numerical point of view. Also, to avoid this kind of pitfall, we have integrated a validation mechanism that will check that the received data are consistent before they are used. The consistency check is conveniently performed by comparing the total size of the data received by each component node against the size of the data to be received at all. If this is consistent, then the reception buffer data is placed in the working memory of each node of the receiving component.

5.3.4.3 Implementation for Heterogeneous Platforms with Multi-GPU

TO DO

5.4 Experiment and Evaluation

5.4.1 Hardware Platforms

We test its convergence acceleration, fault tolerance and scalability on the large-scale platforms. UCGLE method has been installed on the supercomputer *Tianhe-2*, which is installed at the National Super Computer Center in Guangzhou of China. It is a heterogeneous system made of Intel Xeon CPUs and Intel Knights Corner (KNC), with 16000 compute nodes in total. Each node composes 2 Intel Ivy Bridge 12 cores @ 2.2 GHz. In this article, we do not test UCGLE with KNC on *Tianhe-2* since PETSc do not support it with good performance.

5.4.2 Parameters Evaluation

5.4.2.1 Test Parameters Setup

- Krylov subspace size for GMRES
- LS applied times:
- LS Frequency:
- Number of eigenvalues:
- LS polynomial degree:

5.4.2.2 Test Matrix Suite:

Matrices from Matrix Market Collections:

Table 5.1 – Test Matrix from Matrix Market Collection.

Matrix	Size	s NNZ	s Domain
utm300	300	3155	\mathbb{R}
utm1700b	1700	21509	\mathbb{R}
pde2961	2961	14585	\mathbb{R}
young4c	841	4089	\mathbb{C}

Matrices generated by SMG2S:

5.4.2.3 Experiments

In order to highlight the impacts of different parameters inside UCGLE, we conducted several sets of experiments, which varies one parameter mentioned above, and keeps the other parameters fixed. In this section, we will present the results of these experiments, and then analysis the effect of each parameter on the preconditioning, thus the acceleration of convergence. We study the parameters including the Krylov subspace size of GMRES m_g , the times of LS preconditioning applied on the GMRES lsa , the frequence of LS preconditioning applied $freq$, the number of eigenvalues approximated by ERAM Component $neigen$, and the degree of LS polynomial l .

Krylov subspace size:

The parameter m_g , which means the restarted subspace size of GMRES, has important influence on the convergence of UCGLE. This effect is similiar with the case on the conventional GMRES without preconditioning. For the experiments of UCGLE, we vary m_g from 50 to 180, and keep $l = 10$, $lsa = 10$, $freq = 10$. Moverover, we evaluate also the classic GMRES with m_g to be 100 and 150. The results are given in Fig. 5.13. First of all, we can conclude that in the case that m_g is too small (see UCGLE($m_g = 50$) in Fig. 5.13), even the LS preconditioning is applied, the convergence can not be achieved. With the augmentation of m_g , UCGLE is able to converge with less iteration steps. Secondly, with the preconditioning of LS polynomial, UCGLE can converge with $m_g = 100$, but the classic GMRES cannot converge with the same value of this parameter.

In conclusion, the Krylov subspace size of GMRES Component is a very important parameter of UCGLE. If this parameter is too small, it is difficult to get the convergence even with the LS polynomial preconditioning. It is not practical to use very large m_g since the limitation of memory. Thus, it is essential to determine a good value of m_g which is able to able to accelerate the convergence by LS polynomial.

LS polynomial degree:

The parameter LS applied times lsa means the number of times the LS parameters will be applied to the temporary solution of GMRES Component before its restart after m_g iterations. In the experiments, lsa ranges from 1 to 25, and the parameters m_g , l , and $freq$ are respectively fixed as 100, 10 and 1. Fig. 5.15 shows the convergence curves of all the tests. Firstly, it is obvious that lsa has the effect on the peaks for each time LS preconditioning. The greater it is, the bigger the peak will be. As talked in Section 5.3.2, these peaks means the Eulidien norm of restart vector produced by LS polynomial. By comparing the curves in the Fig. 5.15, we can conclude that the augmentation of lsa wil accelerate the convergence of UCGLE. But, this parameter cannot be too large, this might lead to a too large norm of the residual of the restarted vector generated by LS polynomial preconditioning processus, and finally damage the convergence.

To conclude on the effect of this parameter, it is necessary to select the best value

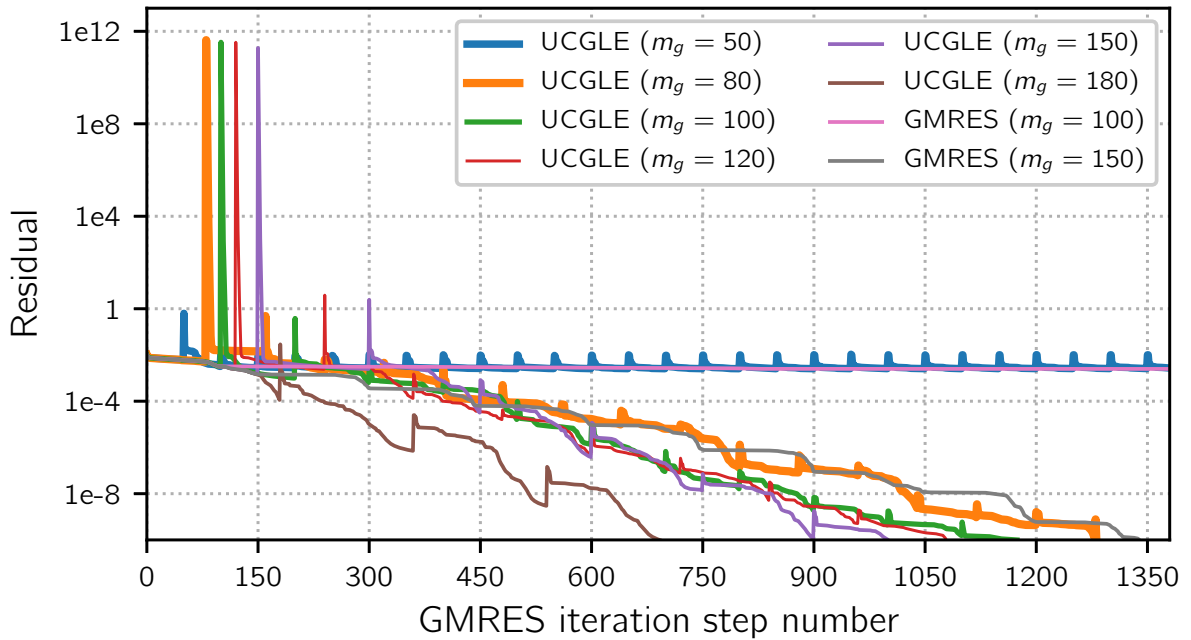


Figure 5.13 – Evaluation of GMRES subspace size m_g varying from 50 to 180. $l = 10$, $lsa = 10$, $freq = 10$.

with considering the selection of the parameter of LS polynomial power l . In fact, the two parameters seem particularly intricate together and the choice of one will depend on the choice of the other. In the practical implementation, this parameter implies a series of SpMV and AXPY operations in parallel. The larger l is, the more operations will be executed, thus the more time will be occupied. The good selection of this parameter should make a balance between the reduction of iteration steps of GMRES components and additional time caused by these SpMV and AXPY operations.

LS applied times:

The parameter LS applied times lsa means the number of times the LS parameters will be applied to the temporary solution of GMRES Component before its restart after m_g iterations. In the experiments, lsa ranges from 1 to 25, and the parameters m_g , l , and $freq$ are respectively fixed as 100, 10 and 1. Fig. 5.15 shows the convergence curves of all the tests. Firstly, it is obvious that lsa has the effect on the peaks for each time LS preconditioning. The greater it is, the bigger the peak will be. As talked in Section 5.3.2, these peaks mean the Euclidian norm of restart vector produced by LS polynomial. By comparing the curves in the Fig. 5.15, we can conclude that the augmentation of lsa will accelerate the convergence of UCGLE. But, this parameter cannot be too large, this might lead to a too large norm of the residual of the restarted vector generated by LS polynomial preconditioning processus, and finally damage the convergence.

To conclude on the effect of this parameter, it is necessary to select the best value with considering the selection of the parameter of LS polynomial power l . In fact, the two parameters seem particularly intricate together and the choice of one will depend on

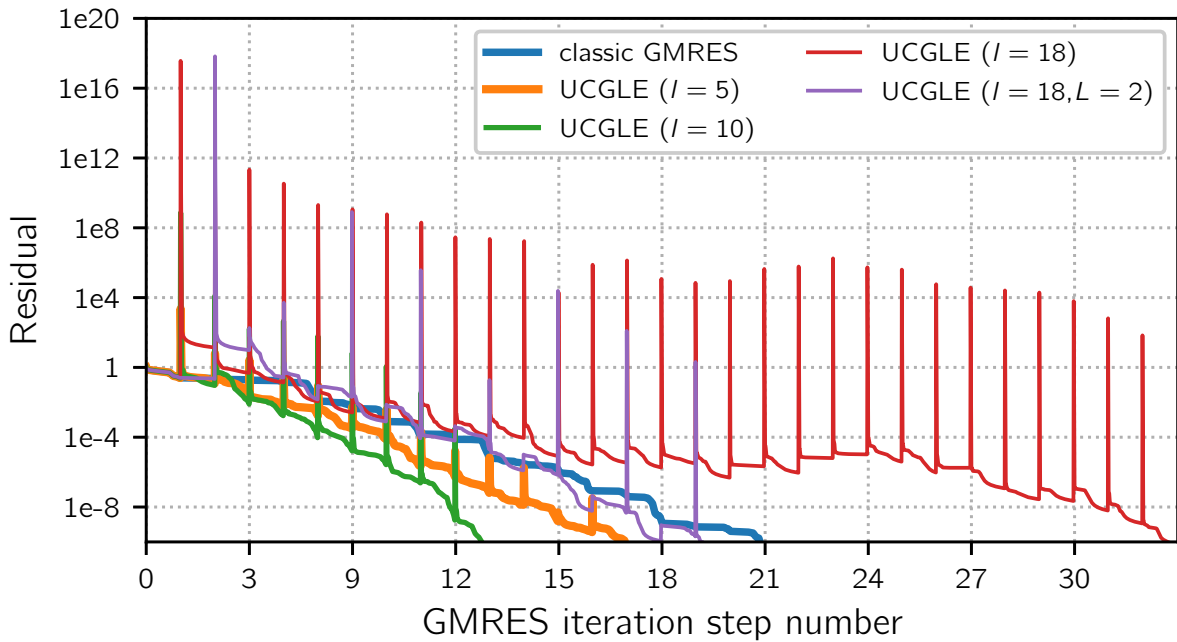


Figure 5.14 – Convergence comparison of UCGLE method vs classic GMRES.

the choice of the other. In the practical implementation, this parameter implies a series of SpMV and AXPY operations in parallel. The larger l is, the more operations will be executed, thus the more time will be occupied. The good selection of this parameter should make a balance between the reduction of iteration steps of GMRES components and additional time caused by these SpMV and AXPY operations.

LS Frequency:

The preconditioning latency represents the number of restarts between which a GMRES preconditioning phase will take place, ie the application of the polynomial to the temporary solution of the resolution method. Also, we noticed previously that after each preconditioning phase corresponded the appearance of a peak of convergence before each acceleration of this one.

In order to characterize the latency parameter (identified by cof in Figures 5.20, 5.21 and 5.22) we conducted a series of tests. These tests were designed to evaluate the number of completed iterations for different latencies, for different subspace sizes.

The results we obtained allowed us to observe several things. The first is that the subspace size is decisive in the preconditioning of the problem. Indeed, if the subspace size is too small then it appears that the preconditioning is not interesting to use. Thus, in the case of too small subspace sizes, preconditioning degrades convergence. Moreover, in the case where the subspace size GMRES is sufficiently large, then the latency parameter loses its importance. This is something we observe in figure 5.22 where the curves corresponding to the resolutions without preconditioning tend to aggregate together.

Ultimately the latency parameter must be chosen to allow sufficient consideration of the preconditioning in the successive cycles at this stage while not being too important

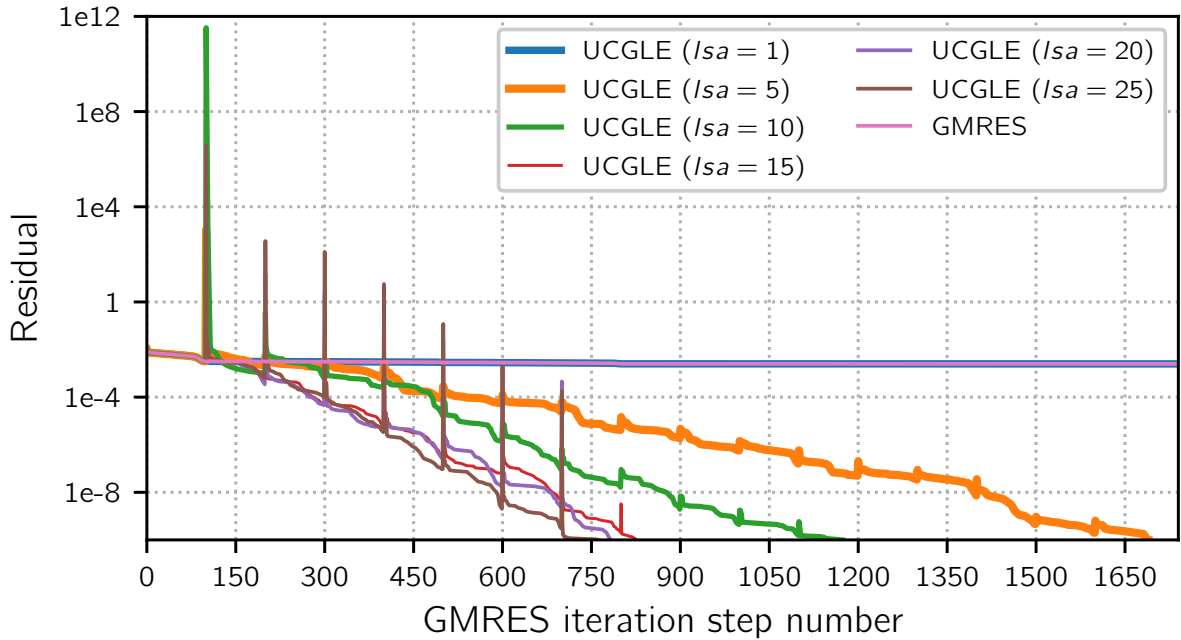


Figure 5.15 – Evaluation of LS applied times lsa varying from 1 to 25, and $m_g = 100$, $l = 10$, $freq = 1$.

so that the convergence can continue to benefit from its effect at a satisfactory pace.

Number of eigenvalues:

The parameter m_g , which means the restarted subspace size of GMRES, has important influence on the convergence of UCGLE. This effect is similiar with the case on the conventional GMRES without preconditioning. For the experiments of UCGLE, we vary m_g from 50 to 180, and keep $l = 10$, $lsa = 10$, $freq = 10$. Moverover, we evaluate also the classic GMRES with m_g to be 100 and 150. The results are given in Fig. 5.13. First of all, we can conclude that in the case that m_g is too small (see UCGLE($m_g = 50$) in Fig. 5.13), even the LS preconditioning is applied, the convergence can not be achieved. With the augmentation of m_g , UCGLE is able to converge with less iteration steps. Secondly, with the preconditioning of LS polynomial, UCGLE can converge with $m_g = 100$, but the classic GMRES cannot converge with the same value of this parameter. The subspace size is a parameter that can be considered as one of the most important in the case of the hybrid method. Too small it does not allow to take into account the preconditioning, too big, it will probably not allow it. Influencing both the effect of preconditioning and the convergence of the method, the subspace size must be dimensioned properly to allow the method to converge and precondition to cause the acceleration of the resolution.

5.4.3 Convergence Evaluation

We have selected four test matrices generated by SMG2S using different given spectra to evaluate the convergence speedup of UCGLE method. The first test matrix *MEG1*

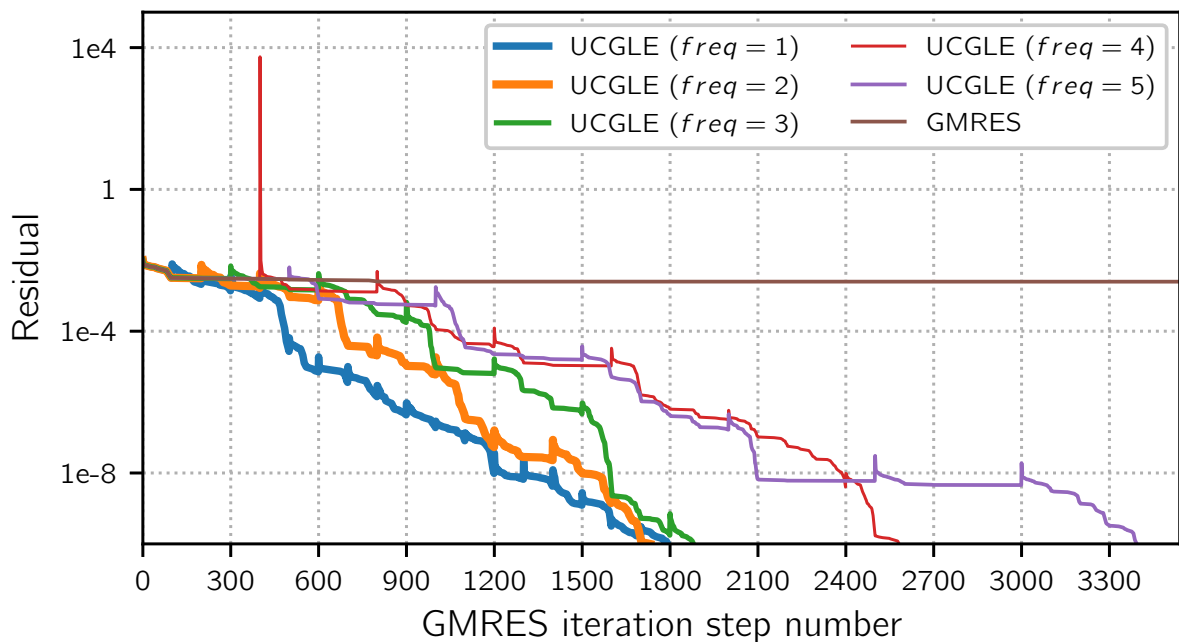
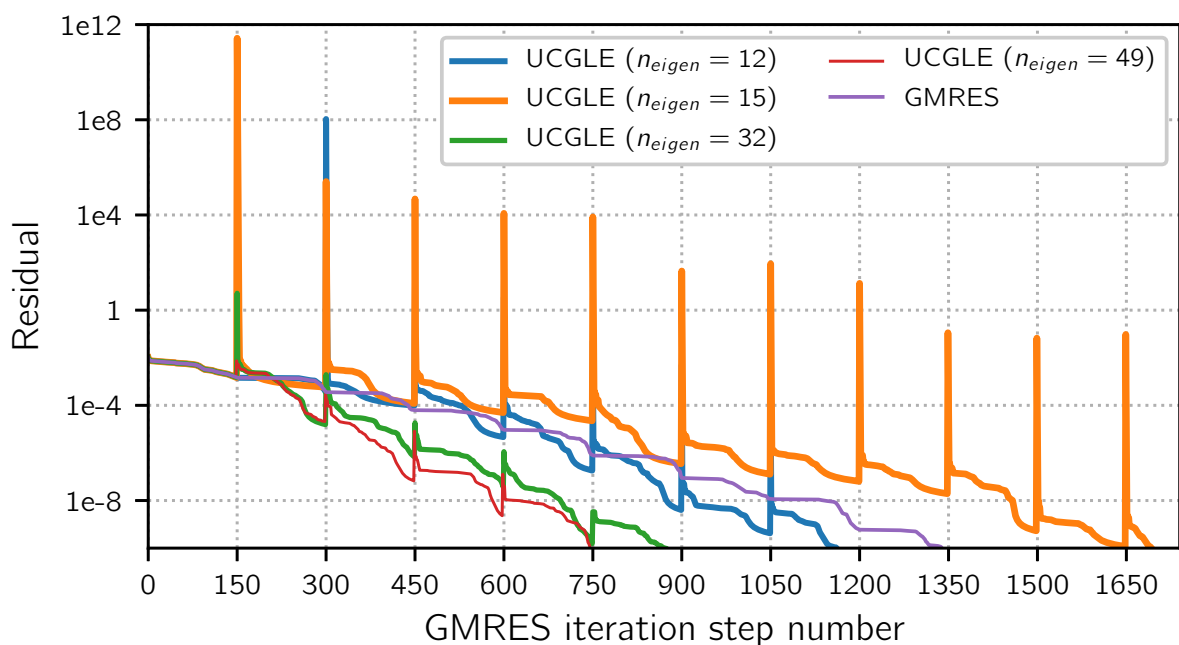

 Figure 5.16 – Evaluation of LS applied times $freq$.

 Figure 5.17 – Evaluation of eigenvalue number n_{eigen} .

Table 5.2 – Test matrices information

Matrix Name	n	nnz	Matrix Type
<i>matLine</i>	1.8×10^7	2.9×10^7	non-Symmetric
<i>matBlock</i>	1.8×10^7	1.9×10^8	non-Symmetric
<i>MEG1</i>	1.024×10^7	7.27×10^9	non-Hermitian
<i>MEG2</i>	5.1×10^6	3.64×10^9	non-Hermitian

and the second matrix *MEG2* are all generated randomly inside an annulus with different scale which is symmetric to the real axis in complex plane. The size of *MEG1* is 1.8×10^7 , and the size of *MEG2* is 1.024×10^7 . The convergence of UCGLE is compared with 1) the restarted GMRES without preconditioning, 2) restarted GMRES with Jacobi preconditioner, 3) restarted GMRES with SOR preconditioner. We select the Jacobi and SOR preconditioners for the experimentations because they are well implemented in parallel by PETSc. The GMRES restarted parameter for *MEG1*, *MEG2*, *MEG3* and *MEG4* are respectively 250, 280, 30 and 40.

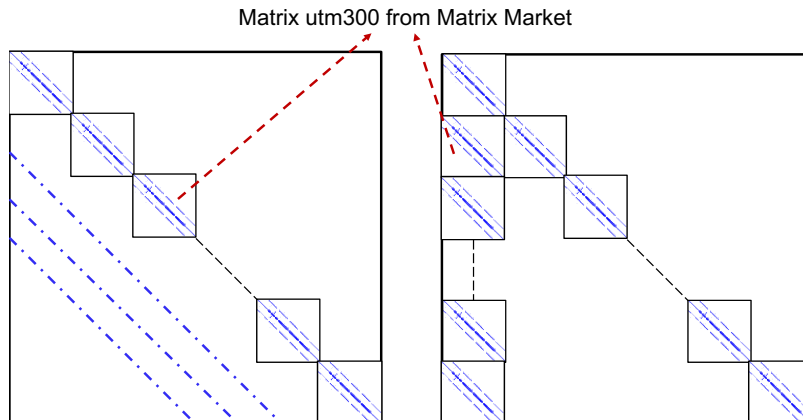


Figure 5.18 – Two strategies of large and sparse matrix generator by a original matrix *utm300* of Matrix Market.

Fig 5.19, Fig 5.20, Fig 5.21 and Fig 5.22 present respectively the convergence experiments of *MEG1*, *MEG2*, *MEG1* and *MEG2*. The numbers of iteration steps for convergence are given in Table 5.3. Obviously, UCGLE method has spectacular acceleration on the convergence for both of them over the conventional preconditioners. It has almost two times of acceleration than the SOR preconditioned GMRES. The SOR preconditioned GMRES is already better than the Jacobi preconditioned GMRES and GMRES without preconditioning for the test matrices.

5.4.4 Scalability Evaluation

This section should be rewritten to compare the scaling performance both on Tianhe-2 and Romeo.

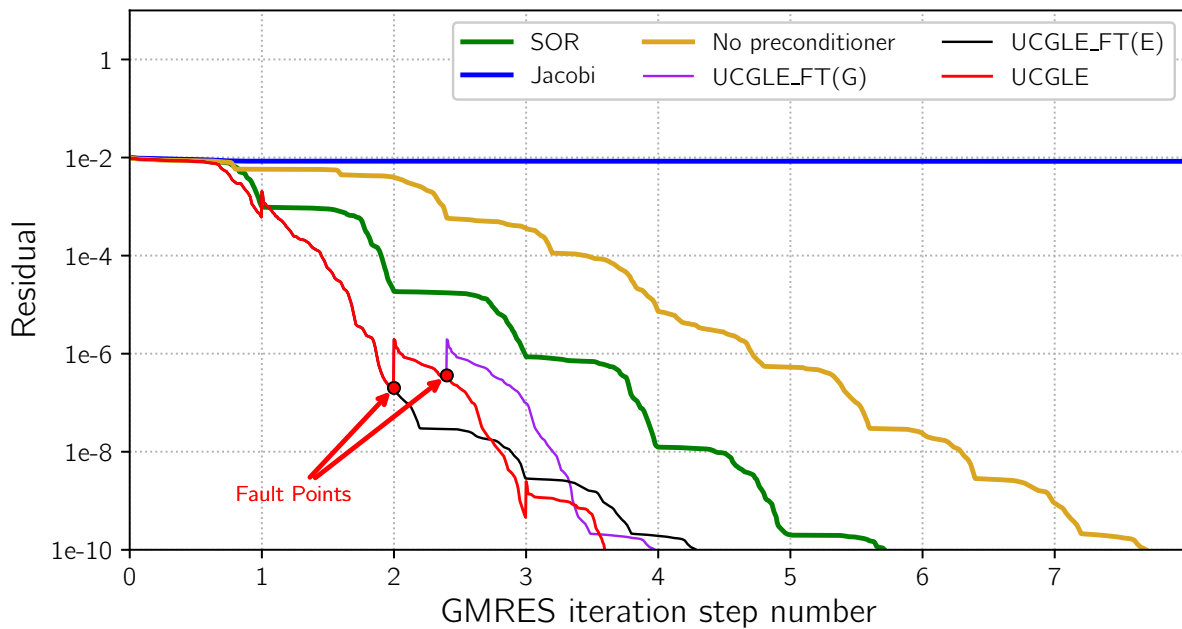


Figure 5.19 – *MEG1*: convergence comparison of UCGLE method vs conventional GMRES

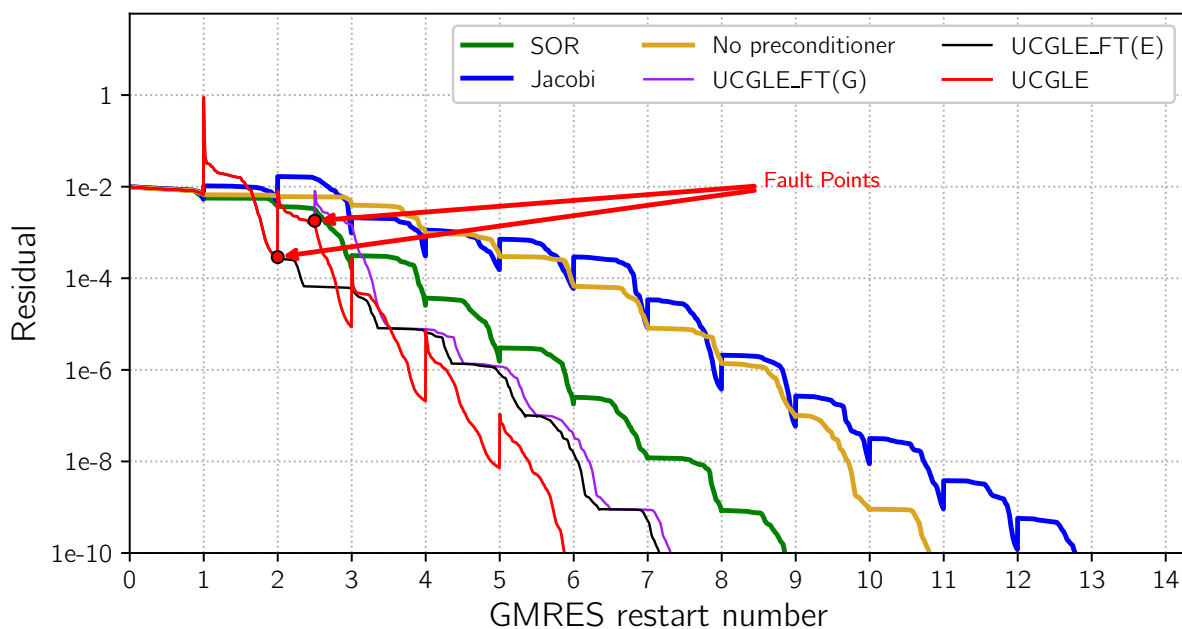


Figure 5.20 – *MEG2*: convergence comparison of UCGLE method vs conventional GMRES

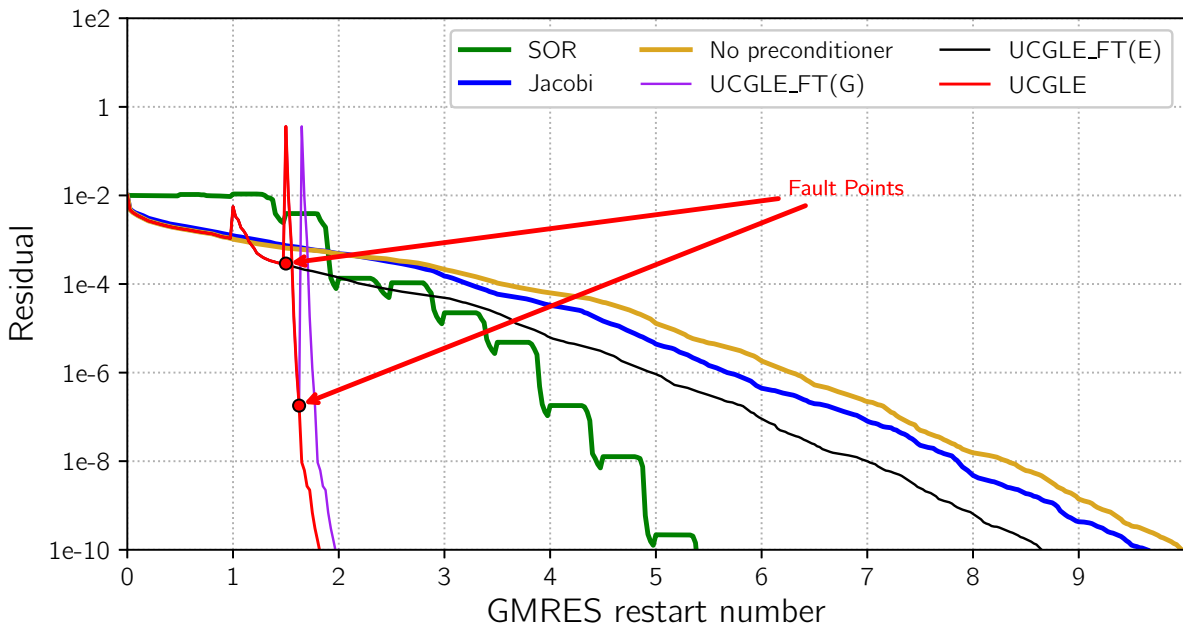


Figure 5.21 – MEG3: convergence comparison of UCGLE method vs conventional GMRES

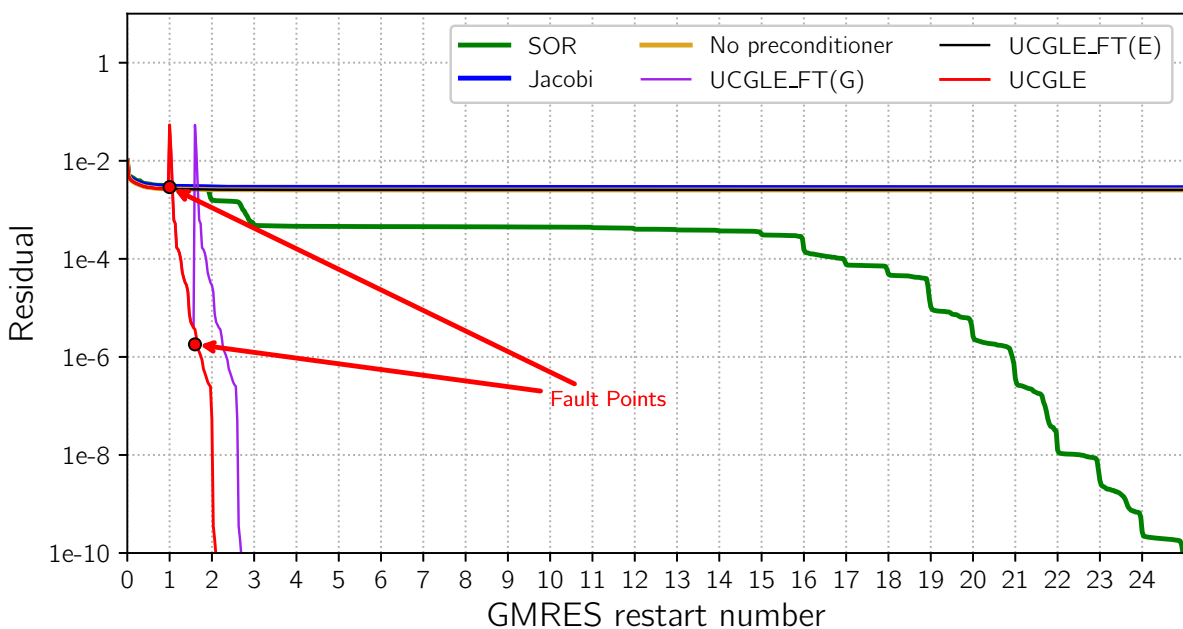


Figure 5.22 – MEG4: convergence comparison of UCGLE method vs conventional GMRES

Table 5.3 – Summary of iteration number for convergence of 4 test matrices using SOR, Jacobi, non preconditioned GMRES,UCGLE_FT(G),UCGLE_FT(G) and UCGLE: red \times in the table presents this solving procedure cannot converge to accurate solution (here absolute residual tolerance 1×10^{-10} for GMRES convergence test) in acceptable iteration number (20000 here).

Matrix Name	SOR	Jacobi	No preconditioner	UCGLE_FT(G)	UCGLE_FT(G)	UCGLE
MEG1	1430	×	1924	995	1073	900
MEG2	2481	3579	3027	2048	2005	1646
MEG3	217	386	400	81	347	74
MEG4	750	×	×	82	×	64

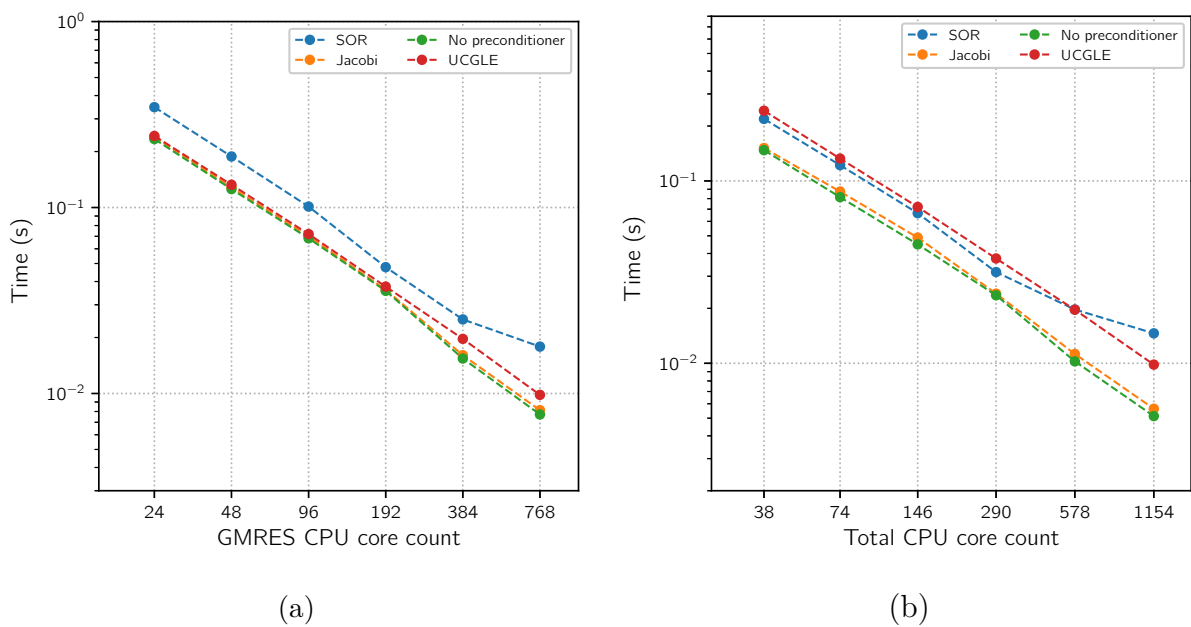


Figure 5.23 – Scalability per iteration comparison of UCGLE with GMRES with or without preconditioners on Tianhe-2.

For the resolution of large-scale linear systems on the modern supercomputing platforms, the main concern of the conventional preconditioned Krylov methods is the cost of the global communication and synchronization overheads. We select the test matrix *MEG2* for the scalability evaluation. The average time cost per iteration of these methods is computed by a fixed number of iterations. Time per iteration is suitable for demonstrating scaling behavior.

For the evaluation of UCGLE on the homogeneous cluster, the core number of GMRES Component is set respectively to be 24, 48, 96, 192, 384, 768, and both the core number of LS Component and Manager Component is 1. ERAM Component should ensure to supply the approximated eigenvalues in time for each time restart of GMRES Component. Thus we select the core number is respectively 16, 32, 64, 128, 256, 512 referring to different GMRES Component core number. The GMRES core number of conventional GMRES is equal to the one of GMRES Component in UCGLE.

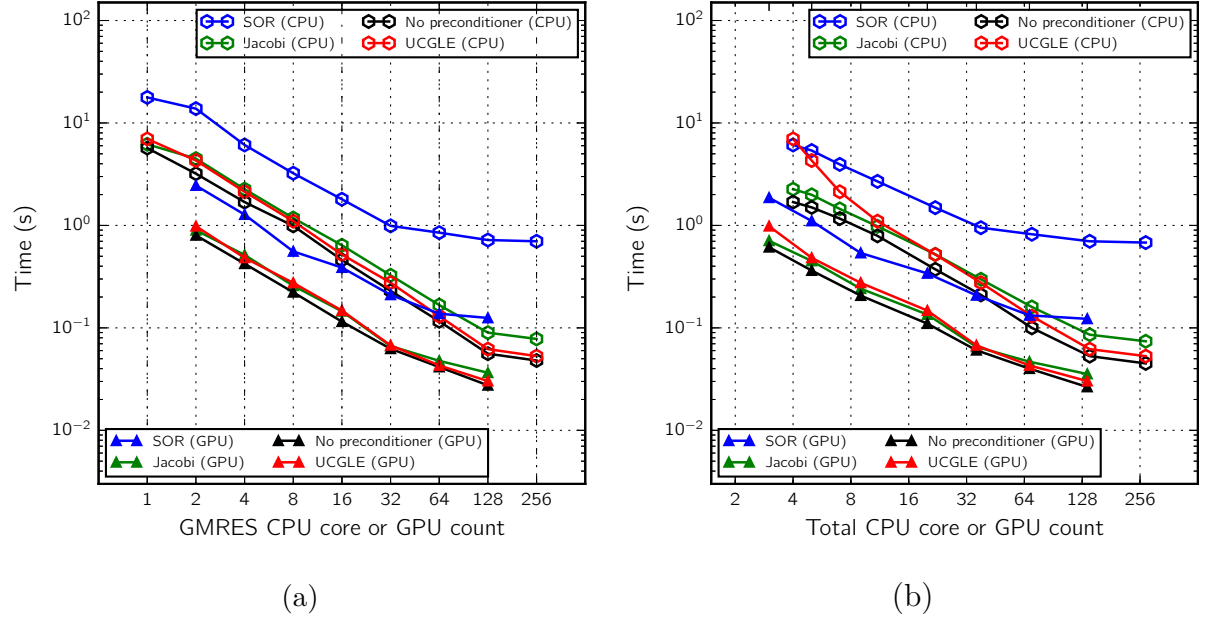


Figure 5.24 – Scalability per iteration comparison of UCGLE with GMRES with or without preconditioners on ROMEO.

In Fig. 5.23 (a), we can find that these methods have good scalability with the augmentation of computing units except the SOR preconditioned GMRES. The classic GMRES has the smallest time cost per iteration. The Jacobi preconditioner is the simplest preconditioning form for GMRES, and its time cost per iteration is similar to the classic GMRES. The GMRES with SOR preconditioner has the largest time cost per iteration since SOR preconditioned GMRES has the additional matrix-vector and matrix-matrix multiplication operations in each step of the iteration. These operations have global communication and synchronization points. The communication overhead makes the SOR preconditioned GMRES more easily lose its good scalability with the augmentation of computing unit number. There is not much difference between the time cost per iteration of classic GMRES and UCGLE with the help of the asynchronous communication implementation of UCGLE method. Since the resolving part and preconditioning part of UCGLE work independently, its global communication and synchronize points is similar to the classic GMRES without preconditioning. That is the benefits UCGLE’s asynchronous communication.

Since UCGLE requires additional computing units for the master, LS Component and especially ERAM Component, it is necessary to compare UCGLE with other methods when the total computing resource number of UCGLE and other methods keeps the same. Thus we test also the matrix *MEG2* using conventional methods with the computing unit number to be 38, 74, 146, 290, 578, 1154. The performance comparison is given in Fig. 5.23 (b). We can find that if the computing resource number is small, the time per iteration of classic and conventional preconditioned GMRES is much better than UCGLE since the latter allocates extra computing resources for other components. With the augmentation

of computing resources, the scalability of the SOR preconditioned GMRES tends to be bad, and the average time cost per iteration of UCGLE method tends to be better than the SOR preconditioned GMRES with good scalability. Although the scalability of classic and Jacobi is good, and their time per iteration is smaller than UCGLE, but since UCGLE can accelerate the convergence of solving linear systems, thus better performance can be expected.

5.4.5 Fault Tolerance Evaluation

The fault tolerance of UCGLE is studied by the simulation of the loss of either GMRES or ERAM Components. UCGLE_FT(G) in Fig. 5.19, Fig. 5.20, Fig. 5.21 and Fig. 5.22 represents the fault tolerance simulation of GMRES, and UCGLE_FT(E) implies the fault tolerance simulation of ERAM.

The failure of ERAM Component is simulated by fixing the execution loop number of ERAM algorithm, in this case, ERAM exits after a fixed number of solving procedures. We mark the ERAM fault points of the two test matrices in Fig. 5.19, Fig. 5.20, Fig. 5.21 and Fig. 5.22 : respectively 500, 560, 60 and 30 iteration step for each case. The UCGLE_FT(E) curves of the experimentations show that GMRES Component will continue to resolve the systems without LS acceleration. Table 5.3 shows that the iteration number for convergence of UCGLE_FT(E) is greater than the normal UCGLE method but less than the GMRES method without preconditioning.

The failure of GMRES Component is simulated by setting the allowed iteration number of GMRES algorithm to be much smaller than the needed iteration number for convergence. The values of these cases are respectively 600, 700, 70 and 48. They are also marked in Fig. 5.19, Fig. 5.20, Fig. 5.21 and Fig. 5.22. We can find that after the quitting of GMRES Component without the finish of its task, ERAM computing units will automatically take over the jobs of GMRES component. The new GMRES resolving procedure will use the temporary solution x_m as a new restarted initial vector received asynchronously from the previous restart procedure of GMRES Component before its failure. In this case, ERAM Component no longer exists. Thus the resolving task can be continued as the classic GMRES without LS preconditioning. In Fig. 5.19, Fig. 5.20, Fig. 5.21 and Fig. 5.22, we can find the difference between UCGLE_FT(E) and UCGLE_FT(G). In UCGLE_FT(G), the new GMRES Component takes x_m of previous restart procedure. Thus it will repeat the iteration steps of previous restart iterations until the failure of GMRES. Another fact of UCGLE_FT(G) which cannot be concluded, but can be easily obtained, is that the resolving time will be different if the computing unit numbers of previous GMRES and ERAM Components are different.

5.5 Conclusion

CHAPTER 6

UCGLE for Linear Systems with Sequences of Right-hand-sides

Many problems in science and engineering often require to solve a long sequence of large-scale non-Hermitian linear systems with different Right-hand sides (RHSs) but a unique operator. Efficiently solving such problems on extreme-scale platforms requires the minimization of global communications, reduction of synchronization points and promotion of asynchronous communications. Unite and Conquer GMRES/LS-ERAM (UCGLE) method presented in the last chapter is a suitable candidate with the reduction of global communications and the synchronization points of all computing units. In this chapter, we extend both the mathematical model and the implementation of UCGLE method to adapt to solve sequences of linear systems. The eigenvalues obtained in solving previous linear systems by UCGLE can be recycled, improved on the fly and applied to construct a new initial guess vector for subsequent linear systems, which can achieve a continuous acceleration to solve linear systems in sequence. Numerical experiments using different test matrices to solve sequences of linear systems on supercomputer Tianhe-2 indicate a substantial decrease in both computation time and iteration steps when the approximate eigenvalues are recycled to generate the initial guess vectors.

6.1 Demand to Solve Linear Systems in Sequence

We consider the solution of a long sequence of general linear systems

$$Ax^{(i)} = b^{(i)}, i = 1, 2, \dots \quad (6.1)$$

where $A \in \mathbf{C}^{n \times n}$ is a fixed matrix, and the right-hand side $b^i \in \mathbf{C}^n$ which changes from one system to another. Moreover, these systems are typically not available simultaneously. Many scientific applications require the resolution this kind of sequent linear systems, such

as the finite element analysis in modeling fatigue [Newman \[1976\]](#); [Gullerud and Dodds Jr \[2001\]](#); [Sukumar et al. \[2003\]](#), diffuse optical tomography [Kilmer and De Sturler \[2006\]](#); [Arridge et al. \[1993\]](#); [Schweiger et al. \[1995\]](#), electromagnetic [Bastos and Sadowski \[2003\]](#); [Pridmore et al. \[1981\]](#); [Ye et al. \[2008\]](#) and wave-propagation for the earthquake simulation [Fujita et al. \[2018\]](#); [Moczo et al. \[2007\]](#); [Chen et al. \[2015\]](#), etc. Generally, these systems are formatted by the time-dependent applications, where the operator matrix A keeps the same, but the right-hand side $b^{(i)}$ cannot be gotten in the same time. In many fields, the next right-hand side of the linear system depends on the previous solution. Thus only one linear system is available at a time. Another application of these sequent linear systems are the Newton methods for solving nonlinear equations (e.g., [Brown and Saad \[1990\]](#); [Knoll and Keyes \[2004\]](#); [Bellavia and Morini \[2001\]](#); [Flueck and Chiang \[1998\]](#); [An and Bai \[2007\]](#)).

If the direct solvers are applicable, their decompositions can be shared and reused for the successive linear systems by the forward/backward solves. When the matrix has a large dimension or special sparsity pattern, and the direct solvers are not applicable, then the iterative methods based on Krylov subspace, such as CG (Conjugate Gradient) method [Kershaw \[1978\]](#) for symmetric systems, and GMRES (Generalized minimal residual) method [Saad and Schultz \[1986\]](#) for non-Hermitian systems, are considerable. Obviously, this naive implementation is not efficient enough, since the sequence of linear systems shares the same matrix A . The intermediate information computed from the previous system's solution can be reused to speed up the solution of the next systems. There are already several methods proposed to take advantage of this temporary information in order to speed up resolving the sequences of linear systems. The first approach is to use the seed methods (e.g., [Saad \[1987a\]](#); [Papadrakakis and Smerou \[1990\]](#); [Smith et al. \[1989\]](#); [Gu \[2002\]](#); [Simoncini and Gallopoulos \[1995\]](#); [Abdel-Rehim et al. \[2014\]](#)). This method selects one seed system and solve it by the Krylov iterative method, and then a Galerkin projection of the other right-hand sides is performed onto the Krylov subspace generated by the seed system. It is efficient since the Krylov subspace generated by the previous time resolution develops a good approximation to the eigenvectors of small eigenvalues of A , and the projection of the other right-hand sides over this subspace can remove the components of their residual vectors in the directions these eigenvectors. The seed method requires more memory space to store the subspace of seed systems. The speedup cannot always be guaranteed for the uncorrelated right-hand sides. It can also be inefficient for the restarted methods, in this case, even the convergence of resolving the seed systems maybe stagnate. Another approach is to improve the convergence for a sequence of linear systems by the process of Krylov Subspace Recycling (e.g. [Parks et al. \[2006\]](#); [Jolivet and Tournier \[2016\]](#); [Kilmer and De Sturler \[2006\]](#); [Ye et al. \[2008\]](#)). For example, by recycling the Krylov subspace generated by previous resolution, the method GCRO-DR (Generalized Conjugate Residual method with inner Orthogonalization and

Deflated Restarting) proposed by M.L. Parks [\[2006\]](#) allows to speed up the solution of systems from one right-hand side to another or even between two times restart of iterative methods through the maintain of the Arnoldi subspace orthogonalization and the deflation of smallest eigenvalues. Additionally, Block iterative methods are a popular way to solve systems with multiple-right hands (e.g., [Simoncini and Gallopoulos \[1995\]](#); [Calvetti and Reichel \[1994\]](#); [Baker et al. \[2006\]](#); [Gutknecht \[2006\]](#)), but the different right-hand sides should simultaneously known, which is not the exact case talked in this paper.

6.2 Existing Methods and Analysis

6.2.1 Seeds Method

This section needs analyze in details the seeds method, espacially the instability for uncorreleated RHSs.

Algorithm 23 gives one kind of implementation of seeds method.

Algorithm 23 The seed-GMRES algorithm

- 1: Choose n_{max} , the maximum size of the subspace. For each RHS $b^{(l)}$, choose an initial guess $x_0^{(l)}$ and compute $r_0^{(l)} = b^{(l)} - Ax_0^{(l)}$. The recast problem is the error system $A(x^{(l)} - x_0^{(l)}) = r_0^{(l)}$, choose a RHS k , the first on which a cycle of GMRES is applied. Set $Z_p = (z_1, \dots, z_p)$, p vectors of size m , to zero.
 - 2: run one cycle of GMRES(n_{max}) on $r_0^{(k)}$, either it converges in $n = n_1$ step or stops after $n = n_{max}$ steps. This GMRES provides us with V_{n+1} , that has orthonormal columns, and $\underline{H}_{n+1,n}$ such that $AV_n = V_{n+1}\underline{H}_{n+1,n}$. The approximate solution for the k -th system writes $x_n = x_0^{(k)} + MV_n y_n^{(k)}$ but is not computed as such. The vector z_k is updated via $z_k = z_k + V_n y_n^{(k)}$ and the residual can be formattted via $x^{(k)} = x_0^{(k)} + Mz_k$. If all the systems have converged, stop.
 - 3: For each RHS $L \neq k$ that has not converged, form $c^{(l)} = V_{n+1}^T r_0^{(l)}$ and compute $y_n^{(l)}$ the solution of the least squares problems $\|\underline{H}_{n+1,n}y - c^{(l)}\|_2$. Compute $z_l = z_l + V_n y_n^{(l)}$ and the residual $r_n^{(l)} = (I_m - V_{n+1}V_{n+1}^T)r_0^{(l)} + V_{n+1}(c^{(l)} - \underline{H}_{n+1,n}y_n^{(l)})$. If the system has l converged, form the approximate solution $x^{(l)} = x_0^{(l)} + Mz_l$. If all the systems have converged, stop.
 - 4: For each RHS l that has not converged, set $r_0^{(l)} = r_n^{(l)}$. Choose a vector to run a cycle of GMRES. Traditionally we take the first l in the list $k, k+1, \dots, p$, so that the system l has not converged and go to step 2.
-

6.2.2 Krylov Subspace Recycling Methods

This section gives an example as GCR-DO, anaylze the synchronization points, etc.

The workflow of GCR-DO is given in Fig. 6.1.

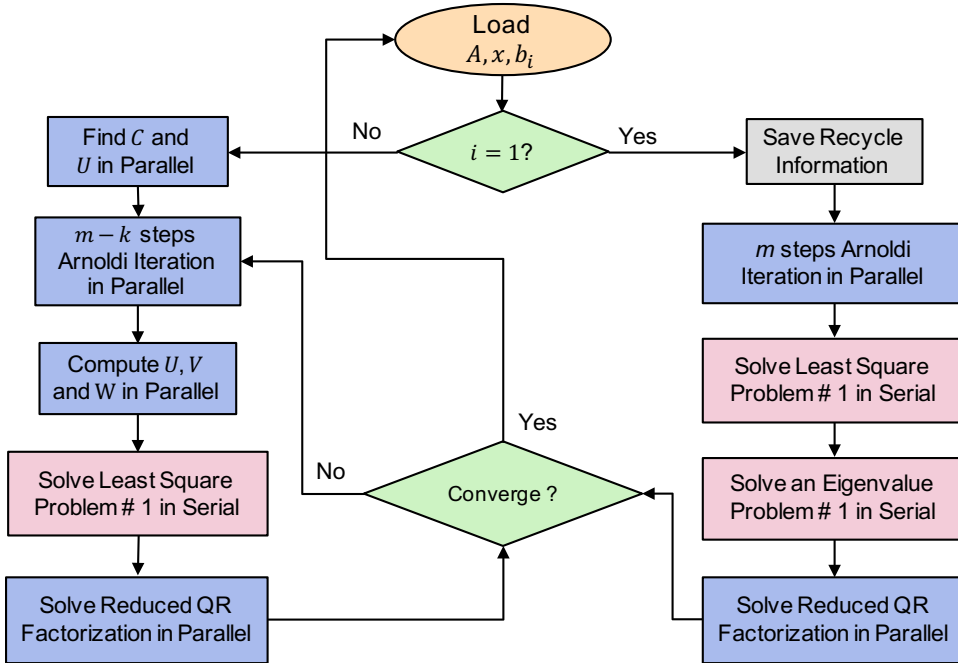


Figure 6.1 – GCR-DO workflow.

6.2.3 Challenges of Existing Methods

TO DO

6.3 UCGLE method for Linear Systems with Sequent Right-hand-sides

In this section, we introduce another point of view to solve sequences of non-Hermitian linear systems for modern computer architectures, based on UCGLE method. Inside of UCGLE, the dominant eigenvalues are used to accelerate the convergence of iterative methods. The more the eigenvalues are calculated, the more accurate these values are, the more significant the acceleration will be. When using UCGLE to solve the sequences of linear systems, the eigenvalues computed during the previous resolution can be reused, and sometimes improved, to resolve the following sequences of different linear systems. Theoretically, the continuous amelioration of convergence for the rest of the linear systems can be achieved. Moreover, the eigenvalues computed from the previous resolution can be used to construct an approximative solution by LS method and serve as an initial guess vector to speedup up the next time resolution.

6.3.1 Relation between LS Residual and Dominant Eigenvalues

Suppose that the computed convex hull by Least Squares contains eigenvalues $\lambda_1, \dots, \lambda_m$, the residual given by Least Squares polynomial of degree $d - 1$ is

$$r = \sum_{i=1}^k \rho_i(R_d(\lambda_i))^l u_i + \sum_{i=m+1}^n \rho_i(R_d(\lambda_i))^l u_i, \quad (6.2)$$

this residual can be divided into two parts. The first part is formulated with the first known m eigenvalues which are used to computed the convex hull by LS Component, the second part represents the residual with unknown eigenpairs.

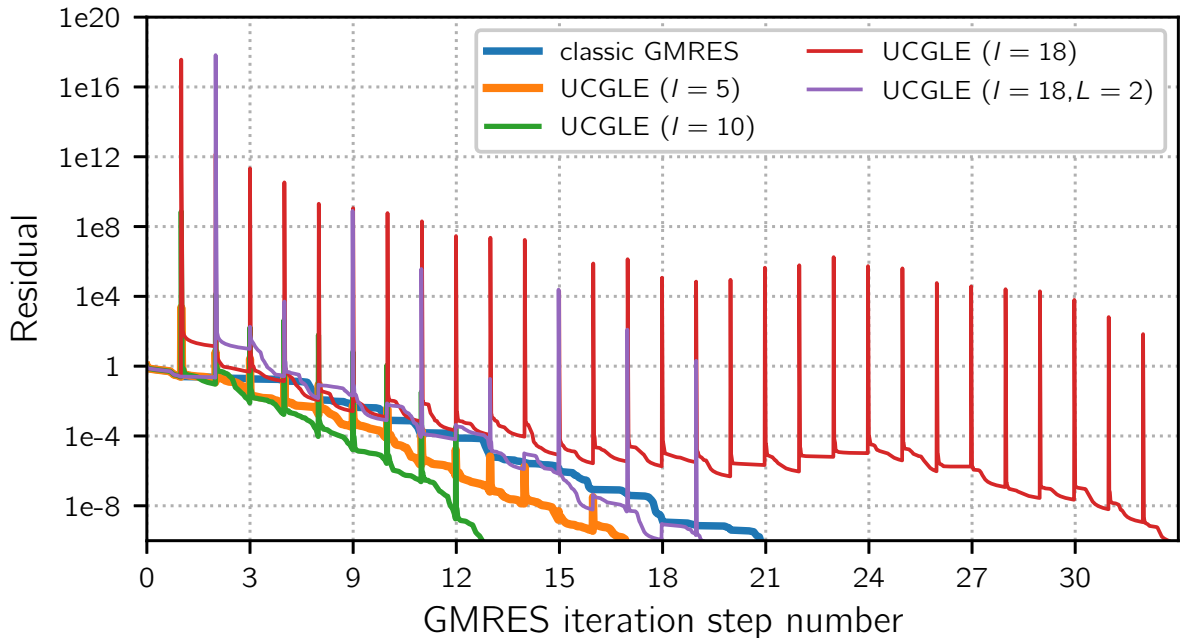


Figure 6.2 – Convergence comparison of UCGLE method vs classic GMRES.

In practice, for each time preconditioning by LS polynomial method, it is often repeated for several times to improve its acceleration of convergence, that is the meaning of parameter l in Equation (6.2). The LS polynomial preconditioning applies r_d as a deflation vector for each time GMRES restart process. Fig. 5.8 gives the comparison between classic GMRES and UCGLE with different values for the parameter l . As shown in this figure, the first part in Equation (6.2) is small since the LS method finds R_d minimizing $|R_d(\lambda)|$ in the convex hull, but not with the second part, where the residual will be rich in the eigenvectors associated with the eigenvalues outside H_k . As the number of approximated eigenvalues k increasing, the first part will be much closer to zero, but the second part keeps still large. This results in an enormous increase of restarted GMRES preconditioned vector norm. Meanwhile, when GMRES restarts with the combination of a number of eigenvectors, the convergence will be faster even if the residual is enormous, and the convergence of GMRES can still be significantly accelerated. The peaks are shown in Fig. 6.2 for each time restart of UCGLE represent these enormous residuals. The l times repeat of r_d before applying to next time restart can still enlarge its norm, and the selection of l is important for the acceleration. In the example of Fig. 6.2, we conclude that if l is too large, the norm trends enormous, which slows down the speedup, if l is small, the

acceleration may not be evident. In some situation, the preconditioned residual may be too large, and it results that GMRES cannot converge enough before the next restart. Hence the LS preconditioning can be applied each L times of GMRES restart, and the best l should be found.

6.3.2 Eigenvalues Recycling to Solve Linear Systems in Sequence

After the analysis of relation between LS polynomial residual and the approximated eigenvalues, it is apparent that these dominant eigenvalues used by LS Component to accelerate the convergence, can be recycled and improved from the procedure of solving system with one RHS to another, which will introduce a potential continuous improvement for solving a long sequence of linear systems.

In order to solve the sequence of linear systems $Ax = b_t$ with $t \in 1, 2, 3, \dots$. We enlarge the Krylov subspace size m_a inside ERAM Component to approximate more eigenvalues. Suppose that $(m_a)_1$ for the first system, the exact implementation of ERAM Component for $t \in 2, 3, \dots$ is shown in Equation (6.3), $(m_a)_t$ is equal to the sum of $(m_a)_{t-1}$ and a given constant a . And k_t , the number of eigenvalues computed by ERAM Component for $Ax = b_t$ can be described by a function f which maps the relation between $(m_a)_t$ and k_t . Obviously, $k_t \geq k_{t-1}$. The residual $(r_d)_t$ for each restart of $Ax = b_t$ with $t \in 2, 3, \dots$ is also given in (6.3).

$$\left\{ \begin{array}{l} (m_a)_t = (m_a)_{t-1} + a \\ k_t = f(m_t) \\ (r_d)_t = \sum_{i=1}^{k_t} (R_d(\lambda_i))^l \rho_i u_i + \sum_{i=k_t+1}^n (R_d(\lambda_i))^l \rho_i u_i s \end{array} \right. \quad (6.3)$$

With the enlargement of ERAM Component Krylov subspace size, the more eigenvalues are calculated, then the first part of $(r_d)_t$ in Equation (6.3) are more important, and the more significant the acceleration will be. The continuous amelioration of convergence for solving linear systems in sequence can be gotten. With the changing of ERAM component Krylov subspace size, it may not be guaranteed to get the demanded eigenvalues in time for each restart of GMRES component if this size is too large comparing with GMRES Component Krylov subspace size. In order to improve the robustness of UCGLE, the previously calculated eigenvalues are kept in memory and updated if there come the new ones. These values in memory can be utilized in case that the failure of ERAM component when the parameters are too strict. In Equation (6.3), we did not define the upper limit for $(m_a)_t$, which depends on properties of operator matrices and P_g and P_a for GMRES and ERAM components.

For $t \in 2, 3, \dots$, since the eigenvalues calculated when solving $Ax = b_{t-1}$ are kept in memory, they can be used to construct an approximative solution for the current linear

system $Ax = b_t$ through the LS polynomial method before its solve by GMRES. Obviously, this approximative solution can be used as a non-zero initial guess vector $(x_0)_t$ to solve $Ax = b_t$. It will introduce an acceleration on the convergence for solving the linear systems in sequence. With the number of linear systems to be solved increasing, there will be more eigenvalues approximated, the initial guess vector constructed by LS component will be more accurate, and thus the speedup for solves from one to another can be still gotten. In fact, the impact of initial guess vector on the convergence is different from the restarted residual vector inside the iterative method, we propose a new parameter l'_t for the initial guess generation procedure which is different from the l in LS preconditioning part. The residual vector $(g_d)_t$ for $Ax = b_t$ with $t \in 2, 3, \dots$ is given in Equation (6.4), which is constructed by the k_{t-1} number of eigenvalues calculated when solving $Ax = b_{t-1}$.

$$(g_d)_t = \sum_{i=1}^{k_{t-1}} (R_d(\lambda_i))^{l'_t} \rho_i u_i + \sum_{i=k_{t-1}+1}^n (R_d(\lambda_i))^{l'_t} \rho_i u_i. \quad (6.4)$$

In this section, two parameters are added in order to resolve linear systems in sequence using UCGLE, they are listed as below:

1. $(m_a)_t$: ERAM Krylov subspace size for solving $Ax = b_t$
2. l' : times that LS polynomial applied for the generation of initial guess vector

It is predictable that this speedup for solving successive systems will stagnate after the optimized values of m_a and l' are found. It is useless to use ERAM Component to approximate the eigenvalues continuously. Thus P_a computing units allocated for ERAM Component can be redistributed to GMRES Component. It is expected to get an extra speedup on the performance with more computing resources.

The Algorithm 24 gives the procedure of UCGLE for the resolution of a sequence of linear systems $Ax = b_t$ with $t \in 1, 2, 3, \dots$. Initially, P_g and P_a are respectively set to be $proc_g$ and $proc_a$. If $t = 1$, UCGLE loads normally the three computation components with the ERAM component's Krylov subspace to be $(m_a)_1$, and the initial guess vector for GMRES component to be zero. For the resolution of the successive linear systems, before the update of three components, a *INITIAL_GUESS* function is performed which is the same as the LS component but with different parameter l' . The *INITIAL_GUESS* function will generate an initial guess vector g_{dt} . Inside GMRES component, the initial guess vector is updated by g_{dt} before the start of resolution. Moreover, the Krylov subspace Size of ERAM Component is replaced by $(m_a)_t$. When the optimized values of $(m_a)_{op}$ and l'_{op} are found, the eigenvalues are kept into a local file *eigenvalue.bin*. The P_g and P_a are respectively updated as $proc_g + proc_a - 1$ and 1. The *INITIAL_GUESS* function executes by loading *eigenvalue.bin*. *LOADGMRES* is restarted with the redeployment of its data onto $proc_g + proc_a - 1$ computing units. *LS* also executes with *eigenvalue.bin*. The

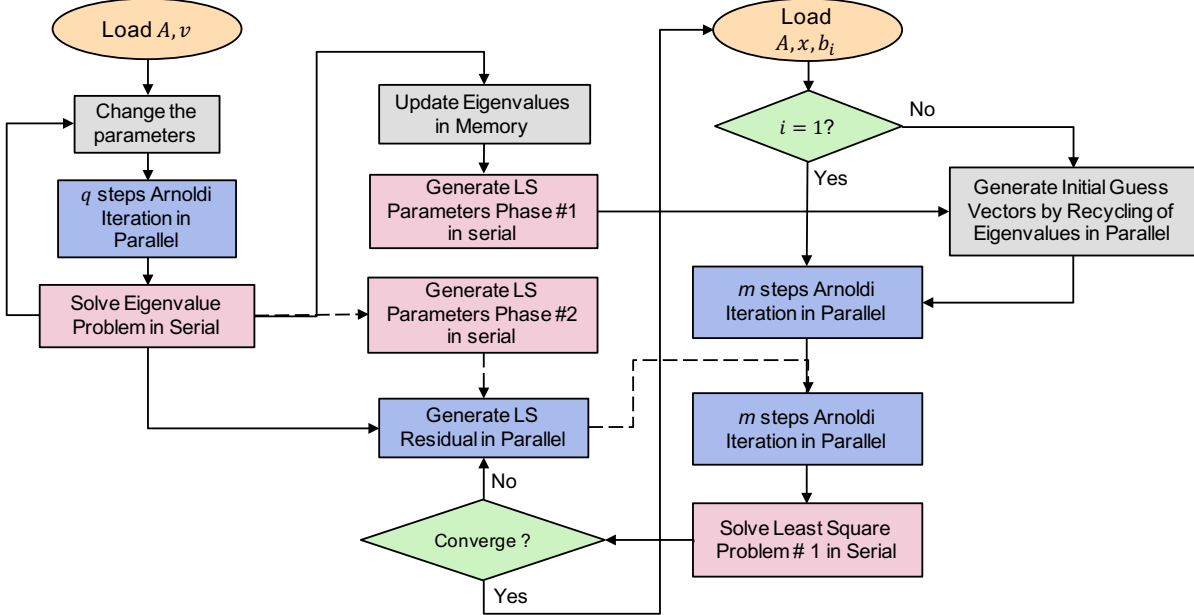


Figure 6.3 – Workflow of UCGLE to Solve Linear Systems In Sequence.

retainment of 1 computing unit for ERAM Component aims to ensure the distributed and parallel implementation of UCGLE with high fault tolerance. However, the inside kernel of ERAM Component is replaced by a simple function with keeping the data sending and receiving functionalities.

6.3.3 Experiments of UCGLE for Sequences of Linear Systems

In this section, we evaluate the UCGLE for solving the sequences of linear systems on the supercomputer using different generated test matrices. UCGLE with or without initial guess vector generation is compared with conventional restarted GMRES with or without available preconditioners (Jacobi and SOR) in our implementations. The parallel performance on different homogeneous and heterogeneous platforms is presented in [Wu and Petiton \[2018a\]](#). Thus this paper concentrates on the numerical performance of UCGLE for solving non-Hermitian linear systems in sequence, and the parallel performance comparison will not be discussed. Indeed, the performance of UCGLE can achieve further improvement with unique implementation targeting at different computer architectures, but this is not the purpose of this paper. *Unite and Conquer approach* (including UCGLE) is a particular programming model which introduces a better performance on top of classic solvers and makes them be more suitable for modern computers. It is fair to prove the benefits of *Unite and Conquer approach* by comparing it with the implementations of classic solvers based on the same basic operations (distribution of matrix across the cores, parallel sparse matrix-vector operation, the orthogonalization in Arnoldi reduction, etc.) without specific optimization for different platforms. In fact, if we optimize the parallel implementation of classic solvers and also the components (especially GMRES

Algorithm 24 UCGLE for sequences of linear systems

```

1: for ( $t \in (1, 2, 3, \dots)$ ) do
2:   if ( $t = 1$ ) then
3:     set  $P_g = proc_g$  and  $P_a = proc_a$ 
4:      $LOADERAM(input : A, m_a, v, r, \epsilon_a)$ 
5:      $LOADLS(input : A, b, d)$ 
6:      $LOADGMRES(input : A, m_g, x_0, b_1, \epsilon_g, L, l, output : x_m)$ 
7:   else
8:     set  $P_g = proc_g$  and  $P_a = proc_a$ 
9:      $INITIAL\_GUESS(input : A, b_t, d, output : g_{dt})$ 
10:    update  $LOADGMRES(input : A, m_g, g_{dt}, b_t, \epsilon_g, L, l, output : x_m)$ 
11:    update  $(m_a)_{t-1}$  by  $(m_a)_t$  in  $LOADERAM(input : A, (m_a)_t, v, r, \epsilon_a)$ 
12:    update  $LOADLS(input : A, b_i, d)$ 
13:    if (optimized  $(m_a)_{op}$  and  $l'_{op}$  found) then
14:      save the eigenvalues to eigenvalues.bin
15:      set  $P_g = proc_g + proc_a - 1$  and  $P_a = 1$ 
16:       $INITIAL\_GUESS(input : A, b_t, d, output : g_{dt})$  by loading
        eigenvalues.bin
17:       $LOADGMRES(input : A, m_g, g_{dt}, b_t, \epsilon_g, L, l'_{op}, output : x_m)$ 
18:      replace  $LOADERAM$  by a simple useless function
19:       $LOADLS(input : A, b_i, d)$  by loading eigenvalues.bin
20:    end if
21:  end if
22: end for

```

Component) in UCGLE at the same time, the benefits of UCGLE by reducing the global communications and promoting the synchronization are still there.

6.3.3.1 Experimental Hardwares

UCGLE is implemented on the supercomputer *Tianhe-2*, installed at the National Super Computer Center in Guangzhou of China. It is a heterogeneous system made of Intel Xeon CPUs and Matrix2000, with 16000 compute nodes in total. Each node composes 2 Intel Ivy Bridge 12 cores @ 2.2 GHz. In this paper, we did not test UCGLE with co-processor Matrix2000 on *Tianhe-2* since our implementation does not support it with good performance.

6.3.3.2 Experimental Results

We evaluate UCGLE for solving sequences of linear systems using three test matrices of size 1.572×10^7 generated by SMG2S with different given spectra. They are respectively denoted as *Mat1*, *Mat2* and *Mat3*. The different right-hand sides of these sequent linear systems are generated at random. The parameter l for all tests using UCGLE keeps the same as 10. The numbers of process for GMRES and ERAM Components in UCGLE are respectively 768 and 384. Five methods are compared in the experiments, and the notations of different methods are given as below:

- GMRES: classic restarted GMRES;
- GMRES+SOR or SOR: GMRES with SOR preconditioner;
- GMRES+Jacobi or Jacobi: GMRES with Jacobi preconditioner;
- UCGLE without initial guess: UCGLE without using previously obtained eigenvalues to generate an initial guess vector for the next system by LS polynomial method;
- UCGLE with initial guess: UCGLE using previously obtained eigenvalues to generate an initial guess vector for the next systems by LS polynomial method.

ERAM and LS components in UCGLE demand additional computing units. It is unfair to test only the conventional methods of their numbers of CPUs equal to the number of GMRES components in UCGLE. Therefore, experiments have also been tested that the numbers of computing units of the classical iterative method are equal to the total CPU in UCGLE (hence, the CPUs for GMRES and ERAM components are included). In the captions of figures, a given method "with total CPUs" means that its number of CPUs equals the total CPU in UCGLE. The time comparisons for solving nine sequent linear systems of *Mat1*, *Mat2* and *Mat3* are given respectively in Fig. 6.4 (a), Fig. 6.5 (a) and

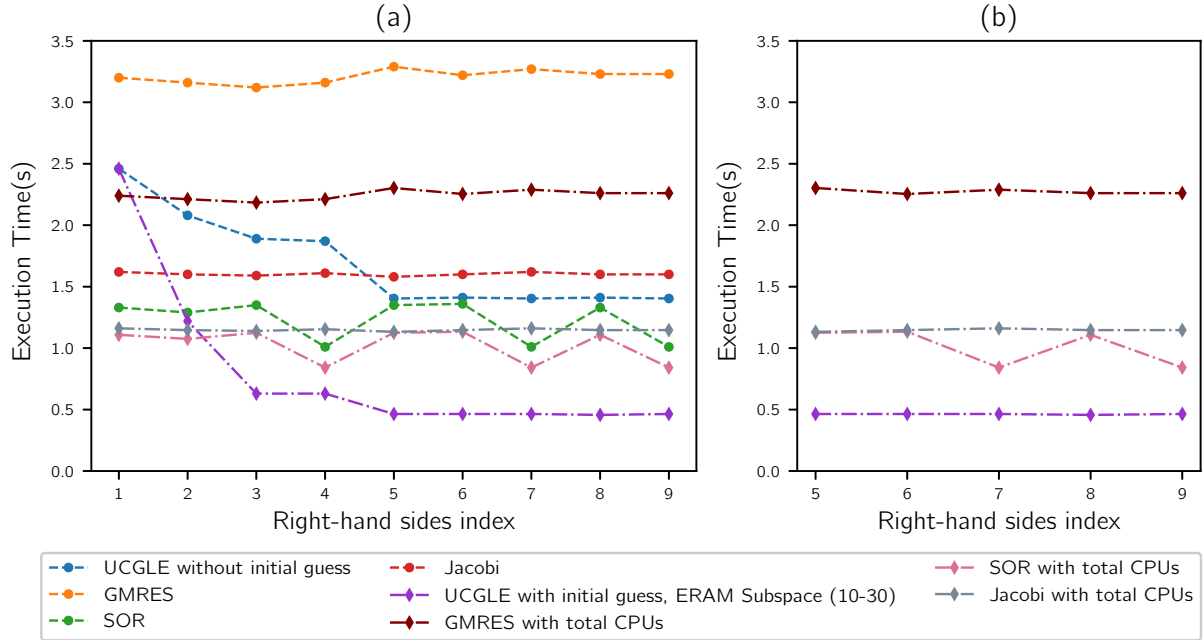


Figure 6.4 – *Mat1*: time comparison for solving a sequence of linear systems. (a) shows the solution time for 9 sequent linear systems; (b) shows the cases extracted from (a) after the good selection of parameters in UCGLE.

Fig. 6.6 (a), the comparison of the number of iteration for convergence are respectively given in Table 1, Table 2 and Table 3. From these three tables, we conclude that UCGLE can speed up the convergence to solve linear systems with test matrices comparing with the conventional methods. The generation of initial vectors using the eigenvalues for subsequent linear systems can still speed up the convergence over the UCGLE without initial guess.

Table 6.1 – *Mat1*: iterative step comparison for solving a sequence of linear systems.

Method	1	2	3	4	5	6	7	8	9
GMRES	509	505	501	505	527	510	523	516	518
GMRES+SOR	169	165	172	130	172	173	130	170	130
GMRES+Jacobi	274	273	270	276	269	274	280	276	273
UCGLE w/o initial guess	120	90	90	90	90	90	90	90	90
UCGLE with initial guess	120	36	35	35	36	36	36	33	35

For the tests of *Mat1*, the GMRES restart size is 30, the Krylov subspace of ERAM Component for solving the first three linear systems are respectively 10, 20 and 30, the size of this subspace of ERAM for the remaining systems keeps being 30. For the tests of *Mat2*, the GMRES restart size is 300, the Krylov subspace of ERAM Component for solving the first three linear systems are respectively 100, 150 and 200, the size of this

subspace of ERAM for the remaining systems keeps being 200. For the cases that UCGLE with initial guess, the parameter l' for *Mat1* and *Mat2* keeps 30. With the augmentation of the size of ERAM Krylov subspace, there will be more eigenvalues to be approximated, and we find that there is acceleration with the accumulation of more eigenvalues for both the case UCGLE with and without initial guess. The influence of subspace of ERAM can be found through the curves of UCGLE with/without initial guess in Fig. 6.4 (a) and Fig. 6.5 (a). However, it is not practical to enlarge too much the Krylov subspace of ERAM to approximated more eigenvalues, since if it is too large, it takes too much time by ERAM, LS Component cannot receive the eigenvalues in time, thus it will be difficult for the GMRES Component to perform the LS preconditioning for it each time restart.

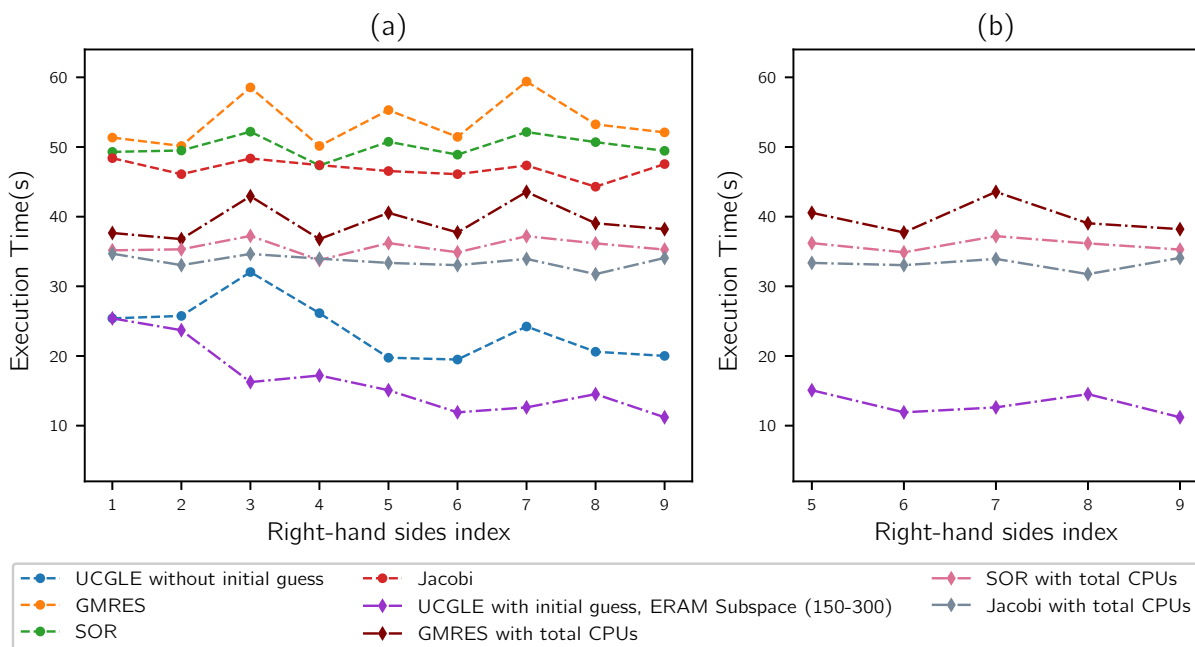


Figure 6.5 – *Mat2*: time comparison for solving a sequence of linear systems. (a) shows the solution time for 9 sequent linear systems; (b) shows the cases extracted from (a) after the good selection of parameters in UCGLE.

Table 6.2 – *Mat2*: iterative step comparison for solving a sequence of linear systems.

Method	1	2	3	4	5	6	7	8	9
GMRES	1316	1277	1460	1278	1409	1325	1472	1369	1342
GMRES+SOR	1197	1219	1336	1173	1290	1194	1335	1289	1213
GMRES+Jacobi	1278	1185	1283	1220	1191	1184	1218	1159	1239
UCGLE w/o initial guess	666	671	831	689	701	685	837	736	714
UCGLE with initial guess	666	595	470	491	544	464	485	532	440

For the tests of *Mat3*, the GMRES restart size is 150, and the Krylov subspace size of

ERAM Components keeps the same to be 200. Meanwhile, for the 2nd, 3rd and 4th linear systems, the parameter l' of initial guess are respectively 20, 30 and 40, for the remaining linear systems, this parameter keeps 40. For the solving the linear systems by UCGLE with an initial guess, we can find that with the augmentation of l' , the iteration numbers for the first four linear systems decrease quickly from 360 to 283 with approximately $1.3\times$ speedup. For *Mat3*, SOR preconditioned GMRES is already good, but UCGLE with initial guess has still about $2.2\times$ speedup of convergence. Even in the case that the computing unit number of SOR preconditioned GMRES equals the total number of UCGLE, UCGLE with initial guess can achieve $2.2\times$ of execution time speedup. With the augmentation of the parameter l' , there will be a strong impact on the convergence. Since the *Mat3* is generated with the clustered eigenvalues which are randomly distributed inside a fixed region of the real-imaginary plan, if l' is larger, it can be seen as there are much more eigenvalues generated, even they are not very accurate compared with the real ones. The inaccuracy of eigenvalues can result in the enlargement the norm in Equation (6.3), but it can still very quickly converge. It is effective to generate an initial guess vector with very large l' , but not the same case for the parameter l inside each preconditioning, since the too many times of repeats for each time restart will amplify quickly this inaccuracy of norm, and it is easy to result in the difficulties of convergence.

In order to use UCGLE for solving a large number of linear systems in sequence, it is necessary to choose the suitable parameters by the evaluation of a small number of sequent linear systems. After the selection of parameters, we compare the best cases of each method with the least time consumption. The results for three test matrices are shown in Fig. 6.4 (b), Fig. 6.6 (b) and Fig. 6.5 (b). We conclude that for *Mat1*, UCGLE with initial guess has about $4.4\times$ for the acceleration of convergence and $1.7\times$ for the speedup of execution time. For *Mat2*, it has about $2.6\times$ acceleration for the convergence and $4.3\times$ for the speedup of time. For *Mat3*, it has about $3.2\times$ acceleration for the convergence and $2.0\times$ for the speedup of time.

Table 6.3 – *Mat3*: iterative step comparison for solving a sequence of linear systems.

Method	1	2	3	4	5	6	7	8	9
GMRES	914	912	892	885	895	905	911	892	904
GMRES+SOR	895	871	856	885	879	870	868	838	868
GMRES+Jacobi	894	888	875	864	876	887	892	888	872
UCGLE w/o initial guess	673	364	355	360	367	363	363	351	364
UCGLE with initial guess	673	396	291	283	339	338	274	279	267

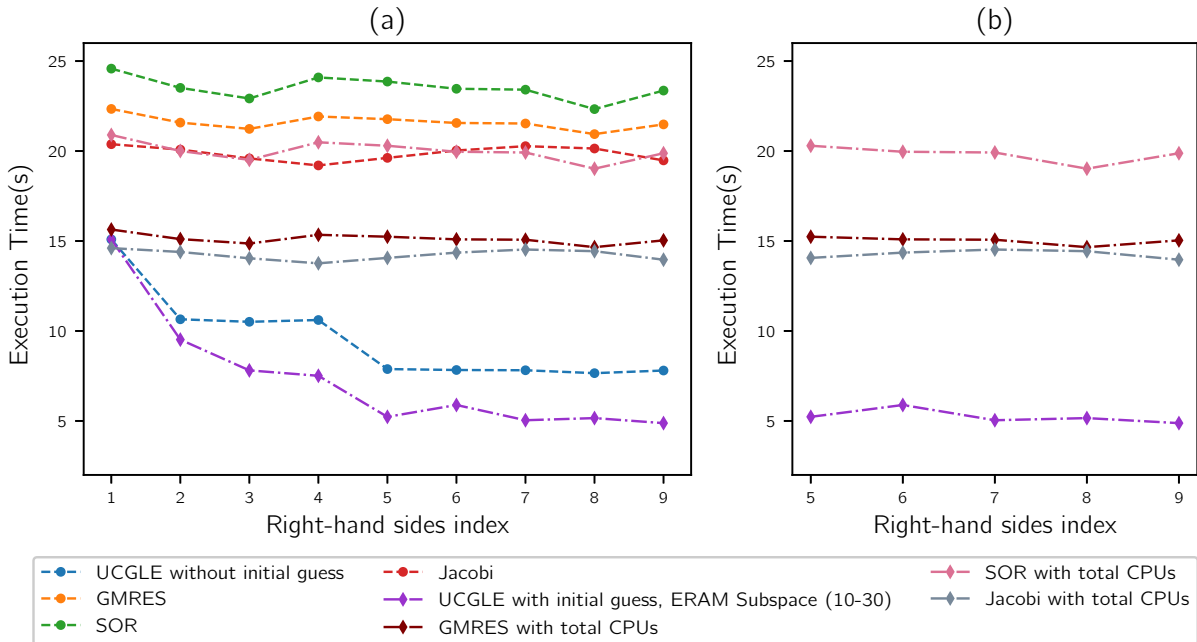


Figure 6.6 – *Mat3*: time comparison for solving a sequence of linear systems. (a) shows the solution time for 9 sequent linear systems; (b) shows the cases extracted from (a) after the good selection of parameters in UCGLE.

6.3.3.3 Analysis and Conclusions

In conclusion, the UCGLE, especially it with the recycling eigenvalues to generate initial guess vector using the eigenvalues, can significantly accelerate the convergence and reduce the time consumption for solving a sequence of linear systems. However, the time employed by the LS iterative recurrence, especially a small number of Sparse Matrix-Vector Product operations inside makes the time speedup not consistent with the convergence speedup. For example, in Table 3, UCGLE with initial guess has almost $3.0\times$ acceleration on the convergence over the classic GMRES for solving the 3rd linear system. However, it has only about $2.0\times$ acceleration on the performance in the case that the classic GMRES and GMRES Component inside UCGLE have the same number of computing units. It is caused by the recurrence of LS iterations to perform the preconditioning on GMRES Component after receiving the parameters from LS Component. Nevertheless, UCGLE is more efficient to solve the sequences of linear systems, and with its distributed and parallel communication framework, it is a good candidate for solving non-Hermitian linear systems in sequence on much larger machines.

6.4 Conclusion

CHAPTER 7

UCGLE for Linear Systems with Multiple Right-hand-sides

Many problems in science and engineering often require to solve simultaneously large-scale non-Hermitian sparse linear systems with multiple right-hand sides (RHSs). Efficiently solving such problems on extreme-scale platforms also requires the minimization of global communications, reduction of synchronization points and promotion of asynchronous communications. Unite and Conquer GMRES/LS-ERAM (UCGLE) method is also a suitable candidate with the reduction of global communications and the synchronization points of all computing units. In this chapter, we develop another extension of the Unite and Conquer GMRES/LS-ERAM (UCGLE) method by combining it with Block GMRES method to solve non-Hermitian linear systems with multiple RHSs, with novel designed manager engine implementations. This engine is capable of allocating multiple Block GMRES at the same time, each Block GMRES solving the linear systems with a subset of RHSs and accelerating the convergence using the eigenvalues approximated by other eigensolvers. Dividing the entire linear system with multiple RHSs into subsets and solving them simultaneously with different allocated linear solvers allow localizing calculations, reducing global communication, and improving parallel performance. Meanwhile, the asynchronous preconditioning using eigenvalues can speed up the convergence and improve the fault tolerance and reusability. Numerical experiments using different test matrices on supercomputer ROMEO indicate that the proposed method achieves a substantial decrease in both computation time and iterative steps with good scaling performance.

7.1 Demand to Solve Linear Systems with Multiple Right-hand-sdes

In this chapter, we consider solving the system

$$AX = B, \quad (7.1)$$

where $A \in \mathbb{C}^{n \times n}$ is a large, sparse and non-Hermitian matrix of order n , $X = [x_1, \dots, x_s] \in \mathbb{C}^{n \times s}$ and $B = [b_1, \dots, b_s] \in \mathbb{C}^{n \times s}$ are rectangular matrices of dimension $n \times s$ with $s \leq n$. In this paper, the rectangular matrices such as B is also called multi-vector, which can be seen as the combination of s vectors $b_i \forall i \in 1, 2, \dots, s$. This kind of linear systems with multiple RHSs arise from a variety of applications in different scientific and engineering fields, such as the Lattice Quantum Chromodynamics (QCD) [Sakurai et al. \[2010\]](#); [Nakamura et al. \[2012\]](#); [Fiebach et al. \[1997\]](#), the wave scattering and propagation simulation [Malhotra et al. \[1997\]](#), dynamics of structures [Barbella et al. \[2011\]](#); [Ferraz and Dos Santos \[2001\]](#); [Nour-Omid and Clough \[1985\]](#), etc. The block Krylov methods are good candidates if we want to solve these large linear systems at the same time because the block methods can expand the search space associated with each RHS and may accelerate the convergence. Another feature of block Krylov methods is that they can be implemented using BLAS3, which improves the locality and reusability of data and reduces the memory requirement on modern computer architectures [Agullo et al. \[2014\]](#). The block Krylov methods replace the Sparse Matrix-Vector Multiplication (SpMV) in each iterative step of the conventional Krylov methods with the Sparse Generalized Matrix-Matrix (SpGEMM) Multiplication.

7.2 Existing Methods and Analysis

This section should talk a little in details about Block GMRES

7.2.1 Block Method

Algorithm 25 Block Arnoldi Algorithm

```

1: function BLOCK ARNOLDI(input: $A, m, V \in \mathbb{C}^{N \times s}$  of full rank, output:  $H_m, \Omega_m$ )
2:    $V_0 P_0 := V$                                  $\triangleright$  QR factorization:  $P_0 \in \mathbb{C}^{s \times s}, V_0 \in \mathbb{C}^{N \times s}, V_0^* V_0 = I$ 
3:   for  $j = 0, 1, 2, \dots, m$  do
4:      $U_j = AV_j$                                  $\triangleright s$  MVs
5:     for  $i = 1, 2, 4, \dots, j$  do
6:        $H_{i,j} = V_i^T U_j$                        $\triangleright s^2$  SDOTs
7:        $U_j = U_j - V_i H_{i,j}$                    $\triangleright s^2$  SAXPYs
8:     end for
9:      $U_j = V_{j+1} H_{j+1,j}$   $\triangleright$  QR factorization:  $H_{j+1,j} \in \mathbb{C}^{s \times s}, V_{j+1} \in \mathbb{C}^{N \times s}, V_{j+1}^* V_{j+1} = I$ 
10:   end for
11: end function

```

Then we define the $N \times n$ matrices

$$\bar{V}_n = (V_0 \quad V_1 \quad \cdots \quad V_{n-1})$$

Algorithm 26 Block GMRES Algorithm

```

1: function BLOCK GMRES(input: $A, m, B, X_0 \in \mathbb{C}^{N \times s}$  of full rank, output:  $X$ )
2:    $R = B - AX_0$ 
3:    $V_0 R_0 := R$                                  $\triangleright$  QR factorization:  $P_0 \in \mathbb{C}^{s \times s}, V_0 \in \mathbb{C}^{N \times s}, V_0^* V_0 = I$ 
4:   for  $j = 0, 1, 2, \dots, m$  do
5:      $U_j = AV_j$                                  $\triangleright s$  MVs
6:     for  $i = 1, 2, 4, \dots, j$  do
7:        $H_{i,j} = V_i^T U_j$                        $\triangleright s^2$  SDOTs
8:        $U_j = U_j - V_i H_{i,j}$                    $\triangleright s^2$  SAXPYs
9:     end for
10:     $U_j = V_{j+1} H_{j+1,j}$   $\triangleright$  QR factorization:  $H_{j+1,j} \in \mathbb{C}^{s \times s}, V_{j+1} \in \mathbb{C}^{N \times s}, V_{j+1}^* V_{j+1} = I$ 
11:  end for
12:   $W_m = [V_1, V_2, \dots, V_m], H_m = \{H_{i,j}\}_{0 \leq i \leq j; 1 \leq j \leq m}$ 
13:  Find  $y_m$ , s.t.  $\|\beta - H_m y_m\|_2$  is minimized
14:   $X = X + W_m y_m$ 
15: end function

```

Table 7.1 – Operation Cost.

Operations	Block Arnoldi	s times Arnoldi
MVs	ms	ms
SDOTs	$\frac{1}{2}m(m+1)s^2 + \frac{1}{2}ms(s+1)$	$\frac{1}{2}m(m+1)s$
SAXPYs	$\frac{1}{2}m(m+1)s^2 + \frac{1}{2}ms(s+1)$	$\frac{1}{2}m(m+1)s$

Table 7.2 – Storage Requirement.

Operations	Block Arnoldi	s times Arnoldi
y_1, \dots, y_m	$ms(s+1)N$	$(m+1)N$

7.2.2 Cost Comparison

7.2.3 Challenges of Existing Methods for Large-scale Platforms

However, nowadays, HPC cluster systems continue to scale up not only the number of compute nodes and central processing unit (CPU) cores but also the heterogeneity of components by introducing graphics processing units (GPUs) and many-core processors. This

Table 7.3 – Extra cost of Block GMRES comparing with s times GMRES.

Operations	Block GMRES	s times GMRES
MVs	s	s
SDOTs	ms^2	ms
scalar work	$\mathcal{O}(m^2s^3)$	$\mathcal{O}(m^s)$

Table 7.4 – Extra cost of Block GMRES comparing with s times GMRES.

Operations	Block GMRES	s times GMRES	ratio
MVs	$(1 + \frac{1}{m})s$	$(1 + \frac{1}{m})s$	1
SDOTs	$\frac{1}{2}(m+1)s^2 + \frac{1}{2}s(s+1)$	$\frac{1}{2}(m+1)s$	$s + \frac{s+1}{m+1}$
SAXPYs	$\frac{1}{2}(m+3)s^2 + \frac{1}{2}s(s+1)$	$\frac{1}{2}(m+3)s$	$s + \frac{s+1}{m+3}$
scalar work	$\mathcal{O}(ms^3)$	$\mathcal{O}(m^s)$	$\mathcal{O}(s^2)$

results in the tendency of transition to multi- and many cores within computing nodes, which communicate explicitly through faster interconnection networks. These hierarchical supercomputers can be seen as the intersection of distributed and parallel computing. Indeed, for a large number of cores, the communication of overall reduction operations and global synchronization of applications are the bottleneck. The seed and recycling methods talked above for solving a sequent of linear systems, introduce the special process (e.g., the image projection and sparse matrix-vector product) to accelerate the next time resolution, which has much more additional global communication operations and synchronization points. They will lose their advantages on the large-scale hierarchical platforms. When solving linear systems by block Krylov methods on large-scale distributed memory platforms, the cost of using BLAS3 operations to enlarge search space and reduce the memory requirement is apparent: the communication bound of SpGEMM in each step of Arnoldi projection damages heavily their performance, which cannot be compensated by the advantages of the block methods.

Even using classic Krylov methods, such as GMRES (Generalized Minimal Residual method), to solve a large-scale problem on parallel clusters, the cost per iteration of them becomes the most significant concern, typically caused by communication and synchronization overheads. Consequently, large scalar products, overall synchronization, and other operations involving communication among all cores have to be avoided. The numerical applications should be optimized for more local communication, less global communication, and synchronization. That is the reason for the recent tendance to study the communication avoiding techniques for linear algebra operations [Demmel et al. \[2008\]](#); [Hoemmen \[2010\]](#); [Carson \[2015\]](#) and different pipelined strategies for Krylov methods

Ghysels et al. [2013]; Morgan et al. [2016]; Cools and Vanroose [2017]. For benefiting the full computational power of such hierarchical systems, it is central to explore novel parallel methods and models for the solving of linear systems. These methods should accelerate not only the convergence but also have the abilities to adapt to multi-grain, multi-level memory, to improve the fault tolerance, reduce synchronization and promote asynchronization.

7.3 ***m*-UCGLE for Multiple Right-hand-sides**

We propose to combine the Block GMRES (BGMRES) Vital [1990] with UCGLE Wu and Petiton [2018b] to solve Equation (7.1) in parallel on modern computer architectures. In this paper, firstly, we develop a block version of Least Squares Polynomial (B-LSP) method based on Saad [1987b], then replace the three computing components of UCGLE respectively by the BGMRES, Shifted Krylov-Schur (*s*-KS), and B-LSP. Additionally, in order to solve linear systems with multiple RHSs and reduce the global communication, we design and implement a new manager engine to replace the former one in UCGLE. This novel engine allows to allocate and deploy multiple BGMRES and/or *s*-KS Components at the same time and support their asynchronous communications. Each allocated BGMRES is assigned to solve the linear systems with a subset of RHSs. This extension is denoted as multiple-UCGLE or *m*-UCGLE even though the ERAM Component is replaced by *s*-KS method.

7.3.1 Shifted Krylov-Schur Algorithm

UCGLE uses the dominant eigenvalues to accelerate the convergence of GMRES, and theoretically, the more eigenvalues are applied, the acceleration of Least Squares Polynomial will be more significant Wu and Petiton [2018b]. In order to approximate more eigenvalues by ERAM Component, the easiest way is to enlarge the size of related Krylov Subspace. In *m*-UCGLE, we replace ERAM Component by *s*-KS method which is another variant of the Arnoldi algorithm with an effective and robust restarting scheme and numerical stability Stewart [2002]. The Krylov subspace of *s*-KS cannot be too large. Otherwise BGMRES Component is not able to receive the eigenvalues in time to perform the B-LSP acceleration. With the novel developed manager engine of *m*-UCGLE in this paper, several different *s*-KS components can be allocated at the same time to approximate efficiently the different part of dominant eigenvalues of matrix A , by the shift with different values and thickly restarting with smaller Krylov subspace sizes. The algorithm of *s*-KS is given in Algorithm 27.

Algorithm 27 Shifted Krylov-Schur Method

```

1: function s-KS(input:  $A, x_1, m, \sigma$ , output:  $\Lambda_k$  with  $k \leq p$ )
2:    $A \leftarrow A - \sigma I$ 
3:   Build an initial Krylov decompostion of order  $m$ 
4:   Apply orthogonal transformations to get a Krylov-Schur decompostion
5:   Reorder the diagonal blocks of the Krylov-Schur decompostion
6:   Truncate to a Krylov-Schur decompostion of order  $p$ 
7:   Extend to a Krylov decomposition of order  $m$ 
8:   If not satisfied, go to step 3
9: end function

```

7.3.2 Least Squares Polynomial for Multiple Right-hand sides

The Least Squares polynomial method is an iterative method proposed by Saad [\[1987b\]](#) to solve linear systems. It is applied to calculate a new preconditioned residual for restarted GMRES in UCGLE. In this section, we will present the B-LSP method, which is a block extension of Least Squares polynomial method to solve linear systems with multiple RHSs at the same time. The iterates of B-LSP method can be written as $X_n = X_0 + \mathcal{P}_d(A)R_0$, where $X_0 \in \mathbb{C}^{N \times s}$ is a selected initial guess to the solution, $R_0 \in \mathbb{C}^{N \times s}$ the corresponding residual multi-vector, and \mathcal{P}_d a polynomial of degree $d - 1$. We set a polynomial of n degree \mathcal{R}_n such that

$$\mathcal{R}_d(\lambda) = 1 - \lambda\mathcal{R}_d(\lambda)$$

The residual of n^{th} steps iteration R_n can be expressed as equation $R_n = \mathcal{R}_d(A)R_0$, with the constraint $\mathcal{R}_d(0) = 1$. We want to find a kind of polynomial which can minimize all $\|\mathcal{R}_d(A)R_0^{(p)}\|_2$, with $p \in 0, 1, \dots, s - 1$, $R_0^{(p)}$ the p^{th} vector in the multi-vector R_0 and $\|\cdot\|_2$ the Euclidean norm.

Suppose A is a diagonalizable matrix with its spectrum denoted as $\sigma(A) = \lambda_1, \dots, \lambda_n$, and the associated eigenvectors u_1, \dots, u_n . Expanding the each component of R_n in the basis of these eigenvectors as as $R_n^{(p)} = \sum_{i=1}^n \mathcal{R}_d(\lambda_i)\rho_i u_i$, which allows to get the upper limit of $\|R_n^{(p)}\|_2$ with $p \in 0, 1, \dots, s - 1$ as:

$$\|R_0^{(p)}\|_2 \max_{\lambda \in \sigma(A)} |\mathcal{R}_d(\lambda)| \quad (7.2)$$

In order to minimize the norm of $R_n^{(p)}$, it is possible to find a polynomial \mathcal{P}_d which can minimize the Equation (7.2) $\forall p \in 0, 1, \dots, s - 1$.

As presented in [Wu and Petiton \[2018b\]](#), \mathcal{P}_d can be expanded with a basis of Chebyshev polynomial $t_j(\lambda) = \frac{T_j(\frac{\lambda-c}{b})}{T_j(\frac{c}{b})}$, where t_i is constructed by an ellipse englobing the convex hull formulated by the computed eigenvalues, with c the centre of ellipse, and b the focal distance of this ellipse. \mathcal{P}_d is under form that $\mathcal{P}_d = \sum_{i=0}^{d-1} \eta_i t_i$. The selected Chebyshev

polynomials t_i meet still the three terms recurrence relation (7.3).

$$t_{i+1}(\lambda) = \frac{1}{\beta_{i+1}} [\lambda t_i(\lambda) - \alpha_i t_i(\lambda) - \delta_i t_{i-1}] \quad (7.3)$$

For the computation of parameters $H = (\eta_0, \eta_1, \dots, \eta_{d-1})$, we construct a modified gram matrix M_d with dimension $d \times d$, and matrix T_d with dimension $(d+1) \times d$ by the three terms recurrence of the basis t_i . M_d can be factorized to be $M_d = LL^T$ by the Cholesky factorization. The parameters H can be computed by a least squares problem of the formula:

$$\min \|l_{11}e_1 - F_d H\| \quad (7.4)$$

With the definition of $\Omega_i \in R^{N \times s}$ by $\Omega_i = t_i(A)R_0$, we can obtain the Equation (7.5), and in the end iteration (7.6).

$$\Omega_{i+1} = \frac{1}{\beta_{i+1}} (A\Omega_i - \alpha_i \Omega_i - \delta_i \Omega_{i-1}) \quad (7.5)$$

$$X_n = X_0 + \mathcal{P}_d(A)R_0 = X_0 + \sum_{i=1}^{n-1} \eta_i \Omega_i \quad (7.6)$$

The pre-treatment of this method to obtain the parameters $A_d = (\alpha_0, \dots, \alpha_{d-1})$, $B_d = (\beta_1, \dots, \beta_d)$, $\Delta_d = (\delta_1, \dots, \delta_{d-1})$, and $H_d = (\eta_0, \dots, \eta_{d-1})$ is presented in Algorithm 28, where A is a $n \times n$ matrix, B represents the multi-vector of RHSs, d is the degree of Least Squares polynomial, Λ_r the collection of approximate eigenvalues, a, c, b the required parameters to fix an ellipse in the plan, with a the distance between the vertex and centre, c the centre position and b the focal distance. The iterative recurrence implementation of Equation (7.5) and (7.6) using the parameters gotten from the pre-treatment procedure to construct the restarted residual for BGMRES by B-LSP is given in Algorithm 29. In this algorithm, X_0 is the temporary solution in BGMRES before performing the restart. Compared with Least Squares polynomial method for single RHS, the difference in B-LSP is to replace the SpMV in each iteration step with SpGEMM, as shown in Equation (7.6).

7.3.3 Analysis

Suppose that the computed convex hull by B-LSP contains eigenvalues $\lambda_1, \dots, \lambda_m$, the restarted residual for BGMRES generated by B-LSP for solving Equation (7.1) can be divided into two parts:

$$R_n = \sum_{i=1}^m \sum_{j=1}^s \rho((\mathcal{R}_d^{(j)})(\lambda_i)^{\nu}) u_i + \sum_{i=m+1}^n \sum_{j=1}^s \rho((\mathcal{R}_d^{(j)})(\lambda_i)^{\nu}) u_i \quad (7.7)$$

The first part is constructed with the m known eigenvalues used to compute the convex

Algorithm 28 Least Square Polynomial Pre-treatment

```

1: function LS(input:  $A, B, d, \Lambda_r$ , output:  $A_d, B_d, \Delta_d, H$ )
2:   construct the convex hull  $C$  by  $\Lambda_r$ 
3:   construct  $ellispe(a, c, b)$  by the convex hull  $C$ 
4:   compute parameters  $A_d, B_d, \Delta_d$  by  $ellispe(a, c, b)$ 
5:   construct matrix  $T$   $(d+1) \times d$  matrix by  $A_d, B_d, \Delta_d$ 
6:   construct Gram matrix  $M_d$  by Chebyshev polynomials basis
7:   Cholesky factorization  $M_d = LL^T$ 
8:    $F_d = L^T T$ 
9:    $H_d$  satisfies  $\min \|l_{11}e_1 - F_d H\|$ 
10: end function
```

Algorithm 29 Update BGMRES residual by LS Polynomial

```

1: function LSUPDATERESIDUAL(input:  $A, B, A_d, B_d, \Delta_d, H_d$ )
2:   Get  $X_0$ , which is temporary solution in BGMRES
3:    $R_0 = B - AX_0$ ,  $\Omega_1 = R_0$ 
4:   for  $k = 1, 2, \dots, l$  do
5:     for  $i = 1, 2, \dots, d-1$  do
6:        $\Omega_{i+1} = \frac{1}{\beta_{i+1}}[A\Omega_i - \alpha_i\Omega_i - \delta_i\Omega_{i-1}]$ 
7:        $X_{i+1} = X_i + \eta_{i+1}\Omega_{i+1}$ 
8:     end for
9:   end for
10:  Update GMRES restarted residual by  $X_d$ 
11: end function
```

hull in B-LSP Component, and the second part represents the residual with unknown eigenpairs. In the practical implementation, for each time preconditioning by the B-LSP method, it is often repeated for several times to improve its acceleration of convergence, that is the meaning of parameter l in Equation (7.7). The B-LSP preconditioning applies R_d as a deflation vector for each time restart of BGMRES. The first part in Equation (7.7) is small since the B-LSP finds R_d minimizing $|\mathcal{R}_d(\lambda)|$ in the convex hull, but not with the second part, where the residual will be rich in the eigenvectors associated with the eigenvalues outside H_k . As the number of approximated eigenvalues k increasing, the first part will be much closer to zero, but the second part keeps still large. This results in an enormous increase of restarted BGMRES preconditioned vector norm. Meanwhile, when BGMRES restarts with the combination of some eigenvectors, the convergence will be faster even if the residual is enormous, and the convergence of BGMRES can still be significantly accelerated.

m-UCGLE is a combination of different methods. Thus it has a large number of parameters, which have impacts on the convergence. These parameters are listed and classified according to their relations with different components as follows:

1. BGMRES Component

- (a) m_g : BGMRES Krylov Subspace size
- (b) ϵ_g : relative tolerance for BGMRES convergence test
- (c) P_g : number of computing units for each BGMRES
- (d) l : number of times that polynomial applied on the residual before taking account into the new eigenvalues
- (e) L : number of BGMRES restarts between two times of B-LSP preconditioning
- (f) s : number of RHSs

2. *s*-KS Component

- (a) m_a : *s*-KS Krylov subspace size
- (b) r : number of eigenvalues required
- (c) ϵ_a : tolerance for the *s*-KS convergence test
- (d) P_a : number of computing units for *s*-KS
- (e) σ : shifted value

3. B-LSP Component

- (a) d : Polynomial degree of B-LSP

7.3.4 Manager Engine Implementation

As presented in Chapter 5, the former implementation of manager engine in [Wu and Petiton \[2018b\]](#) based on MPI_Split cannot meet the requirement of m -UCGLE. Thus, in order to extend UCGLE method to solve non-Hermitian linear systems and to reduce the global communication and synchronization points, we design and implement a new manager engine for m -UCGLE. As shown in Figure 7.1, the new engine allows creating a number of different computing components at the same time. Suppose that we have allocated n_g BGMRES Components, n_k s -KS Components and 1 B-LSP Component. The exact implementation for s -KS, B-LSP, BGMRES Components and manager process are respectively given in Algorithms 5, 6, 7 and 8. Denote the BGMRES Components as BGMRES[k] with $k \in 1, 2, \dots, n_g$, and the s -KS Components as s -KS[q] with $q \in 1, 2, \dots, n_a$. The matrix B in Equation (7.1) can be decomposed as:

$$B = [B_1, B_2, \dots, B_k, \dots, B_{n_g}] \quad (7.8)$$

Each BGMRES[k] will solve the linear systems with multiple RHSs B_k , which is a subgroup of B :

$$AX_k = B_k \quad (7.9)$$

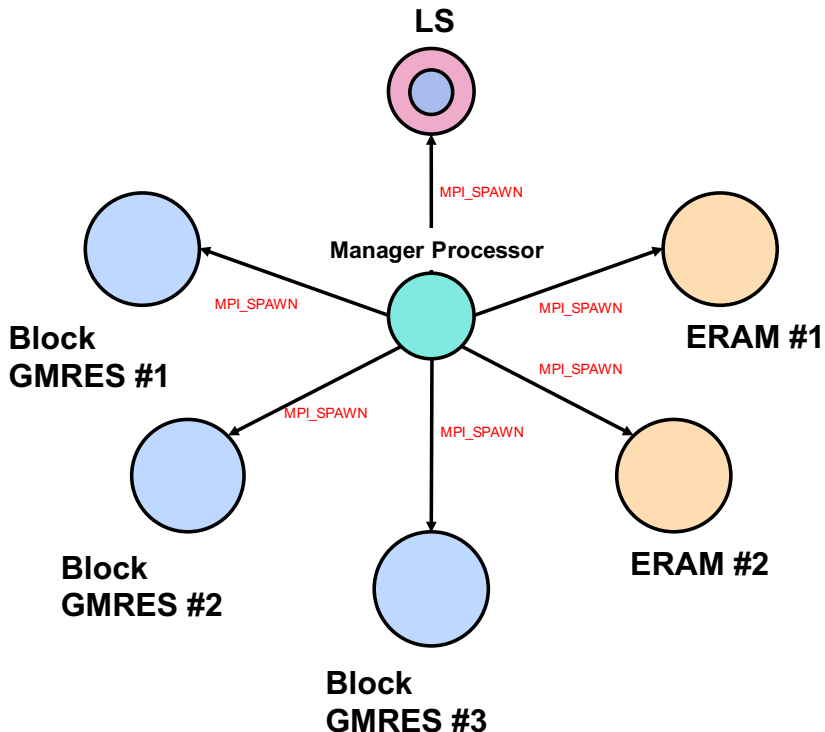


Figure 7.1 – Manager Engine Implementation for m -UCGLE.

Table 7.5 gives the comparison of memory and communication complexity of SpGEMM

operation inside *m*-UCGLE and BGMRES with the same number of RHSs. The factors n , nnz , s , P_g and n_g represent respectively the matrix size, the number of non-zero entries of matrix, the number of multiple RHSs, the total number of computing units for BGMRES Components, and the number of BGMRES Components allocated by the manager engine of *m*-UCGLE. The average memory requirement for BGMRES on each computing unit is $\mathcal{O}(\frac{nnz(1+s)}{P_g})$. For *m*-UCGLE, the matrix is duplicated n_g times into different allocated linear solvers. Thus the required memory to store the matrix should be scaled with the factor n_g comparing with BGMRES. Due to the localization of computation inside *m*-UCGLE, the total number global communication can be reduced with a factor $\frac{1}{n_g}$ comparing with BGMRES. In practice, the selection of the number to allocate the BGMRES Components should make a balance between the increase of memory requirement and the reduction of global communication.

Table 7.5 – Memory and Communication Complexity Comparison between *m*-UCGLE and BGMRES.

	<i>m</i> -UCGLE	BGMRES	ratio
Memory	$\mathcal{O}(\frac{nnz(n_g+s)}{P_g})$	$\mathcal{O}(\frac{nnz(1+s)}{P_g})$	$\frac{n_g+s}{1+s}$
Communication	$\mathcal{O}(\frac{nnzsP_g}{n_g})$	$\mathcal{O}(nnzsP_g)$	$\frac{1}{n_g}$

Algorithm 30 *s*-KS Component

```

1: function s-KS-EXEC(input:  $A, m_a, \nu, r, \epsilon_a$ )
2:   while exit==False do
3:     s-KS( $A, r, m_a, \nu, \epsilon_a$ , output:  $\Lambda_r$ )
4:     Send ( $\Lambda_r$ ) to LS
5:     if Recv (exit == TRUE) then
6:       Send (exit) to LS Component
7:     stop
8:   end if
9:   end while
10: end function

```

Here we present in detail the workflow of this new engine. In the beginning, the manager will simultaneously allocate the required number of three kinds of computing components. For each BGMRES[k], it will load a full matrix A and its related subgroup B_k , and then start to solve Equation (7.9) separately. Meanwhile, each *s*-KS[q] load a full matrix A from local, and start to find the required part of eigenvalues of A , through the *s*-KS method, using different parameters such as the shift value σ_q , the Krylov subspace size $(m_a)_q$, etc. If the eigenvalues of the required number are approximated on *s*-KS[q], these values will be asynchronously sent to the manager process. The manager process will always check if new eigenvalues are available from different *s*-KS Components, if

yes, it will collect and update the new coming eigenvalues together and send them to B-LSP Component. B-LSP Component will use all the eigenvalues received from manager process to do the pre-treatment of the B-LSP, the parameters gotten will be sent back to the manager process. Immediately, these parameters will be distributed to BGMRES[k]. BGMRES[k] can use the B-LSP residual constructed by these parameters to speed up the convergence. If the exit signals from all BGMRES Components are received by manager process, it will send a signal to all other components to terminate their executions.

The allocation of a different number of computing components is implemented with MPI_SPAWN, and their asynchronous communication is assured by the MPI non-blocking sending and receiving operations between the manager process and each computing components.

Algorithm 31 B-LSP Component

```
1: function B-LSP-EXEC(input:  $A, b, d$ )
2:   if Recv( $\Lambda_r$ ) then
3:     LS(input:  $A, b, d, \Lambda_r$ , output:  $A_d, B_d, \Delta_d, H_d$ )
4:     Send ( $A_d, B_d, \Delta_d, H_d$ ) to GMRES Component
5:   end if
6:   if Recv (exit == TRUE) then
7:     stop
8:   end if
9: end function
```

Same as UCGLE, m -UCGLE has multiple levels of parallelism for distributed memory systems:

1. Coarse Grain/Component level: it allows the distribution of different numerical components, including the preconditioning part (B-LSP and s -KS) and the solving part (BGMRES) on different platforms or processors;
2. Medium Grain/Intra-component level, BGMRES and s -KS components are both deployed in parallel;
3. Fine Grain/Thread parallelism for shared memory: the OpenMP thread-level parallelism, or the accelerator level parallelism if GPUs or other accelerators are available.

7.3.5 m -UCGLE Implementation on Multi-GPU

TO DO

7.3.6 Parallel and Numerical Performance Evaluation

In this section, we evaluate the numerical performance of m -UCGLE for solving non-Hermitian linear systems compared with conventional BGMRES.

Algorithm 32 BGMRES Component

```

1: function BGMRES-EXEC(input:  $A, m_g, X_0, B, \epsilon_g, L, l$ , output:  $X_m$ )
2:   count = 0
3:   BGMRES(input:  $A, m, X_0, B$ , output:  $X_m$ )
4:   if  $\|B - AX_m\| < \epsilon_g$  then
5:     return  $X_m$ 
6:     Send (exit == TRUE) to manager process
7:     Stop
8:   else
9:     if count | L then
10:      if recv ( $A_d, B_d, \Delta_d, H_d$ ) then
11:        LSUpdateResidual(input:  $A, B, A_d, B_d, \Delta_d, H_d$ )
12:        count ++
13:      end if
14:    else
15:      set  $X_0 = X_m$ 
16:      count ++
17:    end if
18:  end if
19:  if Recv (exit == TRUE) then
20:    stop
21:  end if
22: end function

```

7.3.6.1 Hardware/Software Settings and Test Sparse Matrices

After the implementation of *m*-UCGLE, we test it on the supercomputer with selected test matrices. The purpose of this section is to give the details about the hardware/software settings and test sparse matrices.

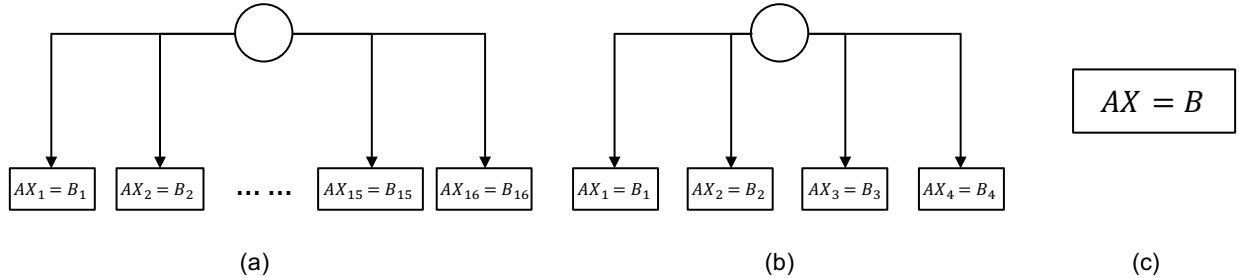


Figure 7.2 – Different strategies to divide the linear systems with 64 RHSs into subsets:
(a) divide the 64 RHSs into to 16 different components of *m*-UCGLE, each holds 4 RHSs;
(b) divide the 64 RHSs into to 4 different components of *m*-UCGLE, each holds 16 RHSs;
(c) One classic BGMRES to solve the linear systems with 64 RHSs simultaneously.

Experiments were obtained on the supercomputer *ROMEO*¹, a system located at University of Reims Champagne-Ardenne, France. Made by Atos, this cluster relies on totally

1. <https://romeo.univ-reims.fr>

Algorithm 33 Manger of m -UCGLE with MPI Spawn

```
1: function MASTER(Input :  $n_g, n_a$ )
2:   for  $i = 1 : n_g$  do
3:     MPI_Spawn executable BGMRES-EXEC[ $i$ ]
4:   end for
5:   for  $j = 1 : n_k$  do
6:     MPI_Spawn executable  $s$ -KS-EXEC[ $j$ ]
7:   end for
8:   MPI_Spawn executable B-LSP-EXEC
9:   for  $j = 1 : n_k$  do
10:    if Recv array[ $j$ ] from  $s$ -KS-EXEC[ $j$ ] then
11:      Add array[ $j$ ] to Array
12:    end if
13:   end for
14:   if Array  $\neq$  NULL then
15:     Send Array to B-LSP-EXEC
16:   end if
17:   if Recv LSPArray from B-LSP-EXEC then
18:     for  $i = 1 : n_g$  do
19:       Send LSPArray to BGMRES-EXEC[ $i$ ]
20:     end for
21:   end if
22:   for  $i = 1 : n_k$  do
23:     if Recv flag[ $i$ ] for BGMRES-EXEC[ $i$ ] then
24:       if flag[ $i$ ] == exit then
25:         flag=true
26:       else
27:         flag=false
28:       end if
29:     end if
30:   end for
31:   if flag == true then
32:     Kill B-LSP-EXEC
33:     for  $i = 1 : n_g$  do
34:       Kill BGMRES-EXEC[ $i$ ]
35:     end for
36:     for  $j = 1 : n_k$  do
37:       Kill  $s$ -KS-EXEC[ $j$ ]
38:     end for
39:   end if
40: end function
```

115 the Bull Sequana X1125 hybrid servers, powered by the Xeon Gold 6132 (products formerly Skylake) and NVidia P100 cards. Each dense Bull Sequana X1125 server accommodates 2 Xeon Scalable Processors Gold bi-socket nodes, and 4 NVidia P100 cards connected with NVLink. In total, this supercomputer includes 3,220 Xeon cores and 280 Nvidia P100 accelerators.

The MPI (Message Passing Interface) used is the OpenMPI 3.1.2, all the shared libraries and binaries were compiled by *gcc* (version 6.3.0). The released scientific computational libraries Trilinos (version 12.12.1) and LAPACK (version 3.8.0) were also compiled and used for the implementation of *m*-UCGLE.

7.3.6.2 Specific Experimental Setup

Table 7.6 – Alternative methods for experiments, and the related number of allocated component, Rhs number per component and preconditioners.

Method	Component nb	RHS nb per component	Preconditioner
BGMRES(64)	1	64	None
<i>m</i> -BGMRES(16) \times 4	4	16	None
<i>m</i> -BGMRES(4) \times 16	16	4	None
<i>m</i> -UCGLE(16) \times 4	4	16	B-LSP
<i>m</i> -UCGLE(4) \times 16	16	4	B-LSP

In the experiments, the total number of RHSs of linear systems to be solved for each test is fixed as 64. As shown in Figure 7.2, we propose three strategies to divide these systems into various subgroup:

1. 1 group with all 64 RHSs solved by classic BGMRES (shown by Figure 7.2(c));
2. 4 allocated BGMRES Components in *m*-UCGLE with each holding 16 Rhs (shown by Figure 7.2(a));
3. 16 allocated BGMRES Components in *m*-UCGLE with each holding 4 Rhs (shown in Figure 7.2(b)).

Moreover, for *m*-UCGLE with 4 or 16 allocated components, they can be applied either with or without the preconditioning of B-LSP using approximate eigenvalues. Denote the special variant of *m*-UCGLE without B-LSP preconditioning as *m*-BGMRES. *m*-BGMRES is also able to reduce the global communications through allocating multiple BGMRES components by the manager engine. Table 7.6 gives the naming of the five alternatives to solve linear systems with 64 RHSs and the numbers of their allocated components and the numbers of RHSs per component.

Table 7.7 – Iteration steps of convergence comparison (SMG2S generation suite SMG2S(1,3,4,*spec*), relative tolerance for convergence test = 1.0×10^{-8}), Krylov subspace size $m_g = 40$, $s_{use} = 10$, $d = 15$, $L = 1$, *dnc* = do not converge in 5000 iteration steps).

Method	<i>spec</i>	<i>m</i> -BGMRES(4) $\times 16$	<i>m</i> -UCGLE(4) $\times 16$	<i>m</i> -BGMRES(16) $\times 4$	<i>m</i> -UCGLE(16) $\times 4$	BGMRES(64)
TEST-1	(rand(21.0, 66.0), rand(-21.0,24.0))	239	160	102	51	51
TEST-2	(rand(0.5, 3.0), rand(-0.5,2.0))	<i>dnc</i>	176	187	62	78
TEST-3	(rand(0.2, 5.2), rand(-2.5,2.5))	<i>dnc</i>	310	<i>dnc</i>	81	657
TEST-4	(rand(-5.2, -0.2), rand(-2.5,2.5))	<i>dnc</i>	320	629	99	942
TEST-5	(rand(-0.23, -0.03), rand(-0.2,0.2))	600	235	170	99	270
TEST-6	(rand(-9.3, -3.2), rand(-2.1,2.1))	80	160	85	51	38

Table 7.8 – Consumption time (s) comparison on CPUs (SMG2S generation suite SMG2S(1,3,4,*spec*), the size of matrices = 1.792×10^6 , relative tolerance for convergence test = 1.0×10^{-8}), Krylov subspace size $m_g = 40$, $l = 10$, $d = 15$, $L = 1$, *dnc* = do not converge in 5000 iteration steps).

Method	<i>spec</i>	<i>m</i> -BGMRES(4) $\times 16$	<i>m</i> -UCGLE(4) $\times 16$	<i>m</i> -BGMRES(16) $\times 4$	<i>m</i> -UCGLE(16) $\times 4$	BGMRES(64)
TEST-1	(rand(21.0, 66.0), rand(-21.0,24.0))	34.2	35.3	133.9	98.9	362.8
TEST-2	(rand(0.5, 3.0), rand(-0.5,2.0))	<i>dnc</i>	40.9	231.3	111.5	580.6
TEST-3	(rand(0.2, 5.2), rand(-2.5,2.5))	<i>dnc</i>	66.0	<i>dnc</i>	145.8	522.5
TEST-4	(rand(-5.2, -0.2), rand(-2.5,2.5))	<i>dnc</i>	68.2	768.3	178.2	6829.3
TEST-5	(rand(-0.23, -0.03), rand(-0.2,0.2))	132.3	50.1	209.4	120.5	1959.5
TEST-6	(rand(-9.3, -3.2), rand(-2.1,2.1))	11.4	34.1	87.8	91.7	275.8

These 64 RHSs for the tests are all generated in random with different given seed states. All the test matrices from TEST-1 to TEST-6 in Table ?? are generated by SMG2S(1, 3, 4, *spec*), the definition of *spec* functions for different tests are shown in Table ???. For example, the *spec* of TEST-1 is given as (rand(21.0, 66.0), rand(-21.0, 24.0)), the first part rand(21.0, 66.0) defines that the real parts of given eigenvalues for TEST-1 are the floating numbers generated randomly in the fixed interval [21.0, 66.0], similarly its imaginary parts are randomly generated in the fixed interval [-21.0, 24.0]. The relative tolerance for the convergence test is fixed as 1.0×10^{-8} , the Krylov subspace size m_g is given as 40 for all tests, the number of times that B-LSP applied in *m*-UCGLE l , the degree of Least Squares polynomial in B-LSP, the number of BGMRES restarts between two times of B-LSP preconditioning are respectively set as 10, 15 and 1. For *m*-BGMRES(16) \times 4, *m*-BGMRES(4) \times 16, *m*-UCGLE(16) \times 4 and *m*-UCGLE(16) \times 4, their iteration steps in Table ?? are defined as the maximal ones among their allocated components to solve the systems.

7.3.6.3 Convergence Result Analysis

The iteration steps of different methods for convergence are shown in Table ?? (*dnc* in this table signifies *do not converge in 5000 iteration steps*). In this table, the blue and red cells represent respectively the worst and the best cases for each test. From Table ??, firstly we can conclude that the enlargement of the Krylov subspace by more RHSs in BGMRES is effective to accelerate the convergence for TEST-1, TEST-2, TEST-3, and TEST-6. However, this acceleration cannot always be guaranteed. Referring to TEST-4 and TEST-5, *m*-BGMRES(16) \times 4 converge faster than BGMRES(64). Secondly, *m*-UCGLE components converge much faster than their related *m*-BGMRES with the same number of RHSs, except in TEST-6. In the TEST-2, TEST-3, TEST-4, and TEST-5 of this table, *m*-UCGLE with 16 RHSs works even much better than BGMRES with 64 RHSs. An extreme special case in TEST-4 shows that convergence of *m*-UCGLE(4) \times 16 and *m*-UCGLE(16) \times 4 have the speedup respectively 3 \times and 9.5 \times over *m*-BGMRES(16).

In conclusion, for most tests, the method that converges the fastest is *m*-UCGLE(16) \times 4. The combination of enlarging the search space by enough number of RHSs and preconditioning by B-LSP makes substantial acceleration on the convergence of solving linear systems. Moreover, compared with classic BGMRES, due to the preconditioning of B-LSP, *m*-UCGLE with less RHSs and smaller search space can still have a better acceleration of the convergence. The potential damages caused by the localization of computation and reduction of global communications with less RHSs of each component in *m*-UCGLE can be covered by the B-LSP preconditioning.

7.3.6.4 Strong Scalability Evaluation

The iteration step for convergence is not the only concern about the iterative methods. After the convergence comparison of m -UCGLE and BGMRES, in this section, we evaluate its strong scalability and performance on supercomputer *ROMEO*.

One important concern of BGMRES is the time cost per iteration, due to the communication bound of SpGEMM. In order to evaluate the parallel performance of m -UCGLE on large clusters, we compare the strong scaling of m -BGMRES(4) \times 16, m -UCGLE(4) \times 16, m -BGMRES(16) \times 4, m -UCGLE(16) \times 4 and BGMRES(64) by their average time cost per iteration.

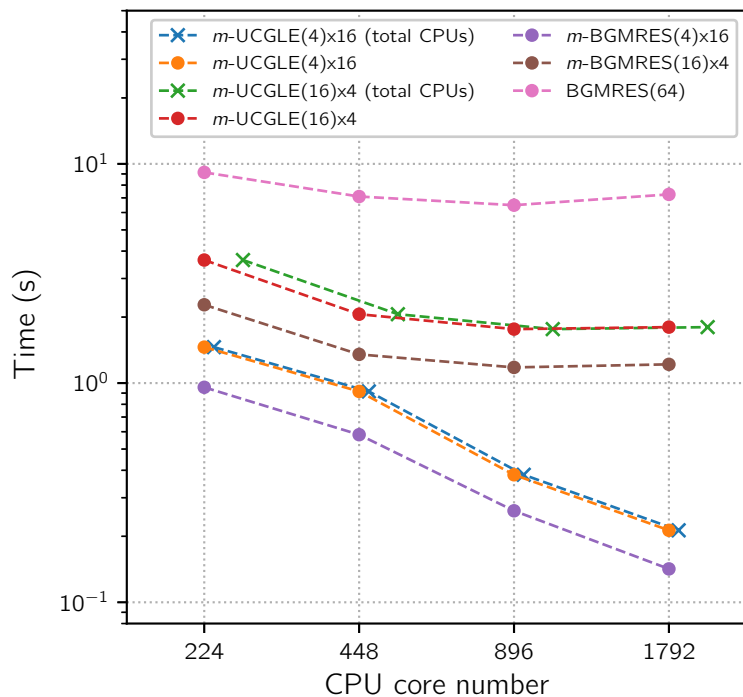


Figure 7.3 – Strong scalability test on CPUs of solving time per iteration for m -BGMRES(4) \times 16, m -UCGLE(4) \times 16, m -BGMRES(16) \times 4, m -UCGLE(16) \times 4, BGMRES(64); test matrix size is 1.792×10^6 ; X-axis refers to the total number of CPUs from 224 to 1792; Y-axis refers to the average execution time per iteration. A base 2 logarithmic scale is used for all X-axis, and a base 10 logarithmic scale is used for all Y-axis.

For the strong scaling evaluation on CPUs, the methods tested are set up the same as in Section ???. The test matrix is generated by $\text{SMG2S}(1, 3, 4, \text{spec})$ with size fixed as 1.792×10^6 . No larger matrices are tested, due to the memory limitation during the Arnoldi projection of BGMRES. The Krylov subspace size m_g for all methods is set as 40. The average time cost for these methods is computed by 100 iterations. Time per iteration is suitable for demonstrating scaling behavior. The total CPU core number for B-GMRES(64) and all BGMRES Components in m -UCGLE and m -BGMRES ranges from 224 to 1792. Thus for each BGMRES Component of m -BGMRES(4) \times 16 and m -UCGLE(4) \times 16, the number ranges from 14 to 112. Similarly, for each BGMRES

Component of m -BGMRES(16) \times 4 and m -UCGLE(16) \times 4, this number ranges from 56 to 448. All the tests allocate only 1 *s*-KS Component which always has the same number of CPU cores with each BGMRES Component inside m -UCGLE.

In Figure 7.3, we can conclude that the strong scaling of m -BGMRES(4) \times 16 and m -UCGLE(4) \times 16 perform very well, the strong scalability of the rest are bad, especially BGMRES(64). In the beginning, the scalability of m -BGMRES(16) \times 4 and m -UCGLE(16) \times 4 is good, but it turns bad quickly with the increase of CPU number. It is demonstrated that the properties of m-UCGLE to promote the asynchronous communication and localize of computation can improve significantly the parallel performance of BGMRES for solving systems with multiple RHSs. Additionally, for the m -BGMRES and m -UCGLE with the same number of RHSs, the time per iteration of former is a little less the latter, since m -UCGLE introduces the iterative operations (SpGEMM) by B-LSP preconditioning.

Since m -UCGLE uses additional computing units for other components especially *s*-KS Component, it is unfair only to compare the scaling performance that total CPU number of all BGMRES Components in m -UCGLE equals to these numbers of m -GMRES and BGMRES(64). Thus we plot two more curves of m -UCGLE(4) \times 16 and m -UCGLE(16) \times 14 with all their CPU numbers (including the CPU of *s*-KS Component) in Figure 7.3. The two additional curves are respectively the blue and green ones with the marker set as the cross. It is shown that m -UCGLE(4) \times 16 and m -UCGLE(16) \times 4 can still have respectively up to 35 \times and 4 \times speedup per iteration against BGMRES(64).

7.3.6.5 Time Consumption Evaluation

After the evaluation of parallel performance, we compare the time consumption of all methods to solve large-scale linear systems with multiple RHSs on CPUs. The test matrices are generated by SMG2S(1, 3, 4, *spec*), the same as the convergence evaluation in Section ???. The size of matrices are all 1.792×10^6 for the experiments on CPUs, the total numbers of CPU cores for different methods (either BGMRES Components in m -UCGLE and m -GMRES or conventional BGMRES) are respectively fixed as 1792, and the Krylov subspace size m_g is set as 40. The results on CPUs is given in Table 7.8, where the blue and red cells represent respectively the worst and the best cases for each test.

We can find that for the TEST-2, TEST-3, TEST-4, TEST-4, m -UCGLE(4) \times 16 take the least time to converge. For TEST-1 and TEST-6, m -BGMRES(4) \times 16 takes a little less time than m -UCGLE(4) \times 16 to get the convergence. For an extremely special case TEST-4, m -UCGLE(4) \times 16 has about 100 \times speedup in time consumption over BGMRES(64) to solve the linear systems with 64 RHSs.

7.3.6.6 Analysis

In conclusion, m -UCGLE(4) \times 16 and m -GMRES(4) \times 16 with the most decrease of global communications have the best strong scaling performance. m -UCGLE cost a little more time per iteration compared with m -BGMRES with the same number of RHSs, but this might be made up by its decrease of iterative steps with B-LSP preconditioning. The experiments in this section demonstrate the benefits of m -UCGLE to reduce global communication and promote the synchronization. Two more important points that cannot be concluded from the experiments in this paper are:

1. The increase of memory requirement should be considered when dividing the whole RHSs into subsets;
2. The number of RHSs per component of m -UCGLE to enlarge the search space and the computation time per iteration should be balanced to achieve the best performance.

7.4 Conclusions

CHAPTER 8

Parameters Autotuning

UCGLE is complex with a number of parameters which have impact on its numerical and parallel performance. The strategy of parameters' autotuning is necessary. In this chapter, we firstly introduce the autotuning scheme for each parameter, and then an adaptive UCGLE/ m -UCGLE which is able to autune automatically all these parameters.

TO DO

8.1 Autotuning of GMRES/BGMRES Component

8.1.1 Krylov Subspace Size

8.1.2 LS Applied Times

8.1.3 LS Frequence

8.1.4 Number of BGMRES Components Allocated

8.2 Autotuning of ERAM/ s -KS Component

8.2.1 Number of Eigenvalues

8.3 Autotuning of LS/BLSP Component

8.3.1 LS Plynomial Degree

8.4 Adaptive UCGLE/ m -UCGLE

8.5 Conlusion

CHAPTER 9

YML and XMP Multi-level Parallelism Programming Paradigm

After the validation of the numerical and parallel performance of *m*-UCGLE, a major difficulty to profit from UC methods including *m*-UCGLE is to implement the manager engine which can well handle their fault tolerance, load balance, asynchronous communication of signals, arrays and vectors, the management of different computing units such as GPUs, etc. In the last chapter, we tried to give a naive implementation of the engine to support the management tasks on the homogeneous platforms based on MPI_SPAWN and MPI non-blocking sending and receiving functionalities. The stability of this implementation of the engine cannot always be guaranteed. Thus we are also thinking about to select the suitable workflow/task based environments to manage all these aspects in the UC approach. YML¹ is a good candidate, which is a workflow environment to provide the definition of the parallel application independently from the underlying middleware used. The special middleware and workflow scheduler provided by YML allows defining the dependencies of tasks and data on the supercomputers [Delanoy \[2008\]](#). YML, including its interfaces and compiler to various programming languages and libraries, will facilitate the implementation of UC based methods with different numerical components. In this chapter, firstly we summarize the YML framework, and then analyze the limitations of existing YML implementation for UC approach. In the end, we propose the solution.

9.1 YML Framework

YML is a workflow environment dedicated to the execution of parallel de distributed applications on various middleware. The YML framework enables the description of the

1. <http://yml.prism.uvsq.fr/>

complex parallel application based on the tasks. The task-based application written based on YML language can be executed on several runtime-systems or middleware without changes. YML is a software layer between the end-user and the runtime system of a supercomputer and/or the middleware of a distributed system, which is in charge of communication. YML is composed of three main parts: an IDL, a kernel and a back-end allowing interactions with the runtime-system or middleware. A high-level workflow language, a just-in-time scheduler and a system of service integration constitute the kernel of YML. The high-level language which is XML-based permits the description of the graph of application. The nodes of the graph correspond to computation while edges correspond to dependencies or communications. A component could be itself a graph. The language integrates the ability to describe components on the one hand and application graphs on the other hand. Both aspects are encapsulated in XML document for homogeneity. This language provides a way to specify the communication between components during the execution of the application. The graph can contain parallel and sequential sections and standard construction of most languages including branching, exceptions, and loops. The graph language describes the dependencies between the components during the execution. These dependencies rest on the notion of events. The compiler translates the graph of components of applications in an internal representation containing a set of components calls. The scheduler manages application execution and acts as a client for the underlying runtime system accurately requiring computing resources. During the application execution, the scheduler detects tasks ready for execution solving dependencies at runtime. Each scheduling step may or may not generate a set of parallel tasks, which are translated in computing requests to runtime system through dedicated backends. A service in YML can be “any kind” of a component such as a library (or some component of), a data repository, or a catalog of binary components. Thanks to the component-oriented design of YML, it is easy to incorporate new ones. The computation components can be written in different programming languages like XMP. In the case of using XMP in YML, the tasks, written in XMP are expected to be executed on sub-clusters or groups of nodes, which are tightly connected. These tasks would be hybrid programs with distributed and shared programming models. The scheduler provided by YML invokes and manages the tasks among the sub-clusters or groups.

Environments such as YML, allowing the realization of the proposed model must be extensible in all their aspects and offer reusability. Furthermore, the ability thereof to provide dynamic integration of end-users expertise is a significant element.

9.1.1 YML Design

The aim of YML is to provide users with an easy-of-use method to run parallel applications on different Grid platform and supercomputer. The framework can be divided into

three parts which are the end-users interface, frontend, and backend. The end-users interface is used to provide an easy-to-use and an intuitive way to submit their applications and applications can be described using a workflow language YvetteML, Frontend is the main part of YML which includes a compiler, scheduler, data repository, abstract and implementation components.

Abstract and implementation components based on function can be reused. The backend is the part to connect different Grid and peer to peer middleware.

The development of a YML application is based on the components approach, and then we will discuss the three kinds of components in detail.

- **Abstract component** defines the communication interface with the other components. This definition gives the name, and the communication channels correspond to a data input, data output or both and are typed. This component is used in the code generation step and to create the graph.
- **Implementation component** is the implementation of an abstract component. It provides the description of computations through YvetteML language. The implementation is done by using common languages like C or C++. They can have several implementations for the same abstract component.
- **Graph component** carries a graph expressed in YvetteML instead of a description of computation. It provides the parallel and sequential parts of an application and the synchronization events between dependent components. It is a straightforward way for scientific researchers to develop their application.

Moreover, those three components are independent of middleware. So, to run an application on another grid environment with a different middleware, the user needs to compile each component for the middleware of his choice. OmniRPC as the backend of YML will be used here.

YML helps the developer in the whole process of parallelizing applications. It starts at the early stage of components creation to the execution of hardly constrained workflow applications on a Grid. Moreover, YML allows the test and validation of those applications on the user computer using a special backend which relies on the multithreading capabilities of the underlying operating system.

YML eases components creation. Existing code can be reused by importing libraries as some new components without any adaptation. Those components are called by the application when computational tasks have to be started. Moreover, the notions of abstract and implementation descriptions of components bring three interesting features for the Grid scheduler that can be included in the framework.

- **data migration** can be easily quantified at the start and at the end of the application thanks to the abstract definition.

- **data used** by a component is clearly defined in the abstract and implementation definitions, therefore this can be used in a checkpointing feature to move a component from a node to an other.
- **computation time** of a component can be evaluated thanks to the implementation definition.

The use of Data Repository Servers hides the data migrations to the developer and ensure that necessary data are always available to all components of the application.

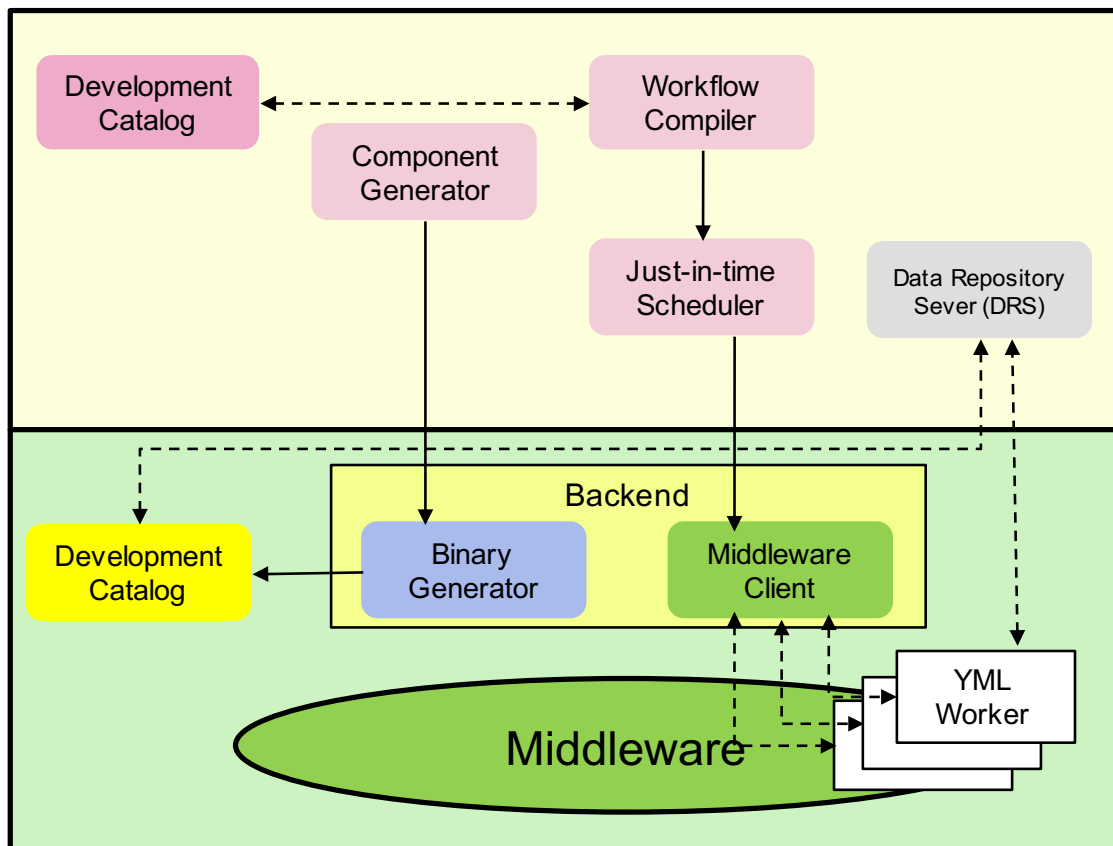


Figure 9.1 – YML Architecture.

9.1.2 Yvette Language

- **Parallel Section:** par section 1 // ... // section N endpar
- **Sequential loop:** seq (i:=begin;end) do ... enddo
- **Parallel loop:** par (i:=begin;end) do ... enddo
- **Conditional structure:** if (condition) then ... else ... endif
- **Synchronization:** wait(event) / notify(event)
- **Component call:** compute NameOfComponent(args,...,...)

9.1.3 YML Example

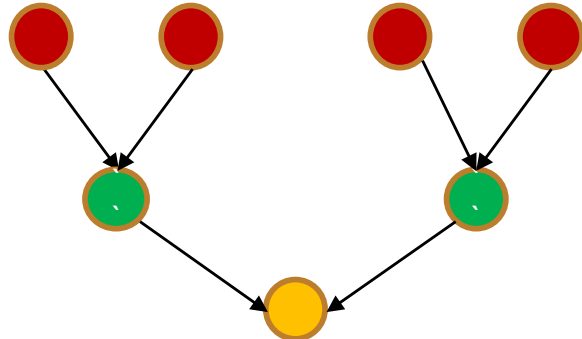


Figure 9.2 – Workflow of Sum Application.

9.1.3.1 Abstract

```

<?xml version="1.0" encoding="utf-8"?>
<component type="abstract" name="test_abstract"
            description="sum_of_two_doubles">
    <param type="real" mode="out" name="res" />
    <param type="real" mode="in" name="a" />
    <param type="real" mode="in" name="b" />
</component>
  
```

9.1.3.2 Implementation

```

<?xml version="1.0" encoding="utf-8"?>
<component type="impl" name="test_impl"
            description="sum_of_two_doubles">
    <impl lang="CXX" libs="">
        <header><! [CDATA [
            #include <stdlib.h>
        ]]>
        </header>
        <source lang="CXX" libs="">
            res = a + b;
        </source>
        <footer></footer>
    </impl>
</component>
  
```

9.1.3.3 Application

```
<?xml version="1.0" encoding="utf-8"?>
<application name="test_app">
    <description>
        sum application
    </description>
    <params></params>
    <graph>
        compute test(res, 1.0, 2.0); #res = 3.0
        compute test(res, results, results); #res = 6.0
    </graph>
</application>
```

9.1.4 Multi-level Programming Paradigm: YML/XMP

The multi-level programming paradigm YML/XMP is supported by the OmniRPC-MPI Middleware. OmniRPC is a thread-safe remote procedure call (RPC) system, based on Ninf, for cluster and grid environment. It supports typical master/worker grid applications. Workers are listed in a XML file named as the host file. For each host, the maximum number of job, the path of OmniRPC, the connection protocol (ssh, rsh) and the user can be defined.

An OmniRPC application contains a client program which calls remote procedures through the OmniRPC agent. Remote libraries which contain the remote procedures are executed by the remote computation hosts, there are implemented like a executable program which contains a network stub routine as its main routine. The declaration of a remote function of remote library is defined by an interface in the Ninf interface definition language (IDL). The implementation can be written in familiar scientific computation language like FORTRAN, C or C++.

There are two versions of OmniRPC, one is for grid computation and the other for supercomputer. The first one (the original version) was designed for the grid computing and distributed architecture of large numbers of computers. The second one was created specially for supercomputers, the XMP language is only usable with this version of OmniRPC if we want to use YML in complement.

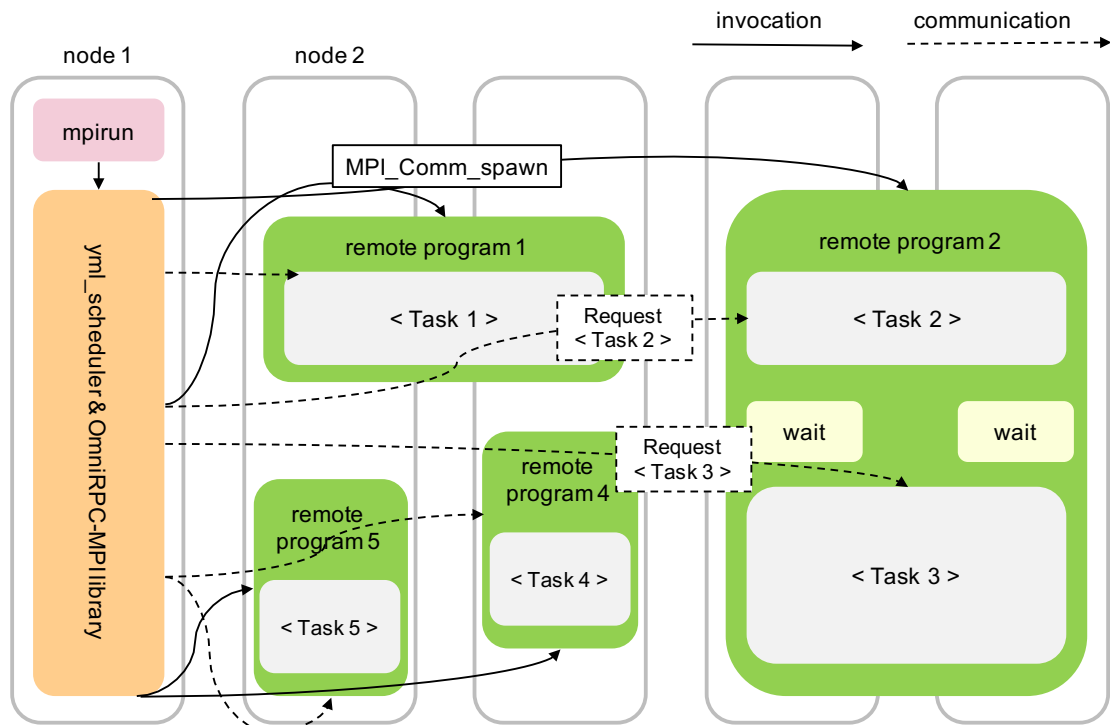


Figure 9.3 – Application Execution with YML + OmniRPC-MPI.

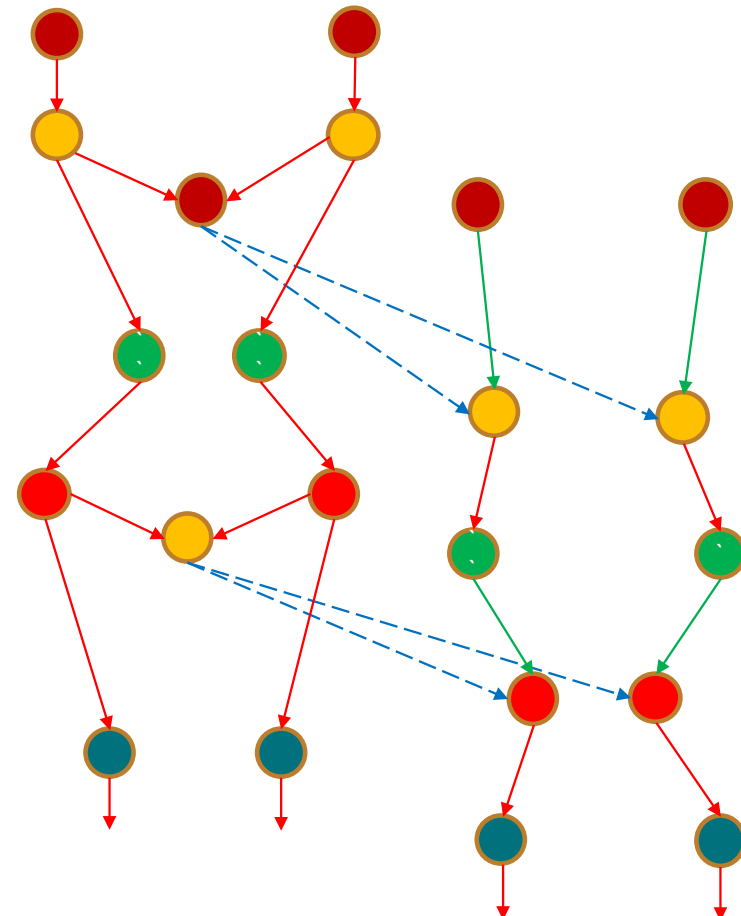


Figure 9.4 – m-UCGLE task.

9.2 Limitations of YML for UC Approach

9.2.1 Workflow of m -UCGLE Analysis

9.2.2 Mechanism for Convergence

9.2.3 Asynchronous Communications

9.3 Proposition of Solution

9.3.1 Dynamic Graph Grammar in YML

We want to have dynamic graphs. The graphs may depend of variable modified into Implement components. Then, in Abstract components :

```
<param type="var_graph" mode="inout" name="foo">
```

The variable for the dynamic graph can be the mode of *in*, *out* or *inout*. These parameter may be evaluated and modified on a task, or only evaluate a logical into Yvette “if (logical) then ... else ...”; If the computation to evaluate the logical is to complex, we may use a task with a special indication, added on the Implementation component, such as “graph_scheduler_evaluation” : then the scheduler may manage those tasks as others, or run it “itself”.

9.3.1.1 Scenario Example

As shown in Fig. 9.5. The red and purple are the addition operations, and the yellow point is the operation to set value. The priority of setting value is: 1) check the output value a of red point, if this value is odd, then set the value to be a ; 2) if a is even, set the value to be b .

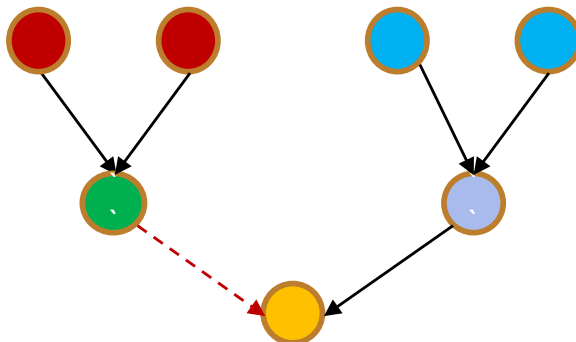


Figure 9.5 – New Scenario with Dynamic Graph.

9.3.1.2 Abstract

```
<?xml version="1.0" encoding="utf-8"?>
<component type="abstract" name="dyntest_abstract"
            description="sum_of_two_doubles#2">
    <param type="real" mode="out" name="val" />
    <param type="real" mode="in" name="a" />
    <param type="real" mode="in" name="b" />
    <param type="var_graph" mode="out" name="odd" />
</component>
```

```
<?xml version="1.0" encoding="utf-8"?>
<component type="abstract" name="dyntest_abstract"
            description="set_value">
    <param type="real" mode="out" name="val" />
    <param type="real" mode="in" name="a" />
    <param type="var_graph" mode="inout" name="odd" />
</component>
```

9.3.1.3 Implementation

```
<?xml version="1.0" encoding="utf-8"?>
<component type="impl" name="dyntest_impl"
            description="sum_of_two_doubles#2">
    <impl lang="CXX" libs="">
        <header><![CDATA[
            #include <stdlib.h>
        ]]>
        </header>
        <source lang="CXX" libs="">
            res = a + b;
            if(res % 2 ==0){
                odd = false;
            } else {
                odd = true;
            }
        </source>
        <footer></footer>
    </impl>
</component>
```

```
<?xml version="1.0" encoding="utf-8"?>
<component type="impl" name="setvalue_impl"
            description="set_value">
    <impl lang="CXX" libs="">
        <header><! [CDATA [
            #include <stdlib.h>
        ]]>
        </header>
        <source lang="CXX" libs="">
            val = a;
        </source>
        <footer></footer>
    </impl>
</component>
```

9.3.1.4 Application

```
<?xml version="1.0" encoding="utf-8"?>
<application name="dyntest_app">
    <description>
        set value application
    </description>
    <params></params>
    <graph>
        compute dyntest(res1, 1.0, 2.0, odd); #res = 3.0
        compute test(res2, 4.0, 6.0); #res = 10.0
        if(odd) then
            compute setvalue(val, res1, odd); #val = 3.0
        else
            compute setvalue(val, res2, odd); #val = 10.0
        endif
    </graph>
</application>
```

9.3.2 Exiting Parallel Branch

If the graph is dynamic and if we decide to exit a parallel branch:

- we have to specify is all the running task as to be completed or not;

- we may want to finish all the task of the parallel branch before to exit;
- we may also decide to exit several level of parallelism;
- we may stop completely the computation.

Exit(level=p) : we exit p levels of parallelism (p loops if it is parallel loops)

Exit(complete=all) : all the running tasks of the level are finished (data?) before to exit

Exit(level=p,auto) : we add to each abstract components if the task has to be finished, data saved or not, if the task is running and we exit the parallel branch (</exit finish = "yes" />) ; and we may ask in the abstract component:

```
<param type="Matrix" mode="inout" name="A" save_exit="yes" />
```

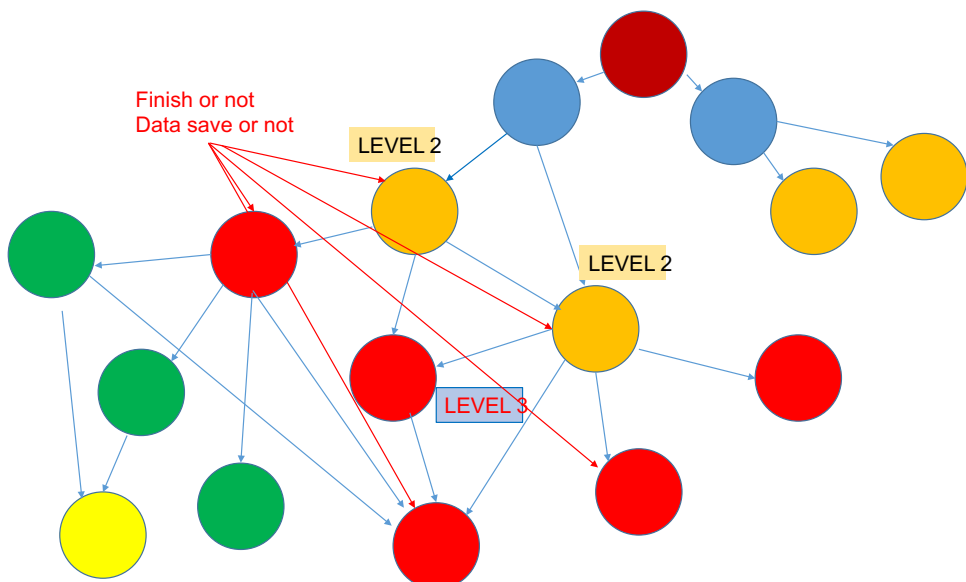


Figure 9.6 – Exiting Parallel Branch.

9.3.3 Check Pointing

9.3.4 Scheduler for YML/MPI

9.4 Demand for MPI Correction Mechanism

MUST² detects usage errors of the Message Passing Interface (MPI) and reports them to the user. As MPI calls are complex and usage errors common, this functionality is extremely helpful for application developers that want to develop correct MPI applications. This includes errors that already manifest - segmentation faults or incorrect results - as

2. <https://tu-dresden.de/zih/forschung/projekte/must>

well as many errors that are not visible to the application developer or do not manifest on a certain system or MPI implementation.

To detect errors, MUST intercepts the MPI calls that are issued by the target application and evaluates their arguments. The two main usage scenarios for MUST arise during application development and when porting an existing application to a new system. When a developer adds new MPI communication calls, MUST can detect newly introduced errors, especially also some that may not manifest in an application crash. Further, before porting an application to a new system, MUST can detect violations to the MPI standard that might manifest on the target system. MUST reports errors in a log file that can be investigated once the execution of the target executable finishes.

9.5 Conclusion

CHAPTER 10

Conclusion and Perspectives

In conclusion

Scientific Communication

Peer-reviewed publications

- Xinzhe Wu and Serge G. Petiton, "A Distributed and Parallel Asynchronous Unite and Conquer Method to Solve Large Scale Non-Hermitian Linear Systems" in HPC Asia 2018: International Conference on High Performance Computing in Asia-Pacific Region, Tokyo, Japan.
- Xinzhe Wu, Serge G. Petiton and Yutong Lu, "A Parallel Generator of Non-Hermitian Matrices computed from Given Spectra" in VECPAR 2018: 13th International Meeting on High Performance Computing for Computational Science, São Pedro, Brazil.
- Xinzhe Wu and Serge G. Petiton, "A Distributed and Parallel Unite and Conquer Method to Solve Sequences of Non-Hermitian Linear Systems". Submitted to Japan Journal of Industrial and Applied Mathematics. [Under Review].
- Xinzhe Wu and Serge G. Petiton, "A Distributed and Parallel Asynchronous Unite and Conquer Method to Solve Large Scale Non-Hermitian Linear Systems with Multiple Right-hand Sides". Submitted to Parallel Computing. [Submitted].

Invited and Contributed Talks

- Serge G. Petiton and Xinzhe Wu, "An Asynchronous Distributed and Parallel Unite and Conquer Method to Solve Sequences of Non-Hermitian Linear systems" in MATHIAS 2018: Computational Science Engineering & Data Science by TOTAL, Serris, France.
- Xinzhe Wu, Serge G. Petiton and Yutong Lu, "A Parallel Generator of Non-Hermitian Matrices Computed from Given Spectra" in VECPAR 18: 13th International Meeting on High Performance Computing for Computational Science, São Pedro, Brazil.

-
- Xinzhe Wu and Serge G. Petiton, "A Parallel Generator of Non-Hermitian Matrices Computed from Given Spectra" in PMAA18: 10th International Workshop on Parallel Matrix Algorithms and Applications, Zurich, Switzerland.
 - Xinzhe Wu and Serge G. Petiton, "A Parallel Generator of Non-Hermitian Matrices Computed from Known Given Spectra" in 3rd Workshop on Parallel Programming Models - Productivity and Applications, Aachen, Germany.
 - Xinzhe Wu and Serge G. Petiton, "A Parallel Generator of Non-Hermitian Matrices Computed from Known Given Spectra" in SIAM PP18: SIAM Conference on Parallel Processing for Scientific Computing, Tokyo, Japan.
 - Serge G. Petiton and Xinzhe Wu, "The Unite and Conquer GMRES-LS/ERAM method to solve sequences of Linear Systems" in EPASA 2018: International Workshop on Eigenvalue Problems: Algorithms, Software and Applications, in Petascale Computing, Tsukuba, Japan.
 - Xinzhe Wu and Serge G. Petiton, "A Distributed and Parallel Asynchronous Unite and Conquer Method to Solve Large Scale Non-Hermitian Linear Systems" in HPC Asia 2017: International Conference on High Performance Computing in Asia-Pacific Region, Tokyo, Japan.
 - Serge G. Petiton, Xinzhe Wu and Tao Chang, "A Distributed and Parallel Asynchronous Unite and Conquer Method to Solve Large Scale Non-Hermitian Linear Systems" in Preconditioning 2017: International Conference On Preconditioning Techniques For Scientific And Industrial Applications, Vancouver, Canada.

Posters

- Xinzhe Wu and Serge G. Petiton, "Large Non-Hermitian Matrix Generation with Given Spectra" in EPASA 2018: International Workshop on Eigenvalue Problems: Algorithms, Software and Applications, in Petascale Computing, Tsukuba, Japan.

Software Manual/Technical Reports

- Xinzhe Wu, "SMG2S Manual" in Maison de la Simulation, France - Version 1.0, 2018.

Bibliography

Abdou M Abdel-Rehim, Ronald B Morgan, and Walter Wilcox. Improved seed methods for symmetric positive definite linear equations with multiple right-hand sides. *Numerical Linear Algebra with Applications*, 21(3):453–471, 2014.

Nabil FT Abubaker, Kadir Akbudak, and Cevdet Aykanat. Spatiotemporal graph and hypergraph partitioning models for sparse matrix-vector multiplication on many-core architectures. *IEEE Transactions on Parallel and Distributed Systems*, 2018.

Loyce Adams and J Ortega. A multi-color sor method for parallel computation. In *ICPP*, pages 53–56. Citeseer, 1982.

Emmanuel Agullo, Luc Giraud, and Y-F Jing. Block gmres method with inexact breakdowns and deflated restarting. *SIAM Journal on Matrix Analysis and Applications*, 35(4):1625–1651, 2014.

José I Aliaga, Hartwig Anzt, Maribel Castillo, Juan C Fernández, Germán León, Joaquín Pérez, and Enrique S Quintana-Ortí. Unveiling the performance-energy trade-off in iterative linear system solvers for multithreaded processors. *Concurrency and Computation: Practice and Experience*, 27(4):885–904, 2015.

Heng-Bin An and Zhong-Zhi Bai. A globally convergent newton-gmres method for large sparse systems of nonlinear equations. *Applied Numerical Mathematics*, 57(3):235–252, 2007.

Hartwig Anzt, Stanimire Tomov, and Jack Dongarra. Energy efficiency and performance frontiers for sparse computations on gpu supercomputers. In *Proceedings of the sixth international workshop on programming models and applications for multicores and manycores*, pages 1–10. ACM, 2015.

Pierre-Yves Aquilanti, Serge Petiton, and Henri Calandra. Parallel gmres incomplete orthogonalization auto-tuning. *Procedia Computer Science*, 4:2246–2256, 2011.

Walter Edwin Arnoldi. The principle of minimized iterations in the solution of the matrix eigenvalue problem. *Quarterly of applied mathematics*, 9(1):17–29, 1951.

SR Arridge, M Schweiger, M Hiraoka, and DT Delpy. A finite element approach for modeling photon transport in tissue. *Medical physics*, 20(2):299–309, 1993.

Arash Ashari, Naser Sedaghati, John Eisenlohr, and P Sadayappan. An efficient two-dimensional blocking strategy for sparse matrix-vector multiplication on gpus. In *Proceedings of the 28th ACM international conference on Supercomputing*, pages 273–282. ACM, 2014.

Thomas J Ashby, Pieter Ghysels, Wim Heirman, and Wim Vanroose. The impact of global communication latency at extreme scales on krylov methods. In *International Conference on Algorithms and Architectures for Parallel Processing*, pages 428–442. Springer, 2012.

Cédric Augonnet, Samuel Thibault, Raymond Namyst, and Pierre-André Wacrenier. Starpu: a unified platform for task scheduling on heterogeneous multicore architectures. *Concurrency and Computation: Practice and Experience*, 23(2):187–198, 2011.

Owe Axelsson. A generalized ssor method. *BIT Numerical Mathematics*, 12(4):443–467, 1972.

Zhaojun Bai, David Day, James Demmel, and Jack Dongarra. A test matrix collection for non-hermitian eigenvalue problems. *Prof. Z. Bai, Dept. of Mathematics*, 751:40506–0027, 1996.

Allison H Baker, John M Dennis, and Elizabeth R Jessup. On improving linear solver performance: A block variant of gmres. *SIAM Journal on Scientific Computing*, 27(5):1608–1626, 2006.

Chris G Baker, Ulrich L Hetmaniuk, Richard B Lehoucq, and Heidi K Thornquist. Anasazi software for the numerical solution of large-scale eigenvalue problems. *ACM Transactions on Mathematical Software (TOMS)*, 36(3):13, 2009.

Christopher G Baker and Michael A Heroux. Tpetra, and the use of generic programming in scientific computing. *Scientific Programming*, 20(2):115–128, 2012.

Satish Balay, Kris Buschelman, William D Gropp, Dinesh Kaushik, Matthew G Knepley, L Curfman McInnes, Barry F Smith, and Hong Zhang. Petsc web page, 2001.

Satish Balay, Shrirang Abhyankar, M Adams, Peter Brune, Kris Buschelman, L Dalcin, W Gropp, Barry Smith, D Karpeyev, Dinesh Kaushik, et al. Petsc users manual revision 3.7. Technical report, Argonne National Lab.(ANL), Argonne, IL (United States), 2016a.

Satish Balay, Shrirang Abhyankar, Mark F. Adams, Jed Brown, Peter Brune, Kris Buschelman, Lisandro Dalcin, Victor Eijkhout, William D. Gropp, Dinesh Kaushik, Matthew G. Knepley, Lois Curfman McInnes, Karl Rupp, Barry F. Smith, Stefano Zampini, Hong Zhang, and Hong Zhang. PETSc users manual. Technical Report ANL-95/11 - Revision 3.7, Argonne National Laboratory, 2016b. URL <http://www.mcs.anl.gov/petsc>.

Randolph E Bank, Todd F Dupont, and Harry Yserentant. The hierarchical basis multigrid method. *Numerische Mathematik*, 52(4):427–458, 1988.

Gianluca Barbella, Federico Perotti, and V Simoncini. Block krylov subspace methods for the computation of structural response to turbulent wind. *Computer Methods in Applied Mechanics and Engineering*, 200(23-24):2067–2082, 2011.

Achim Basermann. Qmr and tfqmr methods for sparse nonsymmetric problems on massively parallel systems. In *AMS-SIAM Summer Seminar in Applied Mathematics*, number FZJ-2014-04512. Zentralinstitut für Angewandte Mathematik, 1996.

João Pedro A Bastos and Nelson Sadowski. *Electromagnetic modeling by finite element methods*. CRC press, 2003.

Eric Bavier, Mark Hoemmen, Sivasankaran Rajamanickam, and Heidi Thornquist. Amesos2 and belos: Direct and iterative solvers for large sparse linear systems. *Scientific Programming*, 20(3):241–255, 2012.

Nathan Bell and Michael Garland. Efficient sparse matrix-vector multiplication on cuda. Technical report, Nvidia Technical Report NVR-2008-004, Nvidia Corporation, 2008.

Nathan Bell and Michael Garland. Implementing sparse matrix-vector multiplication on throughput-oriented processors. In *Proceedings of the conference on high performance computing networking, storage and analysis*, page 18. ACM, 2009.

Stefania Bellavia and Benedetta Morini. A globally convergent newton-gmres subspace method for systems of nonlinear equations. *SIAM Journal on Scientific Computing*, 23(3):940–960, 2001.

Pietro Berkes. Handwritten digit recognition with nonlinear fisher discriminant analysis. In *Proceedings of the 15th international conference on Artificial neural networks: formal models and their applications-Volume Part II*, pages 285–287. Springer-Verlag, 2005.

Ronald F Boisvert, Roldan Pozo, Karin Remington, Richard F Barrett, and Jack J Dongarra. Matrix market: a web resource for test matrix collections. In *Quality of Numerical Software*, pages 125–137. Springer, 1997.

Achi Brandt. Algebraic multigrid theory: The symmetric case. *Applied mathematics and computation*, 19(1-4):23–56, 1986.

Marian Brezina, Andrew J Cleary, Robert D Falgout, Van Enden Henson, Jim E Jones, Thomas A Manteuffel, Stephen F McCormick, and John W Ruge. Algebraic multigrid based on element interpolation (amge). *SIAM Journal on Scientific Computing*, 22(5):1570–1592, 2001.

Claude Brezinski and M Redivo-Zaglia. Hybrid procedures for solving linear systems. *Numerische Mathematik*, 67(1):1–19, 1994.

Peter N Brown and Youcef Saad. Hybrid krylov methods for nonlinear systems of equations. *SIAM Journal on Scientific and Statistical Computing*, 11(3):450–481, 1990.

D Calvetti and L Reichel. Application of a block modified chebyshev algorithm to the iterative solution of symmetric linear systems with multiple right hand side vectors. *Numerische Mathematik*, 68(1):3–16, 1994.

Erin Claire Carson. *Communication-avoiding Krylov subspace methods in theory and practice*. PhD thesis, UC Berkeley, 2015.

Umit V Catalyurek and Cevdet Aykanat. Hypergraph-partitioning based decomposition for parallel sparse-matrix vector multiplication. *IEEE Transactions on parallel and distributed systems*, 10(7):673–693, 1999.

Langshi Chen, Serge G Petiton, Leroy A Drummond, and Maxime Hugues. A communication optimization scheme for basis computation of krylov subspace methods on multi-gpus. In *International Conference on High Performance Computing for Computational Science*, pages 3–16. Springer, 2014.

Xiaojun Chen, Carolin Birk, and Chongmin Song. Transient analysis of wave propagation in layered soil by using the scaled boundary finite element method. *Computers and Geotechnics*, 63:1–12, 2015.

Siegfried Cools and Wim Vanroose. The communication-hiding pipelined bicgstab method for the parallel solution of large unsymmetric linear systems. *Parallel Computing*, 65:1–20, 2017.

Christophe Croux and Gentiane Haesbroeck. Principal component analysis based on robust estimators of the covariance or correlation matrix: influence functions and efficiencies. *Biometrika*, 87(3):603–618, 2000.

Leonardo Dagum and Ramesh Menon. Openmp: an industry standard api for shared-memory programming. *IEEE computational science and engineering*, 5(1):46–55, 1998.

Timothy A Davis and Yifan Hu. The university of florida sparse matrix collection. *ACM Transactions on Mathematical Software (TOMS)*, 38(1):1, 2011.

David Day and Michael A Heroux. Solving complex-valued linear systems via equivalent real formulations. *SIAM Journal on Scientific Computing*, 23(2):480–498, 2001.

Eric De Sturler. Truncation strategies for optimal krylov subspace methods. *SIAM Journal on Numerical Analysis*, 36(3):864–889, 1999.

Olivier Delannoy. *YML: un workflow scientifique pour le calcul haute performance*. PhD thesis, Université de Versailles Saint-Quentin, France, 2008.

James Demmel and Alan McKenney. A test matrix generation suite. In *Courant Institute of Mathematical Sciences*. Citeseer, 1989.

James Demmel, Mark Hoemmen, Marghoob Mohiyuddin, and Katherine Yelick. Avoiding communication in sparse matrix computations. In *Parallel and Distributed Processing, 2008. IPDPS 2008. IEEE International Symposium on*, pages 1–12. IEEE, 2008.

Alejandro Duran, Eduard Ayguadé, Rosa M Badia, Jesús Labarta, Luis Martinell, Xavier Martorell, and Judit Planas. Ompss: a proposal for programming heterogeneous multi-core architectures. *Parallel Processing Letters*, 21(02):173–193, 2011.

H Carter Edwards, Christian R Trott, and Daniel Sunderland. Kokkos: Enabling many-core performance portability through polymorphic memory access patterns. *Journal of Parallel and Distributed Computing*, 74(12):3202–3216, 2014.

Howard C Elman, Youcef Saad, and Paul E Saylor. A hybrid chebyshev krylov subspace algorithm for solving nonsymmetric systems of linear equations. *SIAM Journal on Scientific and Statistical Computing*, 7(3):840–855, 1986.

Nahid Emad and Serge Petiton. Unite and conquer approach for high scale numerical computing. *Journal of Computational Science*, 14:5–14, 2016.

Nahid Emad, Serge Petiton, and Guy Edjlali. Multiple explicitly restarted arnoldi method for solving large eigenproblems. *SIAM Journal on Scientific Computing*, 27(1):253–277, 2005.

Jocelyne Erhel, Kevin Burrage, and Bert Pohl. Restarted gmres preconditioned by deflation. *Journal of computational and applied mathematics*, 69(2):303–318, 1996.

Azeddine Essai, Guy Bergére, and Serge G Petiton. Heterogeneous parallel hybrid gmres/ls-arnoldi method. In *PPSC*, 1999.

Michael Feldman. Top500 cea to deploy arm-powered supercomputer, 2018a. URL <https://www.top500.org/news/cea-to-deploy-arm-powered-supercomputer/>.

Michael Feldman. Top500 fujitsu completes prototype of arm processor that will power exascale supercomputer, 2018b.

Alexandre Fender, Nahid Emad, Serge Petiton, and Joe Eaton. Leveraging accelerators in the multiple implicitly restarted arnoldi method with nested subspaces. In Emerging Technologies and Innovative Business Practices for the Transformation of Societies (EmergiTech), IEEE International Conference on, pages 389–394. IEEE, 2016.

Alexandre Fender, Nahid Emad, Serge Petiton, and Maxim Naumov. Parallel modularity clustering. Procedia Computer Science, 108:1793–1802, 2017.

Fabio Guilherme Ferraz and José Maria C Dos Santos. Block-krylov component synthesis and minimum rank perturbation theory for damage detection in complex structures. Proceeding of the IX DINAME, Florianópolis-SC-Brazil, pages 329–334, 2001.

Peter Fiebach, Andreas Frommer, and Roland Freund. Variants of the block-qmr method and applications in quantum chromodynamics. In 15th IMACS World Congress on Scientific Computation, Modelling and Applied Mathematics, volume 3, pages 491–496, 1997.

Alexander J Flueck and Hsiao-Dong Chiang. Solving the nonlinear power flow equations with an inexact newton method using gmres. IEEE Transactions on Power Systems, 13(2):267–273, 1998.

Valérie Frayssé, Luc Giraud, and Serge Gratton. Algorithm 881: A set of flexible gmres routines for real and complex arithmetics on high-performance computers. ACM Transactions on Mathematical Software (TOMS), 35(2):13, 2008.

Roland W Freund and Noël M Nachtigal. Qmr: a quasi-minimal residual method for non-hermitian linear systems. Numerische mathematik, 60(1):315–339, 1991.

Haohuan Fu, Junfeng Liao, Jinzhe Yang, Lanning Wang, Zhenya Song, Xiaomeng Huang, Chao Yang, Wei Xue, Fangfang Liu, Fangli Qiao, et al. The sunway taihulight supercomputer: system and applications. Science China Information Sciences, 59(7):072001, 2016.

Seiji Fujino and Kosuke Iwasato. An estimation of single-synchronized krylov subspace methods with hybrid parallelization. In Proceedings of the World Congress on Engineering, volume 1, 2015.

Kohei Fujita, Keisuke Katsushima, Tsuyoshi Ichimura, Masashi Horikoshi, Kengo Nakajima, Muneo Hori, and Lalith Maddegedara. Wave propagation simulation of complex multi-material problems with fast low-order unstructured finite-element meshing and analysis. In Proceedings of the International Conference on High Performance Computing in Asia-Pacific Region, HPC Asia 2018, pages 24–35, New York, NY, USA, 2018. ACM. ISBN 978-1-4503-5372-4. doi: 10.1145/3149457.3149474. URL <http://doi.acm.org/10.1145/3149457.3149474>.

Hervé Galicher, France Boillod-Cerneux, Serge Petiton, and Christophe Calvin. Generate very large sparse matrices starting from a given spectrum. in lecture notes in computer science, 8969, Springer (2014).

Pieter Ghysels and Wim Vanroose. Hiding global synchronization latency in the preconditioned conjugate gradient algorithm. Parallel Computing, 40(7):224–238, 2014.

Pieter Ghysels, Thomas J Ashby, Karl Meerbergen, and Wim Vanroose. Hiding global communication latency in the gmres algorithm on massively parallel machines. SIAM Journal on Scientific Computing, 35(1):C48–C71, 2013.

Andrew Grimshaw, W Wulf, J French, A Weaver, and Paul F Reynolds Jr. A synopsis of the legion project. Technical report, Technical Report CS-94-20, Department of Computer Science, University of Virginia, 1994.

William D Gropp, William Gropp, Ewing Lusk, Anthony Skjellum, and Argonne Distinguished Fellow Emeritus Ewing Lusk. Using MPI: portable parallel programming with the message-passing interface, volume 1. MIT press, 1999.

Gui-Ding Gu. A seed method for solving nonsymmetric linear systems with multiple right-hand sides. International journal of computer mathematics, 79(3):307–326, 2002.

Arne S Gullerud and Robert H Dodds Jr. Mpi-based implementation of a pcg solver using an ebe architecture and preconditioner for implicit, 3-d finite element analysis. Computers & Structures, 79(5):553–575, 2001.

Martin H Gutknecht. Block krylov space methods for linear systems with multiple right-hand sides: an introduction. 2006.

Azzam Haidar, Stanimire Tomov, Jack Dongarra, and Nicholas J Higham. Harnessing gpu tensor cores for fast fp16 arithmetic to speed up mixed-precision iterative refinement solvers. In Harnessing GPU Tensor Cores for Fast FP16 Arithmetic to Speed up Mixed-Precision Iterative Refinement Solvers, page 0. IEEE, 2018.

Haiwu He, Guy Bergère, and Serge Petiton. A hybrid gmres/lstarnoldi method to accelerate the parallel solution of linear systems. *Computers & Mathematics with Applications*, 51(11):1647–1662, 2006.

V Hernandez, JE Roman, A Tomas, and V Vidal. Single vector iteration methods in slepc. *Scalable Library for Eigenvalue Problem Computations*, 2005a.

Vicente Hernandez, Jose E Roman, and Vicente Vidal. Slepcc: A scalable and flexible toolkit for the solution of eigenvalue problems. *ACM Transactions on Mathematical Software (TOMS)*, 31(3):351–362, 2005b.

Michael A Heroux. Epetra performance optimization guide. *Sandia National Laboratories, Tech. Rep. SAND2005-1668*, 2005.

Michael A Heroux, Roscoe A Bartlett, Vicki E Howle, Robert J Hoekstra, Jonathan J Hu, Tamara G Kolda, Richard B Lehoucq, Kevin R Long, Roger P Pawlowski, Eric T Phipps, et al. An overview of the trilinos project. *ACM Transactions on Mathematical Software (TOMS)*, 31(3):397–423, 2005.

Michael Allen Heroux. Aztecoo user guide. Technical report, Sandia National Laboratories, 2004.

Ralf Hiptmair. Multigrid method for maxwell’s equations. *SIAM Journal on Numerical Analysis*, 36(1):204–225, 1998.

Mark Hoemmen. *Communication-avoiding Krylov subspace methods*. University of California, Berkeley, 2010.

BR Hutchinson and GD Raithby. A multigrid method based on the additive correction strategy. *Numerical Heat Transfer, Part A: Applications*, 9(5):511–537, 1986.

Pierre Jolivet and Pierre-Henri Tournier. Block iterative methods and recycling for improved scalability of linear solvers. In *SC16-International Conference for High Performance Computing, Networking, Storage and Analysis*, 2016.

M Ozan Karsavuran, Kadir Akbudak, and Cevdet Aykanat. Locality-aware parallel sparse matrix-vector and matrix-transpose-vector multiplication on many-core processors. *IEEE Transactions on Parallel & Distributed Systems*, (1):1–1, 2016.

Takahiro Katagiri, Pierre-Yves Aquilanti, and Serge Petiton. A smart tuning strategy for restart frequency of gmres (m) with hierarchical cache sizes. In *International Conference on High Performance Computing for Computational Science*, pages 314–328. Springer, 2012.

David S Kershaw. The incomplete cholesky—conjugate gradient method for the iterative solution of systems of linear equations. *Journal of Computational Physics*, 26(1):43–65, 1978.

Misha E Kilmer and Eric De Sturler. Recycling subspace information for diffuse optical tomography. *SIAM Journal on Scientific Computing*, 27(6):2140–2166, 2006.

Dana A Knoll and David E Keyes. Jacobian-free newton–krylov methods: a survey of approaches and applications. *Journal of Computational Physics*, 193(2):357–397, 2004.

Tomonori Kouya. A highly efficient implementation of multiple precision sparse matrix–vector multiplication and its application to product-type krylov subspace methods. *arXiv preprint arXiv:1411.2377*, 2014.

Moritz Kreutzer, Georg Hager, Gerhard Wellein, Holger Fehske, and Alan R Bishop. A unified sparse matrix data format for efficient general sparse matrix–vector multiplication on modern processors with wide simd units. *SIAM Journal on Scientific Computing*, 36(5):C401–C423, 2014.

L Lasdon, S Mitter, and A Waren. The conjugate gradient method for optimal control problems. *IEEE Transactions on Automatic Control*, 12(2):132–138, 1967.

Jeonghwa Lee, Jun Zhang, and Cai-Cheng Lu. Incomplete lu preconditioning for large scale dense complex linear systems from electromagnetic wave scattering problems. *Journal of Computational Physics*, 185(1):158–175, 2003.

Jinpil Lee and Mitsuhisa Sato. Implementation and performance evaluation of xcalablemp: A parallel programming language for distributed memory systems. In *Parallel Processing Workshops (ICPPW), 2010 39th International Conference on*, pages 413–420. IEEE, 2010.

Koung Hee Leem, Suely Oliveira, and DE Stewart. Algebraic multigrid (amg) for saddle point systems from meshfree discretizations. *Numerical linear algebra with applications*, 11(2-3):293–308, 2004.

Weifeng Liu and Brian Vinter. Csr5: An efficient storage format for cross-platform sparse matrix–vector multiplication. In *Proceedings of the 29th ACM on International Conference on Supercomputing*, pages 339–350. ACM, 2015.

Tahir Malas and Levent Gürel. Incomplete lu preconditioning with the multilevel fast multipole algorithm for electromagnetic scattering. *SIAM Journal on Scientific Computing*, 29(4):1476–1494, 2007.

Manish Malhotra, Roland W Freund, and Peter M Pinsky. Iterative solution of multiple radiation and scattering problems in structural acoustics using a block quasi-minimal residual algorithm. *Computer methods in applied mechanics and engineering*, 146(1-2):173–196, 1997.

Christopher M Maynard and David N Walters. Precision of the endgame: Mixed-precision arithmetic in the iterative solver of the unified model. *arXiv preprint arXiv:1811.03852*, 2018.

Duane Merrill and Michael Garland. Merge-based sparse matrix-vector multiplication (spmv) using the csr storage format. In *ACM SIGPLAN Notices*, volume 51, page 43. ACM, 2016.

Takeshi Mifune, Takeshi Iwashita, and Masaaki Shimasaki. New algebraic multigrid preconditioning for iterative solvers in electromagnetic finite edge-element analyses. *IEEE transactions on magnetics*, 39(3):1677–1680, 2003.

Peter Moczo, Jozef Kristek, M Galis, P Pazak, and M Balazovjech. The finite-difference and finite-element modeling of seismic wave propagation and earthquake motion. *Acta Physica Slovaca. Reviews and Tutorials*, 57(2):177–406, 2007.

Eurípides Montagne and Anand Ekambaram. An optimal storage format for sparse matrices. *Information Processing Letters*, 90(2):87–92, 2004.

Hannah Morgan, Matthew G Knepley, Patrick Sanan, and L Ridgway Scott. A stochastic performance model for pipelined krylov methods. *Concurrency and Computation: Practice and Experience*, 28(18):4532–4542, 2016.

Ronald Morgan. On restarting the arnoldi method for large nonsymmetric eigenvalue problems. *Mathematics of Computation of the American Mathematical Society*, 65(215):1213–1230, 1996.

Ronald B Morgan. A restarted gmres method augmented with eigenvectors. *SIAM Journal on Matrix Analysis and Applications*, 16(4):1154–1171, 1995.

Aaftab Munshi. The opencl specification. In *Hot Chips 21 Symposium (HCS), 2009 IEEE*, pages 1–314. IEEE, 2009.

Noël M Nachtigal, Lothar Reichel, and Lloyd N Trefethen. A hybrid gmres algorithm for nonsymmetric linear systems. *SIAM Journal on Matrix Analysis and Applications*, 13(3):796–825, 1992.

Yoshifumi Nakamura, K-I Ishikawa, Y Kuramashi, Tetsuya Sakurai, and Hiroto Tadano. Modified block bicgstab for lattice qcd. *Computer Physics Communications*, 183(1):34–37, 2012.

-
- James C Newman. A finite-element analysis of fatigue crack closure. In Mechanics of crack growth. ASTM International, 1976.
- Bahram Nour-Omid and Ray W Clough. Short communication block lanczos method for dynamic analysis of structures. Earthquake engineering & structural dynamics, 13(2):271–275, 1985.
- CUDA Nvidia. Nvidia cuda c programming guide. Nvidia Corporation, 120(18):8, 2011.
- Edson Luiz Padoin, Laércio Lima Pilla, Francieli Zanon Boito, Rodrigo Virote Kassick, Pedro Velho, and Philippe OA Navaux. Evaluating application performance and energy consumption on hybrid cpu+ gpu architecture. Cluster Computing, 16(3):511–525, 2013.
- Christopher C Paige and Michael A Saunders. Solution of sparse indefinite systems of linear equations. SIAM journal on numerical analysis, 12(4):617–629, 1975.
- Manolis Papadrakakis and S Smerou. A new implementation of the lanczos method in linear problems. International Journal for Numerical Methods in Engineering, 29(1):141–159, 1990.
- Michael L Parks, Eric De Sturler, Greg Mackey, Duane D Johnson, and Spandan Maiti. Recycling krylov subspaces for sequences of linear systems. SIAM Journal on Scientific Computing, 28(5):1651–1674, 2006.
- Serge G Petiton. Parallel subspace method for non-hermitian eigenproblems on the connection machine (cm2). Applied Numerical Mathematics, 10(1):19–35, 1992.
- Gernot Plank, Manfred Liebmann, Rodrigo Weber dos Santos, Edward J Vigmond, and Gundolf Haase. Algebraic multigrid preconditioner for the cardiac bidomain model. IEEE Transactions on Biomedical Engineering, 54(4):585–596, 2007.
- DF Pridmore, GW Hohmann, SH Ward, and WR Sill. An investigation of finite-element modeling for electrical and electromagnetic data in three dimensions. Geophysics, 46(7):1009–1024, 1981.
- Nikola Rajovic, Alejandro Rico, Filippo Mantovani, Daniel Ruiz, Josep Oriol Vilarrubí, Constantino Gomez, Luna Backes, Diego Nieto, Harald Servat, Xavier Martorell, et al. The mont-blanc prototype: an alternative approach for hpc systems. In High Performance Computing, Networking, Storage and Analysis, SC16: International Conference for, pages 444–455. IEEE, 2016.
- John W Ruge and Klaus Stüben. Algebraic multigrid. In Multigrid methods, pages 73–130. SIAM, 1987.

Karl Rupp, Josef Weinbub, Ansgar Jüngel, and Tibor Grasser. Pipelined iterative solvers with kernel fusion for graphics processing units. *ACM Transactions on Mathematical Software (TOMS)*, 43(2):11, 2016.

Y Saad. Sparsekit: a basic tool kit for sparse matrix computation (version2), university of illinois, 1994a.

Youcef Saad. Chebyshev acceleration techniques for solving nonsymmetric eigenvalue problems. *Mathematics of Computation*, 42(166):567–588, 1984.

Youcef Saad. On the lanczos method for solving symmetric linear systems with several right-hand sides. *Mathematics of computation*, 48(178):651–662, 1987a.

Youcef Saad. Least squares polynomials in the complex plane and their use for solving nonsymmetric linear systems. *SIAM Journal on Numerical Analysis*, 24(1):155–169, 1987b.

Youcef Saad and Martin H Schultz. Gmres: A generalized minimal residual algorithm for solving nonsymmetric linear systems. *SIAM Journal on scientific and statistical computing*, 7(3):856–869, 1986.

Youcef Saad. Krylov subspace methods for solving large unsymmetric linear systems. *Mathematics of computation*, 37(155):105–126, 1981.

Youcef Saad. Ilut: A dual threshold incomplete lu factorization. *Numerical linear algebra with applications*, 1(4):387–402, 1994b.

Youcef Saad. *Iterative methods for sparse linear systems*. Siam, 2003.

Youcef Saad. *Numerical Methods for Large Eigenvalue Problems: Revised Edition*. SIAM, 2011.

Tetsuya Sakurai, Hiroto Tadano, and Y Kuramashi. Application of block krylov subspace algorithms to the wilson–dirac equation with multiple right-hand sides in lattice qcd. *Computer Physics Communications*, 181(1):113–117, 2010.

Patrick Sanan, Sascha M Schnepp, and Dave A May. Pipelined, flexible krylov subspace methods. *SIAM Journal on Scientific Computing*, 38(5):C441–C470, 2016.

Martin Schweiger, SR Arridge, M Hiraoka, and DT Delpy. The finite element method for the propagation of light in scattering media: boundary and source conditions. *Medical physics*, 22(11):1779–1792, 1995.

Kubilay Sertel and John L Volakis. Incomplete lu preconditioner for fmm implementation. *Microwave and Optical Technology Letters*, 26(4):265–267, 2000.

Valeria Simoncini and Efstratios Gallopoulos. An iterative method for nonsymmetric systems with multiple right-hand sides. *SIAM Journal on Scientific Computing*, 16(4):917–933, 1995.

Gerard LG Sleijpen and Diederik R Fokkema. Bicgstab (l) for linear equations involving unsymmetric matrices with complex spectrum. *Electronic Transactions on Numerical Analysis*, 1(11):2000, 1993.

Charles F Smith, Andrew F Peterson, and Raj Mittra. A conjugate gradient algorithm for the treatment of multiple incident electromagnetic fields. *IEEE Transactions on Antennas and Propagation*, 37(11):1490–1493, 1989.

Dennis Chester Smolarski. Optimum semi-iterative methods for the solution of any linear algebraic system with a square matrix. PhD thesis, University of Illinois at Urbana-Champaign, 1982.

Danny C Sorensen. Implicitly restarted arnoldi/lanczos methods for large scale eigenvalue calculations. In Parallel Numerical Algorithms, pages 119–165. Springer, 1997.

Pyrrhos Stathis, Stamatis Vassiliadis, and Sorin Cotofana. A hierarchical sparse matrix storage format for vector processors. In Parallel and Distributed Processing Symposium, 2003. Proceedings. International, pages 8–pp. IEEE, 2003.

Gilbert W Stewart. A krylov–schur algorithm for large eigenproblems. *SIAM Journal on Matrix Analysis and Applications*, 23(3):601–614, 2002.

N Sukumar, DL Chopp, and B Moran. Extended finite element method and fast marching method for three-dimensional fatigue crack propagation. *Engineering Fracture Mechanics*, 70(1):29–48, 2003.

Kasia Swirydowicz, Julien Langou, Shreyas Ananthan, Ulrike Yang, and Stephen Thomas. Low synchronization gmres algorithms. *arXiv preprint arXiv:1809.05805*, 2018.

TheNextPlatform. TheNextPlatform argonne hints at future architecture of aurora exascale system, 2018. URL <https://www.nextplatform.com/2018/03/19/argonne-hints-at-future-architecture-of-aurora-exascale-system/>.

Raymond van Venetië and Jan Westerdiep. Induced dimension reduction. 2015.

Petr Vaněk, Jan Mandel, and Marian Brezina. Algebraic multigrid by smoothed aggregation for second and fourth order elliptic problems. *Computing*, 56(3):179–196, 1996.

Brendan Vastenhout and Rob H Bisseling. A two-dimensional data distribution method for parallel sparse matrix-vector multiplication. *SIAM review*, 47(1):67–95, 2005.

Brigitte Vital. Etude de quelques méthodes de résolution de problèmes linéaires de grande taille sur multiprocesseur. PhD thesis, Rennes 1, 1990.

John Von Neumann. First draft of a report on the edvac, 30 june 1945. Contract No W-670-ORD-492, Moore School of Electrical Engineering, University of Pennsylvania, Philadelphia. Google Scholar, 1945.

Heinrich Voß. An arnoldi method for nonlinear eigenvalue problems. BIT numerical mathematics, 44(2):387–401, 2004.

Olof Widlund. A lanczos method for a class of nonsymmetric systems of linear equations. SIAM Journal on Numerical Analysis, 15(4):801–812, 1978.

Sandra Wienke, Paul Springer, Christian Terboven, and Dieter an Mey. Openacc—first experiences with real-world applications. In European Conference on Parallel Processing, pages 859–870. Springer, 2012.

WikiChips. WikiChips matrix-2000 - nudt, 2017. URL <https://en.wikichip.org/wiki/nudt/matrix-2000>.

Michael Wilde, Mihael Hategan, Justin M Wozniak, Ben Clifford, Daniel S Katz, and Ian Foster. Swift: A language for distributed parallel scripting. Parallel Computing, 37(9):633–652, 2011.

Markus Wittmann, Georg Hager, Thomas Zeiser, and Gerhard Wellein. An analysis of energy-optimized lattice-boltzmann cfd simulations from the chip to the highly parallel level. CoRR, vol. abs/1304.7664, 2013.

Xinzhe Wu. Smg2s manual v1. 0. Technical report, 2018.

Xinzhe Wu and Serge G. Petiton. A distributed and parallel asynchronous unite and conquer method to solve large scale non-hermitian linear systems. In Proceedings of the International Conference on High Performance Computing in Asia-Pacific Region, HPC Asia 2018, pages 36–46, New York, NY, USA, 2018a. ACM. ISBN 978-1-4503-5372-4. doi: 10.1145/3149457.3154481. URL <http://doi.acm.org/10.1145/3149457.3154481>.

Xinzhe Wu and Serge G Petiton. A distributed and parallel asynchronous unite and conquer method to solve large scale non-hermitian linear systems. In Proceedings of the International Conference on High Performance Computing in Asia-Pacific Region, pages 36–46. ACM, 2018b.

Ichitaro Yamazaki, Stanimire Tomov, and Jack Dongarra. Mixed-precision cholesky qr factorization and its case studies on multicore cpu with multiple gpus. SIAM Journal on Scientific Computing, 37(3):C307–C330, 2015.

Ichitaro Yamazaki, Mark Hoemmen, Piotr Luszczek, and Jack Dongarra. Improving performance of gmres by reducing communication and pipelining global collectives. In Parallel and Distributed Processing Symposium Workshops (IPDPSW), 2017 IEEE International, pages 1118–1127. IEEE, 2017.

Ulrike Meier Yang et al. Boomeramg: a parallel algebraic multigrid solver and preconditioner. Applied Numerical Mathematics, 41(1):155–177, 2002.

Xiyang IA Yang and Rajat Mittal. Acceleration of the jacobi iterative method by factors exceeding 100 using scheduled relaxation. Journal of Computational Physics, 274:695–708, 2014.

Zuochang Ye, Zhenhai Zhu, and Joel R Phillips. Generalized krylov recycling methods for solution of multiple related linear equation systems in electromagnetic analysis. In Proceedings of the 45th annual Design Automation Conference, pages 682–687. ACM, 2008.

Seokkwan Yoon and Antony Jameson. Lower-upper symmetric-gauss-seidel method for the euler and navier-stokes equations. AIAA journal, 26(9):1025–1026, 1988.

